TRANSPORT PROPERTIES OF SOLIDS AT LOW TEMPERATURES IN HIGH MAGNETIC FIELDS

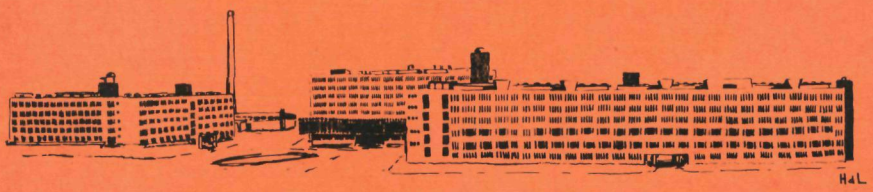

H. N. DE LANG

Part of this work has been supported by the Stichting voor Fundamenteel Onderzoek der Materie (FOM) with financial support from the Nederlandse Organisatie voor Zuiver Wetenschappelijk Onderzoek (ZWO).

TRANSPORT PROPERTIES OF SOLIDS AT LOW TEMPERATURES IN HIGH MAGNETIC FIELDS

PROMOTOR PROF. DR. P. WYDER

CO-REFERENT: DR. H. VAN KEMPEN

TRANSPORT PROPERTIES OF SOLIDS AT LOW TEMPERATURES IN HIGH MAGNETIC FIELDS

PROEFSCHRIFT

TER VERKRIJGING VAN DE GRAAD VAN DOCTOR IN DE WISKUNDE EN NATUURWETENSCHAPPEN AAN DE KATHOLIEKE UNIVERSITEIT TE NIJMEGEN, OP GEZAG VAN DE RECTOR MAGNIFICUS PROF.DR. A.J.H. VENDRIK, VOLGENS BESLUIT VAN HET COLLEGE VAN DECANEN IN HET OPENBAAR TE VERDEDIGEN OP WOENSDAG 23 NOVEMBER 1977 DES NAMIDDAGS TE 4 UUR

door

HERMAN NICOLAAS DE LANG
geboren te Klaten (Indonesië)

1977
Druk: Krips Repro Meppel

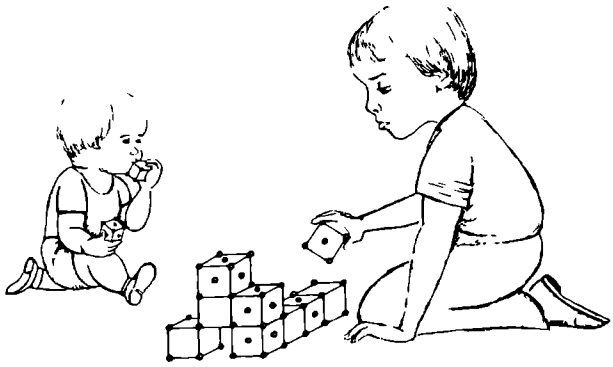

voor pap en mam,l.g.
voor tineke,dennis en quirijn,
en misschien ook een beetje
voor coen en/of merel

Naast allen die mij behulpzaam waren bij de in dit proefschrift beschreven onderzoek,zou ik graag de volgende personen in het bijzonder willen danken :
Herman van Kempen,voor zijn evangelisch geduld,zijn onuitputtelijke kennis van elektronica,cryogenie en fysica,zijn genereuze behulpzaamheid en zijn subtiele humor,
Ap van Gelder voor vele verhelderende en verwarrende,maar altijd interessante gesprekken,
Hans Stoelinga,voor hulp en inspiratie bij het probleem van de 2-dimensionale fononen roosters,
Joe Lass,for inducing some Cantabridgean sense for perfection into our measurements,
Prof.A.R.Miedema,voor het aanreiken van problemen en zijn levendige belangstelling bij de uitwerking ervan,
Erik Mischgofsky,voor zijn gulle,steeds aanwezige bereidheid tot het leveren van perfect gegroeide kristallen,
Kees Beers,Leo Coenen,Jan Hermsen en Riki Gommers,voor technische,illustratieve en administratieve hulp,
Felix Meier en Jos Perenboom,mijn kamergenoten,voor hulp en vriendschap,
alsmede de medewerkers van de technische diensten,in het bijzonder de heer H.W.Boltze.
Vooral ook mijn ouders zou ik willen danken voor hun steun,liefde en medeleven.
Maar bovenal gaat mijn dank uit naar Tineke voor haar steun en toewijding.Moge het begin van ieder hoofdstuk daarvan getuigen.

CONTENTS

1. INTRODUCTION. 1

1.1 Many particle physics 1
1.2 Transport properties of magnetic insulators 5
1.3 Transport properties of pure metals 8
1.4 Transport properties of superconductors 11
1.5 The Blue Monster 14
References 16

2. THE BLUE MONSTER 19

2.1 Cryostat and cooling system 19
2.2 The superconducting magnet 25
2.3 Sample space and leads 25
2.4 Temperature measurement and thermometers 28
2,5 Calibration 37
2.6 Measuring and control system 38
References 43

3. MAGNON AND PARAMAGNON THERMAL CONDUCTIVITY IN TWO-DIMENSIONAL MAGNETIC SYSTEMS 45

3.1 Introduction 45

3.2 Two-dimensional Heisenberg magnetic systems 49
3.3 Theoretical background 54
3.3.1 The Sato model of magnon thermal conduction 54
3.3.2 Influence of the magnetic field 58
3.3.3 Two-dimensional magnon thermal conductivity 62
3.4 Experimental details and results 71
3.4.1 Sample preparation 71
3.4.2 Sample mounting and measurement 73
3.4.3 Experimental Results 77
3.4.4 Field dependence 79
3.4.5 Phonon conductivity 86
3.4.6 Magnon and paramagnon conductivity 93
References 105

4. THE LATTICE THERMAL CONDUCTIVITY OF PURE METALS: ALUMINIUM AND INDIUM 111

4.1 Introduction 111
4.2 Theoretical background 115
4.2.1 Thermal conduction in metals 115
4.2.2 Theoretical estimate of the lattice conductivity 126
4.2.3 The separation of the lattice and electronic conductivities 134
4.2.4 Reduction of λ_e in the superconducting state 137
4.2.5 Reduction of λ_e by alloying 143

4.2.6 Reduction of λ_e by the application of a magnetic field 155
4.2.7 The magnetic field dependence 164
4.2.8 The linear magnetoresistance 177
4.2.9 The Corbino effect 191
4.3 Experimental details and results 197
4.3.1 Experimental Arrangement 197
4.3.2 Samples 198
4.3.3 The lattice conductivity 201
4.3.4 Thermal linear magnetoresistance 209
4.3.5 The so-called quadratic magnetoresistance 232
4.3.6 Curve crossing: the Kagan effect 237
References 252

5. METASTABLE STATES IN SUPERCONDUCTORS : SUPERCOOLING AND SUPERHEATING 265

5.1 Introduction 265
5.2 The metastable states 275
5.2.1 The Ginzburg-Landau equations 275
5.2.2 Supercooling 277
5.2.3 Superheating 281
5.2.4 Influence of the boundary condition 286
5.2.5 Flaws and nucleation centers 290
5.2.6 The quench effect 291
5.3 Influence of the geometry 292
5.4 Experimental results 301

5.4.1 Sample preparation 301
5.4.2 Unplated wires 305
5.4.3 Gold-plated wires 308
5.4.4 Discussiun 309
References 315

6. SUMMARY 319
SAMENVATTING 321

1. INTRODUCTION

1.1 Many Particle Physics.

> Nature,it seems,is the popular name
> For milliards and milliards and milliards
> Of particles,playing their infinite game
> Of billiards and billiards and billiards...
>
> Piet Hein,"Grooks"

The leader of our group,when pressed for a nutshell description of the physical investigations his group is engaged in,likes to summarize these research activities into three words : many-particle-physics.

'Particle' here stands for quasiparticle,while 'many' is meant,not only to indicate the huge number of particles involved ($\sim 10^{23}$),but also to convey a qualitative feeling for the number of different quasiparticles ($10 \sim 10^{2}$),which may play a role in the physical processes under consideration.

In the physics of condensed matter,systems are studied involving a great many individual constituent particles,usually interacting strongly with one another. A complete microscopic analysis of such systems is clearly impossible,as even three-body problems cannot in general be solved analytically.Fortuitously,however,in most many-body systems the low energy states,which dominates the low temperature properties,behave like those of arti-

ficial weakly interacting systems,even though the interaction between the constituent particles of the real system may be strong.Hence,the excitation energies may be taken as additive to a good approximation,leading to considerable simplification in the analysis.These excitations are known as 'elementary excitations' or 'quasiparticles'.

Elementary excitations exist in two different classes,i.e.

i) quasiparticle excitations,e.g. electrons

ii) collective excitations,e.g. phonons,magnons

In a system of non-interacting particles,one can raise the energy of one of the particles without in the least affecting the others.On the other hand,if an interaction between the particles does exist,one expects these particle excitations to decay,since the excited particles will scatter off the unexcited ones. However,if the particles obey the Pauli "exclusion principle" and the excitation energies are low,there will be very few empty states into which the particles can be scattered,and the excitation will acquire a sufficiently long lifetime for the particle concept to be applicable.It is excitations such as these that we call 'quasiparticle excitations'.

By appropriate quantum mechanical transformations the system of interacting particles can be described as a system of non- or weakly interacting quasiparticle excitations,although,because of the interactions,the energy of such excitations will differ from those of

the non-interacting particles.
Hence,quasiparticles have the same qualitative character as the bare constituent particles of the system, e.g. a quasi-electron can be visualised as a bare electron,surrounded by a cloud of virtual collective excitations.

Collective excitations,on the other hand,depend for their existence on the interaction between the bare constituting particles.For example,because the interatomic forces in a solid are so strong,it is not practicable to consider the motions of a lattice ion in terms of the motions of an individual particle. Any momentum given to one lattice ion is so quickly transmitted to its neighbours that after a very short period one cannot tell which ion initially has been displaced.A motion through the lattice is specified, not by the change in coordinates of just one ion,but by those of every ion in the solid collectively.
A 'collective excitation' can then be defined as the quantum of a collective normal mode of an interacting system.
Thus a phonon is a the quantum unit of a lattice vibration (oscillations in the relative position of atoms in a lattice) and a magnon the quantum unit of a spin-wave (oscillations in the relative orientations of spins in a lattice).Such quanta are bosons with no restriction on occupation number.

The study of quasiparticles has served not only

transport properties,they can all be analysed,using the same general methods and techniques.

1.2 Transport Properties of Magnetic Insulators.

The magnetic insulators studied in this thesis are two-dimensional Heisenberg ferromagnets of the general formula : $(C_nH_{2n+1}NH_3)_2CuCl_4$,n=1,2,....(henceforth abbreviated by C_nCuCl).The magnetic ions in these crystals are arranged in sheets or layers with relatively long distances between them,formed by the organic alkylammonium $(C_nH_{2n+1}NH_3)$-chains.Hence,due to the exponential form of the space dependence of the exchange interaction, the intralayer magnetic interactions are about a thousand to a million times stronger than the interlayer interactions,and these crystals approximate a two-dimensional Heisenberg ferromagnet to an almost ideal degree.

Besides a two-dimensional magnetic lattice,these crystals possess other highly interesting magnetic (2,3), dielectric (4,5,6) and transport (7,8,9) properties,but we shall limit ourselves to a discussion of the thermal energy transport only.

The conduction of heat in insulators is generally carried out by phonons.For magnetic systems the specific heat consists of a spin and a phonon part,and in a certain temperature range the former may even exceed the latter.One would therefore expect that magnons may

also contribute to the heat transport.In practice,however,the appearance of magnon conductivity turns out to be a rather rare phenomenon : there are only very few magnetic crystals where magnon conductivity has been unambiguously shown to exist.
The reason for this is the following :
It should be realized that thermal energy can only enter and leave the crystal via the phonon system.Therefore, for the magnon system to contribute to the heat transport,an interaction between the two systems must exist. If this interaction is too small,no heat will escape into the magnon system in an experimentally detectable degree.If the interaction is too large,the magnons will mainly serve to impede rather than to contribute positively to the heat transport.
Thus,only when the interaction lies within a certain range of strength will magnon thermal conductivity be possible.

In general,magnons only exist at temperatures below a well-defined critical temperature T_c (also called Curie-temperature for ferromagnets).However, under certain conditions large long-living spinfluctuations can occur above T_c.At temperatures not far above T_c,the exchange interaction is still able to induce some limited amount of order over small volumes of the crystal,the extent of which is determined by the correlation length.In this way,small assemblies of correlated spins appear in different parts of the crystal.

The process is dynamic and time dependent, so that at a given temperature small ordered spin-assemblies (each having a net spontaneous magnetization) are continuously forming and dissolving in different parts of the crystal. The total net magnetization, however, remains practically zero (paramagnetic state).

The appearance of these paramagnetic short-range order magnons or paramagnons is highly influenced by the dimensionality of the magnetic system. As a consequence of the two-dimensionality, the length over which the spins are correlated will be considerably larger than in three-dimensional systems at the same temperature relative to T_c. Therefore, one expects for low-dimensional systems more pronounced magnon modes above T_c.

We have shown by thermal conductivity measurements on C_1CuCl- and C_2CuCl-crystals, that besides exhibiting a two-dimensional magnetic system, the phonon system of these crystals is two-dimensional in character as well. Furthermore, below T_c magnon conductivity completely dominates the heat transport, comprising about 90 % of the total thermal conductivity - the largest magnon contribution yet observed. Above T_c, we have found for the first time a magnetic contribution to the transport of thermal energy up to 95 % of the total heat transport, which can mainly be attributed to paramagnons. Unfortunately, no theory for the energy transport by paramagnons exists as yet to allow quantitative comparasons. These experimental results, as well as the theory of magnon conductivity, shall be

described in chapter 3.

1.3 Transport Properties of Pure Metals.

The transport properties of pure metals are largely determined by electrons and phonons.The electronic contribution,however,completely dominates the phononic part,and where heat conduction is concerned,the former is about ten thousand times greater than the latter.

In pure metals both modes of thermal transport are interrelated by electron-phonon interactions. The electron-phonon interaction is intrinsic to several low-temperature phenomena,such as the electrical resistance in pure metals (10-13),the thermal boundary resistance (14,15),the characteristics of ballistic phonon pulses (15),certain single-particle tunneling phenomena (14-18),point-contact spectroscopy (19-21) and the thermal impedance between electrons and phonons in small specimen (22,23).

A question which continues to arise regarding these and other phenomena is how tightlythe phonons are coupled to the electron system.The experimental technique often used to study this question is to measure the lattice conductivity of metals.This measurement is possible only,if the thermal conductance contributed by the electrons can drastically be reduced.

Three methods exist to accomplish this reduction :

i) by going into the superconducting state

ii) by alloying the metal

iii) by applying a magnetic field

A critical and comprehensive discussion of these methods is given in chapter 4.

In chapter 4 is also described our measurements of the lattice thermal conductivities of pure Aluminium and Indium by the magnetic field method in the so-called Corbino configuration.In this arrangement the heat current enters the sample,which consists of a circular disk,in the center of the disk while the magnetic field is applied perpendicular to it.Under the influence of the field the electrons do not reach the outer circumference of the sample in a straight line but are deviated.Proportional to the strength of the applied field, this deviation causes a decrease of the electronic conductivity,while the phonons remain unaffected (24,25).The essence of the Corbino method lies in the fact that,because of the particular geometry,the (electrical or thermal) Hall-field cannot be established, increasing highly its effectiveness in reducing the electronic conductivity.This in contrast to the conventional configuration,whereby the sample consists of a long wire or thin plate with the magnetic field applied perpendicular to it.In fact,the conventional configuration displays a minimal magnetoresistance, due to the correcting influence of the Hall effect, while in the Corbino configuration the highest possible value of the magnetoresistance is obtained.

Historically,the lattice thermal conductivity of metals were mostly measured by the alloying method,because no magnetic fields could be produced of sufficiently high strengths to reduce the electronic conductivity adequately.But it is not clear at all if the considerable alloying does not change the intrinsic properties of the material in a drastic way.
Indeed,our measurements provide the first reliable values of the lattice conductivity of Al and In,obtained with the magnetic field method.Even though,especially at Nijmegen (26),very high continuous magnetic fields can now be generated with relative ease,in our opinion the formerly available fields were of sufficient strength to produce reliable data on the lattice conductivity,had the Corbino method been used.

Closely connected to these problems is the magnetoresistance.The field dependence of the electrical and thermal magnetoresistance became convincingly explicable only, after the topology of the Fermi surface was taken into account by I.M.Lifshitz,M.Y.Azbel and M.I. Kaganov in 1957.Despite the successes of the LAK-theory however,one mystery remained,i.e. the linear magnetoresistance.Although at sufficiently high fields for closed orbit,uncompensated metals like Aluminium and Indium,the LAK-theory predicted a saturation of the magnetoresistance, experimentally one found a magnetoresistance which increases linearly with field.
A comprehensive review of the anomalous magnetoresistance (27-29) as well as a discussion of its influence

on the determination of the lattice conductivity by the Corbino method,is also given in chapter 4.

Recently it was found that the thermal conductivity of Potassium showed a quadratic field dependence, a fact which could not be understood in terms of any of the available theories.Furthermore,a straightforward extrapolation of these results lead to a lattice thermal conductivity which was about 5 to 8 times too high, compared with the theoretically predicted values.
We could show that the quadratic field dependence is not a real effect,but stems from a misinterpretation of a partial Corbino effect.
This is also described in chapter 4.

Lastly,when plotted as a function of temperature, a maximum appears in the thermal conductivity when a magnetic field is applied.
We were able to interprete this phenomenon in terms of a theory,formulated by Kagan and collaborators in 1974. This is the first time that evidence of the Kagan effect in the thermal conductivity has been obtained.

1.4 Transport Properties of Superconductors.

In 1911 Kamerlingh Onnes - rather serendipitously - discovered superconductivity,but for almost half a century it remained 'the shame and despair of theoretical physics' as no quantitative,fundamental interpretation of its origin and effects could be given.

It was not until 1957 that J.Bardeen,L.N.Cooper and J.R. Schrieffer succeeded at last to develop a microscopic explanation of superconductivity - the famous BCS-theory - and not until a decade later that an experimental group was established at Nijmegen University (30) to study superconducting phenomena.

The most fundamental property of a superconductor is its perfect diamagnetism (Meissner state) rather than its infinite conductivity,as the latter is a consequence of the former and not vice versa (31). The transition from the Meissner state to the normal state occurs at a thermodynamically well-defined critical field H_c.However,in an increasing field the specimen can remain in the Meissner state even for fields $H>H_c$: superheating.

Equally,in a decreasing field the specimen can remain in the normal state even for fields $H<H_c$: supercooling.

These metastable states (32) can be most adequately described within the framework of the phenomenological Ginzburg-Landau (GL) theory of superconductivity (31). It can also be shown on the basis of the same theory, that the presence of a boundary increases the supercooling field (33-37).The influence of a boundary can be mitigated by coating the superconductor with a normal metal.This destroys the surface superconductivity, enhances the supercooling effect and decreases superheating.

The interest in supercooling-superheating effects stems from the fact that it provides one of the few means to measure the most important Ginzburg-Landau parameter κ, which plays a crucial role in the theory of superconductivity (31).

We have studied the supercooling and superheating effects in pure and goldplated,thin Indium wires,by measuring the resistive transitions in a changing magnetic field.A discussion of our results together with an account of the Ginzburg-Landau theory shall be given in chapter 5.

In its general three-dimensional non-linear form, the GL-equations have not been solved and it is only for special configurations that they can be reduced into a tractable form.For thin cylinders the GL-equations have been solved analytically for the case where the field is applied parallel to the cylinders.For the case where the magnetic field is applied perpendicular to the cylinders,as in our measurements,the GL-equations have not been solved analytically but only numerical solutions have been given.
We have been able to provide an analytical solution for the perpendicular configuration,exact to first order of $(f_0 r)$,where f_0 is the order parameter in zero field and r the radius of the cylinder.

Tied with these problems is the influence of the shape of the sample and the demagnetization factor.To determine the superheating field,for instance,one

usually considers the configuration of a magnetic field parallel to the boundary of a semi-infinite halfspace, for which the GL-equations reduce to analytically solvable one-dimensional differential equations.For samples of different shape,one adapts this halfspace solution by the introduction of an appropriate demagnetization factor.In this way,however,the influence of the locally variable penetration depth of the magnetic field is completely neglected.In our analytical treatment of the three-dimensional problem of a magnetic field perpendicular to a superconducting cylinder the demagnetization factor emerges in a most natural way into the solution of the superheating field and we could show that the influence of the penetration depth is of negligible consequence.

1.5 The Blue Monster

The measurements,reported in this thesis,were performed at temperatures ranging between 0.3 K and 25 K and in fields up to 7 tesla.These temperatures and fields are produced in a ^{3}He-cryostat,with a home-made insert and which is commonly referred to in our group as the "Blue Monster".
It received its name from my supervisor and co-referent,Dr. H. van Kempen,because of its blue metallic colour.

In naive optimism and youthful overconfidence and because of its elevated position - rather than to set it on the ground we have decided to hang it from the ceiling to prevent vibrational disturbances - I proposed to call it the "Blue Angel" instead,when I first began working with it.

But with the progress of time and no progress of results, I had to acknowledge the far more experienced eye of my supervisor.No Angel would hide its leaks so deviously in the most intricate parts of its system,freeze its inlet shut when we needed it open,jam its electronics, short-circuit its leads and swallow so many liters of precious liquid helium without producing results in return.

A Monster it is and,although now tamed and behaving reasonably well,a Monster it remains.

Its anatomy and functions shall be described in the next chapter.

References

1) A P van Gelder,"Veeldeeltjes Effecten" (Lecture Notes Cath.Univ.Nijmegen,1972)unpublished.

2) H van Kempen,F H M Mischgofsky and P Wyder in "Proc.12th Int.Conf.on Low Temp.Phys."(ed.E Kanda, Ac.Press of Japan,Kyoto,1971),p. 811.

3) H van Kempen,F H M Mischgofsky and P Wyder,Phys. Rev. B15(1977)4386

4) J H M Stoelinga and P Wyder, J.Chem.Phys. 61(1974) 478

5) J H M Stoelinga and P Wyder,J.Chem.Phys. 64(1976) 4612

6) J Holvast,J H M Stoelinga and P Wyder,Ferroelectrics 13(1976)543

7) H N De Lang,H van Kempen and P Wyder,Phys.Rev. Letters 39(1977)467

8) L H M Coenen,H N De Lang,J H M Stoelinga,H Van Kempen and P Wyder,Solid State Commun. 20(1976)713

9) L H M Coenen,H N De Lang,J H M Stoelinga,H Van Kempen and P Wyder,Physica 86-88B(1977)968

10) H van Kempen,J S Lass,J H J M Ribot and P Wyder in"Proc.14th Int.Conf.on Low Temp.Phys."(eds.M Krusius and M Vuorio,North Holland,Amsterdam,1975) vol.3,p.94

11) H van Kempen,J S Lass,J H J M Ribot and P Wyder, Phys.Rev.Letters 37(1976)1574

12) H van Kempen in"Proc. EPS-Conf. on Transport Properties of Normal Metals,1977, invited paper,to be published

13) H van Kempen,J H J M Ribot and P Wyder,Phys.Rev. 1977, to be published

14) J W M Bakker,"Tunneling Experiments with Superconductors",Ph.D.-thesis Cath.Univ.Nijmegen (Studentenpers,Nijmegen,1973)

15) H W M Salemink,"Ultra high-frequency phonon Experiments with Superconducting Tunnel Junctions", doctoraal-thesis Cath.Univ.Nijmegen 1973 (unpublished) and to be published.

16) H N De Lang,Ned.Tijdschr.v.Natuurk. 39(1973)298

17) H N De Lang,Chem.Weekblad 69(1973)8

18) H N De Lang in "Winkler Prins Jaarboek 1974" (Elsevier,Amsterdam,1974),p.342

19) A G M Jansen,F M Mueller and P Wyder in "Superconductivity in d- and f-band metals" (ed.D H Douglass,Plenum Press,New York,1976),p.607

20) A G M Jansen and F M Mueller,Ned.Tijdschr.v. Natuurk. A43(1977)83

21) A G M Jansen,F M Mueller and P Wyder,Phys.Rev. 1977,to be published

22) F Meier,"Small Particles and Boundary Conditions" Ph.D.-thesis Cath.Univ.Nijmegen (De Kleyn Offset, Nijmegen,1973)

23) F Meier,J A A J Perenboom and P Wyder,Phys.Reports,to be published

24) M Hubers,J F M Klein,H van Kempen,H N de Lang, J S Lass,A R Miedema and P Wyder in "Proc.1st Int.Conf.on Phonon Scattering in Solids" (ed.H J Albany,Service de Documentation du CEN,Saclay,1972) p.169

25) H van Kempen,H N de Lang, J S Lass and P Wyder, Phys.Letters 42A(1972)277

26) H N De Lang and P Wyder,Ned.Tijdschr.v.Natuurk. 43A(1977)95

27) J S Lass,Phys.Rev. B13(1976)2247

28) A P van Gelder,to be published

29) C J Beers,H van Kempen and P Wyder,to be published

30) 5 Jaar ACTION (ed.H N de Lang,Offsetdrukkerij FWN de K U Nijmegen,Nijmegen,1972)

31) P Wyder, "Notizen zur Vorlesung über Supraleitung" (Lecture Notes Cath.Univ.Nijmegen,1968) unpublished

32) R Deltour,H N de Lang and P Wyder,Phys.Letters 31A(1970)515

33) A P van Gelder,J W Hendriks and P Wyder in "Proc. 11th Int.Conf.on Low Temp.Phys.(eds. J F Allen, D M Finlayson and D M McCall,St.Andrews,1968) vol.2,p.956

34) A P van Gelder,Phys.Rev.Letters 20(1968)1435

35) A P van Gelder,J W Hendriks and P Wyder,Phys.Rev. B4(1971)2950

36) P Wyder,FOM-Jaarboek 1972,p.109

37) J W Hendriks," Measurements on Superconducting Films",Ph.D-thesis Cath.Univ.Nijmegen(Krips Repro,Meppel,1976)

2. THE BLUE MONSTER

2.1 Cryostat and Cooling System.

In recent years the commercial availability of ^{3}He has instigated the development of new types of cryostats, i.e. the helium-3 cryostat and the dilution refrigerator, which has brought the cryogenic region from 1 K down to several millikelvin, within relatively easy reach. The importance of ^{3}He as a cooling agent is due to three highly useful cryogenic properties, i.e.

i) ^{3}He has a higher vapour pressure than ^{4}He at low temperatures (Table 1)

Hence, by reducing the vapour pressure by pumping, much lower temperatures can be reached with ^{3}He than is possible with ^{4}He.

ii) ^{3}He does not become superfluid down to 3 mK, with a subsequent absence of film flow.

In ^{4}He-cryostats, the lowest obtainable temperature is mainly limited by film flow : at temperatures below the λ-point (2.17 K), a superfluid film creeps up the walls of the container until it evaporates at a higher level, which is warm enough. This causes a continuous loss of helium and a steady inflow of heat.

iii) ^{3}He has a larger heat capacity than ^{4}He (Table 2)

The disadvantage of ^{3}He is that it is not available in large quantities and rather expensive. This can

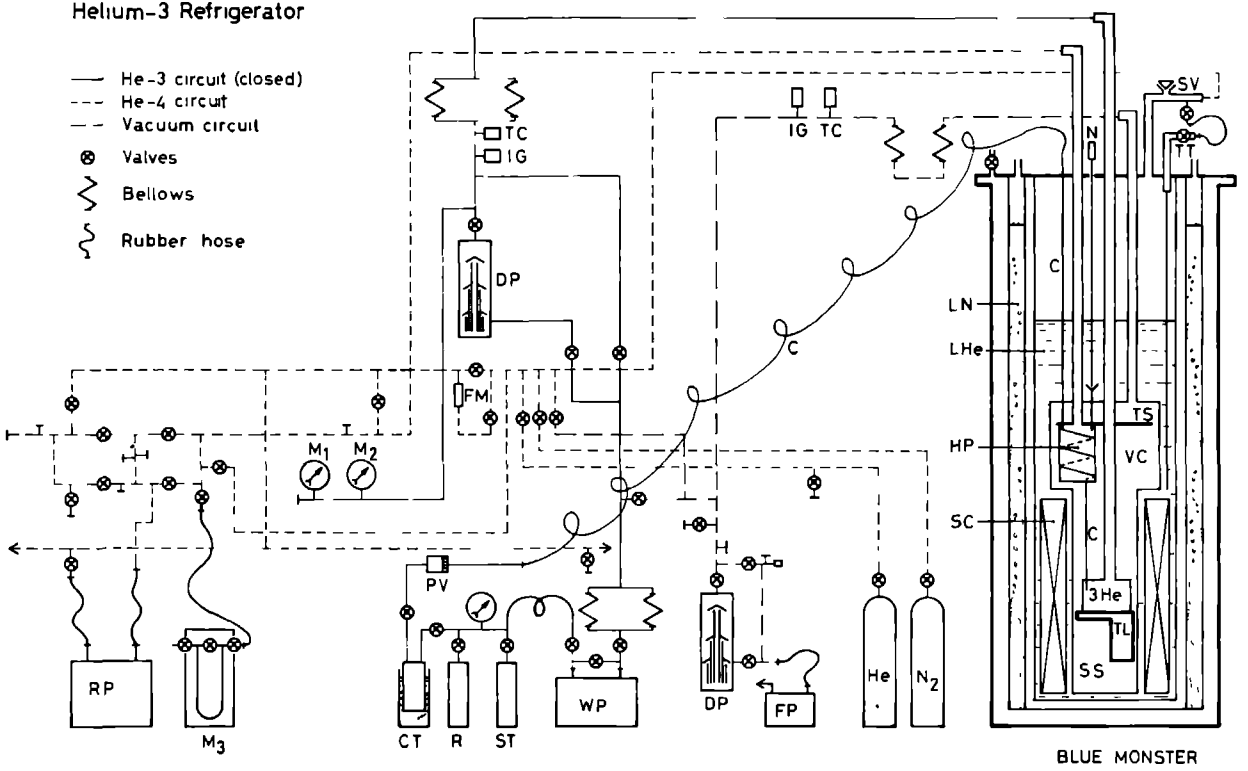
Helium-3 Refrigerator
He-3 circuit (closed)
He-4 circuit
Vacuum circuit
Valves
Bellows
Rubber hose
TC
IG
DP
FM
M1
M2
PV
RP
M3
CT
R
ST
WP
IG
TC
SV
N
TT
C
LN
LHe
HP
SC
TS
VC
3He
TL
SS
He
N2
FP
BLUE MONSTER

be partly compensated for by recirculating the ^{3}He in a closed system, so that only small quantities - typically 15 ml liq. ^{3}He - are needed.

The "Blue Monster" is a ^{3}He-cryostat in which temperatures from 25 K to 0.3 K and magnetic fields (from a superconducting magnet) up to 7 tesla, can be generated. (For modern descriptions of ^{3}He-cryostats, see refs.(1-3)) In the conventional ^{4}He-cryostats, temperatures down to approximately 1 K, or at most down to 0.8 K, can be reached. With a ^{3}He-cryostat the cooling range can be extended down to about 0.25 K.

In Fig.2.1 is shown the pumping scheme of the high vacuum and the ^{4}He-system, together with the closed ^{3}He-system and a schematic view of the ^{3}He-cryostat, as used for the Blue Monster.

Fig.2.1 : Helium-3 Refrigeration System.

C: 3He-capillary, CT: cooling trap, DP: diffusion pump, FM: flow meter, FP: forepump (cap: 330 1/h), He: 4He-gas vessel (200 atm.), 3He: 3He-can (0.3 K), HP: auxillary 4He-pot (1 K), IG: ionisation gauge, LHe: liquid 4He-bath (4.2 K), LN: liquid nitrogen bath (77 K), M1: WT (Wallace and Tiernan) absolute pressure manometer: 0-50 torr, M2: WTmanometer: 0-800 torr, NV: needle valve, N2: N2-gas vessel (200 atm.), PV: precision valve, R: 3He-reservoir, RP: rotation pump (cap: 500 1/h), SC: superconducting magnet (7 T), SS: sample space, ST: 3He storage tank, SV: safety valve, TC: thermocouple gauge, TL: copper thermal link to 3He-bath, TS: top-flange thermal shield (1 K), TT: transfer tube (inner section), VC: vacuum can (4.2 K), WP: Welch-pump.

Table 2.1 : The vapour pressure P of ^4He and ^3He.

T	P(^4He)	P(^3He)
K	mm Hg	mm Hg
1	0.12	8.6
0.6	2.8×10^{-4}	0.50
0.3	$3. \times 10^{-10}$	1.5×10^{-3}

Table 2.2 : The heat capacity C of Copper, ^4He and ^3He.

T	C(Cu)	C(^4He)	C(^3He)
K	erg/cm^{3}K	erg/cm^{3}K	erg/cm^{3}K
1	1.2×10^2	1.2×10^5	1.2×10^6
0.5	$6. \times 10$	3.7×10^3	1.0×10^6

The cryostat consists of three sections,which fit concentrically into each other,i.e.

i) the liq.N_2- and liq.^{4}He-dewar (Oxford Instruments,type SMD 8)

ii) the home-made metallic heatshield and support for the SC-magnet (only the magnet is shown in Fig.2.1)

iii) the home-made insert,comprising the vacuum chamber and the ^{3}He-system.

The cooling procedure involves the following steps :

i) After precooling with liq.N_2 and filling the dewar with liq.^{4}He,using ^{4}He-gas as an exchange medium,the sample in the vacuum can (VC) is cooled down to 4.2 K.

ii) The exchange gas is pumped out, and from the ^{4}He-bath (LHe) liquid helium is sucked into an auxillary ^{4}He-pot (HP) by means of a needle valve (NV). By pumping on the pot the temperature is lowered down to 1 K. The ^{4}He-level in the pot is monitored by means of a Speer carbon thermometer,glued to the pot : when all the helium in the pot has been evaporated,the temperature rises and this could be immediately detected by the subsequent decrease of the thermometer resistance.

iii) The ^{3}He storage-vessel (ST) is opened and the ^{3}He-gas brought into the system. A stainless steel capillary tube (C) of the ^{3}He-system has been wound around the the ^{4}He-pot and hard-soldered onto it,

to obtain as good a thermal contact as possible. When flowing past the ^{4}He-pot, the ^{3}He-gas condenses (boil.pnt. ^{3}He: 3.19 K) and trickles into the ^{3}He-can (He3). By pumping on the ^{3}He-can, the temperature can be subsequently reduced down to about 0.3 K. After all the liq. ^{3}He has been evaporated, the resulting ^{3}He-gas can be recondensed and used for cooling again.

The level of the ^{4}He-bath is monitored by means of four level indicators (NTC-resistors) : the first about 1 cm above the bottom of the ^{4}He-can, the second 3 cm above the top of the superconducting magnet, the third approximately 2 cm above the vacuum pot and the fourth roughly 5 cm above the third. At the fourth level, the dewar contains about 7 liter helium, of which 4 liter are above the second level. To reach the fourth level, approximately 16 liter helium are needed, the excess of which serves mainly to cool the SC-magnet to 4.2 K.

Measurements with field can only be performed down to the second level, as a further reduction of the ^{4}He-level will bare the top of the SC-magnet, which causes the magnet to trip. Without any special precautions the evaporation rate of the helium was measured to be 2 liter/hour. By filling the space of the upper half of the dewar with Styrofoam plugs, the evaporation rate could be reduced to 0.15 liter/hour. With the SC-magnet in use, the effective measuring time from after filling until the helium has been evaporated down to

the second level,is approximately 10 hours.

2.2 The Superconducting Magnet.

The SC-magnet (Oxford Instruments) consists of NbTi-wire,with a maximum field of 7 tesla at 31.14 A, i.e. 0.225 T/A.Its homogeneity is calculated to be better than 1 % over a 2.5 cm diameter spherical volume.As a precaution,however,the field was never allowed to exceed 6.5 T.
The magnet is energized by a 40 A stabilized power supply (Oxford Instruments,type A) with current stability 1 : 10^4 of set current.The sweeptime to full field-strength is about 30 minutes.To avoid heat leaks and reduce evaporation the magnet is kept in a persistent mode during measurements.

2.3 Sample Space and Leads.

The net volume in the tail of the vacuum can, available for the sample is about 75 cm^3,and is enclosed in a 1 mm thick,brass heatshield.The topflange of this shield is hard-soldered onto the ^{4}He-pot,which is always at a constant temperature of about 1 K during the measurements.
Fig.2.2 shows the sample space on scale.

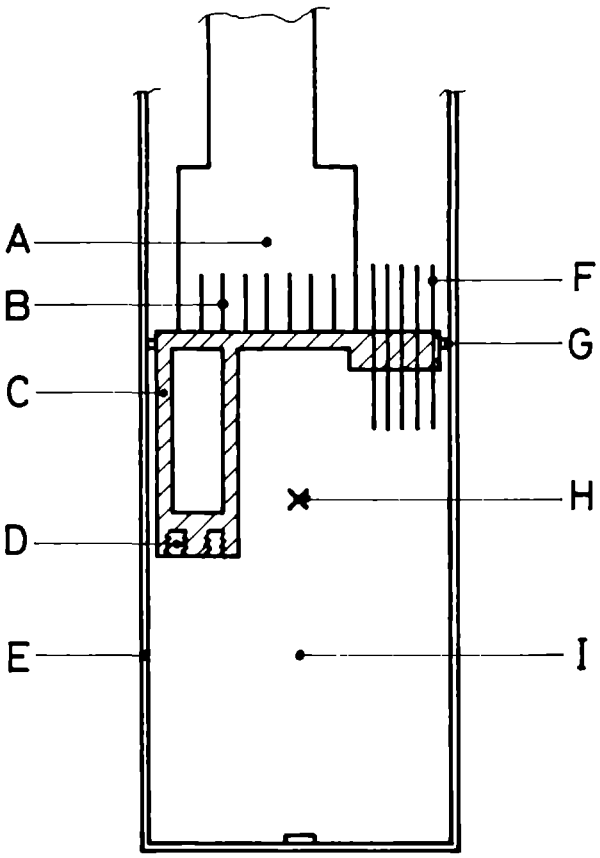

Fig.2.2 : Sample space (scale 1:1)

A: 3He-can,B: copperfoil spiral,C: copper thermal link to 3He-bath (0.3 K),D: screw holes for sample holder, E: brass thermal shield (1 K),F: copper thermal anchors, G: teflon spacer,H: center of magnetic field,I: sample space.

The sample holder can be screwed onto a hollow copper can, the top of which partly serves as the bottom of the ^{3}He-pot. This bottom is furnished with a copper foil spiral, to provide better heat contact with the ^{3}He-liquid. Inside the hollow copper can a cogwheel system has been mounted which, in combination with a specially constructed sample holder, could rotate the sample with respect to the magnetic field.

The top of the copper can is equipped with electrically insulated, copper thermal anchors for the leads of the sample, in order to keep these leads at the same temperature as that of the ^{3}He-bath. Before being let out of the vacuum can, these leads are anchored at the top of the 1 K heatshield and at the topflange of the 4.2 K vacuum pot. In this way, however, no continuous leads from sample to measuring apparatus, in order to minimize thermopower effects, could be used, as the leads have to be ruptured and soldered to the anchors, at least at the topflange of the vacuum pot. When uninterrupted leads are needed, we have used the stainless steel tube of the pumping system (Fig. 2.1) as an inlet into the vacuum can. At the topflange of the dewar, this tube is furnished with a vacuumtight plug, through which the leads can be let out.

From the topflange of the dewar to the topflange of the vacuum can all leads consist of 0.1 mm diameter electrically insulated copper wires. Inside the vacuum can, in order to minimize heat leaks, the sensing leads

(voltage,thermometers) consist of 0.1 mm diameter,manganine wires,while the leads through which the electrical currents are passed (heaters) consist of coppercoated superconducting NbTi (T_c=18 K) wires.To prevent still further the leakage of heat,the coppercoating is etched away over a range of approximately 2 cm,just before those spots where the wires are anchored.
Outside the dewar,all connections consist of shielded wires.

All the leads emanating from the Blue Monster are gathered into a terminal box and the connections to the measuring apparatus made via appropriate plugs at the front panel.This way,necessary changes in the connections can be made easily and rapidly,while at the same time a clear surveyability is maintained.

2.4 Temperature Measurement and Thermometers.

For the measurement of the thermal conductivity a method is employed,whereby in essence only one precision thermometer is used,in contrast to the more common technique,which consists of the use of two calibrated thermometers.In the latter method,slight errors or changes in one or both of the calibrations,can result in large errors in the temperature difference ΔT between the thermometers.When ΔT is small,large errors in the value of the thermal conductivity λ,as calcula-

ted from the measurements, are induced.

Let A (hot end) and B (cold end) be two points of the sample (Fig.2.3) between which the thermal conductivity is to be measured. To these points are attached the thermometers R_A and R_B and the heaters H_A and H_B, respectively. The cold end B is connected to the cooling system and provided with an extra stabilizing heater H_S. During a measurement, the power to the heaters H_B and H_S is continuously adjusted to keep point B at a constant temperature T_B as determined by the thermometer R_B. This control may be either electronic and automatic, or manual.

The measuring procedure involves the following steps :

i) The temperature control is set at the required fixed temperature T_B, while no heatflux is applied at the hot end (Q=0). Hence, when thermal equilibrium is reached, $T_A = T_B$.

ii) An electrically measured thermal heatflux $\dot{Q}$ is then applied at point A by means of H_A. By adjusting H_B and H_S the temperature is brought back to T_B. At thermal equilibrium, the temperature at point A is now T'_A, and the thermal conductivity λ is obtained by

$$\lambda = \frac{L}{A} \frac{\dot{Q}}{T'_A - T_A} \qquad (2.1)$$

where L is the distance between A and B and A is the cross-sectional area. The ratio L/A is called the geometry factor.

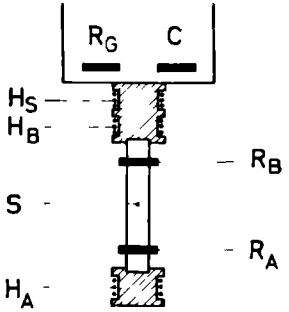

Fig.2.3 : Thermometer and Heater Arrangement (schematic)

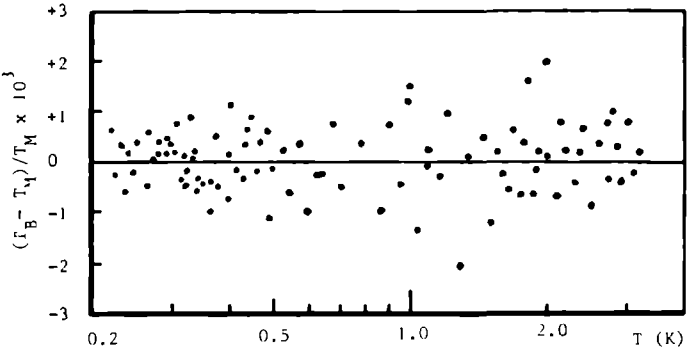

Fig.2.4 : Deviation plot for the Germanium Thermometer.

T_M is the temperature as given by Eq.(2.2) and the Cryocal data, T_B is the temperature as obtained from Eq.(2.4) with m= 11.

iii) To compensate for thermal drift,one mostly returns once again to the situation of i),and T_A is taken as the average of the two obtained values.

For the thermometers R_A and R_B semiconducting carbon resistors are used.For a large temperature range, one single thermometer will generally not suffice and to maintain sufficient temperature resolution we have used two thermometers,i.e. both for R_A and R_B a 10 Ω 1/10 W, and a 220 Ω 1/10 W (Allen Bradley) carbon resistor.

The carbon resistors are usually covered by an insulating mantle.To enhance heat contact and reduce the thermal relaxation time,part of the mantle was grinded away until the carbon was laid bare.This was done in a controlled way,and during grinding the resistance was constantly monitored so that for R_A and R_B pairs of resistors were obtained of the same room temperature resistance and with the same temperature characteristics. After grinding,the carbon was electrically insulated again by a thin layer of GE 7031 varnish.

One drawback of carbon thermometers is an instability on thermal cycling,probably due to change in orientation of some graphite particles.In contrast,a germanium thermometer,which consists of one single crystal,is completely reproducible.The commercially available Ge-resistor (Cryocal,S/N 2667) we have used, was only calibrated from 40 K down to 1.5 K.We have

extended the calibration down to 0.22 K (Fig.2.4) by calibrating the Ge-thermometer against a large single crystal of the paramagnetic salt cerium magnesium nitrate (CMN),by means of susceptibility measurements in a dilution refrigerator.In magnetic thermometers the measured temperature may deviate from the true, thermodynamic temperature T at very low temperatures, i.e. when the interaction energy between the paramagnetic spins becomes comparable with $k_B T$,but for CMN the Curie-Weiss law

$$\chi = C/(T - \theta) \qquad (2.2)$$

(χ is the susceptibility,C and θ are constants) is ideally followed down to 6 mK.

All thermometers which depend on electron transport properties,e.g. the semiconducting carbon and germanium resistors,are susceptible to the influence of a magnetic field,the Ge-thermometer far more so than the carbon thermometer.

However,recently Lawless and collaborators (4-10) have developed a glass-ceramic capacitance thermometer,produced by controlled crystallisation of the peroskite $SrTiO_3$ in an alumino-silicate glass matrix.Its dielectric constant is strongly temperature dependent but remains indifferent to intense magnetic fields.Hence, for our experiments in a magnetic field we have used a glass-ceramic capacitance thermometer (Lake Shore, CS-400 GR) as a reference thermometer.A disadvantage

of this type of temperature sensor,however,is an aging effect (10): a drift in the capacitance occurs under isothermal conditions,necessitating relatively long waiting periods before each measurement for the temperature to stabilize.

To summarize,the temperature sensing system of the Blue Monster contains the following thermometers (Fig.2.3) :

i) Two AB carbon resistors R_A and R_B of about the same thermal characteristics,connected to the sample: a'cold end'and a'hot end'thermometer.
The cold end thermometer R_B serves as a temperature sensor for the temperature regulator,which by means of the heaters H_B or H_S keeps the sample at the required constant temperature.
The hot end thermometer R_A serves to measure the temperature difference due to the alternative presence and absence of a thermal current.

ii) One germanium-resistor R_G connected to the cold end part of the sample holder and which serves as a primary reference thermometer.

iii) One glass-ceramic capacitance thermometer C,also connected to the cold end part of the sample holder,and which serves as a secondary reference thermometer in the presence of a magnetic field.

The measuring procedure at each run involves the following steps :

i) At the start,the two carbon resistors,connected

to the sample,and the capacitance thermometer,are accurately calibrated against the germanium resistor.The calibration should occur before the SC-magnet has been switched on,as switching off the magnet does not reduce the field to zero but due to trapped flux a residual field of about 500 gauss remains.At this stage also the zero field measurements of the thermal conductivity are started.

ii) As soon as possible the calibration results are computerally processed,and graphs are constructed of the resistance R and the sensitivity $S = (R/T)(dT/dR)$ as a function of temperature T, especially for the hot end carbon thermometer (Fig.2.5).These graphs allows for a rapid calculation of λ from the measured R- and ΔR-values :

$$\lambda = \frac{L}{A}\frac{R}{T}\left(\frac{I \times V}{\Delta R}\right) S \qquad (2.3)$$

where L/A is the geometry factor,I the current, V the voltage and $\dot{Q} = I \times V$ the heatflux of the hot end heater.This way, λ can be continuously monitored during the experiment and a deviative behaviour more closely scrutinized and corrected for immediately,considerably enhancing the reliability of the measurements.The computations of λ with the help of a computer occurs only after all the measurements have been completed.

iii) For the λ-measurements at non-zero fieldstrengths

the field-independent capacitance thermometer now serves to measure the temperature; the carbon resistor R_A serves only to measure the temperature difference.

When the measurements involve a field dependent behaviour of λ at a constant temperature, a different procedure is followed to evade the long waiting periods, necessitated by the thermal drift of the capacitance thermometer : at each required constant temperature, a rapid sweep of the field was made from zero to 6.5 T and the magnetoresistance of R_A and R_B was measured. At the actual measurement of λ, this magnetoresistance can be taken into account and R_B, which is connected to the temperature regulator, set to the appropriate value at each different field.

iv) When the measurements have to be terminated temporarily, the temperature is not allowed to reach room temperature, but is kept at the temperature of liquid nitrogen (77 K), this to avoid an all too drastic change in the thermal characteristics of the carbon thermometers. Recalibration after a return to liq. helium temperatures proved that the changes were indeed small (less than 1 %) and that the shape of the R-T curves remained the same, i.e. the consequence of a thermal cycling to liq. nitrogen temperatures amounts but to a systematic shift of the whole R-T curve to slightly

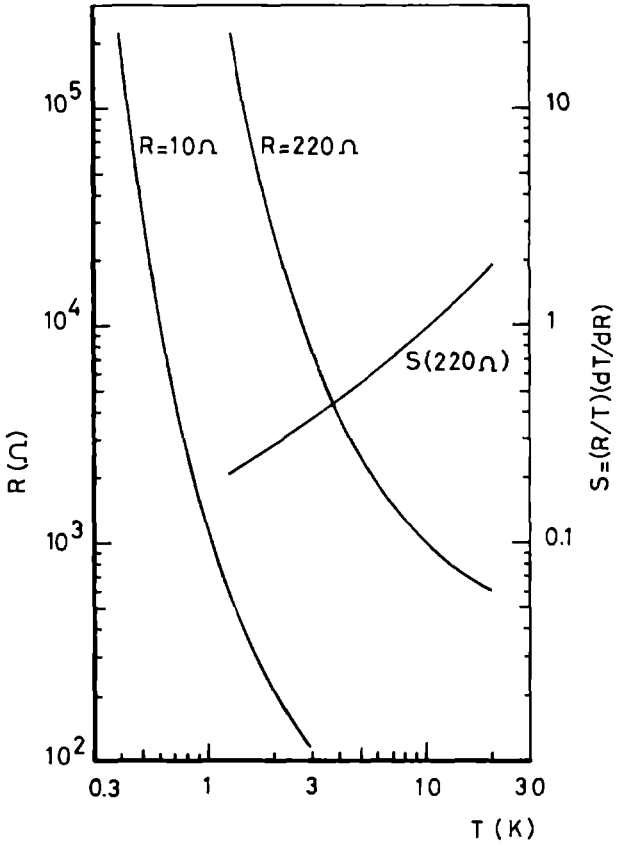

Fig.2.4 : Resistance and Sensitivity curves as a function of temperature for 10 Ω and 220 Ω Allen-Bradley carbon resistors.The temperature is obtained from a computer fit,using Eq.(2.5)

higher values of R.Hence,recalibration can be restricted to about 5 or 10 points of the whole temperature range.

2.5 Calibration.

i) Germanium resistor.

The employed Ge-resistor (Cryocal) was commercially calibrated only down to 1.5 K.We have extended the calibration down to 0.22 K,starting from about 3 K and using a magnetic thermometer (CMN-salt) for reference. The calibration data were computerally fitted to the 'brute force' equation (11)

$$\ln R = \sum_{n=0}^{m} A_n (\ln T)^n \qquad (2.4)$$

using the principle of least squares.From 1.5 K to 3 K the 'Cryocal'-data from the commercial calibration were included,and the total data of the range between 0.22 K and 3 K amounted to about 92 points.Fits of different order of m (from 6 to 14) were generated, and the best results were obtained for m = 11 (Fig.2.4).Consequently,as an interpolation formula,a polynomial of order m = 11 was used.

ii) Carbon resistors.

For the carbon resistors,the measured R- and T-

values were fitted according to the formula (12)

$$\frac{1}{T} = \sum_{i=0}^{j} a_i (\ln R)^i \qquad (2.5)$$

with j = 8 providing the best results.The T-values were obtained by means of the germanium thermometer.
The same program used for the computer fit generates also values for the sensitivity S (Fig.2.5),i.e.

$$S = \frac{R}{T} \left(\frac{dT}{dR}\right) \qquad (2.6)$$

All the computations were performed on the IBM 370/158 computer at the Computer Center of the University of Nijmegen,housed at the Faculty of Science.

iii) Capacitance Thermometer.

The results of the capacitance thermometer were not fitted to an interpolation formula (8) but were plotted graphically as a function of T.

2.6 Measuring and Control System.

Fig.2.6 shows a block diagram of the measuring and electronic control system.The thermal conductivity was obtained by measuring a temperature difference at a constant temperature by means of the carbon thermometer R_A at the hot end of the sample,as explained in subsection 2.5.

The resistance of R_A was measured with a home-made ac Wheatstone bridge, coupled to a phase sensitive detector for detection. For the variable reference resistance, 5-decade ESI Dekaboxes, with ranges $1-10^6\ \Omega$ for the low temperature, and $0.1-10^5\ \Omega$ for the high temperature region with an accuracy of $1:10^4$, were used. The accuracy of the bridge was estimated at 0.02 %, permitting temperature measurements with an accuracy better than 1 mK. At intermediate and high temperatures, however, the accuracy is limited by the lowest ranges of the Dekaboxes.

The current through the hot end heater H_A was generated by a voltage/current calibrator (John Fluke, type 382A) capable of producing a calibrated dc current between 0 and 2 A, with a stability of 0.0025 % and a ripple less than 0.002 % of range RMS.

The voltage over the heater H_A was measured by means of a digital voltmeter (Solatron, type LM 1480.3) with an accuracy of 0.008 % of reading ± 10 μV.

At the cold end R_B is connected to the temperature regulator for the temperature control. The temperature regulator was home-made, based on a design by Ries and Moore (13) and also described by M A Weenen (14). The bridge circuit is a guarded conductance bridge with a toroidal transformer. By winding the two primary windings together in a bifilar manner, it was possible to insure to high precision that the two windings had identical effect on the transformer core. Hence, the

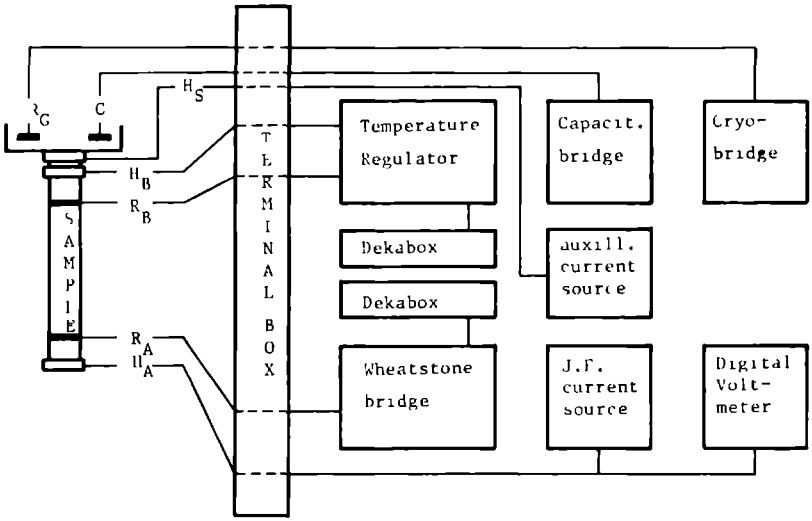

Fig.2.6 : Block diagram of the Measuring and Control System.

accuracy was inherently high because the balance of the ratio arms is created by geometric symmetry and is not affected by temperature fluctuations within the bridge circuit.The accuracy was measured to be $\Delta R/R=10^{-5}$
As the bridge reference element an external precision decade resistor (ESI Dekabox) was used.Temperature regulation could be executed automatically as well as manually.The controller circuit provides both linear proportional regulation,to compensate fast thermal fluctuations,and integral regulation, to compensate for drift in the temperature;the temperature can be controlled to better than 5×10^{-6} K.
A temperature change can be achieved by simply adjusting the setting of the Dekabox reference resistor to the appropriate value and if this temperature change is not too large to require readjustment of the cooling rate,stable temperature control can be attained in about 10 to 15 seconds.
Extra heating power can be produced by connecting H_S to an auxillary,manually operated current source.

The resistance of the germanium thermometer was measured with a commercial automatic digital potentiometer (ASL Cryobridge) of unusual precision (15).
The measuring principle consists of balancing the voltage over the unknown resistor R_X and the reference resistor R_1 to the voltage over parts n_1 and n_2 of the secondary windings of the transformer. At balance, $R_X=(n_2/n_1)R_1$ or,by choosing n_1 conveniently,$R_X=n_2R_1$.

The accuracy is 0.002 % of full scale in the range 10-$10^4\Omega$, better than 0.01 % in the range 10^4-$10^6\Omega$, unaffected by ambient temperature changes and thermal e.m. fs. (lead errors) and free of drift.
The reason that such high precision can be achieved is the exceptional accuracy and stability of the transformers. Sensitivity approaches the theoretically possible, being limited by the Johnson noise in the resistors only. The operation is completely automatic with a digital reading of the resistance and a six-decade resolution. Balancing occurs within seconds.

The capacitance thermometer was measured with a capacitance bridge (General Radio, type 1615-A) in combination with an audio-oscillator (General Radio, type 1311-A) as a generator, and a two-phase sensitive phase locked integrating voltmeter (ASL, model 110) as a null-detector with a sensitivity of typically 10 nV to 1 V f.s.d. depending on gain control setting.
When used to keep the temperature at a constant value, e.g. in the presence of a magnetic field, a deviation could be returned to the original value by manually operating the temperature regulator and employing the capacitance thermometer as a temperature null-detector.

References

1) O V Lounasmaa,"Experimental Principles and Methods below 1 K" (Academic Press,New York,1974)

2) R R Conte,"Eléments de Cryogénie"(Masson et Cie, Paris,1972)

3) D S Betts,"Refrigeration and Thermometry below One Kelvin" (Sussex University Press,Sussex,1976)

4) W N Lawless,Rev.Sci.Instr. 42(1971)561

5) W N Lawless,R Radebaugh,R J Soulen,Rev.Sci.Instr. 42(1971)567

6) L G Rubin,W N Lawless,Rev.Sci.Instr.42(1971)571

7) W N Lawless in "Temperature,its Measurement and Control in Science and Industry,(ed.H H Plumb, Instrument Society of America,Pittsburgh,1972) vol.4,p.1143

8) W N Lawless,E A Panchyk,Cryogenics 12(1972)196

9) D Bakalyar,R Swinehart,W Weyhmann,W N Lawless, Rev.Sci.Instr. 43(1972)1221

10) W N Lawless,Rev.Sci.Instr.46(1975)625

11) J S Blakemore,J Winstel,R V Edwards,Rev.Sci.Instr. 41(1970)835

12) A C Anderson in "Temperature,its Measurement and Control in Science and Industry"(ed.H H Plumb, Instrument Society of America,Pittsburgh,1972) vol.4,part 2,p.773

13) R P Ries,B K Moore,Rev.Sci.Instr.41(1970)996

14) M A Weenen,"Thermal Processes in He-II",doctoraal thesis Cath.Univ.Nijmegen,1972 (unpublished)

15) P C F Wolfendale,J.Sci.Instrum.(J.Phys:E) 2(1969)659

3. MAGNON AND PARAMAGNON THERMAL CONDUCTIVITY IN TWO-DIMENSIONAL MAGNETIC SYSTEMS

3.1 Introduction.

Nearly all the heat transport in solids are executed by electrons and phonons and although a host of other quasiparticles exist,none of them have been found to contribute positively to the actual transfer of thermal energy. Indeed,the presence of other quasiparticles provide but added scattering mechanisms for the electrons and phonons,leading to a decrease rather than an increase of the thermal conductivity.
At low temperatures the only known exception to this rule are formed by magnons.
What is a magnon ?
If in a ferromagnet the groundstate,with all the spins parallel,is perturbed by a spinreversal,this perturbation will not stay confined to one local spin.Owing to the exchange interaction between the magnetic ions,the perturbation will be spread out over all the spins of the crystal.The propagations of the perturbation through the spins of the crystal have a wavelike form and are called spinwaves or,when quantized,magnons.

Suggestions for the energy transport by spinwaves could be found as early as 1936 (1).It was Sato (2), however,who first developed a theory of heat conduction

by spinwaves and pointed out the experimental conditions by which these predictions could be tested. Since then, evidence of magnon heat conduction was indeed observed in several magnetic materials, e.g. in the ferrimagnetic yttrium iron garnets (YIG) (3,4,5,10) the ferromagnetic EuS (6) and EuO (59), the anti-ferromagnetic $GdVO_4$ (11), as well as in the metallic transition alloys ferromagnets $Ni_{81}Fe$ (12), $Ni_{70}Fe$ (12) and $Fe_{68}Co$ (13).

In this chapter we shall report on thermal conductivity measurements of the two-dimensional (2d), $S=\frac{1}{2}$ Heisenberg ferromagnets $(CH_3NH_3)_2CuCl_4$ and $(C_2H_5NH_3)_2CuCl_4$. The thermal conductivity of these magnetic compounds were measured as a function of temperature over the range 1 K to 25 K and as a function of magnetic field from zero to 6.5 tesla. The magnon contribution to the heat transport in these crystals was found to be the highest ever observed as yet, i.e. between 75 % and 90 %.

For fields above 4.5 T and temperatures below T_c, the magnon conductivity is quenched and the lattice conductivity is obtained. An estimate is given of the magnon and phonon mean free path and of the dislocation density of the crystals.

Not only do these compounds constitute a 2d magnetic system, but the temperature dependence of the lattice conductivity indicates, that the acoustical phonon system is two-dimensional as well. This corroborates the

results previously obtained in this laboratory by means of far infrared measurements,which show that in these compounds the optical phonon system is two-dimensional. In the paramagnetic region,i.e. for temperatures above T_c in zero field,we have found that a large magnetic contribution to the heat transport is still present in the $(CH_3NH_3)_2CuCl_4$-crystal.
This is the first time that the thermal conductivity by paramagnetic magnon modes or paramagnons has been measured.

Previous measurements of the thermal conductivity of these compounds have been done by Miedema and collaborators at the University of Amsterdam (14,15,16) Preliminary results of our measurements have been published in refs.(17,18,78).

In the following section 3.2 we shall describe the physical properties of the 2d Heisenberg ferromagnets.In section 3.3 a discussion is given of the Sato model and an expression is derived for the magnon thermal conductivity in a 2d spinsystem.In the last section 3.4 our experimental results are presented and discussed

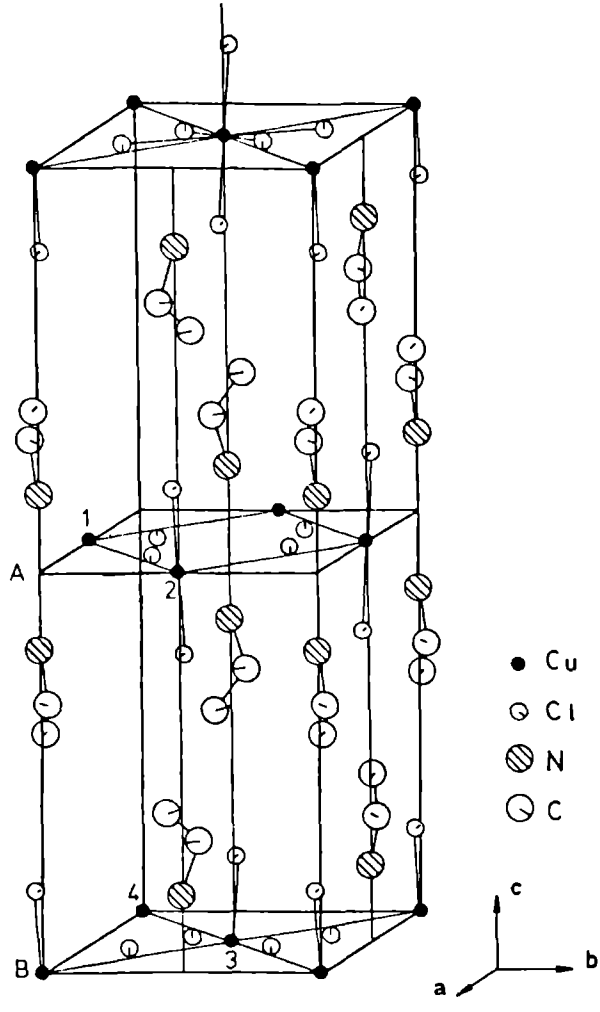

Fig.3.1 : Unit cell of $(C_2H_5NH_3)_2CuCl_4$
The numbers 1 to 4 refer to the four types of copper sites, A and B refer to the two magnetic sublattices.For the sake of clarity the hydrogen atoms are not shown.(After ref.(20))

3.2 Two-dimensional Heisenberg Magnetic Systems.

The alkylammoniummetalhalogenides $(C_nH_{2n+1})_2MX_4$ (abbreviation: C_nMX), with n= 1,2,3,4,5,6,10,15,18; M= Cu(ferromagnetic),Fe,Mn(anti-ferromagnetic),Cd,Pd (diamagnetic); X= Br,Cl, exhibit several striking structural characteristics,which reflect themselves in many interesting magnetic,dielectric and transport properties.

These compounds consist of sheets in which the doubly positively charged metal ions M^{2+} are arranged in a nearly quadratic configuration.These sheets are widely separated by a double layer of the alkylammonium $(C_nH_{2n+1}NH_3)$-chains.Fig.3.1 shows the crystalstructure of the $(C_2H_5NH_3)_2CuCl_4$ compound (19,20).
For the magnetic compounds (M= Cu,Mn,Fe),the magnetic interaction between the metal-ions within one sheet is far stronger - because of their closer proximity - than the interaction between the ions from different sheets. As such,these crystals form a nearly ideal approximation to a two-dimensional Heisenberg magnet and have become model systems to study two-dimensional magnetic phenomena.

Physics in lower dimensions is highly interesting in itself (19-22).Calculations are often simplified when the dimensionality is lowered and exact solutions of several one- and two-dimensional models can be obtained.Furthermore,certain minor aspects of thermodynamic quantities bloom into salient features at lower

dimensions.For instance,long wavelength fluctuations, which tend to be of low energy because of their slow spatial variation,play an increasingly important role with decreasing dimensionality of a system.

Two-dimensional isotropic Heisenberg magnetic systems derive an added interest from the fact,that according to theory (23) no spontaneous magnetization for non-zero temperatures can occur,in contrast to the anisotropic case,where the exact solution of the $S=\frac{1}{2}$ Ising-model presents an example of a second order phase transition (24).

Although theoretically no long range order exist in a 2d Heisenberg system at temperatures other than zero,a so-called Stanley-Kaplan (SK) phase transition (25) does seem to occur at non-zero temperatures.This transition connects the high temperature paramagnetic state with a low temperature state without long range order, but with divergent susceptibility.

The question then remains,whether or not it is possible to have a non-zero transition temperature,characterized by a divergence of the susceptibility,yet below which no spontaneous magnetization exists.

From an experimental point of view the problem is compounded by the fact that in realistic cases the slightest deviations from the pure two-dimensional system (anisotropies,three-dimensional interlayer interactions,finite size of the crystal,crystal imperfections, etc.) have proved by themselves sufficient,to induce

long range order at temperatures equal or even higher than the SK-transition temperature of the ideal case (26). Thus, in all practical cases encountered, the transition at T_{SK} (defined as the temperature at which the susceptibility reaches infinity) has been from the paramagnetic state to a state with ordinary long range order. As yet, no unambigous example of a pure 2d Heisenberg magnet which exhibit an SK-transition has been found.

The very extensive investigations of Miedema and collaborators at the University of Amsterdam have done much to clarify many aspects of the questions at issue (for a review, see e.g. refs.(19,20)).
In a series of beautiful experiments they have varied the structural properties of these crystals in a systematic and controlled way. These feats of 'molecular engineering' have been performed by

i) varying the interlayer distance by changing the number of carbon atoms in the $(C_nH_{2n+1}NH_3)$-chain. In this way, for instance, the separation between Cu^{2+}-ions from neighbouring layers can be varied from 9.97 Å (n=1) to 25.8 Å (n=10), resulting in a variation of the interlayer distance from 2 to 5 times the Cu-Cu distance within a layer, which itself remains unaffected.
This technique allows one to study various properties as a function of the interlayer distance and to extrapolate to the ideal 2d system.

ii) complete or partial substitution of the protons

Table 3.1 : Parameters of C_1CuCl and C_2CuCl (After refs.(19,20))

Parameter	C_1CuCl	C_2CuCl
a_o (Å)	7.535	7.47
b_o (Å)	7.3	7.35
c_o (Å)	18.6	21.2
M	269.5	297.5
T_c (K)	8.895	10.20
J/k_B	19.2	18.6
R= J'/J	5.5×10^{-4}	8.5×10^{-4}

by deuterons in the alkylammonium-chain.
This gives added information about the lattice properties.

iii) substitution of the magnetic ions (Cu,Mn,Fe) by diamagnetic ions (Cd,Pd).
A comparison of the magnetic crystals with their diamagnetic counterparts allows one to isolate the magnetic from the lattice properties.

iv) substitution of Cl or Br,alternatively.
This influences the interlayer anisotropy.

The structural properties in the paramagnetic phase of these compounds have received enhanced attention recently,because of their analogy to smectic liquid crystals and membrane structures.By measuring the dielectric properties,first and second order phase transitions have been found between monoclinic,tetragonal and orthorombic modifications of these crystals (27,37), connected to the ordening of the alkylammonium-group. As n is enlarged,the number of structural phase transitions grows,due to the increasing degree of freedom of the alkyl-chains,and a complex polymorphic pattern results.

The magnetic and crystallographic properties of these compounds have been investigated by means of susceptibility (28),specific heat (29,30,31),magnetic torque (32),ESR (33,34),NMR (83),NQR (35,82),neutron diffraction (27,36,37),röntgen diffraction (27,38), optical birefringence (27),magneto-optical (40,41), faraday-rotation (39,79),far infrared (42,43,44),di-

electric constant (45), thermogravimetric (46) and differential thermal analysis (38,46) measurements.
The transport properties at low temperatures have been studied by means of thermal conductivity (14-18) measurements and shall be discussed in the subsequent sections of this chapter.
For methylammoniumcopperchloride $(CH_3NH_3)_2CuCl_4$ and ethylammoniumcopperchloride $(C_2H_5NH_3)_2CuCl_4$, henceforth abbreviated to C_1CuCl and C_2CuCl, respectively, the relevant physical data are summarized in Table 3.1.

3.3 Theoretical Background.

3.3.1 The Sato-model of Magnon Thermal Conduction.

Sato (2) presented his theory of magnon heat conduction, using the following assumptions :

i) no phonon-magnon interaction
ii) no ferromagnetic anisotropy
iii) sufficiently low temperatures so that the phonon and magnon mean free paths become boundary limited only, hence temperature independent and of equal magnitude.

These assumptions effectuate a complete separation of the spinwave and lattice vibrational wave systems, with the magnons and phonons as independent carriers of the thermal energy. Consequently, one can write the total heat conductivity λ_{tot} as the sum of the magnon con-

ductivity λ_s and the phonon conductivity λ_{ph}, i.e.

$$\lambda_{tot} = \lambda_s + \lambda_{ph} \qquad (3.1)$$

At low temperatures, with only boundary scattering present, λ_s and λ_{ph} can be calculated, using the well known kinetic formula

$$\lambda = \frac{1}{3} C l v \qquad (3.2)$$

where C is the specific heat per unit volume, l the average mean free path, v the average group velocity of the respective heat carriers.

For a 3d Heisenberg ferromagnetic spinwave system the magnon heat capacity $C_s \propto T^{3/2}$, the magnon mean free path l_s is constant and, using the quadratic dispersion relation, the magnon group velocity $v_s \propto T^{1/2}$.
Hence, the thermal conductivity by magnons is proportional to T^2, i.e. $\lambda_s \propto T^2$.

For the lattice wave system, the heat capacity per unit volume $C_{ph} \propto T^3$, the phonon mean free path l_{ph} is again constant, while the phonon group velocity v_{ph} is equal to the velocity of sound and a constant also. Consequently, one finds a T^3 temperature dependence for the phonon thermal conductivity, i.e. $\lambda_{ph} \propto T^3$.
At sufficiently low temperatures λ_s compares favourably with λ_{ph}. By measuring the total conductivity

$$\lambda_{tot} = \alpha T^2 + \beta T^3 \qquad (3.3)$$

as a function of temperature and plotting λ_{tot}/T^2 versus T, the possible presence of magnon thermal conduct-

ivity can thus be detected.

Some comments are appropriate here.

i) The measurement of magnon thermal conduction always involves a certain amount of magnon-phonon interaction(47).The experimental technique consists of attaching a heater at one end of the crystal and measuring the temperature gradient produced by the heat current.Since heaters generate phonons only,the heat cannot get into the magnon system unless a certain degree of interaction between the magnon and the phonon system exists.This interaction must be neither too strong,nor too weak.A too strong magnon-phonon interaction reduces both the magnon and phonon mean free paths and the net experimental result is a decrease in the thermal conductivity.On the other hand,if the magnon-phonon interaction is too weak,no heat can leak into the magnon system and a thermal conductivity experiment will reveal the phonon conductivity only.

Indeed,as Akhiezer (48) has first shown,a magnon-phonon interaction is always present in a magnetic system,because,whereas the exchange interactions and dipolar couplings depend upon the interatomic spacings,the modulations of these interatomic distances by lattice vibrations induces a coupling between the phonons and the magnons.The magnetic dipolar and spin-orbit interactions are relativistic in origin and much weaker than the exchange interactions.But they are very important, as no statistical equilibrium could be established be-

tween an external heat source and the spin system without their presence.

ii) The same ubiquitous relativistic-magnetic interactions are also responsible for the fact,that in a ferromagnet a nonzero anisotropy field is always present.Due to this anisotropy field the actual magnon spectrum,even at zero external field,has always a gap at k=0. This leads to a reduction of the population of the magnon modes and an ensuing decrease of the magnon conductivity.

iii) The assumption of a mean free path,limited by boundary scattering only,is also difficult to realize in practiceBoth the magnons and phonons are scattered from impurities and crystal imperfections, while phonon-magnon interactions may also have a dampening effect.These influences are hard to estimate,however,because of computational difficulties and of our limited knowledge of these effects in real crystals.

iv) These deviations from the simple Sato-model may result in a far more complicated temperature dependence than the T^2- and T^3-behaviour of the magnon and phonon conductivity.Furthermore,as a consequence of the magnon-phonon interaction,one can no longer equate the total thermal conductivity to the sum of the magnon and phonon conductivities,as these two are not independent of each other.For these reasons it appears questionable if the presence of magnon conductivity can be unambiguously tested by simply measuring the thermal

conductivity as a function of temperature,as proposed by Sato.Even in the unlikely event that the simplifications of the model are reproduced in a given substance,the magnitude and the temperature dependence of the thermal conductivity would not provide unequivocal identification of the mechanisms involved.

3.3.2 Influence of the Magnetic Field.

As originally propounded by Douthett and Friedberg (49),an external magnetic field can be exploited to reduce the magnon conductivity in a predictable way and thereby to signal its presence.
If an external field is applied the spinwave energy spectrum is changed by a Zeeman-term $g\mu_B H$,i.e.

$$E(k) = Dk^2 + g\mu_B H$$

where D is a constant,g the spectroscopic splitting factor,μ_B is the Bohr magneton and H can be regarded the resultant of the external field and the anisotropy field.The resultant gap

$$E_g = g\mu_B H$$

at k=0, reduces the magnon conductivity roughly as

$$\lambda_s \propto \exp(-E_g/k_B T)$$

due to the decrease in the population of the magnon modes.However,a decrease in the measured thermal con-

ductivity in the presence of a magnetic field is by no means sufficient evidence for the existence of a sizable magnon conduction at zero field.

The presence of spinwaves can affect the thermal conductivity in two ways : either by contributing to the heat transport and increasing the conductivity,or by interfering with the phonon conductivity and decreasing the thermal flow.If a small field is applied,both effects can lead to a decrease of the thermal conductivity but when the latter effect predominates,the thermal conductivity,after an initial decrease,increases again and saturates at a value above the zero-field value.In that case,because of the relatively strong magnon-phonon interaction,the spinwaves serve mainly to scatter the phonons and no magnon conductivity will be apparent in zero field (50,51).

For an unambiguous determination of the presence of magnon conductivity

i) explicit account should be taken of the influence of the field-dependent spinwave modes on the thermal conductivity at intermediate fields

ii) sufficiently high fields should be applied until a real saturation of the spinsystem is achieved, to effectuate a complete quenching of the magnon conductivity.

Only when this last condition is fulfilled will a separation between magnon and phonon conductivity be possible.Typically,fields of 4 tesla and higher are needed

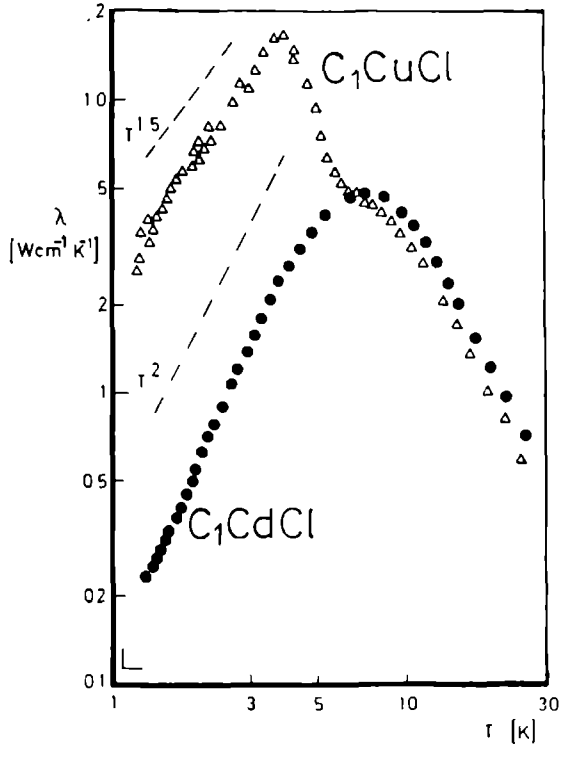

Fig.3.2 : The thermal conductivity of C_1CuCl as compared with that of the isomorphous, non-magnetic Cd-compound. The Cd-data are assumed to represent the lattice conductivity. Hence the surplus conductivity observed below T_c = 8.90 K of the Cu-compound can be attributed to the magnon conductivity. (After ref. (19))

for this purpose.

The above criteria for the detection of magnon conductivity are not met in the measurements on $Cu(NH_4)_2Br_4.2H_2O$ (7), $Cu(NH_4)_2Cl_4.2H_2O$ (8), and $CoCl_2(NH_2)_2CS_4$ (10), where fields of about 1 tesla only were employed. In fact, measurements by Dixon et al. (52, 60), using fields up to 4.8 T, proved that for instance $Cu(NH_4)_2Br_4.2H_2O$ and $Cu(NH_4)_2Cl_4.2H_2O$ do not have a measurable amount of heat conduction.
To be sure, only in the measurements of Douglass (5) on YIG, Martin and Dixon on EuO (59) and our measurements on $(CH_3NH_4)_2CuCl_4$ and $(C_2H_5NH_4)_2CuCl_4$ (17,18,78) are these criteria fully met and an absolute determination achieved of the magnon and phonon conductivities involved.

An ingenious method to separate the phonon from the magnon conductivity without the use of magnetic fields have been employed by Miedema and co-workers (14,15,16) in the thermal conductivity measurements of $(CH_3NH_4)_2CuCl_4$. To estimate the phonon conductivity, they use the thermal conductivity of the diamagnetic, isomorphous Cd-compound (Fig.3.2). Unfortunately, this method does not lend itself for a general application as it is essentially dependent on the existence of a diamagnetic isomorphous specimen. Furthermore, the thermal conductivity is highly sensitive to the crystalline purity and sample history. Therefore, the estimate of the lattice conductivity by the employment of isomorphous samples

cannot be considered as reliable as when applied,for instance,to the thermodynamic analysis of the specific heat (20).

3.3.3 Two-dimensional Magnon Thermal Conductivity.

The model,as proposed by Sato (2),provides but the bare framework for a theory of magnon conductivity, without the blur of modification and detail.It has the advantage,however,of keeping all the physically relevant mechanisms transparent and of making the theory of heat transport in ferromagnets more easily accessible mathematically. As for the restrictions to the model : what has been said for the three-dimensional case applies also,mutatis mutandis,to a two-dimensional system.

We shall now derive a formula for the magnon thermal conductivity,based mainly on the Sato-model,but adapted to the two-dimensional case.

Consider a two-dimensional isotropic square lattice of magnetic ions,with lattice constant a and periodic boundary conditions,applied to a square of side L. The 2d magnon conductivity $\lambda_s(2)$ can be obtained by generalizing the simple kinetic formula of Eq.(3.2),so that one considers a sum over all the possible spin-wave modes,i.e.

$$\begin{aligned} \lambda_s(2) &= \frac{1}{2} \sum_k C(k)v(k)l(k) \\ &= \frac{1}{2} \int C(k)v(k)l(k)g(k)d^2k \end{aligned} \qquad (3.4)$$

Here, $C(k)$ is the contribution of the k-mode spinwave to the specific heat, $v(k)$ and $l(k)$ are the k-dependent group velocity and magnon mean free path, respectively, and $g(k)=(L/2\pi)^2$ is the mode density, i.e. the number of modes in the surface element d^2k.

To evaluate the integral of Eq.(3.4), we make use of the Debye assumptions, which presuppose a continuous isotropic homogeneous system. To determine the number of allowed k-modes, these assumptions permit the replacement of the correct region of integration over the Brillouin zone by a circular region with an upperbound, corresponding to a cut-off wavevector k_{max}. This upper limit can be found by using the condition that the total number of modes must equal the number of degrees of freedom of the spinsystem, i.e.

$$\int g(k)\,dk=(\frac{L}{2\pi})^2\int_0^{2\pi}\int_0^{k_{max}} 2\pi k\,d\theta\,dk = N_s$$

where N_s is the number of spins in the area under consideration. Furthermore, we use the magnon dispersion relation in the low temperature ($T \ll T_c$), low k ($ka \ll 1$) approximation and assuming nearest neighbour interactions only, i.e.

$$\begin{aligned} E(k) &= Dk^2 + g\mu_B H \\ D &= 2JSa^2 \end{aligned} \qquad (3.6)$$

which has the same form as for a 3d cubic lattice. Here, D is the stiffness constant, J is the exchange con-

constant, S is the spin quantum number, g is the spectroscopic splitting or Landé factor, μ_B is the Bohr magneton and H is the local resultant field, composed of the internal anisotropy field and the external applied field.

Spinwaves obey Bose-Einstein statistics, and therefore the specific heat per magnon mode is

$$C(k) = \frac{\partial}{\partial T}\left(\frac{E}{\exp(E/k_BT)-1}\right) = k_B\left(\frac{E}{k_BT}\right)^2 \frac{\exp(E/k_BT)}{(\exp(E/k_BT)-1)^2} \tag{3.7}$$

where E is given by Eq.(3.6). The magnon group velocity is determined by Eq.(3.6) as well, i.e.

$$v(k) = \frac{1}{\hbar}\nabla_k E = \frac{2D}{\hbar}k \tag{3.8}$$

The magnon mean free path is assumed boundary limited only and hence a constant, independent of temperature

$$l(k) = l_s \tag{3.9}$$

Gathering our results and introducing the dimensionless variables

$$x = \frac{Dk^2}{k_BT}; \quad \delta = \frac{g\mu_B H}{k_BT}; \quad x + \delta = \frac{E}{k_BT} \tag{3.10}$$

we find from Eq.(3.4) for the 2d magnon conductivity (L = 1) :

$$\lambda_s(2) = \pi l_s \frac{k_B}{\hbar} \frac{(k_BT)^{3/2}}{D^{1/2}} \int_0^{x_{max}} (x+\delta)^2 \frac{e^{x+\delta}}{(e^{x+\delta}-1)^2} x^{1/2} dx$$

At low temperatures the upper limit may be extended to infinity, since in that case only the low k - modes

contribute significantly to the integral.

It should be realized,however,that an actual crystal is always three-dimensional and in the case considered,consists of two-dimensional layers stacked on top of each other.If c is the distance between two successive layers,1/c is the number of layers per unit length. Hence,the magnon conductivity for a layered system becomes

$$\lambda_s = \frac{1}{c}\,\lambda_s(2) \qquad (3.12)$$

$$= 2\pi\,\frac{1}{c\hbar D}\left(\frac{k_B T}{D}\right)^{1/2}\left(\frac{k_B T}{\hbar}\right)^{3/2}\int_0^\infty (x+\delta)^2\,\frac{e^{x+\delta}}{(e^{x+\delta}-1)^2}\,x^{1/2}dx$$

$$= \frac{1}{c\,\hbar\,D}\left(\frac{k_B T}{D}\right)^{1/2}\left(\frac{k_B T}{\hbar}\right)^{3/2}\sum_{n=1}^{\infty}\left(\frac{5}{2}\,\frac{\Gamma(5/2)}{n^{5/2}} + 3\,\frac{\Gamma(3/2)}{n^{3/2}}\,\delta + \right.$$

$$\left. + \frac{1}{2}\,\frac{\Gamma(1/2)}{n^{1/2}}\,\delta^2\right)\,e^{-n\delta}$$

where $\Gamma(x), x > 0$ is the Gamma-function

The principal approximations used in the derivation of Eq.(3.12) are the Debye assumptions,the quadratic magnon dispersion relation as given by Eq.(3.5),and the use of a constant magnon mean free path,restricted by boundary scattering only.

It is estimated that in the 3d case the Debye procedure as applied to magnons,is valid only for temperatures $T < 2T_c/3(S+1) \approx 0.1\ T_c$ (53).Furthermore,the quadratic magnon dispersion relation is also restricted to a temperature range of about an order of magnitude below T_c

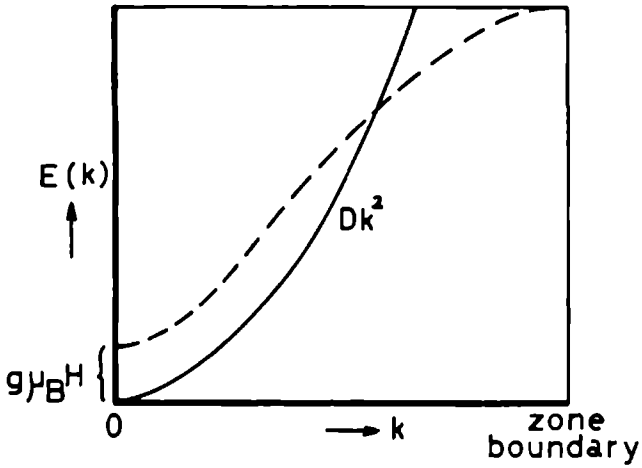

Fig.3.3 : Modification of the quadratic dispersion relation by the zone boundary and a field H (broken line.

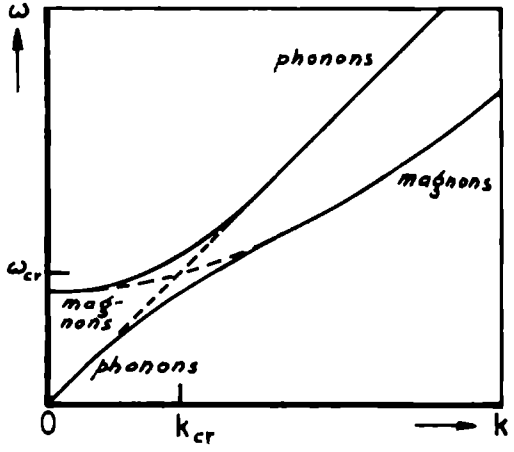

Fig.3.4 : Perturbation of the magnon and phonon dispersion relation due to resonant coupling.The unperturbed dispersion relations are indicated by dashed lines.

For k-values near the zone boundary,the dispersion relation is modified drastically (Fig.3.3).Also,only nearest neighbour interaction is considered and the variation of magnon energy with the angle of propagation,magnetic dipolar coupling and magnon-magnon interactions are neglected.Using the correct form of the dispersion relation and integrating over the Brillouin zone,Dyson (54) found higher order terms in the specific heat of the spinwaves,i.e.

$$C = AT^{3/2} + BT^{5/2} + CT^{7/2} + DT^{4} + \ldots$$

where the first three terms evolve from non-interacting spinwaves while the T^4-term is a correction term for the interaction of spinwaves with each other.

As for 2d systems,Colpa (29) found for the specific heat of the 2d C_nCuCl,n= 1,....6,

$$C = AT + BT^{-2}$$

for temperatures below 0.7 K $\approx$ 0.1 T_c and where the T^{-2}-term is attributed to the energy level splittings of the Cu-nuclei.Although indeed a linear term was observed,as predicted by 2d spinwave theory,the prefactor A is too large by about 16 %. At higher temperatures,the experimental results could only be fitted to higher order T-terms (30,31).

These considerations show that one cannot hope to obtain from simple spinwave theory detailed predictions for the experimental behaviour of a 2d ferromagnetic system.To describe the gross features,however,the spin-

wave approximation is well suited.As such,the simple spinwave theory shall be used throughout this chapter.

With regard to the magnon mean free path,other limiting scattering processes may include,besides boundary scattering, magnetic and non-magnetic impurity and defect scattering,normal magnon-magnon scattering and magnon-phonon scattering,while at higher temperatures Umklapp magnon-magnon processes may also play a significant role.These different possibilities shall not be discussed here.The scattering processes thought relevant,shall be discussed with the experimental results. Here,we shall confine ourselves to some remarks.

Generally,normal scattering processes,which conserve the total quasimomentum of the quasiparticles,do not lead by themselves to a finite resistance.Normal collisions produce at most an internal equilibrium in the quasiparticle system which can as a whole move in relation to the crystal lattice with an arbitrary velocity.Only when one takes into account processes where the quasimomentum is not conserved does a thermal resistance occur.Therefore,normal scattering is usually neglected.But at low temperatures,where the normal processes dominate,they can exert an appreciable influence on the other scattering processes,e.g. modifying the order of magnitude,the temperature dependence or other parameters (54).

If for instance,normal magnon-magnon scattering occurs more frequently than boundary scattering,the magnons

will undergo many normal collisions before they reach the boundary.As a result,the path traversed between two collisions with the boundary will be appreciably increased,and the effective mean free path for boundary scattering can be larger than the linear dimensions of the sample (55).

As for the magnon-phonon interactions,they can be divided into resonant and non-resonant processes.

Resonant coupling is confined to the region where the magnon modes have the same frequency and wave vectors as the phonon modes,i.e. where the magnon and phonon dispersion relations cross (Fig.3.4).In this cross-over region a hybridization between the modes occur, which then become neither magnons nor phonons but magneto-elastic waves.This resonant coupling produces a perturbation of the dispersion relations,leading to an effective gap in the phonon branch,whose width depends on the coupling strength (56).For weak coupling no such hybridization occurs.The effect of the gap is to eliminate the phonons of the cross-over region from the heat transport.This can be demonstrated by applying a magnetic field.Increasing the field translates the magnon dispersion relation upwards in energy and the cross-over region is equally swept upwards along the phonon spectrum.As for a certain temperature T, the phonons are peaked between k_BT and $4k_BT$,the thermal conductivity will decrease to a minimum when the cross-over region coincides with the peak in the phonon distribution.

Thus,if in zero field the cross-over region occurs at energies below the peak energy,an increase in field leads to a decrease in the conductivity,which after a minimum recovers again.

If in zero field the cross-over region occurs at energies above the peak energy,an increase in field results in an increasing conductivity.

In both cases,the high field values of the conductivity are higher than the zero-field value due to a complete quenching of the interfering magnon modes.Examples of this behaviour have been encountered in $GdCl_3$ (47,50), and $MnCl_2.4H_2O$ (51).

In non-resonant coupling (57),which is usually weaker,the most important processes turn out to be the transformation of two magnons into one phonon and the inverse process in which a phonon decays into two magnons,as well as the Cerenkov radiation of phonons with a magnon as the incident particle.The interactions occur over a wide range of phonon and magnon frequencies and are strongly temperature dependent,but no theoretical account of their effect on the thermal conductivity has been given as yet.

3.4 Experimental Details and Results.

3.4.1 Sample Preparation.

The C_1CuCl and C_2CuCl crystals have a brown transparent colour and are highly hygroscopic,acquiring a whitish tinge at the surface when contaminated with watervapour.The samples were cut from large single crystals,typically of dimensions 15x15x2 mm^3.These large single crystals were grown hydrothermally by Dr.F H M Mischgofsky of the Laboratory of Crystal Growth of the Delft Technical University.The directions of the a- and b-axis could be easily noticed visually and lie along the diagonals of the single crystals.These crystals were observed between two polarizers,to determine the possible presence of water inclusions,crystal imperfections, etc.Water inclusions expand on solidification and,when cooled,would crack the crystal,leading to a decrease of the thermal conductivity.The crystals appeared to be of exellent quality and surprisingly few irregularities were detected.

The samples were cut from those areas of the single crystals where no inclusions and imperfections occur.The obtained samples have the following dimensions

C_1CuCl : 9.7 x 1.8 x 1.7 mm^3

C_2CuCl : 26.1x 3.0 x 1.3 mm^3

The cutting was done by hand,with a cotton wire moistened with distilled water.Immediately after cutting,the samples were kept in vacuum for about 24 hours,to remove

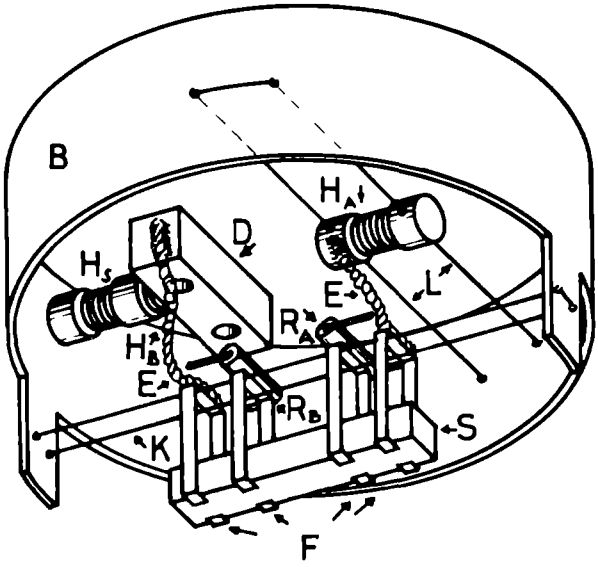

Fig.3.5 : Sample holder and sample mounting.
(See text for an explanation of the synbols)

all traces of water vapour.Attempts to cut the samples mechanically with a crystal saw failed because of the extreme brittleness of the crystals.

This brittleness is most pronounced perpendicular to the c-axis,where the Van der Waals bonds between the adjacent layers by means of the alkylammonium-chains make these links very weak;the crystals are easily split between the layers.These bonds are the weaker the longer the alkylammonium-chains.For these reasons only measurements on crystals with n=1 and n=2 proved to be possible.Also,due to anisotropic magnetostriction,the crystals may break easily when a magnetic field is applied. Attempts to measure the magnetostriction of these compounds failed,probably for these reasons (58).

It is clear from the above considerations,that extreme care is required in the handling and mounting of these crystals,as well as in the cooling down to liquid helium temperatures and the application of a magnetic field.

3.4.2 Sample Mounting and Measurement.

The thermal conductivity of these crystals was measured in the temperature range between 1.5 K and 20 K and in fields up to 6.5 T. The measurements were done in the Blue Monster by the conventional steady state method, as described in chapter 2.

The samples were oriented in such a way that the heat flow was parallel to the magnetic layers,while the magnetic field was applied perpendicular to the heat flow and parallel to the c-axis.
The mounting of the sample in the sample holder is shown in Fig.3.5.

The thermal conductivity perpendicular to the layers has been found to be lower by a factor 10^{-2}- 10^{-3}(14) compared to the conductivity parallel to the layers. For that reason the heaters and thermometers were not mounted on top of the sample (S),as in that case the heat would flow in the toplayer only.Instead,four phosphor bronze clamps (F) (thickness: 0.2 mm,width: 1 mm) were attached to the sides of the crystal,so as to make contact with all the layers, and the heaters and thermometers were connected to these clamps.Between the clamps and the crystal a thin layer of Apiezon-N grease was applied to improve the thermal contact.To support the sample two cotton wires (K) were then threaded through the clamps and fastened to extensions of the circular copper frame (B).In this way a flexible and strain-free mounting of the crystal was achieved.

For the temperature measurements,two 220 Ω,1/10 W Allen-Bradley carbon resistors R_A and R_B were used.To enhance the thermal contact they were soldered at one point to the two inner clamps (F).The cold end heating system consists of a cold end heater H_B(max.output 0.5W) and a stabilization heater H_S(max.output 1.0 W),made of

manganine wire wound around a copper spool which at one end was hard-soldered to the circular frame (B).This frame was attached to the ^{3}He-chamber with copper screws. The other end consists of a copper encasing (D) for a Ge-resistor R_G and a field-independent capacitance thermometer C. At the hot end the heater H_A(max.output 0.5 W) was kept in place by two cotton wires (L) fastened to the circular frame.The heaters H_A and H_B were connected to the respective clamps by a bundle of 0.1 mm diameter copper wires (E).

To avoid thermal shock a very slow cooling pace was observed,especially at about 100 K where a discontinuous structural phase transition occurs (27,37).The cooling from room temperature to liquid nitrogen temperature (77 K) took about 24 hours.After that,filling with liq. helium could proceed in the usual way.As thermal cycling would crack and destroy the crystal,or at least greatly reduce the thermal conductivity in an irreproducible way (14),the temperature was not allowed to exceed the liq.nitrogen temperature during the whole of the experiment.

Changes in the magnetic field were also executed very slowly.Magnetic cycling,however,could not be avoided.A slight decrease in the thermal conductivity was observed,each time after the field had reached 6.5 T.The decrease due to magnetic cycling was estimated to be of the order of 5 %.

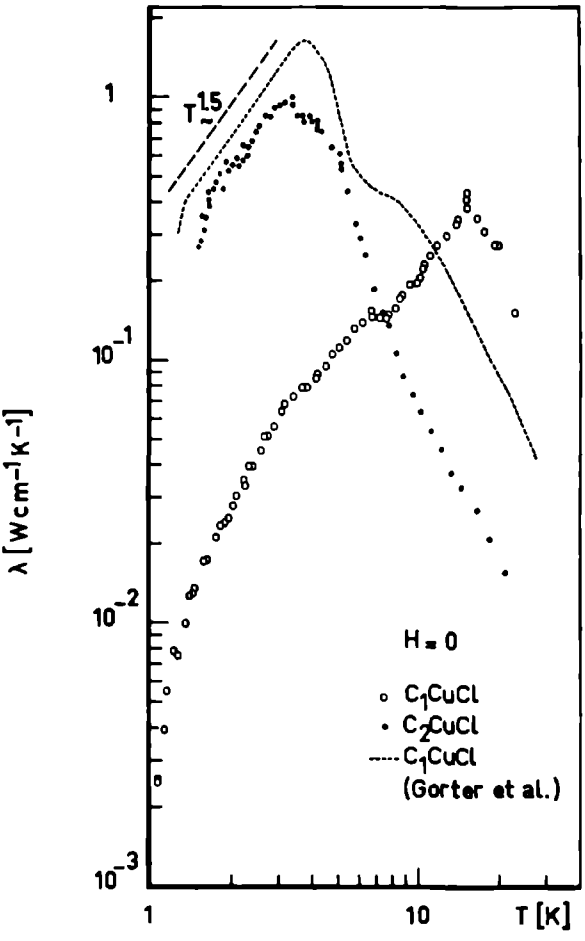

Fig.3.6 : Temperature dependence of the thermal conductivity of C_1CuCl and C_2CuCl at zero field. The broken line is proportional to $T^{3/2}$.

3.4.3 Experimental Results.

Fig.3.6 shows the temperature dependence of the thermal conductivity of the C_1CuCl (methyl) and the C_2CuCl (ethyl) crystals in zero field.For reasons of comparison,the thermal conductivity at zero field for the methyl compound as measured by Gorter et al.(15) is also drawn.The values of the methyl crystal are about an order of magnitude smaller than those of the ethyl compound,while the latter is of the same order of magnitude as the methyl values obtained by Gorter. This is due to the difference in the quality of the crystals.On examination after the experiments,the C_2CuCl crystal was still found to be of exellent quality,but the C_1CuCl crystal showed some cracks.The difference in crystal quality is also reflected in the temperature dependent behaviour of the respective compounds. While below 4 K the ethyl compound,as well as the methyl values obtained by Gorter et al. show a clear $T^{3/2}$-dependence - evidence of a dominating magnon conductivity - this behaviour is far less manifest in the methyl results.

Figs.3.7 and 3.8 show typical examples of the thermal conductivity of the methyl and ethyl single crystals as a function of magnetic field at a constant temperature..Both curves show the same characteristics. After an initial increase in the low field region,the total thermal conductivity decreases until at fields between 4 T and 5 T it reaches a saturation value of

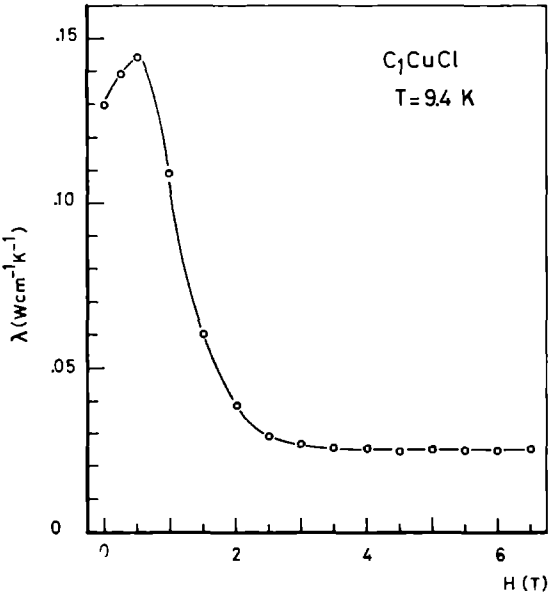

Fig.3.7 : Field dependence of the thermal conductivity of C_1CuCl at a constant temperature of 9.4 K.

about 10 % of the original magnitude at zero field for the methyl compound,and about 25 % for the ethyl crystal. Clearly at zero field the heat flow consists of a large magnon contribution and a much smaller phonon current. When a magnetic field is applied,the magnon conductivity is reduced until at sufficiently high fields it is completely quenched for temperatures below T_c,and one measures the lattice conductivity only.
Fig.3.9 and Fig.3.10 show the temperature dependence of the thermal conductivity of the methyl and ethyl crystals,respectively,at zero and at the highest measured field (6.5 T),the high field values representing the lattice conductivity for $T < T_c$.
We shall first concern ourselves with the field dependence of the thermal conductivity,then proceed to analyse the lattice contribution and finally examine the magnon conduction.

3.4.4 Field Dependence.

Fig.3.11 and Fig.3.12 show the field dependence of the thermal conductivities of the methyl and ethyl crystals at several constant temperatures.
At low fields a positive magnetoconductivity occurs for C_2CuCl (Fig.3.12),with a maximum for fields between 0.2 T and 0.3 T,regardless of temperature.This behaviour was also observed in the measurements of Gorter (16) on

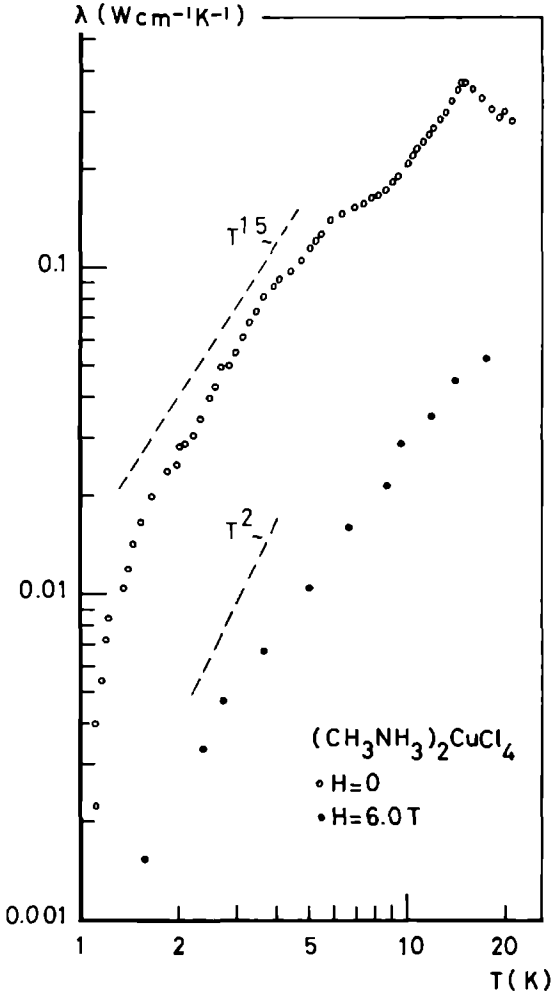

Fig.3.9 : Temperature dependence of the total (H= 0 T) and lattice (H= 6.0 T) thermal conductivity of C_1CuCl.

the good quality C_1CuCl crystal. In the C_1CuCl crystal of lesser quality the maximum occurs at different field strengths. Several possible explanations could be advanced for the occurence of this maximum.

As was shown by Van Kempen et al (39,79) by means of the Faraday rotation effect, in similar compounds below 10 K, even at zero field, magnetic domains are present. Presumably, the magnon mean free path is then limited by the domain boundaries. When the field is increased, the size of the domains is increased as well, thereby lengthening the magnon mean free path until at a sufficiently high field the domainsize comprises the whole crystal. Thus, at low fields the subsequent enhancement of the magnon conductivity by the lengthening of the magnon mean free path up to a certain value of the field, may offset and even exceed the quenching influence of the magnetic field. To determine, therefore, the zero field value of the thermal conductivity in the absence of these effects, a linear extrapolation is used, from conductivity values with fields higher than the field where the maximum occurs. This extrapolated value is then used as the zero field value $\lambda(0)$ of the thermal conductivity of the sample.

A second explanation for this low field maximum was proposed by Douglass (5). He postulated that the thermal conductivity depends mainly on the magnetization direction, rather than on the field direction. In zero field most of the magnetization aligns along the

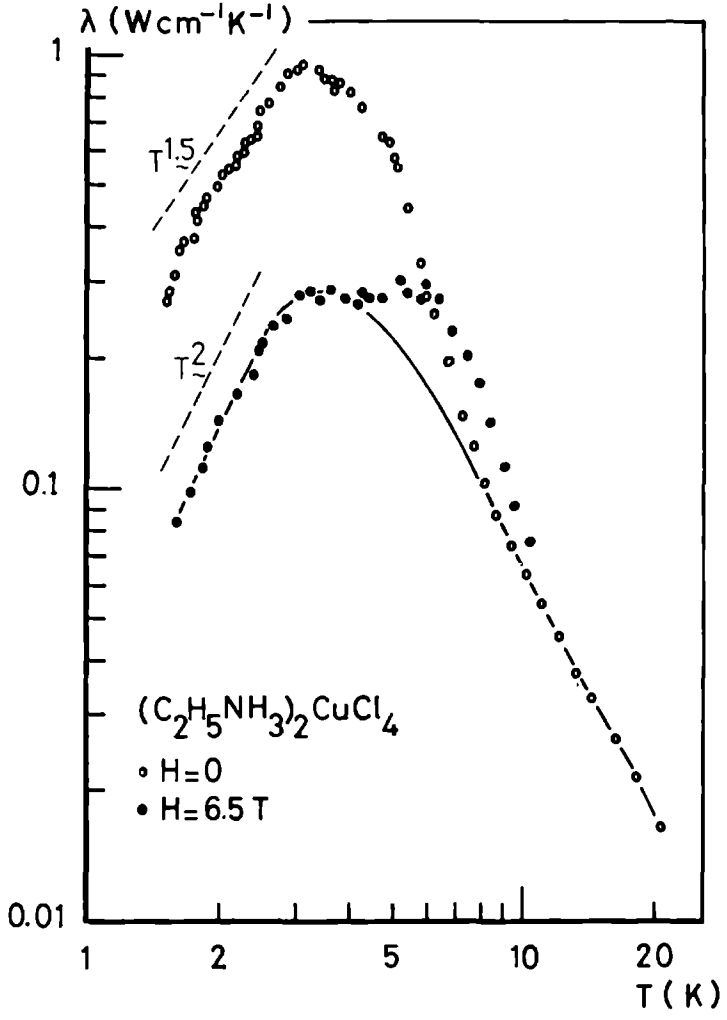

Fig.3.10: Temperature dependence of the total (H= 0 T) and lattice (H= 6.5 T) thermal conductivity of C_2CuCl. For T > 4.5 K the lattice conductivity is represented by a drawn line.

easy directions.If the direction of the thermal gradient is parallel to these directions,the thermal conductivity would be maximal and no positive magnetoconductivity would appear if an external magnetic field is applied. If the thermal gradient subtend an angle to the easy directions of magnetization,the conductivity would be less.In the last case,if a magnetic field normal to the heat flow is switched on,the magnetization will be reoreinted in a direction perpendicular to the thermal gradient and the conductivity increases again.The zero field value of the sample,i.e. for the case where the thermal gradient lies parallel to one of the easy directions,is again obtained by a linear extrapolation from the high field side of the maximum.
From our measurements it cannot be deduced which of the two possible explanations for the the initial positive magnetoconductivity,as outlined above,is the correct one.In both cases,the extrapolation to the theoretical zero-field value $\lambda(0)$ is executed in the same way.
A measurement of the angle-dependence of the thermal conductivity at different constant field strength could decide the case,however, as the domain growth is not angle dependent in contrast to the Douglass-mechanism.

Fig.3.13 shows $\lambda(H)/\lambda(0)$ versus H/T for the C_1CuCl and C_2CuCl samples in about the same temperature region.Here $\lambda(0)$ is obtained by the above procedure. The drawn line represents the values obtained from Eq.(3.12) for a two-dimensional magnon gas in the sim-

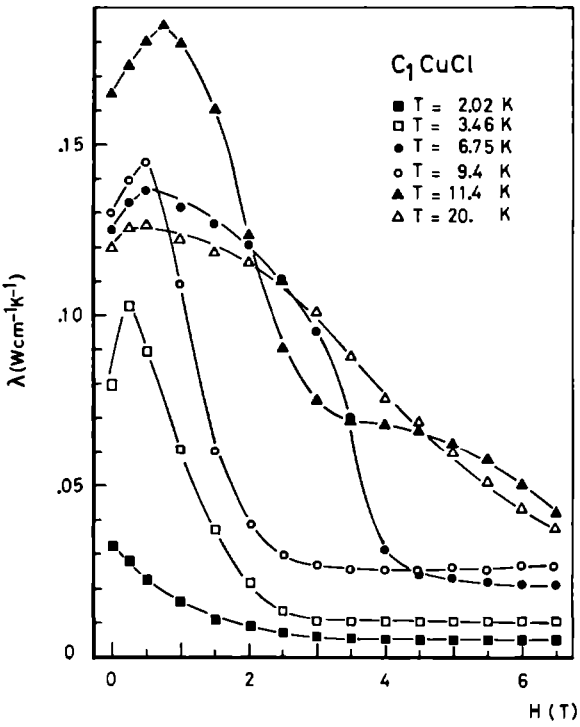

Fig.3.11: Field dependence of the thermal conductivity of C_1CuCl for different constant temperatures.

ple spinwave approximation,enhanced by the lattice conductivity.As can be seen from Fig.3.13 the good quality C_2CuCl crystal follows the prediction for a 2d noninteracting magnon gas far better than the lesser quality C_1CuCl crystal,which reaches its saturation value in a much steeper decrease with field.These saturation values comprise about 10 % to 15 % of the total thermal conductivity,implying a magnon thermal conductivity,especially at the lower temperatures,of about 90 % to 85 %.
This is the largest fractional contribution from magnons to the heat transport as yet observed.

Apparently,the crystal defects affect the phonon conductivity far stronger than they do the magnon conductivity,resulting in a quenching of the lattice heatflow and a higher magnon contribution in the lesser quality C_1CuCl crystal,as compared to the good quality C_2CuCl crystal.

For the high temperatures (Fig.3.11: T = 11.4 K, T = 20 K),the thermal conductivity values of C_1CuCl do still pursue a downward trend,even at the highest attainable field of 6.5 T. As $g\mu_B H/k_B T = 1$ corresponds to $H/T = 0.72\ TK^{-1}$,at least fields higher than 8.5 T and 14.5 T,respectively,are required for these temperatures to obtain their saturation values.Both these temperatures are above the Curie-temperature of C_1CuCl (T_c=8.895 K) This indicates that even at temperatures more than twice the critical temperature,a sizeable contribution of magnetic origin to the thermal conductivity is found.

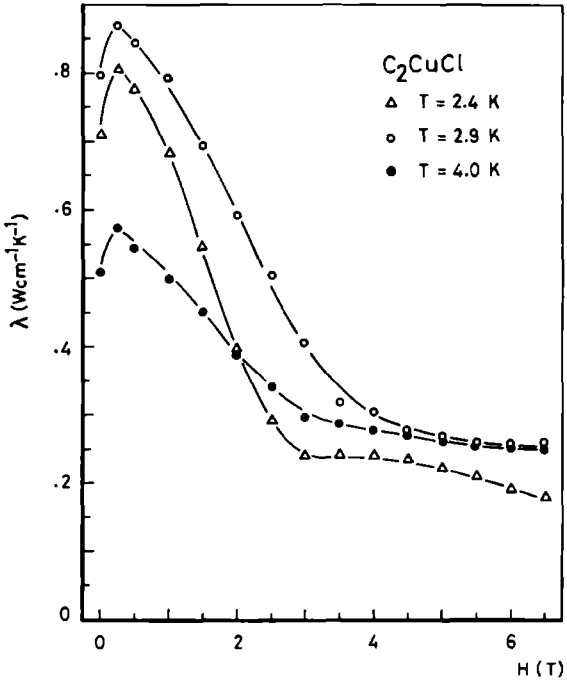

Fig.3.12: Field dependence of the thermal conductivity of C_2CuCl for different constant temperatures.

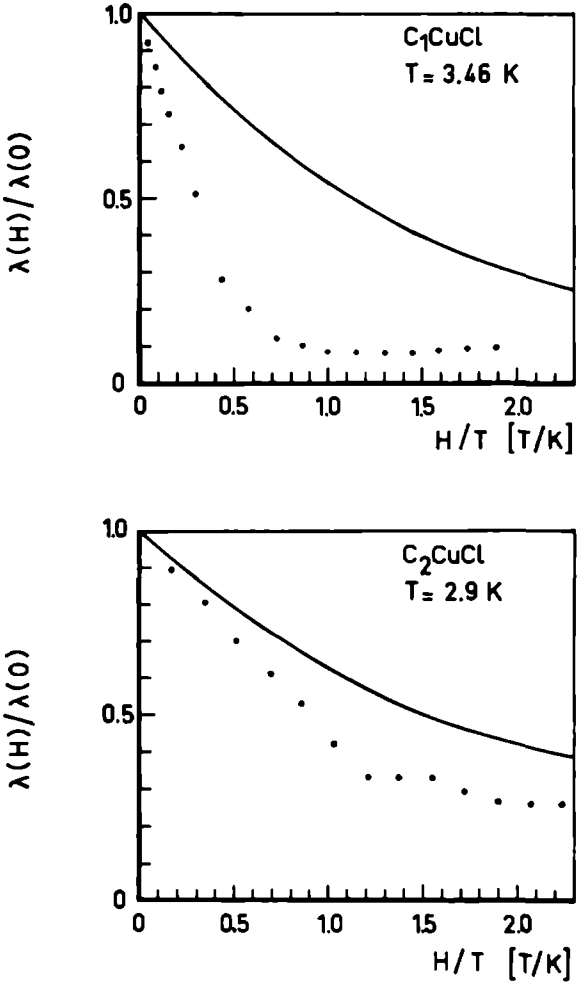

Fig.3.13: Field dependence of the reduced thermal conconductivity of C_1CuCl and C_2CuCl. The solid line represents the sum of the theoretically calculated conductivity of the non-interacting magnongas and the estimated lattice conductivity.

This shall be treated in the last section of this chapter.

3.4.5 Phonon Conductivity.

From Fig.3.11 and Fig.3.12 it can be seen that the thermal conductivity saturates for fields above 4.5 T, at least for temperatures below T_c. As these saturation values can be identified with the lattice thermal conductivity, the curves with H = 6.5 T as obtained in Fig. 3.9 and Fig.3.10 , represent the lattice conductivity of the C_1CuCl and C_2CuCl compounds in the temperature region up to T_c. The high field values for temperatures above this region cannot be interpreted unambiguously as the lattice conductivity and shall be dealt with in the last section.

The lattice conductivity of the C_1CuCl crystal shows a $T^{1.9}$-dependence at low temperatures and a $T^{1.4}$-dependence at higher temperatures (Fig.3.9), while the C_2CuCl crystal shows a T^2-dependence up to about 3 K (Fig.3.10). This clearly indicates a phonon lattice of lower dimensionality, as a 3d lattice would lead to a T^3-dependence of the thermal conductivity.
These indications are amplified by the results of far infrared measurements on these compounds with n= 1,2, 3,4, performed by Stoelinga et al (42,43,44) of our laboratory, who found that the optical phononic system

of these crystals is two-dimensional.More specifically, they could show,that the optical phonon system is two-dimensional for wavenumbers above 50 cm^{-1},i.e. the alkylammonium-groups do not play a significant role in the FIR-spectra,which could wholly be explained by the fundamental modes of the layers alone.Below 50 cm^{-1},no optical phonons could be detected,indicating that in the low energy region the acoustical phonons dominate.From our measurements of the lattice conductivity of these compounds,information on the acoustical part of the phonon spectrum can now be obtained.

Using again the Debye approximation and employing the same generalization of the kinetic formula for the phonon conductivity as for magnons,i.e.

$$\lambda_{ph}(2)= \frac{1}{2}\int C(\omega)v(\omega)l(\omega)g(\omega)d\omega \qquad (3.13)$$

the expression for the 2d lattice thermal conductivity $\lambda_{ph}(2)$ is easily derived.Here $g(\omega)= g(k)(dk/d\omega)$ is the spectral density.Since for phonons there are three polarization directions per wave vector,the mode density is given by $g(k)= 3(L/2\pi)^2$.

Using the phonon dispersion relation $\omega(k)= v\,k$,where v is the sound velocity,taken as constant,and $l(\omega)= v\,\tau(\omega)$,with $\tau(\omega)$ the phonon relaxation time,while also using the dimensionless variable $x= \hbar\omega/k_B T$ and taking L=1,we find for the lattice conductivity λ_{ph} of a layered system

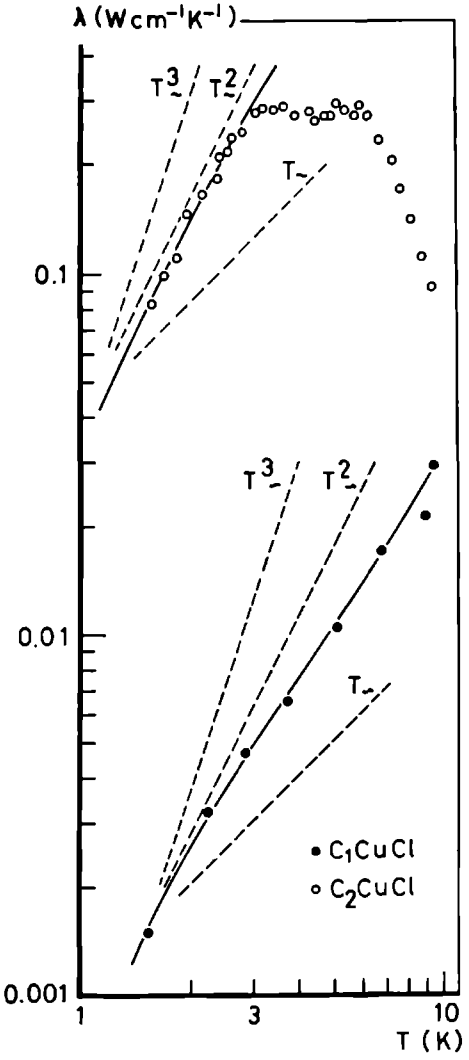

Fig.3.14: Temperature dependence of the lattice conductivity of C_1CuCl and C_2CuCl (H= 6.5 T). The solid lines are a two-parameter fit of the theoretical curve as explained in the text.The broken lines represent a cubic,quadratic and linear temperature dependence,respectively.

$$\lambda_{ph} = \frac{1}{c}\,\lambda_{ph}(2)$$
$$= \frac{3}{c}\,Nk_B v^2 \left(\frac{T}{\theta}\right)^2 \int_0^{\infty} \frac{x^3 e^x}{(e^x-1)^2 \tau^{-1}}\,dx \qquad (3.14)$$

Here, $\lambda_{ph}(2)$ is the thermal conductivity in a 2d lattice, $1/c$ is the number of layers per unit length ($c = 0.5\,c_o$ is the distance between two magnetic layers), $N = 4/(a_o b_o)$ is the number of atoms per unit area, a_o, b_o, c_o are the lattice constants of the unit cell, v is the average sound velocity and θ is the Debye temperature.
The upper limit on the integral is arrived at in the conventional way : equating the total number of modes to the degrees of freedom, we express this condition by

$$\int_0^{\omega_{max}} g(\omega)\,d\omega = 3N$$

where $\omega_{max} = v(4\pi N)^{1/2}$ is the cut-off frequency. Defining the Debye temperature as $\theta = \hbar\omega/k_B$, the upper bound becomes $x_{max} = \theta/T$, and can be extended to infinity in the low temperature limit.

We have included, besides boundary scattering, scattering at line dislocations, hence the phonon relaxation time at low tempreatures can be written as (61)

$$\frac{1}{\tau} = \frac{1}{\tau_1} + \frac{1}{\tau_2}$$
$$= \frac{v}{l} + 0.05\,b^2\gamma^2 N_d \omega \qquad (3.15)$$

where τ_1 is the relaxation time from boundary scatter-

ing and τ_2 is the relaxation time from scattering at line dislocations, $l = l_{ph}$ is the phonon mean free path, b is the Burgers vector, γ is the Grüneisen constant, N_d is the number of dislocations per unit area and ω is the frequency of the relevant phonon mode. We have not included scattering at impurities or point dislocations as in that case the scattering probability varies as the fourth power of frequency in the limit of long wavelengths (61), and its influence on the thermal conductivity can be neglected.

In the limit $\tau_2^{-1} \leqslant \tau_1^{-1}$, indicating that only a relatively small amount of dislocations are present, Eq.(3.14) and Eq.(3.15) give a T^2-dependence for the case of a 2d lattice. For a 3d lattice one obtains a T^3-dependence in this limit, using Eq.(3.15) and the 3d equivalent of Eq.(3.14).

In the other limit $\tau_2^{-1} \gg \tau_1^{-1}$, for a large amount of dislocations, one obtains a T- and a T^2-dependence for the 2d and the 3d case, respectively.

In Fig.3.14 the lattice thermal conductivity of the C_1CuCl and C_2CuCl crystals are shown as a function of temperature, together with curves representing a cubic, quadratic and linear temperature dependence. The measured temperature dependence of λ_{ph} for both crystals, lies between a T- and a T^2-dependence, thus following the behaviour of a 2d lattice. This is confirmed by a computer fit of the measured data to Eq.(3.14) nd Eq.(3.15). The fitted curves of the two crystals

are indicated in the figure.

By straightforward mathematics, Eq.(3.14) can be rewritten as

$$\lambda_{ph} = \alpha\beta^2 T^2 \int_0^\infty \frac{x^3 e^x}{(e^x-1)^2(1+\beta T x)}\, dx \qquad (3.16)$$

for the fitting procedure, with

$$\alpha = (3Nv/ck_B l)(20\,\hbar v/\theta b^2\gamma^2 N_d)^2$$

$$\beta = k_B l b^2 \gamma^2 N_d/20\,\hbar v$$

From these fits we obtained the following results:

C_1CuCl: $\alpha = 1.5$ $Wm^{-1}K^{-1}$; $\beta = 0.1$ K^{-1}
C_2CuCl: $\alpha = 2.6\times10^2$ $Wm^{-1}K^{-1}$; $\beta = 0.05$ K^{-1}

These results can be used to derive the phonon mean free path l_{ph} and the dislocation density N_d.
From specific heat measurements on these compounds by Bloembergen and Miedema (30), an average Debye temperature $\theta \approx 300$ K can be obtained for the two-dimensional lattice. Using this value and the value of the unit cell parameters as quoted in Table 3.1, and assuming b= 10 Å, $\gamma = 1.5$, $v = 3\times10^5$ cms^{-1}, one finds

C_1CuCl: $l_{ph} = 1.2\times10^{-4}$ cm; $N_d = 1.5\times10^{12}$ cm^{-2}
C_2CuCl: $l_{ph} = 2.5\times10^{-2}$ cm; $N_d = 1.5\times10^{10}$ cm^{-2}

which are reasonable values (62).

From their specific heat data Bloembergen and Miedema (30) also obtained indications for the two-dimensionality of the phonon spectrum of these compounds. For a 3d lattice the low temperature lattice specific

heat C_{lat} should vary proportional to T^3, whereas for a 2d lattice C_{lat} should show a T^2-dependence. Bloembergen and Miedema found a clear difference in the temperature behaviour between compounds with even and uneven n-values, in that compounds with even n are "less two-dimensional" than compounds with uneven n, e.g. for the C_1CuCl compound $C_{lat} \propto T^{2.25}$, while for the C_2CuCl compound $C_{lat} \propto T^{2.95}$. No such systematic differences could be detected in the optical phonon spectrum as measured by far infrared measurements. Nor did we notice such difference in behaviour from our lattice thermal conductivity measurements.

The failure to detect a "less two-dimensional" behaviour for compounds with even n by our thermal conductivity measurements can be understood by assuming for these even n compounds a much larger value for vl within the magnetic layers than in the direction normal to these layers. Such an anisotropy in the mean free path and for the sound velocity would cause the much larger values of vl within the layers to dominate completely the small vl-components normal to these layers in the thermal conductivity measurements.

3.4.6 Magnon and Paramagnon Conductivity.

It was established in the preceding section that the high field values can be taken to represent the lattice thermal conductivity in the temperature region below T_c. The magnon contribution can now be computed, by substracting the high field values from the zero field values of the thermal conductivity. The results are shown in Fig.3.15. As can be seen from this figure, the C_2CuCl crystal shows a far better $T^{3/2}$-behaviour, in accordance with Eq.(3.12), than the C_1CuCl compound, due to the lesser quality of the latter.

At zero field, Eq.(3.12) reduces to

$$\lambda_s = \frac{l_s k_B (k_B T)^{3/2}}{c\,h\,D^{1/2}} \int_0^\infty \frac{x^{5/2} e^x}{(e^x-1)^2}\,dx \qquad (3.17)$$

$$= \frac{k_B^2 l_s}{a_o c_o h (J/k_B)^{1/2}} \frac{5}{2} \Gamma(5/2)\zeta(5/2)\, T^{3/2}$$

where the Gamma-function $\Gamma(5/2) = \frac{3}{4}\sqrt{\pi}$ and the Riemann-Zeta-function $\zeta(5/2) = 1.341$ (63).

Using the values summarized in Table 3.1, we obtain

$$C_1CuCl: \lambda_s = 20.4\, l_s T^{3/2}\ Wcm^{-1}K^{-1} \qquad (3.18)$$
$$C_2CuCl: \lambda_s = 18.1\, l_s T^{3/2}\ Wcm^{-1}K^{-1}$$

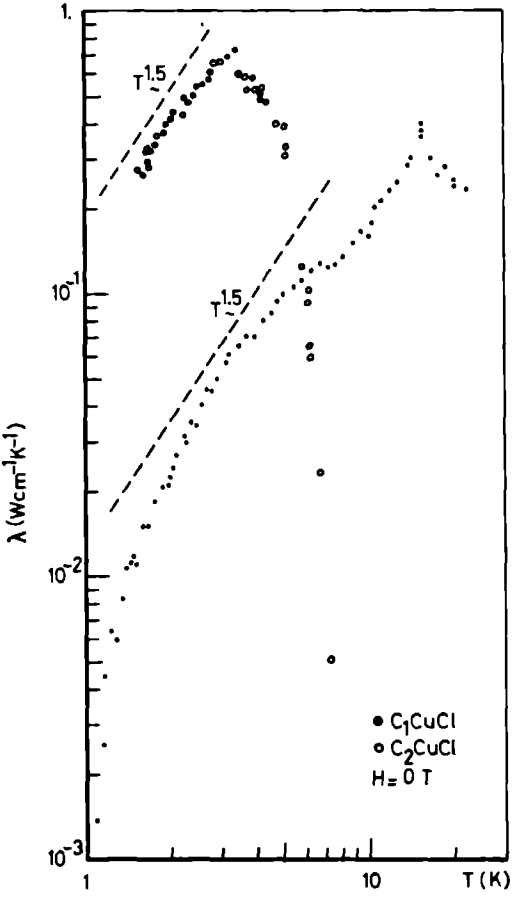

Fig.3.15: Temperature dependence of the magnon thermal conductivity of C_1CuCl and C_2CuCl.

From the measured results of λ_s we find for the magnon mean free path at T= 3 K

C_1CuCl: $l_s = 1.3 \times 10^{-3}$ cm

C_2CuCl: $l_s = 1.8 \times 10^{-2}$ cm

in agreement with other estimates (14-16).

In view of these results it can be considered established that below T_c magnons play a dominating role in the energy transport in these compounds. The situation becomes more complicated, however, for temperatures near and above T_c, in the paramagnetic phase.

The zero field values, as obtained for the good-quality crystals C_1CuCl (Fig.3.2) and C_2CuCl (Fig.3.10) show that near T_c the magnon contribution has decreased to a negligible fraction. In C_2CuCl (T_c= 10.20 K) a kink appears at 10 K, suggesting that above T_c phonons completely dominate the conduction of the heat flow, while for C_1CuCl (14-16) a shoulder appears at T_c= 8.895 K, attributed to phonon conduction.

For C_2CuCl this suggestion is intensified by the fact that a linear extrapolation from values above T_c reaches the first maximum of the lattice conductivity curve, as represented by the high field values (Fig.3.10). The high field values of C_2CuCl show two maxima with peaks at 3.5 K and 5.5 K, and a dip at approximately 4.5 K, while above T= 6 K they display a higher conductivity than at zero field. Probably this is due to the fact that at the higher temperatures a field of 6.5 T is not sufficient to suppress completely all magnetic

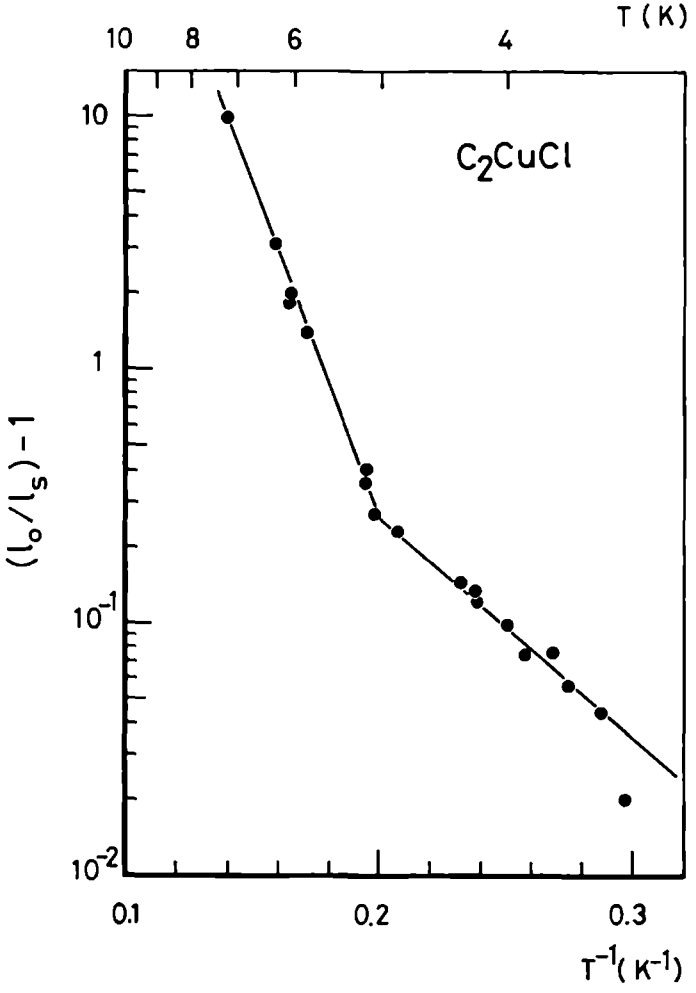

Fig.3.16: Reduced magnon mean free path as a function of T^{-1}.

contributions to the thermal conductivity.This was also observed by Gorter et al.(15,16).Consequently,for the lattice conductivity above 4.5 K we have used the curve as drawn in Fig.3.10,which connects the first maximum at 3.5 K to the zero field values at 10 K.

The magnon conductivity of C_2CuCl (Fig.3.15) is seen to fall off rather steeply after a maximum at about 3.5 K.Miedema et al.(14) have analysed this steep decrease in terms of a temperature dependent mean free path

$$\frac{1}{l_s} = \frac{1}{l_o} + \frac{1}{l(T)} \qquad (3.19)$$

of which l_o is the constant low temperature value as found below 3 K,while l(T) shows an exponentially decreasing temperature dependence,i.e.

$$l(T) = a\, e^{\Delta/k_B T} \qquad (3.20)$$

Following the same analysis for the C_2CuCl values above 3 K,we have taken (Eq.(3.18))

$$l_s = \frac{\lambda_s}{18.1\ T^{3/2}}\ \text{cm}$$

$$l_o = 1.8 \times 10^{-2}\ \text{cm}$$

and plotted $(l_o/l_s)-1 = (l_o/a)\exp(-\Delta/k_B T)$ versus T^{-1} on a half-log. scale.The results are shown in Fig.3.16, where indeed straight lines were obtained,with values

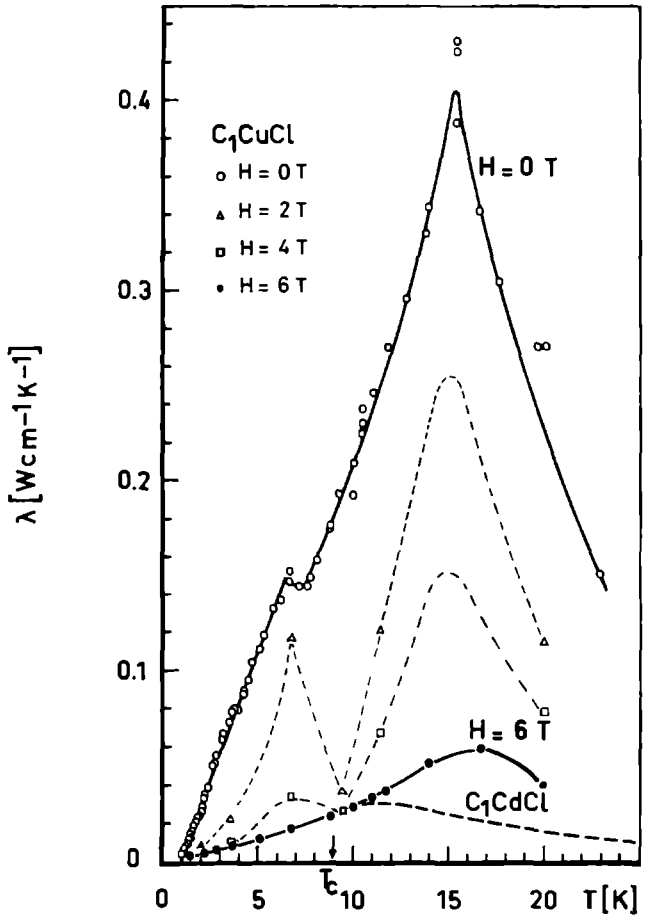

Fig.3.17: Temperature dependence of the thermal conductivity of C_1CuCl at different constant field strengths. For $T < T_c$ the 6 T-line represents the lattice conductivity. For $T > T_c$ the lattice conductivity is represented by the thermal conductivity of the diamagnetic C_1CdCl (broken line), properly scaled to fit the 6 T-curve below T_c

$a = 7 \times 10^{-5}$ cm; $\Delta/k_B = 10$ K for 3.4 K < T < 4.8 K

$a = 3 \times 10^{-8}$ cm; $\Delta/k_B = 76$ K for 4.8 K < T < 6.8 K

This compares reasonably well with the results found by Miedema et al. (14) for C_2CuCl, i.e.

$l_o = 1.3 \times 10^{-2}$ cm; $a = 4 \times 10^{-7}$ cm; $\Delta/k_B = 35$ K

The exponential decrease of the magnon mean free path with increasing temperature can be accounted for by both magnon-magnon as well as magnon-phonon interactions (48).

The C_1CuCl crystal shows a rather different behaviour.

At $T_c = 8.895$ K, no decrease in the zero field magnon conductivity can be observed, although a slight dip appears at 7.5 K (Fig.3.9 and Fig.3.15).

From Fig.3.11 an estimate of the temperature dependent behaviour of the thermal conductivity at various constant fields can be obtained and this is shown in Fig. 3.17. As for temperatures above T_c it appears that the thermal conductivity has not yet reached a saturation value at fields of 6.5 T and the magnon contribution is still not completely suppressed at that high field value, we have estimated the lattice conductivity for $T > T_c$ by using the same procedure as employed by Gorter et al.(15,16). This consists of equating the lattice conductivity (i.e. the 6.5 T values for $T < T_c$) to the properly scaled thermal conductivity of the diamagnetic isomorphous C_1CdCl compound, which has phonon conduction only.

It follows from Fig.3.17 that for $T < T_c$, the

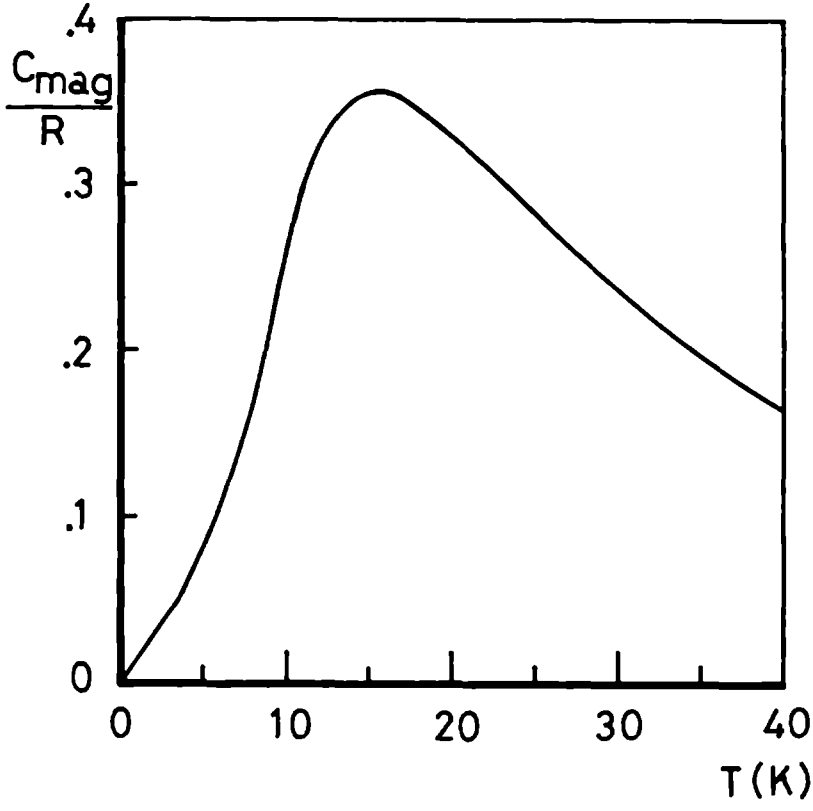

Fig.3.18: Reduced magnetic heat capacity of $C_4CuCl.R$ is the gas constant (After refs.(20,31)).

magnon contribution is found to possess a peak at about 7 K. At T_c, the magnon contribution is already completely quenched for fields of 4 T. But at $T > T_c$, an added contribution to the thermal conductivity, evidently of magnetic origin, is seen to appear, not only in zero field but in the largest field as well. Furthermore, Fig.3.17 shows, that in the neighbourhood of T_c, the magnon contribution is quenched drastically, only when a magnetic field is applied. Apparently, a large magnon contribution can still be found above T_c at zero field.
Indeed, as can be seen from Fig.3.6, the thermal conductivity of the C_1CuCl crystal at zero field, apart from a slight dip somewhat below T_c, rises monotonically to a maximum at 15.5 K, and even exceeds the zero field values of the good quality C_1CuCl crystal. At this maximum value the magnetic contribution comprises about 95 % of the total thermal conductivity. This observed thermal conductivity maximum coincides with the maximum of the specific heat of C_1CuCl (Fig.3.18), as measured by Bloembergen (20,31). This behaviour stands in marked contrast to the zero field temperature dependence of the good quality C_1CuCl- (14,15) and C_2CuCl- (Fig.3.10) crystals, which show a decrease above 3.5 K and for which the non-zero field values coincides with the zero field values above T_c.

The persistence of magnons or magnonlike excitations, even in the absence of long range order and well into the paramagnetic region, has previously been esta-

blished experimentally,for instance in the 3d Heisenberg antiferromagnet $RbMnF_3$ (64).For magnetic systems of lower dimensionality,the effect is even more pronounced as is shown by neutron scattering measurements on the 2d Heisenberg antiferromagnet K_2NiF_4 (65-67) and on the 1d Heisenberg antiferromagnet $(Cd_3)_4NMnCl_3$ or TMMC (68).

A theoretical explanation for the existence of paramagnetic spinwaves was first provided by Marshall (19,69,70).Although no long range order exists above T_c,short range order still prevails,leading to regions of correlated spins the extent of which is determined by the correlation length.Damped excitations or quasi-spinwaves of wavelengths shorter than the correlation length,can still exist and propagate within these correlated regions.

In systems of lower dimensionality,the lengths over which the spins are correlated will be considerably larger than in a 3d system,resulting in even more pronounced magnon modes above T_c. Indeed,nothing special happens at T_c itself (19),as not T_c but the correlation length is the prime quantity that determines the disappearance of the paramagnetic magnons when the temperature is raised.

Despite the fact that the existence of paramagnetic magnon modes or paramagnons has been well established,both by theory and experiment,one still suffers from a paucity of information regarding the possible

energy transport by these paramagnons.
Huber has speculated (71),that the paramagnetic magnon contribution to the conductivity may increase in the vicinity of the critical temperature as the volume of the Brillouin zone increases,but no meaningful calculation has been carried out as yet.

Besides paramagnon thermal conductivity,energy transport by diffusive magnon modes may also be present. Huber et al. (74,75) have shown,that energy transport is non-diffusive in 1d systems with S=1/2,but that in 1d systems with S > 1/2 and 2d and 3d lattices with S=1/2,energy diffusion is present in H=0. On the other hand,Kruger (76) has proved that for 1d systems with S=1/2,a uniform magnetic field reestablishes the energy diffusion at all temperatures,if spin diffusion is present,and that the introduction of weak next nearest neighbour interactions also contribute to the reestablishment of energy diffusion.

Using the theory of Kawasaki (72) and of Lurié et al. (73) we have calculated the possible contribution of long wavelength diffusive spinmodes to the thermal conductivity,but this does not exceed 5 % of the observed total thermal conductivity.For that reason we have attributed the magnetic thermal conduction above T_c as mainly due to paramagnetic magnons.
The question then remains why the good quality C_1CuCl and C_2CuCl crystals do not show a large magnetic contribution above T_c.

A clue for this difference in behaviour above T_c might be found in their behaviour below T_c. As can be seen from Fig.3.13, the good quality C_2CuCl crystal shows roughly the expected field dependence for a 2d non-interacting magnon gas; for strongly interacting magnon-phonon systems, a much stronger field dependence is expected (80), such as exhibited by the C_1CuCl sample. This indicates that, probably due to the larger number of dislocations, the C_1CuCl crystal has a much stronger magnon-phonon interaction than the C_2CuCl sample. This again implies that the absence of magnetic conduction above T_c in the C_2CuCl crystal is not due to a small intrinsic magnetic conductivity, but due to a lack of contact between the magnetic system and the lattice.

Certain aspects of our experimental results could also be explained with a model based on interactions between a phonon system and a magnetic system. However, taking into account the results of other very extensive studies on these compounds (14-16,19), which are consistent with our interpretation, we conclude that scattering between phonons and magnetic systems play but a minor role in our experiments.

In conclusion, we have shown experimentally that in 2d Heisenberg ferromagnets, the magnetic system can contribute considerably to the energy transport, even at temperatures far above T_c. The magnitude of this contribution, as observed by thermal conductivity experiments, is strongly dependent on the strength of the magnon-phonon interactions of the crystal.

References.

1) H Fröhlich and W Heitler,Proc.Roy.Soc.(London) A 135(1936)640

2) H Sato, Progr.Theor.Phys. 13(1955)119

3) B Lüthi,J.Phys.Chem.Solids, 23(1962)35

4) S A Friedberg and E D Harris in "Proc.8th Int. Conf.on Low Temp.Phys."(ed.R O Davies,Butterworth, London,1963),p.302

5) R L Douglass,Phys.Rev. 129(1963)1132

6) D C McCollum,R L Wild and J Callaway,Phys.Rev. 136(1964)A426

7) J N Haasbroek and A S M Gieske,Phys.Letters, 31A(1970)351

8) J N Haasbroek and W J Huiskamp,Phys.Letters, 33A(1970)173

9) J N Haasbroek,"Thermal Conductivity at Very Low Temperatures",Ph.D-thesis Univ.of Leiden(Elve/ Labor Vincit,Leiden,1971)

10) D Walton,J E Rives and Q Khalid,Phys.Rev. B8(1973)1210

11) M J Metcalfe and H M Rosenberg,J.Phys.C,5(1972)459

12) W B Yelon and L Berger,Phys.Rev.B 6(1972)1974

13) Y Hsu and L Berger,AIP Conf.Proc. 17(1973)176

14) A R Miedema,P Bloembergen,J H P Colpa,F W Gorter, L J De Jongh and L J Noordermeer,AIP Conf.Proc. 18(1974)806

15) F W Gorter,L J Noordermeer,A R Kop and A R Miedema,Phys.Letters 29A(1969)331

16) F W Gorter,"Some Physics behind Heat Switches", Ph.D-thesis Univ.of Amsterdam,1969

17) L H M Coenen,H N De Lang,J H M Stoelinga,H Van Kempen and P Wyder,Solid State Commun.20(1976)713

18) L H M Coenen,H N De Lang,J H M Stoelinga,H Van Kempen and P Wyder in "Proc.Int.Conf.on Magnetism 1976",Physica, 86-89 B(1977)968

19) L J De Jongh and A R Miedema,Adv.Phys. 23(1974)1

20) P Bloembergen,"An Experimental Study of the Two-Dimensional,Spin 1/2,Heisenberg Ferromagnet",Ph.D thesis Univ.of Amsterdam (Lectura,Leiden,1976)

21) M E Lines,J.Appl.Phys. 40(1969)1352

22) D W Hone and P M Richards,Ann.Rev.of Materials Science, 4(1974)337

23) N D Mermin and H Wagner,Phys.Rev.Letters 17(1966) 1133

24) L Onsager, Phys.Rev. 65(1944)117

25) H E Stanley and J A Kaplan, Phys.Rev.Letters 17(1966)913

26) A R Miedema,J.Phys.(Paris) 32(1971)C1-305

27) K Knorr,I R Jahn and G Heger,Solid State Commun. 15(1974)231

28) L J De Jongh,Physica 82 B(1976)247

29) J H P Colpa,Physica 57(1972)347

30) P Bloembergen and A R Miedema,Physica 75(1974)205

31) P Bloembergen,Physica 85 B(1977)51

32) P Bloembergen,P J Berkhout and J J M Franse, Int.J.Magnetism 4(1973)219

33) Y Ajiro and M Miura, J.Phys.Soc.Japan 35(1973)1787

34) M Tanimoto,T Kato and Yokozawa,Phys.Letters Phys.Letters 58 A(1976)66

35) R Kind and J Roos,Phys.Rev. B 13(1976)45

36) G Heger,E Henrich and B Kanellakopulos,Solid State Commun. 12(1973)1157

37) G Heger,D Mullen and K Knorr,Phys.Stat.Sol. A 31 (1975)455

38) G Chapuis,H Arend and R Kind,Phys.Stat.Sol. 31 (1975)449

39) H van Kempen,F H M Mischgofsky and P Wyder in "Proc.12th Int.Conf. on Low Temp.Phys."(ed.E Kanda,Ac.Press of Japan,Kyoto,1971),p.811

40) H Arend,J Schoenes and P Wachter,Phys.Stat.Sol. B 69(1975)105

41) H Arend,H von Känel and P Wachter,Phys.Stat.Sol. B 74(1976)151

42) J H M Stoelinga and P Wyder,J.Chem.Phys. 61(1974) 478

43) J Holvast,J H M Stoelinga and P Wyder,Ferroelectrics, 13(1976)543

44) J H M Stoelinga and P Wyder,J.Chem.Phys.64(1976) 4612

45) A Levstik,Solid State Commun. 20(1976)127

46) H Arend,R Hofmann and F Waldner,Solid State Commun. 13(1973)1629

47) D Walton in "Proc.1st Int.Conf.on Phonon Scattering in Solids"(ed. H J Albany,Service de Documentation du CEN,Saclay,1972),p.295

48) A I Akhiezer,J.Phys.(USSR), 10(1946)217
See also: A I Akhiezer,V G Baryaktar and S R Peletminskii,"Spinwaves"(North Holland,Amsterdam,1968)

49) D Douthett and S A Friedberg,Phys.Rev. 121(1961) 1662

50) J E Rives,G S Dixon and D Walton,J.Appl.Phys. 40(1969)1555

51) J E Rives,Phys.Letters 36 A(1971)327

52) G S Dixon,J E Rives and D Walton,J.Phys.(Paris) 32(1971)C1-528

53) F Keffer in "Handbuch der Physik"(ed.S Flügge, Springer Verlag,Berlin,1966),vol.18/2,p.115

54) J Callaway and R Boyd,Phys.Rev. 134(1964)A1655

55) R N Gurzhi,Sov.Phys.Uspekhi, 11(1968)255

56) C Kittel,Phys.Rev. 110(1958)836

57) A Bachellerie,J Joffrin and A Levelut,J.Phys.(Paris),32(1971)993

58) H R Ott,private communication

59) J J Martin and G S Dixon,Phys.Stat.Sol. B 54(1972) 707

60) G S Dixon,Phys.Rev. B 8(1973)3206

61) P G Klemens in "Handbuch der Physik"(ed.S Flügge, Springer Verlag,Berlin,1956),vol.14,p.198

62) C Kittel,"Introduction in Solid State Physics", 5th edition(John Wiley,New York,1976),p.578

63) M Abramowitz and I A Stegun,"Handbook of Mathematical Functions"(Dover,NewYork,1965)

64) R Nathans,F Menzinger and S J Pickart,J.Appl.Phys. 39(1968)1237

65) J Skalyo,G Shirane,R J Birgenau and H J Guggenheim, Phys.Rev.Letters 23(1969)1394

66) R J Birgenau,J Skalyo and G Shirane,J.Appl.Phys. 41(1970)1303

67) R J Birgenau,J Skalyo and G Shirane,Phys.Rev. B 3(1971)1736

68) M T Hutchings,G Shirane,R J Birgenau and S L Holt, Phys.Rev. B 5(1972)1999

69) W Marshall in "Proc.Conf.on Critical Phenomena" (NBS,Washington,1965)

70) W Marshall and R D Lowde,Rep.Progr.Phys. 31(1968) 705

71) D L Huber,Solid State Commun. 6(1968)685

72) K Kawasaki,Progr.Theor.Phys. 29(1963)801

73) N A Lurié,D L Huber and M Blume,Phys.Rev. B 9(1974)2171

74) D L Huber and J S Semura,Phys.Rev. 182(1969)182

75) D L Huber,J S Semura and C G Windsor,Phys.Rev. 186(1969)534

76) D A Kruger, Phys.Rev. B 3(1971)2348

77) H Stern,J.Phys.Chem.Solids,26(1965)153

78) H N De Lang,H van Kempen and P Wyder,Phys.Rev. Letters,39(1977)467

79) H van Kempen,F H M Mischgofsky and P Wyder,

Phys.Rev. B 15(1977)4386

80) D Walton,R E Rives and Q Khalid,Phys.Rev. B 8(1973)1210

81) D J Saunders and D Walton,Phys.Rev. B 15(1977)1489

82) J Seliger,R Blinc,H Arend and R Kind,Z.Physik B 25(1976)189

83) H Kubo,N Kaneshima,Y Hashimoto,K Tsuru and K Hirakawa, J.Phys.Soc.Japan 42(1977)484

4 THE LATTICE THERMAL CONDUCTIVITY OF PURE METALS: ALUMINIUM AND INDIUM.

4.1 Introduction.

Electrons and phonons are the only two quasiparticles,which function as energy carriers in simple metals, with the electron contribution generally dominating the phonon conductivity.

Writing the total thermal conductivity λ as a sum of the electronic heat conductivity λ_e and the lattice heat conductivity λ_g,i.e.

$$\lambda = \lambda_e + \lambda_g \qquad (4.1)$$

for most pure metals $\lambda_e/\lambda_g \approx 10^4$ and usually λ_g is completely neglected.Thus the thermal conductivity in pure metals is almost entirely electronic in nature and as such but a different manifestation of the same fundamental transport properties as those,present in the electrical conductivity.As a measurement of either one will yield much the same information about these properties,while electrical measurements are much simpler to perform than thermal conductivity experiments, the measurement of electrical conductivity seems highly preferable above thermal conductivity measurements.

Yet,compelling reasons exist for the measurement

of the thermal conductivity of metals,both from an experimental (1) as well as from a theoretical (3-10) point of view.

When dealing with small-sized,ultra-pure metal samples,the maximal voltages one can generate are of the order of 10^{-8} Volt,using currents of a few Ampères. This is not easy to measure: typical noise levels in high quality voltmeters are of the order of 10^{-10}Volt and although superconducting devices have much lower noise levels,they cannot be used in the presence of large magnetic fields.

In contrast to this,the thermal noise levels in carbon resistance thermometers are about 10^{-5} K in the liquid helium range,while temperature differences along the sample of 10^{-2} K are easily obtained.Hence,experimental considerations of the sensitivities,obtainable in electrical and thermal measurements,may recommend the use of the latter,even at the high and low temperature extremes where the Wiedemann-Franz (WF) law is obeyed and where one can expect to obtain the same information from electrical as from thermal conductivity experiments.

Theoretical interest in thermal conductivity measurements arises from the fact that in the intermediate temperature range,the WF-law is not obeyed and the scattering of electrons by phonons affects the electrical current in a manner,different from the thermal flow. By studying the difference in behaviour of the thermal and the electrical conductivity,preferably simul-

taneously and in the same sample under the same conditions,valuable information can be acquired about,e.g. the electron scattering mechanisms as they manifest themselves in the electrical and thermal mean free paths (2).

Usually,the electron-phonon interactions is studied from the electronic point of view,i.e. one considers how the electrons are scattered by the phonons.An equivalent method would be to regard the electron-phonon interactions from a phononic point of view,i.e. how the phonons are scattered by the electrons.One of the methods by which this can be achieved is to measure the thermal lattice conductivity.

Since in general,measurements of the thermal conductivity cannot be performed with an accuracy greater than 1 %,and λ_g/λ_e is about 0.01 % in pure metals,the lattice conductivity cannot be determined directly.The electronic conductivity has to be reduced to at least the same order of magnitude as the lattice conductivity,before a meaningful measurement of the latter can be obtained. This can be achieved by

i) going into the superconducting state

ii) alloying

iii) reduction by means of a magnetic field

In this chapter we shall report on the measurements of the lattice conductivity of Aluminium and Indium.The magnetic field method was used in the so-called Corbino configuration,whereby a far larger magnetoresis-

tance can be achieved than in the conventional standard geometry.

Presently,sophisticated band structure calculations,electron-phonon many-body theories,etc.seem to be able to calculate a large number of transport properties very accurately.Yet,although these basic interactions have long been identified,detailed understanding continues to be elusive.Our focus here have been on pure simple metals,i.e. those for which the nearly free electron model holds rather well.
Aluminium and Indium can be considered as typical examples of polyvalent simple metals.Potassium,which is a prime example of a monovalent simple metal,shall only be dealt with obliquely in this thesis.

A recent and rather complete review of the lattice conductivity of metals does not exists in the litterature,although the fundamental article by Klemens (3) on the thermal conductivity contains several sections, wherein this subject is treated.In view of the recent developments,however,the Klemens' article is in need of modernization and extension.In the next sections we have attempted such a review.The corresponding discussion of the experimental results shall not cover the whole field,however,but confine itself to Al and In only. Furthermore,an exposition of the prevalent theories about the field dependence of the electronic thermal conductivity is given.

4.2 Theoretical Background.

4.2.1 Thermal Conduction in Metals.

Assuming only two sorts of heat carriers, the thermal conductivity in metals can be approximated by Eq.(4.1)

$$\lambda = \lambda_e + \lambda_g \qquad (4.1)$$

where usually $\lambda_e \gg \lambda_g$.
There are two main scattering processes which limit the electronic conductivity λ_e:

i) The scattering of electrons by imperfections (impurity atoms, lattice defects, etc.), represented by an electron-defect or residual resistivity: $W_o = \beta T^{-1}$

This scattering is important at the very low temperatures and is the thermal counterpart of the temperature independent electrical residual resistance ρ_o. Because the scattering by static imperfections is an elastic process, W_o is related to the residual electrical resistivity ρ_o by the Wiedemann-Franz law

$$\frac{\rho_o}{W_o T} = L_o \qquad (4.2)$$

i.e.

$$\beta = \rho_o L_o^{-1} \qquad (4.2a)$$

where

$$L_o = \rho_o / W_o T = (\pi^2/3)(k_B/e)^2 = 2.443 \times 10^{-8}\ W\Omega K^{-2} \qquad (4.2b)$$

is the value of the Lorenz-constant.

ii) The scattering of electrons by thermal lattice vibrations, leading to an electron-phonon or ideal or intrinsic resistivity: $W_i = \alpha T^2$

This is the thermal equivalent of Bloch's T^5-law for the ideal electrical resistivity, i.e. $\rho_i \sim T^5$, and this scattering is important at low and intermediate temperatures.

The total electronic thermal resistivity $W_e = \lambda_e^{-1}$ is assumed to be the sum of W_o and W_i, i.e.

$$\lambda_e^{-1} = W_e = W_o + W_i = \beta T^{-1} + \alpha T^2 \qquad (4.3)$$

which is referred to as the thermal analogue of Mathiessen's rule, originally formulated for electrical resistivities.

This simplified picture, however, invites several comments:

i) That the presence of static scattering centers induces a temperature independent electrical resistance ρ_o only is by no means self-evident, as was pointed out by De Vroomen (68), but is a consequence of the fact that the electronic system can be regarded as an assembly of independent particles with highly degenerate Fermi statistics. Analysing the influence of static impurities on the transport properties for the case of a general anisotropic metal of arbitrary Fermi surface,

and assuming Fermi statistics,electrons as independent particles and elastic scattering only,he found that

$$\rho_o = \text{constant}, W_o = \beta T^{-1}, \beta = \rho_o L_o^{-1}$$

is indeed correct to terms of the order of $(T/T_F)^2$,which are completely negligible,as for metals the Fermi temperature $T_F = E_F/k_B$ is of the order of 10^4 K.

ii) Magnetic impurities in metals do induce a temperature dependence proportional to log T in the residual resistance,i.e.

$$\rho_s = -b \log T$$

where b is a constant.This is due to an indirect exchange interaction between the magnetic ions and the conduction electrons (the Ruderman-Kittel-Kasuya-Yosida (RKKY) interaction) (220).This results in a minimum in the resistivity versus temperature curves of dilute magnetic alloys at low temperatures,the so-called Kondo effect (221).The resulting temperature dependence of the thermal resistance can be derived by means of the WF-law.

iii) Non-magnetic impurities,however,can also lead to a temperature dependent residual electrical resistance,as was shown by Kagan and Zhernov (222). Actually,due to thermal excitations,the impurity atoms are not static,but oscillate in a way,which may differ greatly from the oscillations of the atoms of the host lattice.Hence,the electrons will be incoherently and inelastically scattered,not only by the impurity atoms

Table 4.1 : Aluminium

Experimental values of α, β and E^{-1}

Sample + ref.	ρ_o Ωcm	$\alpha . 10^5$ $cmK^{-1}W^{-1}$	$\beta . 10^3$ cmK^2W^{-1}	ln β	$E^{-1} . 10^4$ $Wcm^{-1}K^{-3}$
SO1 (29)	1.3×10^{-10}	2.0	5.3	-5.24	1.1
SO2 ,,	1.9×10^{-10}	2.4	8.2	-4.80	0.9
FRW1(28)	5.68×10^{-10}	1.8	23.1	-3.77	1.2
FRW2 ,,	9.03×10^{-10}	2.1	36.4	-3.32	1.0
AWS1(62)	3.04×10^{-9}	2.70	140.	-1.97	0.8
AWS2 ,,	3.85×10^{-9}	2.72	170.	-1.77	0.8
AWS3 ,,	5.51×10^{-9}	2.72	250.	-1.39	0.8
DV1 (68)	5.28×10^{-9}	3.4	214.	-1.54	0.6
DV2 ,,	6.28×10^{-9}	3.4	250.	-1.39	0.6
DV3 ,,	3.90×10^{-9}	3.4	159.	-1.84	0.6
DV4 ,,	4.31×10^{-9}	3.4	174.	-1.75	0.6
R (63)	5.62×10^{-9}	3.2	230.	-1.47	0.7
MR (64)	2.03×10^{-8}	4.8	2300.	0.83	0.45
PHR1(35)	2.5×10^{-8}	3.5	1100.	0.095	0.6
PHR2 ,,	1.71×10^{-7}	5.2	7000.	1.95	0.4
PHR3 ,,	2.0×10^{-7}	5.8	8400.	2.13	0.4
PHR4 ,,	2.8×10^{-7}	5.8	11000.	2.42	0.4

but also by the atoms surrounding the impurity atoms and whose oscillations are perturbed, resulting in a T^2-dependent residual resistivity. As the scattering of the electrons against the thermally excited impurities are inelastic, the thermal resistivity cannot in this case be unequivocally inferred from the WF-law. Furthermore, a temperature dependent residual resistivity will lead to a violation of Matthiessen's rule. However, electron-electron scattering may also produce a T^2-dependent resistive contribution (223,224), i.e.

$$\rho_{e,e} = A\,T^2$$

This was experimentally verified recently, by very precise, high resolution electrical resistivity measurements on K and Al by Van Kempen et al. (225,226,227). In view of the fact that the measured coefficients A of the T^2-contribution were in good agreement with the theoretically predicted values for electron-electron scattering resistivity and that for most metals ρ_o and W_o can indeed to high precision be correlated by the WF-law, the possible T^2-contribution to the resistivity due to the Kagan-Zhernov effect can in most cases be taken as negligibly small.

iv) The constant α of the intrinsic thermal resistivity is related to characteristic properties of the given metal. Unfortunately, a simple general expression for α, covering the whole temperature range, cannot be given. At low temperatures ($T \ll \theta$, where θ is

Table 4.2 : Indium

Experimental values of α, β and E^{-1}

Sample + ref.	ρ_o Ωcm	$\alpha.10^3$ $cmK^{-1}W^{-1}$	$\beta.10^3$ cmK^2W^{-1}	ln β	$E^{-1}10^4$ $Wcm^{-1}K^{-3}$
CCC (13)	1.0×10^{-10}	0.96	1.8	-6.32	5.5
BRC1(14)	1.25×10^{-10}	0.62	4.56	-5.39	8.6
BRC2 ,,	1.59×10^{-10}	0.69	6.76	-5.00	7.7
PW1 (2)	5.1×10^{-10}	0.89	22.5	-3.79	6.0
PW2 ,,	6.9×10^{-10}	1.	33.8	-3.39	5.3
PW3 ,,	8.6×10^{-10}	1.185	40.0	-3.22	4.5
PW4 ,,	1.3×10^{-9}	1.12	45.0	-3.10	4.8
PW5 ,,	1.75×10^{-9}	1.24	68.8	-2.68	4.3
JT (12)	8.3×10^{-10}	1.11	34.0	-3.38	4.8
G1 (11)	8.56×10^{-10}	1.142	35.	-3.35	4.7
G2 ,,	3.45×10^{-9}	1.69	141.	-1.96	3.1
G3 ,,	1.38×10^{-8}	2.17	563.	-0.57	2.5
H (16)	3.4×10^{-9}	1.89	138.	-1.98	2.8
TCJ1(23)	8.3×10^{-10}	1.11	340.	-3.38	4.8
TCJ2 ,,	1.5×10^{-8}	2.42	608.	-0.50	2.2
TCJ3 ,,	3.0×10^{-8}	3.15	1247.	0.22	1.7
TCJ4 ,,	7.1×10^{-8}	3.42	2900.	1.065	1.6

the Debye temperature) α can be approximated (8) by

$$\alpha = 64.0 \frac{b^{2/3}}{\lambda_\infty \theta^2} \qquad (4.4)$$

where b is the valence, i.e. the number of free electrons per atom and λ_∞ is the limiting thermal conductivity at high temperatures.

The theoretical values of α, calculated according to Eq. (4.4), however, appear to be about an order of magnitude greater than the measured values, i.e.

$$\alpha_{theor.} = 10\ \alpha_{exp.}$$

This is due to the neglect of Umklapp processes, the assumption of spherical energy surfaces in the use of λ_∞ and the utilization of a constant Debye temperature (8). At high temperatures, Umklapp processes occur which are absent at low temperatures. Thus the use of λ_∞ will overestimate the low temperature scattering and the value of α will be too large. Furthermore, the use of a constant value for θ implies a simple Debye spectrum, but deviations of this model are most apparent at low temperatures. Therefore, the measured rather than the theoretical value of α should be used in calculations where it appears.

As it constitutes a measure for the intrinsic resistivity, i.e. the resistivity caused by phonon scattering, α should be independent of impurity content. Actually, more elaborate calculations (60) indicate a possible variation of α with mean free path and an increase of α

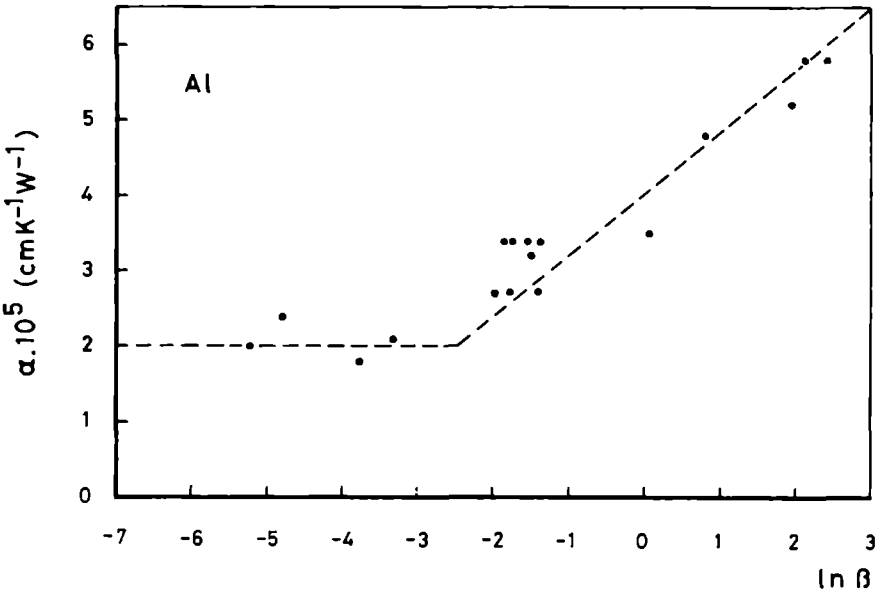

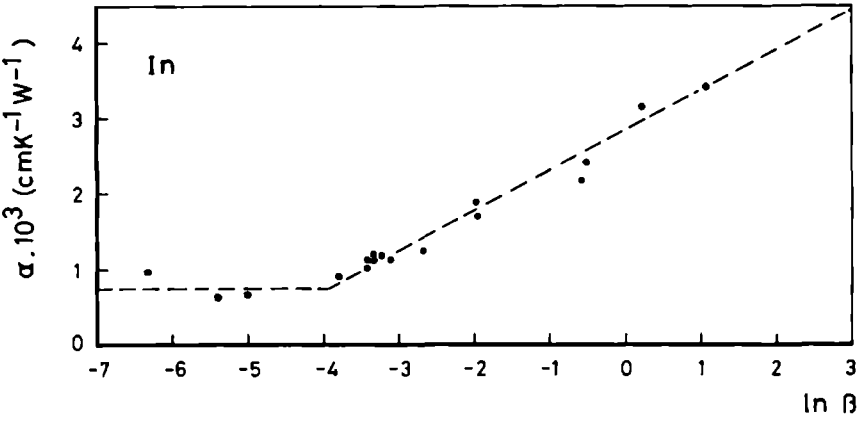

Fig.4.1 and 4.2 : α as a function of $\ln \beta$ for Al and In, respectively.

with increasing residual resistivity.Campbell has observed (61), that α increases linearly with $\ln \rho_o$.This is borne out by our present analysis of Al and In.
In Table 1 and Table 2 we have listed the results of previous measurements of α and β for Al and In of different impurity content.The values of Table 1 for Al are reproduced from Seeberg and Olsen (29),except for the results obtained by De Vroomen (68).No new data has appeared in the litterature since then.
In Fig.1 and Fig.2 we have plotted α against $\ln \beta$,which is proportional to $\ln \rho_o$,according to Eq.(4.2a).As can be seen from these curves, α seems to be independent of β only for very low impurity concentrations,but generally shows a linear $\ln \beta$-dependence.

The interference effects between the phonon and impurity contributions to the resistivity are normally referred to as Deviations from Matthiessen's Rule (DMR), which for the electrical resistivity is defined as

$$\Delta = \rho - \rho_i - \rho_o$$

Here,ρ is the measured electrical resistivity,$\rho_i = \rho_i(T)$ the ideal,temperature dependent resistivity and $\rho_o = \rho_o(c)$ the residual temperature independent resistivity,which is only linearly dependent on impurity concentration.
For the electrical resistivity,the DMR is comprehensively reviewed by Bass (218) and Cimberle et al.(219).No comprehensive study of the DMR for thermal resistivities exists as yet.

In principle,the lattice conductivity λ_g of metals

is governed by the same scattering processes as that of the dielectric solids.At low temperatures the conductivity of insulators increases sharply,and one would therefore expect λ_g of metals to be a significant part of the total thermal conductivity.The scattering of phonons by conduction electrons,which is absent in dielectric insulators,however,forms an additional resistive process.This scattering,particularly at low temperatures,is generally large compared to the other scattering processes (impurities,etc.) prevalent in non-metals.Hence,the lattice thermal conductivity in metals is much smaller than the thermal conductivity of dielectric solids.

In metals,four main processes limit the lattice conductivity λ_g:

i) The scattering of lattice waves by conduction electrons,leading to a phonon-electron resistivity $W_E = E\,T^{-2}$

At low temperatures this is the main contribution to the total phonon resistivity in pure metals.

ii) The scattering by dislocations,represented by a phonon-dislocation resistivity $W_D = D\,T^{-2}$

W_D becomes important in unannealed metals.It has the same temperature dependence as W_E and therefore,the two scattering mechanisms may not be unambigously separated in the same sample.

iii) The scattering by point-imperfections,with a phonon-point defect resistivity $W_P = P\,T$.

This limits the lattice conductivity at higher tempera-

tures.

iv) The scattering by specimen or grain boundaries, expressed by the phonon-boundary resistivity $W_B = B\,T^{-3}$ This occurs only at the lowest temperatures, although it may become important in superconductors.

Again, according to the thermal Matthiessen's rule, the total lattice resistivity $W_g = \lambda_g^{-1}$ can be written as

$$W_g = W_B + W_E + W_D + W_P \qquad (4.5)$$
$$= BT^{-3} + (E + D)T^{-2} + PT$$

B, originating from boundary scattering and P, derived from point imperfection scattering, are effective only at very low and high temperatures, respectively, and shall not be discussed further. Neither shall we include in our discussions W_U, the thermal resistivity due to umklapp processes, as it is important only at high temperatures and negligibly small in the lower temperature regions.

When dislocations are present, calculations of D for a random array of dislocations give

$$D = 0.16\, h^2 v\gamma^2 b^2 N_d k_B^{-3} \qquad (4.6)$$

an expression obtained by Ackerman (15).
Here, h is Planck's constant, v is the sound velocity, γ the Grüneisen constant, b the length of the Burgers vector of the dislocation, N_d the dislocation density and k_B the Boltzmann constant. The Ackerman result of Eq.(4.6), giving a coefficient of 0.16 is well-worth noting, since it is Klemens' earlier result (4,5), giving a numerical coefficient of 0.0435 which is most widely

quoted in published analyses of experimental data,but which overestimates by far the measured dislocation densities.The Ackerman formula is much more in keeping with the experimental findings.

As for W_E,this shall be discussed in the next subsection.

4.2.2 Theoretical Estimate of the Lattice Conductivity.

For pure metals at low temperatures,phonon-electron interactions are the dominant scattering mechanisms,which limit λ_g,i.e.

$$\lambda_g = W_E^{-1} = E^{-1}T^2 \qquad (4.7)$$

Klemens (3-5) has calculated E^{-1} on the basis of the Bloch theory and found for $T \ll \theta$

$$E^{-1} = 313/(\alpha b^{4/3}\ \theta^4) \qquad (4.8)$$

where b is the valence,θ is the Debye temperature and α is defined by Eq.(4.4).For Al and In the values for b and θ are given in Table 4.3.

From Eqs.(4.7) and (4.8) a theoretical value for the lattice thermal conductivity of Al and In may now be estimated.The results are also summarized in Table 4.1 and 4.2. In these calculations the experimental values of α have been used,rather than the theoretical results,obtainable from Eq.(4.4).Of these,only those values of α should be employed,which show no dependence on impurity

content,i.e. for which $\ln \beta < -2.5$.This is equivalent to the condition that $\rho_o < 2.10^{-9}$ Ωcm.
As will be shown later on,these theoretical predictions are in good agreement with the measured values of the lattice thermal conductivity of Al and In,despite the fact that many simplificating assumptions were presupposed to arrive at Eq.(4.8),e.g. Klemens used a spherical energy surface (free electron model),a simple Debye phonon spectrum,and assumed that all the lattice modes - longitudinal as well as transversal - interact equally strongly with the conduction electrons,and that umklapp processes in the phonon-electron interactions can be ignored. However,in contrast to Eq.(4.7),the measured temperature dependence of λ_g may differ somewhat from a quadratic behaviour.Also,more refined theories do not yield a temperature dependence strictly proportional to T^2: using a realistic phonon spectrum,calculations of Amundsen and Verbeek resulted in a $T^{2.3}$-behaviour for λ_g of Al.The current experimental accuracies,however,do not permit a discrimination between a $T^{2.0}$- and a $T^{2.3}$-dependence. In nearly all cases the measured data can,with agreement within the experimental uncertainties,be analysed in terms of T^2-dependence for the lattice conductivity at low temperatures.

Another method for calculating the lattice conductivity of metals is to use the theory of ultrasonic attenuation,whereby the attenuation coefficient α is interpreted as the reciprocal of the mean free path of a

phonon, before it is annihilated by collision with an electron, i.e. (38-43)

$$l_{ph} = \alpha^{-1}$$

According to Pippard (38), in the free electron model the attenuation constant α for longitudinal and transverse phonons is given by

$$\alpha_L = \frac{Nm}{v_L d\tau}\left\{ \frac{1}{3}\frac{a^2 \tan^{-1} a}{a - \tan^{-1} a} - 1\right\}$$

$$= \frac{Nm}{v_L d\tau}\ \frac{a}{F_L(a)} \qquad (4.9)$$

$$\alpha_T = \frac{Nm}{v_T d\tau}\left\{ 1 - \frac{3}{2a}\left(\frac{(a^2+1)\tan^{-1} a}{a} - 1\right)\right\}$$

$$= \frac{Nm}{v_T d\tau}\ \frac{a}{F_T(a)}$$

where N is the number of electrons per unit volume, m is the electron mass, d is the density of the metal, τ is the electron relaxation time, and v_L and v_T are the phonon velocities of the longitudinal and transverse modes, respectively. Furthermore

$$a = q\, l_e$$

where q is the phonon wave number and l_e is the electron mean free path.

For heavy concentrated alloys : $q\, l_e \ll 1$

$$\alpha_L = \frac{4}{15}\frac{Nmv_F}{dv_L}\, l_e q^2$$

$$\alpha_T = \frac{1}{5}\frac{Nmv_F}{dv_T}\, l_e q^2 \qquad (4.10a)$$

For pure metals : $q\,l_e \gg 1$

$$\alpha_L = \frac{\pi}{6}\frac{Nmv_F}{dv_L}\,q$$
$$\alpha_T = \frac{4}{3\pi}\frac{Nmv_F}{dv_T}\,q \qquad (4.10b)$$

For each polarization mode, the lattice conductivity is

$$\lambda_g = \frac{1}{3}\int C(q)v(q)l_{ph}(q)dq$$

where $C(q)dq$ is the Debye specific heat function, i.e.

$$C(q)dq = (k_B^4T^3/2\pi^2v^3(q)\hbar^3)(x^4e^x dx/(e^x-1)^2)$$

with $x = \hbar\omega/k_BT$, and $v(q)$ is the phonon velocity and $l_{ph}(q)$ is the phonon mean free path of wave number q. Substituting $l_{ph} = \alpha^{-1}$, and using $\tau = l_e/v_F$, where v_F is the Fermi velocity, one arrives at

$$\lambda_{g,L} = \frac{dk_B^3T^2}{6\pi^2Nm\hbar^2v_F}\int_0^\infty F_L(a)\frac{x^3e^x}{(e^x-1)^2}\,dx$$
$$\lambda_{g,T} = 2\,\frac{dk_B^3T^2}{6\pi^2Nm\hbar^2v_F}\int_0^\infty F_T(a)\frac{x^3e^x}{(e^x-1)^2}\,dx \qquad (4.11)$$

The total lattice conductivity λ_g is

$$\lambda_g = \lambda_{g,L} + \lambda_{g,T}$$

For $a = ql_e \gg 1$, i.e. in the pure limit where l_e becomes large, $F_L(a)$ reduces to $6/\pi$, and the corresponding conductivity is

$$\lambda_L^0 = \frac{dk_B^3T^2}{\pi^3Nm\hbar^2v_F}J_3 \qquad (4.12a)$$

Table 4.3 : Constants of Al and In.

Constants	Al	In
$\rho_o l_e$ (Ωcm^2)	$4. \times 10^{-12}$	5.8×10^{-12}
Debye temperature θ (K)	428.	108.
Metal density d (gcm^{-3})	2.70	7.29
Atomic weight A	26.98	114.82
Valence b	3	3
Scaling factors :		
$A^s=(10^4 b^{2/3}/A\theta)$	1.80	1.68
$B^s=(b^{2/3} n^{1/3} \theta)^{-1}$	2.42×10^{-3}	11.2×10^{-3}

Table 4.4 : Estimate of λ_g from the theory of ultrasonic attenuation for metals of different impurity content.

ρ_o Ωcm	λ_g $Wcm^{-1}K^{-1}$			
	Aluminium		Indium	
	Curve A	Curve B	Curve A	Curve B
10^{-10}	$8. \times 10^{-2} T^{2.8}$	$4 \times 10^{-5} T^2$	$1.8 \quad T^{2.8}$	$2.7 \times 10^{-4} T^2$
10^{-8}	$1.4 \times 10^{-3} T^{2.8}$	$4 \times 10^{-5} T^2$	$2.7 \times 10^{-2} T^{2.8}$	$2.7 \times 10^{-4} T^2$
10^{-6}	$4. \quad 10^{-5} T^2$	$4 \times 10^{-5} T^2$	$5. \times 10^{-4} T^{2.8}$	$2.7 \times 10^{-4} T^2$

$$J_3 = \int_0^\infty x^3 e^x (e^x-1)^{-2} dx = 7.212 \qquad (4.12b)$$

Normalizing Eq.(4.11),one obtains

$$\lambda_{g,L}/\lambda_L^0 = \frac{1}{J_3}\frac{\pi}{6}\int_0^\infty F_L(a)\,\frac{x^3 e^x}{(e^x-1)^2}\,dx = \frac{I_L}{J_3}$$

$$\lambda_{g,T}/\lambda_L^0 = \frac{2}{J_3}\frac{\pi}{6}\int_0^\infty F_T(a)\,\frac{x^3 e^x}{(e^x-1)^2}\,dx = 2\,\frac{I_T}{J_3} \qquad (4.13)$$

In the longitudinal case

$$a = ql_e = (xk_B/\hbar)(Tl_e/v_L)$$

and hence,the integral I_L is a function of (Tl_e/v_L).The same applies for the transverse case,where I_T is a function of (Tl_e/v_T). I_L and I_T as a function of (Tl_e) have been tabulated by Lindenfeld and Pennebaker (40).
Thus $(\lambda_{g,L}/\lambda_L^0)(Tl_e/v_L)$ is a universal function of (Tl_e/v_L),independent of the sample material,and a similar expression is valid for the transverse case and for the total lattice conductivity.
Using Eq.(4.12),the residual resistivity $\rho_o = mv_F/Ne^2l_e$, the Fermi velocity $v_F = (\hbar/m)(3\pi^2N)^{1/3}$,the Debye temperature $\theta = (v_L\hbar/k_B)(6\pi n)^{1/3}$,the atomic weight A and the valence b= N/n,where n, the number of atoms per unit volume, is taken proportional to d/A,the parameters of the universal function can be rewritten as $A^S(\lambda_g/\rho_o T)$ and $B^S(T/\rho_o)$, respectively,with scaling factors

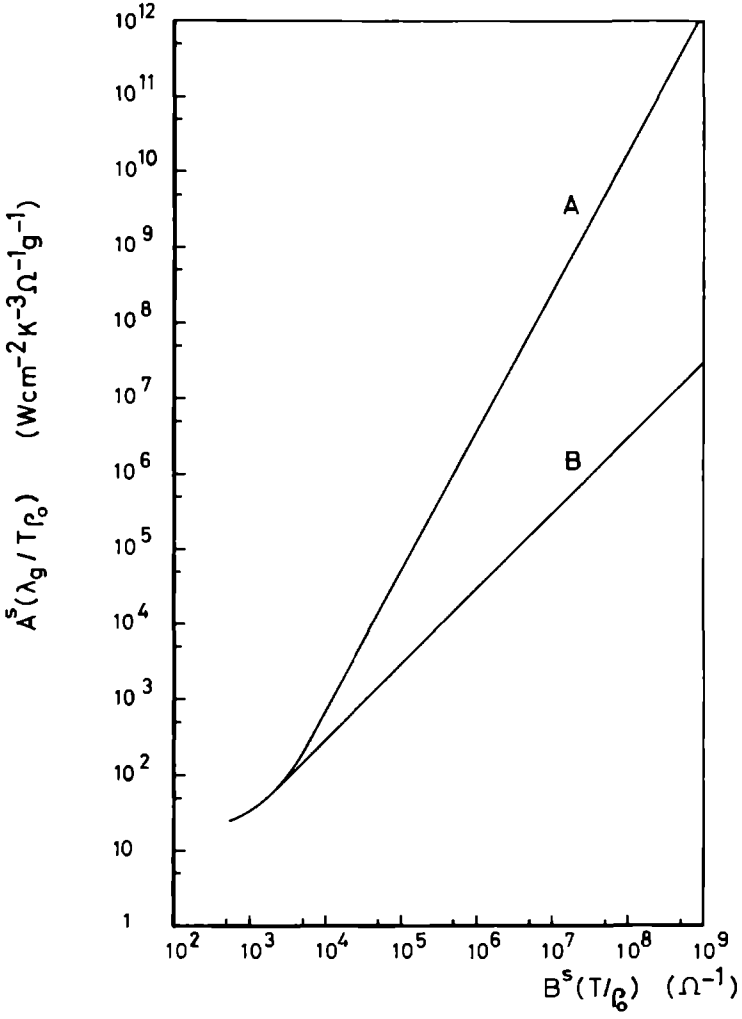

Fig.4.3 : Theoretical universal curves.

$$A^s = 10^4 (b^{2/3}/A\theta)$$
$$B^s = (b^{2/3} n^{1/3} \theta)^{-1} \qquad (4.14)$$

For a specific metal the universal function reduces to a graph of $(\lambda_g/\rho_o T)$ against (T/ρ_o). The relevant constants of Al and In, necessary to obtain the universal function and the scaling factors, are gathered in Table 4.3.

Fig.4.3 shows the universal function (curve A), valid for every metal. The predictive value for the lattice conductivity of this curve is rather low, however, when pure metals are concerned, as can be seen from Table 4.4. It is only for heavy concentrated alloys ($\rho_o \geq 10^{-6}$ Ωcm) that the right order of magnitude for λ_g is approximated. Also, the theory of ultrasonic attenuation leads to a stronger than quadratic temperature dependence of λ_g. In the pure metal limit, the universal function approaches a straight line, with a slope of about 2.8, yielding a temperature dependence of $\lambda_g \sim T^n$, $3 < n < 4$.
To obtain a T^2-dependence, one should have a curve of unity slope (curve B). As noted by Anderson and O'Hara (42), the universal curve A applies only to a metal with a spherical Fermi surface. For a nonspherical Fermi surface the electron-transverse phonon interaction is likely to be stronger (21). If one assumes an identical attenuation of longitudinal and transverse phonons, the lattice conductivity would be represented by curve B. However, there is as yet no theoretical basis for setting α_T equal to α_L.

Since both λ_g^{-1} and α are proportional to the electron-phonon interaction,one can somewhat correct for the deviations of the free electron model,by multiplying λ_g by the ratio $\alpha_{exp}/\alpha_{theor}$,where α_{exp} is the measured acoustic attenuation and α_{theor} the attenuation constant from the Pippard theory.Applying these corrections to the measured lattice conductivity of several metals,collected from the litterature,Anderson and O'Hara (42) found fair agreement with the values of curve B. Indeed,as one can also see from Table 4.4,the values for λ_g,predicted from curve B are far better in keeping with the experimental results than those predicted from curve A. The λ_g-results,derived from curve B,however,are independent of impurity content, which is theoretically unreasonable.

4.2.3 The Separation of the Lattice and Electronic Conductivities.

To measure the lattice conductivity λ_g,the electronic contribution λ_e has to be reduced drastically.The several methods,which exist to achieve this end,can be subdivided into three categories (3,4,6,7) :

i) reduction of λ_e in the superconducting state
ii) reduction of λ_e by alloying
iii) reduction of λ_e by the application of a magnetic field

The question remains,however,whether such a strict separation of the electronic and the lattice conductivity is indeed possible (54).

The standard theory assumes that the electrons move independently of the lattice ions. The coupling between the electrons and the lattice is caused by the alteration in the potential energy,due to the displacement of the lattice,and the ions are supposed to be displaced without being deformed.Evidently,this picture must be oversimplified,since account must be taken of the way in which the self-consistent field of the electrons is affected by the displacement of the lattice (55).Furthermore,the electronic heat conduction is mostly discussed,while assuming that the lattice is in thermal equilibrium,i.e. carries no heat (56). The lattice,however,does conduct heat and the lattice distribution must depart from the equilibrium state when a temperature gradient is present.The effect of this on the electronic distribution is usually ignored. The lattice conductivity in its turn,is usually calculated by setting up a separate Boltzmann-equation for the phonon distribution,under the assumption that the conduction electrons have their equilibrium distribution. This way of calculating the steady-state electronic and phonon distribution is not strictly correct,since the collision integrals,which determine the rate of change either of the phonon or of the electron distribution function,depend upon the actual,non-equilibrium of both the distribution functions,and neither of these are known

until the steady-state equation has been solved.

The magnitudes of these effects have been calculated by Klemens (3). In the case of an electronic deviation from equilibrium, a restoring influence is produced by the thermoelectric field which is built up as a consequence of the condition that the electric current should vanish, and the effect on the phonon distribution is of the order of $(k_B T/\zeta)^2$, where ζ is the chemical potential.
In the case of a phononic deviation from equilibrium, the effect on the electron distribution is of the order of $(k_B T/\zeta)(\lambda_g/\lambda_e)$. Since $k_B T \ll \zeta$ and $\lambda_g \ll \lambda_e$, both these effects are negligible and can safely be disregarded.
Thus, it appears that each system, acting on the other, tends to drive it to an equilibrium state, irrespective of its own non-equilibrium.
A clear, quantitative exposition of these problems has also been given by De Vroomen (68) with the emphasis on phonondrag effects. Furthermore, the problem was also considered by Hanna and Sondheimer (73). Retaining the simplified assumption of a free electron gas, they set up two simultaneous and coupled Boltzmann equations for the distribution functions of the electrons and the phonons and solved these equations by a method of successive approximations. A more rigorous solution was obtained by Bailyn (74), but in all these investigations only the case of zero magnetic field has been treated.

4.2.4 Reduction of λ_e in the Superconducting State.

When the temperature is lowered below the critical temperature T_c, more and more electrons undergo a transition from the "disordered", thermally excited normal state to the "well-ordered" superconducting ground state, where they have zero entropy and therefore, cannot further participate in the heat transport.
The entropy is a measure of the disorder of a system and when the temperature is lowered, the entropy in the superconducting state reduces to zero much more rapidly than in the normal state. As a consequence, the specific heat in the superconducting state and the corresponding electronic thermal conductivity decreases much faster than in the normal state. Hence, at low enough temperatures one might expect the conductivity to be almost entirely due to phonons.

The procedure to separate in the superconducting state the electronic thermal conductivity λ_{es} from the total conductivity λ_s to obtain the lattice conductivity λ_{gs} is generally as follows :
On the basis of the BCS-theory (17), Bardeen, Rickayzen and Tewordt (BRT) (18) obtained an exact expression for the ratio of the electronic thermal conductivity in the superconducting and the normal state, provided that scattering due to static defects is the only significant resistive mechanism, i.e.

$$R_e = \frac{\lambda_{es}}{\lambda_{en}} = \frac{2F_1(-y) + 2y\ln(1+e^{-y}) + y^2/(1+e^{y})}{2F_1(0)}$$

$$F_n(-y) = \int_0^{\infty} \frac{z^n dz}{1+e^{z+y}} \qquad (4.15)$$

$$y = \varepsilon(T)/k_B T$$

Here $2\varepsilon(T)$ is the temperature dependent energy gap (17), which was tabulated by Mühlschlegel (44) for the BCS-case, $F_n(-y)$ is a function, tabulated by Rhodes (45), while recently Ramos and Sanchez (46) has tabulated $R_e = \lambda_{es}/\lambda_{en}$. Assuming lattice defects and impurity scattering only, $\lambda_{en} = L_o T/\rho_o$ is given by the WF-law (Eq.(4.2)) and

$$\lambda_{gs} = \lambda_s - R_e L_o T/\rho_o \qquad (4.16)$$

However, it is difficult to ascertain that electron-defect scattering is indeed the only or dominating resistive mechanism. This may be the case in unannealed metals and alloys, but is not likely for well-annealed, pure metals. If electron-phonon scattering is appreciable, $\lambda_{en} = (\alpha T^2 + \beta T^{-1})^{-1}$ (Eq.(4.3)), and in that case Kadanoff and Martin (19) obtained

$$R_e = \frac{\lambda_{es}}{\lambda_{en}} = \frac{3}{2\pi^2} \int_0^{\infty} d(\beta\varepsilon)(\beta\varepsilon)^2 \operatorname{sech}^2(\beta\varepsilon/2) \times \qquad (4.17)$$

$$\times \frac{1 + at^3}{(\beta\varepsilon/\beta E) + at^3}$$

Here, $\beta^{-1} = k_B T$ and $E = (\xi^2 + \varepsilon^2)^{1/2}$ is the excitation energy of the quasiparticles, where ξ is the Bloch energy in the normal state, relative to the Fermi energy and ε is the superconducting gap energy, while a is defined as the ratio of phonon to impurity resistance at T_c, i.e.

$$a = W_i/W_o = \alpha T_c^3/\beta \qquad (4.18)$$

In the limit of impurity resistance only (a= 0), Eq.(4.17) is identical to the BRT-expression of Eq.(4.15).

Aluminium seems to be in good accord with the BRT-formula (20), while Indium is found to be in better agreement with the Kadanoff-Martin theory, with a=1.3 (21). However, when taking transverse lattice waves into account as well (24), Indium also appears to be in keeping with the BRT-theory. The results of the lattice conductivity measurements in the superconducting state for Al (T_c=1.19 K) and In (T_c= 3.4 K), as obtained from the literature, are summarized in Table 4.5. These results as presented here, do not appear in this straightforward form in the cited references, but had to be extrapolated from the published data.

For Al, the obtained lattice conductivity is more than an order of magnitude too high, as compared with the theoretical predictions of Table 4.1. In view of the high dislocation density ($N_d \sim 10^6$ cm^{-2}) present, this is the more unexpected. The results for Indium, except for the lowest temperatures (25,65), show an increase of λ_{gs} with decreasing temperature. This can be attributed to the fact,

Table 4.5 : Experimental λ_g-values of pure and alloyed Al and In in the superconducting state.
TI = temperature interval of the measurements.

Sample	ρ_o Ωcm	λ_{gs} $Wcm^{-1}K^{-1}$		TI K	Ref.
pure Al		0.0016	$T^{1.7}$	0.05-0.1	(22)
pure In		0.09	T^{3}	0.25-1.0	(65)
pure In		0.05	$T^{1.9}$	0.25-1.0	,,
pure In	1.25×10^{-9}	0.6	T^{4}	0.2 -0.5	(25)
pure In	1.25×10^{-9}	0.4	T^{4}	0.2 -0.5	,,
In-Hg		0.13	$T^{-2.7}$	1.4 -2.	(23)
In-Hg		0.08	$T^{-2.7}$	1.4 -2.	,,
In-Bi	6.9×10^{-7}	0.185	$T^{-2.7}$	1.4 -3.	(24)
In-Bi	2.9×10^{-6}	0.135	$T^{-2.6}$	1.4 -3.	,,
In-Sn	5.3×10^{-7}	0.17	$T^{-2.6}$	1.4 -3	,,
In-Sn	2.1×10^{-6}	0.18	$T^{-2.5}$	1.4 -3	,,

that as the temperature is lowered,more and more electrons are removed as scattering centers of the phonons by going into the superconducting groundstate,so that the lattice conductivity becomes larger.
It should be noted at this point,that λ_{gs} is peculiar to the superconducting state and is not the same as that appertaining to the normal state,where electrons can interact with the phonons and so reduce λ_{gn}.As the electrons fall into the superconducting state,they cannot be scattered by the phonons,but conversely,the phonons themselves will not be scattered by these electrons,and the lattice conductivity increases.At the lowest temperatures, boundary scattering becomes important and the lattice conductivity decreases again,proportional to T^3(25,26,65). Hence,the lattice conductivity of a superconductor appears to follow the behaviour of a dielectric solid, rather than that of a normal metal.

Apart from the fact that not all metals become superconducting,which make this method not generally applicable to all metals,it follows from our analysis that for practical as well as theoretical reasons,the reduction of λ_e by going into the superconducting state cannot be used as a good method for the measurement of the lattice conductivity of pure metals.

In their fundamental article,BRT (18) also obtained expressions for the lattice conductivity of a superconductor in both the normal and the superconducting state.In the low temperature limit λ_{gn} reduces to

Table 4.6 : Experimental λ_g-values of pure and alloyed Al

Sample	ρ_o $10^{-6}\Omega$cm	$10^4\lambda_g/T^2$ $Wcm^{-1}K^{-1}$	$10^{-6}\rho_o^{-1}$ at 1 K	$10^4\lambda_g\rho_o^{-1}$ at 1 K	Ref.
pure Al		5200.			(72)
pure Al	1.89	0.62	0.529	32.80	(32)
pure Al	1.98	0.75	0.505	37.88	,,
pure Al	2.02	0.41	0.495	20.30	,,
pure Al	2.04	0.67	0.490	32.84	,,
pure Al	3.33	0.35	0.300	10.51	,,
Al-Cu	0.123	1.0	8.13	81.30	(33)
AL-Cu	1.10	1.0	0.909	9o.91	,,
Al-Cu	3.3	1.0	0.303	30.30	(35)
Al-Mn	0.95	2.5	1.053	263.16	,,
Al-Mg	2.0	1.5	0.5	75.	,,
Al-Mg	2.3	1.0	0.435	43.48	,,
Al-Mg	3.4	1.1	0.294	32.35	,,
Al-Mg	3.4	1.5	0.294	44.12	,,
Al-Mg	1.83	0.60	0.546	32.79	(32)
Al-Mg	1.84	0.64	0.543	34.78	,,
Al-Mg	1.86	0.81	0.538	43.55	,,
Al-Mg	1.87	0.63	0.535	33.69	,,
Al-Mg	2.05	0.40	0.488	19.51	,,
Al-Mg	2.36	0.64	0.424	27.12	,,
Al-Mg	2.42	0.62	0.413	25.62	,,
Al-Mg	2.52	0.52	0.397	20.63	,,
Al-Mg	0.6	60.			(34)

$$\lambda_{gn} = 7.2\ D(T/\theta)^2 \qquad (4.19)$$

The constant D is independent of temperature and appears also in the BRT-formula for λ_{gs}. Given λ_{gs}, a more sensible procedure would be to fit the measured data to the BRT-expression for λ_{gs} to obtain D, and subsequently calculate λ_{gn} from Eq.(4.19).

4.2.5 Reduction of λ_e by Alloying.

The thermal resistivity of the electronic heat conduction, as expressed by Eq.(4.3)

$$W_e = W_o + W_i = \beta T^{-1} + \alpha T^2 \qquad (4.3)$$

was first obtained by Wilson (10). In a more modern way, Kadanoff and Martin (19), using many-body theory, arrived at the same result. The constant β is related to the electrical residual resistivity ρ_o through the WF-law:

$$\beta = \rho_o L_o^{-1} \qquad (4.2a)$$

while in theory, α is independent of the impurity content. Adding impurities to the host metal will enhance β and consequently, decrease $\lambda_e = W_e^{-1}$. This is most pronounced at low temperatures.

In contrast to their effect on the electronic conduction, the impurity atoms, being point defects, will only scatter the shorter lattice waves, and leave the low tem-

Table 4.7 : Experimental λ_g-values of pure and alloyed In.

Sample	ρ_o $10^{-6}\Omega$cm	$10^4\lambda_g/T^2$ $Wcm^{-1}K^{-1}$	$10^{-6}\rho_\Omega^{-1}$ at 1 K	$10^4\lambda_g\rho_o^{-1}$ at 1 K	Ref.
pure In (extrapolated)		6.0			(31)
In-Th	1.01	6.4	0.99	633.66	,,
In-Th	2.87	3.5	0.35	121.95	,,
In-Th	3.75	4.2	0.27	112.0	,,
In-Th	5.45	3.3	0.18	60.55	,,
In-Th	6.00	1.8	0.17	30.0	,,
In-Th	6.93	1.0	0.14	14.43	,,
In-Sn	0.53	6.5	1.89	1226.42	(24)
In-Sn	2.13	4.3	0.47	201.88	,,
In-Bi	0.69	7.0	1.45	1014.50	,,
In-Bi	2.86	3.8	0.35	132.87	,,

perature, long wavelength phonon conduction unaffected. Thus the addition of impurities will decrease λ_e far more substantially than λ_g, and make λ_g a much larger fraction of the total conductivity at low temperatures than it is the case in the pure metal.

The addition of impurities is best achieved by alloying with suitable elements, ideally with those having different valence but approximately equal atomic mass and radius, so as not to introduce lattice defects.

The measured λ_g values of Al- and In-alloys, as they appeared in the literature, have been assembled in Table 4.6 and Table 4.7, respectively.

To separate λ_g from λ_e, one assumes that at low temperatures

i) λ_e is limited by static, nonmagnetic impurity scattering only, i.e.

$$\lambda_e = W_o^{-1} = \beta^{-1} T = \rho_o^{-1} L_o T \qquad (4.20)$$

This should be checked by measuring the electrical resistivity to see if it is indeed correlated by the WF-law.

ii) λ_g, both for pure and alloyed metals, is limited by phonon-electron scattering, i.e.

$$\lambda_g = W_E^{-1} = E^{-1} T^2 \qquad (4.21)$$

The total conductivity of the alloyed metal will then be of the form

$$\lambda = E^{-1} T^2 + \beta^{-1} T \qquad (4.22)$$

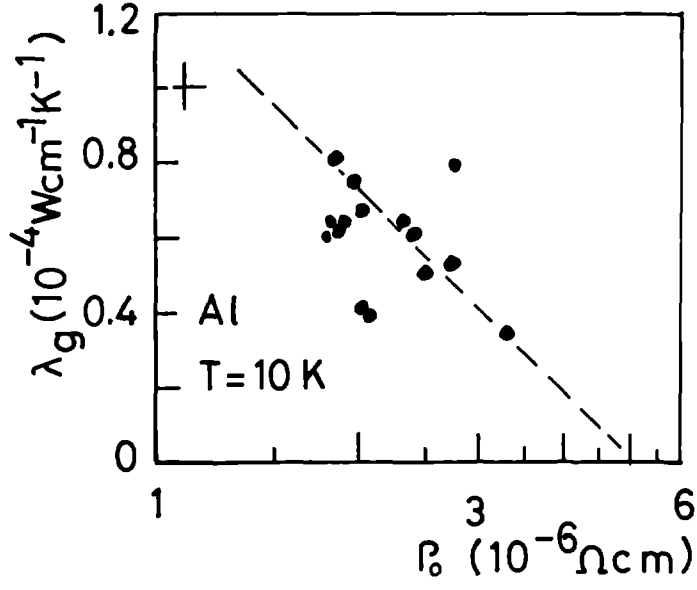

Fig.4.4 : The lattice conductivity of Al-alloys as a function of their residual resistivity (data taken from ref.(32)).The cross-mark represents the result of the lattice conductivity of pure Al,as obtained in this thesis.

Plotting λ/T versus T a straight line is drawn through the data points with a slope,equated to E^{-1},and an intercept β^{-1} on the λ/T-axis.It should be verified that this intercept has indeed the value $\rho_o^{-1}L_o$.
Doing this for alloys containing different percentages of solute atoms,and plotting the resultant E^{-1}-values against the corresponding percentage of solute atoms, $A= E^{-1}$ of the pure (0 % solute atoms) metal can be obtained by extrapolation,and this yields

$$\lambda_g = AT^2$$

This procedure was employed by Sladek (31) for In-Th alloys,to obtain the lattice conductivity of Indium.In this analysis,however, a T^2-dependence is assumed a priori,and what one measures is but the proportionality constant A.

For Aluminium,Klaffky et al.(32) obtained an experimental temperature dependence of λ_g from Al-Mg alloys, by substracting λ_e from the measured thermal conductivity λ ,i.e. $\lambda_g = \lambda - \lambda_e$.
The electronic conductivity $\lambda_e^{-1} = \rho_o^{-1}L_oT + \alpha T^2$ was calculated,using the measured value ρ_o of the alloy and a value for α as obtained by others for pure Al,taken from the literature.
Finding at low temperatures no difference in the lattice conductivity of alloys with different impurity content, they conclude that it also represents the lattice conductivity value for pure Al.More or less the same procedure was followed by Amundsen et al.(33) in the case of Al-Cu

alloys.Both obtained good agreement with the theoretical estimates of Table 4.1.

The fact,however,that two samples with a residual resistivity of 1.86 μΩcm and 2.81 μΩcm,respectively (32),yielded identical values for their lattice conductivity,constitute insufficient evidence for the conclusion that the resultant lattice conductivity is independent of impurity content and may be identified with the lattice conductivity of the pure sample.Indeed,in a plot of all the λ_g-results as obtained by Klaffky et al. (32) against the corresponding residual resistivities,a ρ_o-dependence may still be seen (Fig.4.4).Their result of $\lambda_g = 0.8 \times 10^{-4} T^2$ $Wcm^{-1}K^{-1}$ therefore,despite their claim that it represents the first reliable value for the intrinsic lattice thermal conductivity of well-annealed Aluminium,may be too low.

The values obtained by Powell et al.(35) range from $A = 0.9 \times 10^{-4}$ to 2.5×10^{-4} $Wcm^{-1}K^{-3}$,but no clear dependence on ρ_o could be detected.

The value of $A = 60 \times 10^{-4}$ $Wcm^{-1}K^{-3}$,reported by Täubert et al.(34) for an Al-Mg alloy is far too high and remains unexplicable.

The value of $A = 0.52$ $Wcm^{-1}K^{-3}$,given by Willot (72),is well-nigh impossible.Willot measured on polycrystalline wires with a diameter of 1 mm.Estimating the phonon mean free path from the kinetic formula

$$\lambda_g = \frac{1}{3} Cvl_{ph}$$

where $C = 234\ Nk_B(T/\theta)^3$ is the specific heat, $N = 6\times10^{22}$ cm^{-3} is the atomic density, $v = 3\times10^5$ cm/s is the sound velocity, leads to a value of $l_{ph} = 20$ mm at 1 K, i.e. 20 times the diameter of the sample.

Table 4.6 and Table 4.7 also show the $(\lambda_g/T\rho_o)$- and (T/ρ_o)-values at T= 1 K for the different alloys. These values are plotted in Fig.4.5, together with the theoretical universal curves for Al and In. The good agreement in the case of Indium between the theoretical curve and the experimental values is but a fortuitous coincidence: for T= 10 K, both the $(\lambda_g/T\rho_o)$- and (T/ρ_o)-coordinates would be a factor 10 higher. For intermediate temperatures the values would lie upon a line, parallel to the B-curve, connecting the 1 K point to the 10 K point.

The alloying technique has been the most used method to obtain the lattice conductivity of metals. Much of our present knowledge of λ_g has been derived in that way. Several complications may arise, however, in employing this method :

i) The addition of impurities will alter the phonon spectrum, which will also change λ_g. This can be minimized by using solute atoms of approximately equal atomic weight and radius as that of the solvent metal.

ii) λ_g varies surprisingly rapidly for very small concentrations of solute impurities, which is due to changes in the band structure of the parent metal (36).

iii) The introduction of impurities is associated with the creation of other imperfections, notably dis-

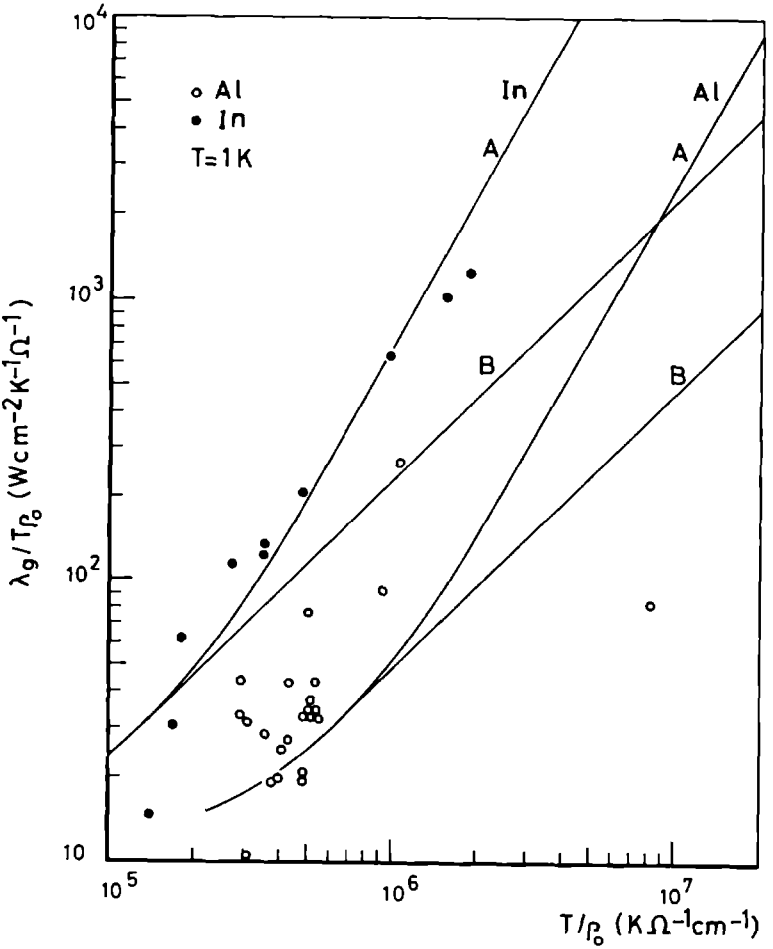

Fig.4.5 : Comparison of the experimental lattice conductivity results of Al- and In-alloys with their respective theoretical curves.

locations,which decrease λ_g at low temperatures.Scattering by dislocations give the same T^{-2}-dependence of the thermal resistivity as scattering by electrons.Thus λ_g of alloys may be systematically smaller than λ_g of pure metals (40).

iv) Alloying changes the electron concentration and hence the amount of scattering (37).

v) The alloying method is not applicable to the alkali metals,because the only alloying elements available for use,also reduce λ_g besides λ_e,so that the λ_g of the alkali alloys may not be a good indication of that of the pure metal (41).

vi) The validity of the thermal Matthiessen's rule,i.e. the approximation,whereby the thermal resistivity is regarded as being additively composed of the resistivities of the different scattering processes present,becomes progressively poorer,the more these scattering processes differ from each other in their frequency dependence.

Particularly in alloys,the phonon-electron scattering and point defect scattering vary as the first and fourth power of frequency (3),respectively,and the resistance is underestimated by the thermal Matthiessen's rule. Furthermore,the effects of point defects become appreciable at somewhat lower temperatures than one would have expected from the additive resistance rule (66).

vii) At low temperatures λ_g may not follow a simple T^2-law for alloys.This can be due to several effects:

a) The magnitude of the electronic mean free path l_e, relative to the phonon wavelength, or its inverse, the phonon wave number q, as first pointed out by Pippard (38).

Using the kinetic formula

$$\lambda_g = \frac{1}{3} C v_s l_{ph}$$

where the lattice specific heat $C \propto T^3$, v_s is the sound velocity and taken as constant and the phonon mean free path $l_{ph} = \alpha^{-1}$, the temperature dependence of λ_g may be derived. The mean phonon frequency $\omega = v_s q$ changes as T. From Eq.(4.10) it follows that if $ql_e \gg 1$, α varies as q, i.e. as T and hence $\lambda_g \propto T^2$; but if $ql_e \ll 1$, α varies as q^2, i.e. as T^2, and thus $\lambda_g \propto T$.

It was indeed found (39) that in alloys of high resistance and using

$$\lambda_g = AT^2 + \beta^{-1}T \qquad (4.22)$$

the T^2-term is smaller than would be expected, and the T-term considerably larger than would be deduced, by using the WF-law. It would be desirable to measure the lattice conductivity of a heavy concentrated alloy over a wide range of temperatures to observe the transition between the two types of behaviour, i.e. from a T^2- to a T-behaviour as the temperature is lowered.

b) In the simple theory the effect of the transverse phonons are either completely neglected or treated on an equal footing with the longitudinal lattice waves : the relative magnitude of the heat, transported by

the transversal and longitudinal branches are taken as either $\lambda_T/\lambda_L \approx 0$ or 1.

It was found, however, that in alloys λ_T, rather than λ_L, is by far the dominating term in the heat conduction, and that $\lambda_T/\lambda_L \approx 1$ for $ql_e \ll 1$ only. But as ql_e becomes larger, λ_T rises more rapidly than λ_L and approaches a cubic dependence on the temperature (40).

c) The effect of boundary scattering may mask the temperature dependence due to electron-phonon interactions in a complicated way (43).

d) Non-static, thermally excited impurities (222) may induced a more complicated temperature dependence of the residual thermal resistivity W_o than was derived by assuming a constant residual resistivity and the validity of the WF-law.

It follows from these considerations that some caution must be exercised in evaluating the results for the lattice conductivity of pure metals, derived by an extrapolation from the values acquired for alloys. Yet, the results obtained by the alloying method are in reasonably good agreement with each other and with the theoretical predictions.

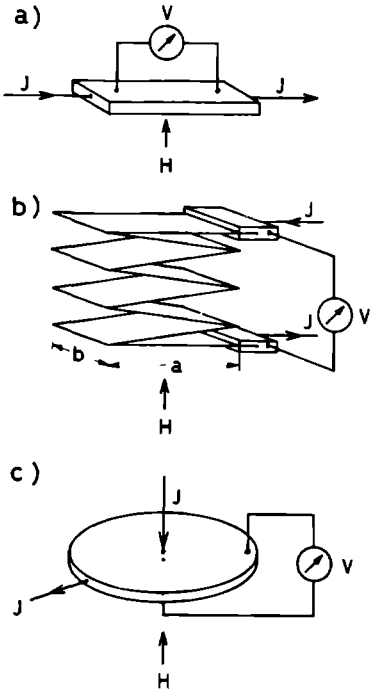

Fig.4.6 : Different configurations to reduce λ_e by means of a magnetic field: a) standard configuration b) zigzag configuration, c) Corbino configuration.

4.2.6 Reduction of λ_e by the Application of a Magnetic Field.

The above considerations show that the superconducting method is not to be recommended for the acquisition of the lattice conductivity of metals,while the alloying method introduces uncertainties in one's knowledge of λ_g of the pure crystal,though the error may be small.

The only method,specifically applicable to a pure-crystalline,normal state metal is the magnetic field method.Furthermore,unlike the alloying technique,where a T^2-dependence is a priori assumed,i.e. $\lambda_g = AT^2$, and only the constant of proportionality A of the pure metal can be obtained,the magnetic field method permits a direct experimental determination of the temperature dependence of λ_g.

When a magnetic field H is imposed on a metal,which is also subjected to an electric field E,the electrons experience an acceleration,due to the so-called Lorentz force

$$F = e(E + (v \times H)/c) \qquad (4.23)$$

where v is the group velocity of the electrons.
To see the effect of the magnetic field on the electronic flow : consider a metal in the nearly free electron approximation,with a spherical Fermi surface,where only closed electron orbits exist.Since the electron motion in the direction of the field is not affected by the Lorentz

force,one would not expect the field to have a large effect on the conductivity parallel to H.
But an electron trying to move at right angles to H, is deflected by the field and goes around in tight circles - the higher the field,the smaller the circles.The acceleration it gets from the electric field on one side of the circle is mostly cancelled by its decelleration on the other side.Thus the transverse magnetoconductivity is lowered at high fields,due to a positive transverse magnetoresistance.

In the standard configuration (Fig.4.6),which consists of a strip,aligned parallel to the xy-plane and through which a current is passed,while the magnetic field is applied perpendicular to it in the z-direction, the electrical or thermal magnetoresistance is counteracted by the Hall effect or its thermal equivalent,the Righi-Leduc effect,respectively.
Indeed,in nearly all the standard textbooks on solid state physics (e.g. 47-49) one finds proved that in the free electron model no transverse magnetoresistance exists.However,the validity of these proofs rest upon the unrealistic assumptions of either a relaxation time independent of electron velocity,or of zero temperature (50). In theory (51),as well as experimentally,a positive transverse magnetoresistance is nearly always present,leading to a field dependent change in the magnetoconductivity.

To separate then,in the standard configuration,the lattice from the electronic conductivity,one generally

measures both the thermal conductivity $\lambda(H,T)$ and the electrical conductivity $\sigma(H,T)$ as a function of field at different temperatures.

Defining the Lorenz function L(T) as

$$L(T) = \lambda_e(H,T)/\sigma(H,T)T \qquad (4.24)$$

one finds for the total thermal conductivity

$$\lambda(H,T) = TL(T)\sigma(H,T) + \lambda_g(T) \qquad (4.25a)$$

Plotting $\lambda(H)$ versus $\sigma(H)$ at different T-values, should then yield straight lines with a slope TL and an intercept λ_g. Alternatively, Eq(4.25a) can also be put into the form

$$L(H,T) = L(T) + \lambda_g(T)\rho(H,T)T^{-1} \qquad (4.25b)$$

where $\rho(H,T)$ is the resistance as a function of field and temperature.

These methods are based upon the assumptions that

i) both the thermal and the electrical magnetoconductivities $\lambda_e(H)$ and $\sigma(H)$ are decreasing with the same dependence upon H.

ii) the Lorenz function L(T) is independent of the applied magnetic field

iii) $\lambda_e(H)$ and $\sigma(H)$ are both zero, when H is infinite

iv) λ_g is not influenced by H

The advantage of the method as expressed by Eq.(4.25a) is, that an exact knowledge of the field dependence of $\lambda_e(H)$ and $\sigma(H)$ is not required. However, doubts exist as to the validity of assumtion ii), which of course, is but a con-

sequence of assumption i).In fact,both theoretical considerations (52) as well as experimental evidence (2,53) adduce,that in general,L is not independent of H.
With regard to assumption iii): this holds only for closed orbit,compensated metals or for metals with open orbits. For uncompensated metals with a closed Fermi surface like Al and In,theory (84-89) predicts a saturation for $\lambda_e(H)$ and $\sigma(H)$ in strong magnetic fields.It is not correct then to extrapolate to $\sigma(H)= 0$,but the graph should be extrapolated to its end point at $\sigma(H)= \sigma(\infty)$ instead.This would give a somewhat larger value for λ_g than extrapolating to $\sigma(H)= 0$.
As for assumption iv): there is of course,no direct effect of H on λ_g,but in the temperature range where λ_g is limited by electron-phonon scattering only,one may surmise an indirect effect on the lattice conductivity as the path of the electrons are changed by the magnetic field.Makinson (56) has shown that the interaction of the lattice with the electrons depends solely upon the equilibrium properties of the lattice,provided that the electronic distribution is in equilibrium.Extending these arguments, Sondheimer and Wilson (52) argued,that no extra complication is introduced by the presence of a magnetic field, and they obtained the same results for λ_g whether a magnetic field was present or not.
Thus,under the assumptions that the lattice non-equilibrium has no influence at all on the electronic distribution and that the electronic non-equilibrium leaves the

lattice distribution unaffected,a magnetic field is expected to have no effect on the lattice conductivity. As explained in subsection 4.2.3,these assumptions rest on a safe basis and the correction terms accounting for the non-equilibrium effects are negligibly small. These effects can also be translated in terms of the phonon drag (68).It will be recalled that phonon drag is a phenomenon,arising from the interaction between an electron current and the phonon system,or equivalently, a phonon current on the electron system.If in a metal a phonon current is set up,say from left to right,as a consequence of a temperature gradient,the electrons are more likely to absorb a phonon which travels to the right than one traveling to the left,since more of the former are present.Consequently,the electrons,absorbing the phonon momentum,are dragged along by the phonons just as in a viscous flow.On the other hand,the excess of hot electrons drifting down the temperature gradient must also drag the phonon distribution preferentially in one direction. Tsuji (75) has considered the effect of an external magnetic field on the phonon drag.He could show that for a free electron gas and an isotropic metal (polycrystalline sample) the phonon drag effect can be seen in the thermoelectric power,but does not appear in the galvanomagnetic and thermomagnetic effects.For anisotropic metals,however, the non-equilibrium distribution of the phonons ads a phonon drag term to the Righi-Leduc coefficient in the presence of a magnetic field,if the departures from a sphe-

rical Fermi surface are significant.Paul (77) has also calculated the effects of the non-equilibrium distribution of the phonons on the thermal conductivity and the thermomagnetic effects of metals,but,as pointed out by Tsuji (75),his article contains some important errors, which invalidate his results.Seemingly unaware of the works of these authors,Flerov (76) has again considered this problem and reach the same conclusions about a negligibly small effect of the electronic and phononic non-equilibrium in non-zero magnetic fields.

The magnetoresistance would be greatly enhanced, if the formation of the Hall field in the electrical,and the Righi-Leduc field in the thermal case could be prevented.These fields arise from boundary conditions and are essentially geometric effects (69).To surmount these boundary effects,special configurations can be utilized, which amounts to an artificial extension of one of the *sample boundaries to infinity*.

A technique,first employed by Cotti (57,58) for the electrical conductivity and subsequently by Thorn and Wyder (59) for the thermal conductivity of Indium, is the so-called Zigzag configuration (Fig.4.6b). The sample consists of a metal strip which is folded in a zigzag form while a magnetic field is applied perpendicular to the planes of the folds.In this configuration the magnetic field will appear to have switched direction in each successive fold with regard to the electronic flow. The sideways deflections due to the field will be alter-

natively in a clockwise and counterclockwise direction, thereby apparently cancelling each other and preventing the formation of the Hall voltage at the boundaries. The data can be analysed,using the theory of Lippmann and Kuhrt (70) of the electronic flow in a rectangular sample, with a magnetic field perpendicular to the plane of the sample. Thorn and Wyder (59) has used this technique to obtain the Righi-Leduc constant for Indium only,but this method can equally well be employed to obtain the lattice conductivity,especially when it is supplemented by a simultaneous measurement of the electrical conductivity. Obviously,this method cannot be used when single crystals or bulk materials are to be measured.This technique is suitable only to measure λ_g in metal foils where size effects have to be included.Also,the folding will introduce extra dislocations which will have a considerable influence on the transport properties of the lattice.

Another geometry,which prevents the formation of the Hall or Righi-Leduc field is the Corbino configuration (Fig.4.6c)The sample consists of a thin cylindrical disk,perforated by a central hole while the magnetic field is applied perpendicular to the plane of the disk.The heat current comes in at the inner boundary and if no field is present,traverses the sample radially to the outer perimeter.If a magnetic field is present,the electronic heat carriers acquire a velocity component,perpendicular to their tangential direction and reach the outer edge not in a straight line but in a logarithmic spiral.In the li-

mit of an infinite magnetic field strength,this velocity component will dominate and the electronic heat current will flow perpendicular to the temperature gradient,whirling around in the sample and not reaching the outer rim at all.In this way a considerable reduction of the electronic thermal component can be achieved.

In the high field limit,standard theory (52) gives for the electronic thermal conductivity

$$\lambda_e(H) = \left(\frac{W(H)}{A_{RL}^2}\right) H^{-2} \qquad (4.26)$$

where W(H) is the thermal resistivity and A_{RL} is the Righi-Leduc constant.The total thermal conductivity is then

$$\lambda(H,T) = \left(\frac{W(H,T)}{A_{RL}^2(T)}\right) H^{-2} + \lambda_g(T) \qquad (4.27)$$

If $W(H,T)/A_{RL}^2(T)$ has a constant value,Eq.(4.27) permits the evaluation of λ_g.At high fields A_{RL} is indeed constant (196) while for uncompensated metals with a closed Fermi surface like Al and In,theory (84-89) predicts W(H) to reach a saturation value.Measuring λ as a function of H at different temperatures and plotting λ versus H^{-2} should then yield straight lines with intercepts λ_g at $H^{-2} = 0$.However,experimental evidence show,that both the electrical and electronic thermal resistivities of Al and In do not saturate but increase linearly with field and that a graph of λ versus H^{-2} does not yield a straight line (72,73),thereby complicating the extrapolation procedure to $H^{-2} = 0$.

The extrapolation to infinite fields is the crucial feature of the magnetic field methods. This extrapolation cannot be executed properly, unless the field dependence of the electronic thermal conductivity is well known. To appreciate this point, we shall discuss the field behaviour of $\lambda_e(H)$ in the next subsection.

There are surprisingly few references in the literature, which report measurements to determine the lattice conductivity of Al and In by means of the magnetic field method.

For Indium there is none, except our preliminary publications (159,160) of the results, fully described in this thesis.

For Aluminium there is only one : Sirota et al.(71) have measured the thermal conductivity of an Al single crystal (RRR= 6000) in the standard configuration in the temperature range between 6 K and 57 K and in fields up to 5 T. In the small temperature interval between 10 K and 12 K they found no change in the thermal conductivity when the field is enhanced from 3 T to 5 T, while for temperatures below and above that interval λ decreases. From this field independent behaviour they conclude that in the 10 - 12 K temperature region they have measured the lattice conductivity of Al, which in that region could be expressed in the following form

$$\lambda_g = 0.383\ T^3 \exp(-0.26\ T)$$

For 10 K, $\lambda_g = 28\ \mathrm{Wcm^{-1}K^{-1}}$. Equating this value to $\lambda_g = AT^2$ for a rough estimate, one obtains $\lambda_g = 0.28\ T^2\ \mathrm{Wcm^{-1}K^{-1}}$,

which is about two orders of magnitude too high as compared with the theoretical estimates (Table 4.1) and the results from Al-alloys (32,33 and Table 4.6).

4.2.7 The Magnetic Field Dependence.

The influence of a magnetic field on the conductivity of a metal is due to its effect on the motions of the electrons.However,the simplest variant of the electron theory of transport phenomena (the relaxation time approximation for one group of charge carriers with an isotropic and quadratic dispersion law, i.e. the free electron model) cannot even qualitatively explain the dependence of the electronic resistivity on the magnetic field.

It can be shown (88) that the resistance in the presence of a field is always greater than the zero-field resistance,both in the electrical as well as in the thermal case,and that this conclusion can be based solely on the observation that the collision operator in the Boltzmann equation is independent of the magnetic field.
Yet,the free electron model does not yield a non-zero magnetoresistance,so that more complicated models must be adopted to explain the experimentally found magnetoresistance (MR) effects.These experimental observations on simple crystals in the limit of high fields,can be subdivided into the following categories :

i) The MR continues to increase proportional to H^2,

irrespective of the field and electronic current orientations with regard to the crystallographic axes.

ii) The MR saturates,i.e. after an initial quadratic increase,changes into a much lower field dependence.

iii) The MR increases proportional to H^2 for certain orientations,but saturates for others.

iv) The longitudinal MR always saturates.

v) Instead of a saturation a linear increase with H, both for transverse and longitudinal MR,is observed.

We have ignored the oscillatory variations of the electrical resistivity,the so-called Shubnikov-De Haas effect. But this effect is usually small and except for Bismuth (83),has not been seen in thermal conductivity measurements. As for the high field limit,an upper bound is posed by the quantum condition

$$\mu_B H \ll \epsilon_F$$

where ϵ_F is the Fermi energy.This condition requires that for most metals the field be smaller than 10^5 T, a limitation not likely to be violated.

To explain the experimentally observed,finite MR, Sondheimer and Wilson (10,52,78) have considered the case of a metal having two overlapping parabolic bands of carriers.They assumed a separate,but constant relaxation time for the carriers in each band and neglected interband transitions.

Defining the thermal magnetoresistance as

$$\frac{\Delta W}{W} = \frac{W(H) - W(0)}{W(0)} = \frac{\lambda(0) - \lambda(H)}{\lambda(H)} \qquad (4.28)$$

where W(0) and W(H) are the thermal resistivities in zero and non-zero fields, respectively, they found in the high field limit

$$\frac{\Delta W}{W} = \frac{\frac{\lambda_1\lambda_2}{(\lambda_1+\lambda_2)^2}\left(\frac{\lambda_1}{n_1} + \frac{\lambda_2}{n_2}\right)^2\left(\frac{H}{ecL_oT}\right)^2}{1 + \frac{\lambda_1^2\lambda_2^2}{(\lambda_1+\lambda_2)^2}\frac{(n_1 - n_2)^2}{n_1^2 n_2^2}\left(\frac{H}{ecL_oT}\right)^2} \qquad (4.29)$$

where n_1, n_2 are the densities of the carriers (electrons and holes) of the respective bands, and λ_1, λ_2 the partial conductivities at zero field.

For $n_1 = n_2$:

$$\frac{\Delta W}{W} = AH^2 \qquad (4.30)$$

which shows the quadratic field dependence.

For $n_1 \neq n_2$:

$$\frac{\Delta W}{W} = \frac{BH^2}{1 + CH^2} \qquad (4.31)$$

which in the limit of infinite fields saturates to the constant value B/C. For the longitudinal MR they found a zero result.

Although the two-band model is capable to explain qualitatively some aspects of the MR, it is too simple to explain all the established features or to enable quantita-

tive results to be obtained.However,as a first approximation it remains useful and for intermediate fields one still has to resort to the two-band model,as fuller fledged theories are not available yet.

For Al (79) and In (80) it follows from the topology of their Fermi surfaces that roughly

i) the first zone is full

ii) the second zone is hole-like,with a hole density of 1 hole per atom and a cyclotron mass $m_c = m_o$ (m_o is the free electron mass)

iii) the third zone is electron-like,with an electron density of a few percent of an electron per atom and $m_c = 0.1\ m_o$

iv) the fourth zone is empty

In dealing with these metals we are thus concerned with two-band conduction in an uncompensated (i.e. $n_e \neq n_h$) metal,and one expects Eq.(4.31) to hold and the MR to saturate at high fields.This is indeed found to be the case,although sometimes a linear increase with field is still observed.

An alternative way to describe the thermal MR is by the similarity relation derived by Kohler (81)

$$\frac{\Delta W}{W} = F\left(\frac{H}{WT}\right) \qquad (4.32)$$

It asserts that a plot of $\Delta W/W$ as a function of H/WT generates the same curve

i) at all temperatures for the same sample

ii) for all specimens of the same material

Kohler's rule can be deduced from general considerations of the Boltzmann transport equation in a relaxation time approximation (2,3,9).Chambers (82) suggested the following criteria for the validity of Kohler's rule:

i) Collisions can be described in terms of a relaxation time $\tau(k)$.

ii) The filled region in k-space does not change appreciably in size over the range of temperature or impurity content considered.

iii) Changes in temperature or purity alter all $\tau(k)$ by the same factor.

Indeed,Eq.(4.32) is but a special case of Eq.(4.29) under the assumption that all charge carriers experience the same relaxation time.

If different scattering mechanisms are simultaneously present,a common relaxation time $\tau^{-1} = \Sigma\tau_i^{-1}$ can only be defined if all the individual scattering processes are isotropic.

Kesternich et al.(109) have developed a derivation of Kohler's rule without applying the relaxation time approximation.They consider only one type of defect and use the fact that the scattering probability of the conduction electrons is proportional to the defect concentration. They could show that Kohler's rule is exactly valid if the concentration but not the kind of scattering centers is changed.Hence,deviations of Kohler's rule is due solely to different types of scattering centers.The effectiveness of their approach is well demonstrated by the mea-

surements of Böning et al.(211,212) who varied the defect concentration in Al by neutron irradiation.Increasing the temperature,however,besides changing the phonon concentration,will also change the type of defect,as the phonon wave number and hence the momentum transfer to the scattered electron increases,and this approach cannot be used to study the temperature dependence of the magnetoresistance.

Kohler's rule can most easily be understood in terms of the characteristic dimensionless parameter $\omega_c\tau$,which determines the role of the magnetic field.Here $\omega_c = eH/m^*$ is the cyclotron frequency, $\tau = l_e/v$ the electron relaxation time and l_e the electron mean free path.It is usual to speak of "strong" or "high fields" when $\omega_c\tau \gg 1$ and of "weak" or "low fields" if the opposite inequality is satisfied.Since $l_e \sim (WT)^{-1}$, $\omega_c\tau$ is equivalent to the Kohler parameter H/WT.Thus it has become standard practice to present magnetoresistance data in a Kohler plot : $\Delta\rho/\rho$ versus H/ρ for the electrical and $\Delta W/W$ versus H/WT for the thermal magnetoresistance,or equivalently,$\Delta\rho/\rho$ versus $\omega_c\tau_{el}$, $\Delta W/W$ versus $\omega_c\tau_{th}$,where different relaxation times are assumed for the electrical (τ_{el}) and the thermal (τ_{th}) case.

The thermal MR measurements of Aluminium (71,155, 156) have not been put into a Kohler plot,but for Indium Jones and Toxen (12) and Wyder (2) found considerable deviations from Kohler's rule,especially at high fields and high temperatures.At low fields better agreement with a

reduced curve was obtained if the MR was plotted against H/W instead of H/WT. De la Cruz et al.(13),however,found the conventional thermal Kohler's rule well satisfied and Bressan et al.(14) could show that their experimental data,properly scaled,could be plotted on a single universal curve; not only for different temperature and field values but also for samples of different impurity content. The deviations from Kohler's rule may be due to the fact that for thermal carriers the presence of a large amount of phonon scattering prohibits the use of a well defined relaxation time.

Recently,however,Kagan and co-workers (213,214) have developed a quantitative theory which may provide an explanation of the deviations of Kohler's rule.According to the Kagan theory the resistivity of a metal depends significantly on the anisotropy of the electron distribution function. This anisotropy arises mainly as a result of umklapp processes in the electron-phonon interactions. For very pure metals at zero field the anisotropy highly reduces the resistivity.When either the impurity content or the magnetic field is increased,however,isotropy is restored with a subsequent increase of the resistivity. The anisotropy function is peaked at a certain temperature and this is reflected in the magnetoresistivity,the more so the higher the field strength or the more impure the sample.Thus the Kagan theory predicts a peak in the temperature behaviour of the magnetoresistance and this prediction has indeed been corroborated by experimental evidence(209).

This peak-effect indicates an obvious violation of Kohler's rule.According to that rule,the magnetoresistance $\Delta\rho/\rho$ is an increasing function,only dependent on H/ρ. For temperatures at the "uphill" side of the peak in the magnetoresistance,an increase in temperature at a fixed field,would mean a higher ρ, consequently a decrease of H/ρ which should always lead to smaller values of $\Delta\rho/\rho$, in contrast to the experimentally observed behaviour. Presumably,the same mechanism is at work in the thermal magnetoresistance.

In 1957,Lifshitz,Azbel and Kaganov (LAK) developed a rigorous,general and microscopic theory of the galvanomagnetic (84) and thermomagnetic (85) effects of metals in the high field limit $\omega_c\tau \gg 1$,which was able to predict all the observed effects,except the linear magnetoresistance.A comprehensive description of their theory can be found in refs.(86-89).

The dependence of the resistivity tensor components on the magnitude and direction of the magnetic field cannot be determined for an arbitrary value of the field,as they vary with the details of the scattering processes and are considerably affected by the dynamic properties of the conduction electrons.In the high field limit,however,LAK have shown that the asymptotic field behaviour of the resistivity tensor components are independent of the nature of the scattering mechanisms and are solely determined by the geometrical structure of the Fermi surface of the metals.

In this,LAK differed from the previous theories,where specific assumptions were made about the electronic scattering mechanisms and the energy distribution of the electrons.However,the temperature dependence and the absolute magnitude of the MR,are still dependent upon the scattering processes.

The LAK theory was mainly developed for the galvanomagnetic processes.But LAK have also shown (85) that the asymptotic form of the thermal conductivity tensor is identical to the electrical conductivity tensor in its field dependence and that in the high field limit the one is related to the other by the WF-law.The conditions for this to be valid are :

i) $\omega_c \tau \gg 1$

ii) elastic scattering

iii) $\lambda_e \gg \lambda_g$

Under these assumptions the general asymptotic form of the thermal conuctivity tensor is

$$\lambda_e(H) \sim \begin{pmatrix} a_{xx}H^{-2} & a_{xy}H^{-1} & a_{xz}H^{-1} \\ -a_{xy}H^{-1} & a_{yy}H^{-2} & a_{yz}H^{-1} \\ -a_{xz}H^{-1} & -a_{yz}H^{-1} & a_{zz}H^{0} \end{pmatrix} \quad (4.33)$$

According to the Onsager relations :

$$a_{ik} = -a_{ki}$$

and in general a_{ik} depends on the collision integral.For a closed Fermi surface,the part involving the collision integral integrates to zero in the case of a_{xy} and a_{yx}.

The remainder can be calculated explicitly and one finds (85)

$$a_{xy} = -a_{yx} = L_o Te(n_e - n_h) \qquad (4.34)$$

where n_e and n_h can be identified with the number density of the electron and hole states, respectively.
To obtain the thermal resistivity tensor, the inverse matrix of Eq.(4.33) has to be calculated.

For an uncompensated metal ($n_e \neq n_h$) with a closed Fermi surface, an electronic thermal current U in the x-direction, i.e. U= (U,0,0) and U is the thermal current density, and a magnetic field H in the z-direction, i.e. H= (0,0,H), one finds to first order in H^{-1}

(4.35)

$$W_e(H) \sim \begin{pmatrix} b_{xx}H^0 & \frac{H}{L_o Te(n_e - n_h)} & 0 \\ \frac{-H}{L_o Te(n_e - n_h)} & b_{yy}H^0 & 0 \\ 0 & 0 & b_{zz}H^0 \end{pmatrix}$$

Under these conditions, $W_{xx} = b_{xx}$ constitutes the transverse MR, which according to the LAK-theory should saturate in the high field limit.
W_{yx} corresponds to the Righi-Leduc coefficient (thermal Hall coefficient) A_{RL}, i.e.

$$A_{RL} = \frac{\nabla T_y}{HU_x} = W_{xy}H^{-1} = b_{xy} = (L_o Te(n_e - n_h))^{-1}$$

$$U_y = U_z = 0 \; ; \; J = 0 \qquad (4.36)$$

Here ∇T represents the thermal gradient and J the electrical current density. In the high field limit, $A_{RL}T$ is a constant (temperature and field independent) according to the LAK-theory

$W_{zz} = b_{zz}$ represents the longitudinal MR, which also tends to a saturation value.

Hence, for uncompensated closed orbit metals, like Al and In, the electronic thermal resistivity becomes

$$W_e(H) \sim \begin{pmatrix} b_{xx} & A_{RL}H & 0 \\ -A_{RL}H & b_{yy} & 0 \\ 0 & 0 & b_{zz} \end{pmatrix} \qquad (4.36a)$$

Under parallel conditions, i.e. electric current J= (J,0,0) and magnetic field H= (0,0,H), the electrical resistivity tensor is of the form

$$\rho(H) \sim \begin{pmatrix} \rho_{xx} & R_H H & 0 \\ -R_H H & \rho_{xx} & 0 \\ 0 & 0 & \rho_{zz} \end{pmatrix} \qquad (4.36b)$$

where ρ_{xx} and ρ_{zz} are constants and ρ_{yx} corresponds to the Hall coefficient R_H, i.e.

$$R_H = \frac{E_y}{HJ_x} = \rho_{yx} H^{-1} = (e(n_e - n_h))^{-1}$$
$$J_y = J_z = 0 \quad ; \nabla T = 0 \qquad (4.37)$$

Note that in the high field limit, according to LAK (85) W_{xy} and ρ_{xy} have the free electron values, with

$$\frac{R_H}{A_{RL}T} = L_o \qquad (4.38)$$

For compensated metals ($n_e = n_h$) : $a_{xy} = 0$ and the dominating term of λ_{xy} is $a_{xy}H^{-2}$ of next lowest order in H^{-1}. Hence, W_{xx} and W_{xy} become proportional to H^2, while W_{zz} again saturates.

For metals with open orbits, more complicated matrices for the tensor $W_e(H)$ are generated. The effect of open orbits will be, that for some directions $W_e(H)$ will saturate while for others $W_e(H)$ will increase quadratically with field.

Although the LAK-theory for the galvanomagnetic and the thermomagnetic behaviour of metals is strictly valid for single crystals only, they apply to polycrystalline metals as well. But some averaging effects of the polycrystalline state on the field dependence of the $W_e(H)$ tensor components is to be expected, especially for a metal with open orbits.

For instance, as early as 1929, Kapitza (90) has studied the field dependent behaviour of the electrical resistance of about 35 different polycrystalline metals in pulsed magnetic fields up to 30 T, and found that in all metals the magnetoresistance first obeyed a quadratic law but in stronger fields changed into a linear dependence on H. For metals with open orbits, Ziman (135) has provided a

a qualitative explanation for the Kapitza effect,based on the averaging of the conductivity tensor over the randomly oriented microcrystals in a polycrystalline specimen.If in a certain microcrystal for certain orientations of the field,all the cross sections of the Fermi surface are closed,the magnetoresistance would saturate. If,on the other hand,in certain field orientations all orbits are open,the magnetoresistance would increase as H^2.Averaging over randomly oriented microcrystals may produce a H-dependence.

A more quantitative study of the averaging effect was performed by Gaidukov (136) on gold single crystals. He measured the dependence of the MR on the angle between the variable field directions and certain crystal axis, and obtained a rotation diagram of the MR with maxima and minima.For the angles of the minima,the MR saturated; for the angles of the maxima,the MR increased as H^2.Averaging over all the angles,he obtained a linear dependence on the magnetic field for the averaged MR.

As yet there is no firm ground for a quantitative theory of this averaging over the effects of open and closed orbits,which appear for a fixed direction of the field and variable crystal orientations or vice versa.

For uncompensated metals with a closed Fermi surface,however,the averaging effect of the polycrystalline state will not alter the nature of the field dependence of the MR.Yet,even in these metals,both for single crystals as well as for polycrystalline samples,a linear MR is found.

4.2.8 The Linear Magnetoresistance

Most of the experimental observations of the galvano- and thermomagnetic effects can now be explained by the LAK-theory and its subsequent refinements (e.g. magnetic breakdown,quantum oscillations,etc.).However,there is still one phenomenon which still eludes firmly founded physical explanation : the linear increase with field of both the transverse and longitudinal magnetoresistance.

For most metals,there is a wide range of the transverse electrical MR,in which the resistivity is a linear function of the field,as was first observed by Kapitza (90).For some metals the linear region separates two quadratic dependences,or is located between the low field quadratic region and the high field saturation level; others show no deviation from the linear law even in strong fields,while in most cases the longitudinal MR also exhibits a linear increase with field (167).

For metals with open orbits,the linear field behaviour could partly be ascribed to averaging effects (135, 136),but in the case of uncompensated,closed orbit metals, like Aluminium (92-110),Indium (2,111-117),Sodium (118, 129) and Potassium (118-129),for which averaging has no effect,the MR seems also to increase with field.This is in complete contrast to the LAK-theory,which unambiguously predicts a saturating behaviour for both the transverse and the longitudinal MR of these matals.

Particularly in the case of Potassium,the deviation

from saturation is rather disturbing.The measured Fermi surface of K (131,132) closely resembles the ideal free electron sphere and its deviations from spericity amounts to about 0.1 %.This is even less than that of a high quality billiard ball (91) so that one would expect its galvanomagnetic properties to be precisely predictable. Potassium is one of the most simple systems in which to study the electron theory of metals,and as such it has become one of the most extensively investigated metals. A summary of the experimental evidence concerning the linear magnetoresistance (LMR) can be found in refs.(124, 133) and a successful theory must account for the following facts :

1) LMR appears also in metals with no open orbits,for which the LAK-theory predicts a saturating behaviour.
2) LMR appears for many experimental geometries and configurations and for various measuring techniques.
3) LMR appears both for low and high fields,i.e. H= 0.5 $\sim$ 11 T,equivalent to $\omega_c\tau$= 10 $\sim$ 350,and showing no tendency to saturate at the highest field strengths.
4) LMR appears both for the longitudinal as well as the transverse component of the resistivity tensor.
5) The dimensionless Kohler slope S,defined as

$$S= \frac{\rho(H,T) - \rho(0,T)}{\rho(0,T)\omega_c\tau} = \frac{\Delta\rho/\rho}{\omega_c\tau} \qquad (4.39)$$

is small and characteristically of the order of $10^{-4}\sim 10^{-2}$.

6) The slope S appears to be quite sensitive to sample preparation and handling,especially to strains(105, 109,117,120,121,124,129)

7) LMR appears to be dependent upon crystal orientations with regard to the field direction (93,102, 109,117,125,155)

8) LMR appears also in the thermal magnetoresistance (156,160,161)

9) In the low temperature,high field limit the Hall coefficient R_H and the Righi-Leduc coefficient A_{RL} appear to be very close to the free electron value and are related to each other by

$$R_H/A_{RL}T = L_o \qquad (4.38)$$

in accordance with the LAK-theory (105,109,117,126, 127,130,134,156,157,158)

However,in the low field region or at higher temperatures Eq.(4.38) does not seem to hold (134,197).

The theoretical models advanced to explain the LMR can be divided into two categories,i.e.

i) intrinsic,i.e. connected with properties of the ideal,defect-free lattice

ii) non-intrinsic

The intrinsic explanations can be subdivided into

a) structural theories

b) transport theories

The structural theories link the LMR to assumed deviations from the closed orbit,free electron-like model.

They introduce energy gaps at the Fermi surface,due either to charge density or spin density waves in the electron ground state (137,138)or to strong spin correlations (139) The LMR occurs through magnetic breakdown of these energy gaps at high fields,thus allowing for open orbits.Combinations of open and closed orbits would then generate the linear term

There are several objections which can be raised against the bandgap plus magnetic breakdown models (124,125):

i) They are only applicable to the transverse MR.

ii) They produce a linear term up to about $\omega_c \tau \sim 150$, after which the MR begins to saturate again.

iii) They should affect the equilibrium properties sufficiently to be observable in other experiments,e. g. De Haas-Van Alphen measurements (132). This is not the case.

iv) They predict either a strongly field dependent Hall coefficient R_H in the high field limit or R_H should be considerably different from the free electron value.

v) They should give rise to a large anisotropy of the magnetoresistance.

The torque measurements of Schaefer and Marcus (123) showed indeed a factor of ten anisotropy in the torque exerted on a single crystal sphere of K,in contrast to an earlier torque experiment by Lass (121).Overhauser(138) took these anisotropy results as evidence for his charge density wave model,but other torque experiments (125,127,

128) completely validated the Lass-results,while Lass (140,141) could argue effectively that the anisotropy could be ascribed to the non-sphericity of the samples.

The transport theories involve extremely anisotropic scattering of the electrons,which cannot be taken care of by the conventional relaxation time approximation. This can arise from electron-phonon umklapp processes at localised scattering centers referred to as 'hot spots' (142),or from anisotropic quantum mechanical fluctuations in the ground state of the electrons,due to electron - phonon and/or electron-electron interactions (133,143). Besides the objections i),iv) and v),which also apply to the'hot spot'theory,the magnitude of the observed Kohler slope S necessitates the size of the hot spots to be extremely large,which is physically unreasonable (124,133).

The macroscopic quantum fluctuation theory,as summarized by Hsu and Falicov (143),predicts that :

i) The transverse MR tends to saturation for fields of $H \sim 100$ T or higher,and the longitudinal MR for fields of $H \sim 10$ T.
   The latter is experimentally accessible and should yield strong support for the correctness of the fluctuation model.

ii) The Hall effect is unaffected by fluctuation scattering.

iii) The fluctuation scattering is strain dependent.

iv) For single crystals as well as for polycrystalline samples $S_L < S_T$.

v) For single crystals the MR is anisotropic.

However,although the quantum fluctuation theory appears the most attractive intrinsic theory,which can explain most of the observed data,there seems to be no reason why such fluctuations should exist.

Theoretically,small-angle scattering (162,168) from phonons or crystal defects may also affect the field and temperature dependence of the MR,but it seems not to be possible to explain the observed experimental results on this basis alone (124).

Besides these models,Cardon de Lichtbuer (144) has obtained a linear MR within the framework of the Boltzmann equation by assuming a field dependent electron scattering probability in the collision integral.This scattering probability is analysed as a series expansion of which the expansion coefficients are field dependent.However,it seems to us that by this method one could obtain almost any field dependence if sufficient expansion terms are included,and the physical reasons for the linear MR remain unclear.

The *non-intrinsic explanations are of two kinds* :

i) geometric

ii) macroscopic

The geometric theories (118,145) are based on non-ideal boundary conditions,the geometry of the experiment and the influence of the electrodes.However,the linear effect has been found in samples of different shape : long wires (118,124),match stick specimen (121),round spheres (121,123,125,127,128), and in samples of different

quality (124) and with different measuring techniques: four probe (118.121.122,124,126),induced torque (121,123, 125,128) and helicon (127) methods.This seems to rule out most of the geometric theories.

The macroscopic theories are connected with the influence of macroscopic (i.e. small compared with sample size,but large compared with the electron mean free path) inhomogeneities like crystallite boundaries,voids,regions of localized strain,etc. on the current flow lines in a magnetic field.The influence of crystallite boundaries can not be the only cause as the linear effect is also seen in single crystals.The current flow around non-conducting voids have been discussed by Lass(121) in terms of 'current jetting',but to explain the magnitude of the effect a void density of the order of 1 % would have to be assumed which is larger than seems reasonable for good samples.In the discussion of Herring (146) the inhomogeneities take the form of continuously variable fluctuations in the carrier density,but the results show that a slope $S = 10^{-2} \sim 10^{-3}$ would require a variation of 10 % $\sim$ 3 % in the carrier density, an unrealistically large variation for a metal.Babiskin and Siebenmann (122,126) noted a correlation between the slope S and the number of voids visible on the surface of their sample.Attributing the linear dependence entirely to the presence of voids, they suggest an unambiguous separation procedure to part the MR into an intrinsic saturating term and a void dependent linear term.However,strong doubts were raised

against their oversimplified model and their separating procedure must be regarded as too crude (147).

Recently,several papers appeared (148-150),which considered the effect of a few isolated (i.e. non-interacting) macroscopic volume inhomogeneities of different conductivity than the host material,upon the galvanomagnetic properties of metals.Schotte and Jacob (148) used an effective medium approach and obtained a region of longitudinal and transverse LMR for an inhomogeneity fraction of 1 %,which is definitely unrealistic.
Sampsell and Garland (149) obtained exact analytic expressions for the magnetic field dependence of the current distribution near non-conducting spherical and cylindrical inclusions in a free electron conductor.For cylindrical voids their theory predicts a Kohler slope $S_L = 1.00\ f$ and $S_T = 0.49\ f$ for the longitudinal and transverse MR,respectively,where f is the volume fraction of the cylindrical inclusions.This requires a void concentrations of $f = 10^{-4} \sim 10^{-2}$ to account for the reported data of K and other metals.Again,the latter figure is unrealistically high.For conducting inclusions,their theory cannot be applied in a simple way.
Stroud and Pan (150),using in essence a mean field approach,obtained Kohler slopes of the same order of magnitude as Samsell and Garland,also requiring void fractions $f = 10^{-4} \sim 10^{-2}$ to fit the observed data.However, according to their theory the Kohler slope is only dependent on f and independent of the shape of the inclu-

sions.Moreover,a conducting inclusion would lead to higher slopes than non-conducting voids,but a linear longitudinal MR would only be generated by zero-conductivity defects.The Hall coefficient R_H,resulting from their calculations,appear to be field independent and nearly equal to the free electron value in the high field limit.

While the theories discussed above are based on macroscopic volume inhomogeneities,the theory proposed by Van Gelder (151) attributes the LMR to sheet- or surface-like inhomogeneities.The Van Gelder theory involves macroscopic lattice imperfections,typically of order 0.1 mm, and characterized by a sheetlike local potential $V= g\delta(x)$, which has the capacity of trapping electrons in its immediate vicinity if a static magnetic field is present. Physically,such potential sheets may be considered typical for interfaces between crystallites or for dislocations. For an imperfection density of 10 mm^{-3},a Kohler slope of $S= 10^{-2} \sim 10^{-3}$ is estimated (152),in good agreement with experiment.In contrast to the former theories,the Van Gelder theory was developed as a microscopic theory.Despite this fact,the resulting expression for the linear MR contained no quantum mechanical entities,and it appeared possible to arrive at the same result out of a macroscopic kinetic theory (152).
As yet,the Van Gelder theory is applicable only to the transverse MR,but an extension to the longitudinal MR seems to be possible.

No theory has been developed explicitly for the linear thermal magnetoresistance (TMR).Generally,one assumes it to mirror the electrical MR via the WF-law, corrected for by the ratio of the electrical and thermal relaxation times τ_{el}/τ_{th},where these are not equal. Although,as compared to the electrical results,but relatively few data exist of the TMR of K (153,154,161,164), Al (155,156) and In (2,13,14,160), the obtained experimental evidence seems not to be in agreement with these simple ideas.

The salient features of the thermal magnetoresistance can be summarized as follows :

i) TMR does not saturate,contrary to the predictions of LAK,but increases linearly with field (13,153, 155,156,161)

ii) The temperature dependence of the linear thermal and electrical MR is the same as that of the zero field resistivities,i.e. the ratio of their magnitude scales as the ratio of the zero field resistivities.

iii) The temperature independent portions of the linear thermal and electrical MR depend on RRR in the same manner (161,164).

iv) The Lorenz ratio is not constant in the high field limit (13,161).The departure of L_o increases with decreasing temperature.

Besides the linear field dependence,Newrock and Maxfield (153,161,164) and also Fletcher (154) have observed a

quadratic increase with field of the TMR of Potassium. They claim this to constitute a new aspect in the TMR of uncompensated closed orbit metals,which has no analogue in the electrical MR.
We shall show in section 4.3.5 that this quadratic behaviour also manifests itself in our measurements of the TMR of Al and In.The quadratic field term arises in our case as a natural consequence of the Corbino geometry. As shall be explained in subsection 4.3.5,the seemingly deviative behaviour of Potassium can be attributed to the same origin.

We should like to conclude this subsection on the linear magnetoresistance with the following observations:
A) As yet,no satisfactory theory for the linear MR exist.The prevalent experimental evidence is not sufficient,even to determine whether the linear term is due to intrinsic or non-intrinsic effects.The intrinsic theories predict either a Hall coefficient that differs considerably from the free electron value,in contrast to experimental observation,or only a delay of the saturation to much higher field strength.The non-intrinsic theories require unrealistically high impurity and defect concentrations to explain the measured Kohler slopes.

From the intrinsic theories,the quantum fluctuation model (133,143) appears to be the most attractive.This theory predicts a saturation of the longitudinal electrical MR at about 10 T,while the transverse MR would remain

increasing linearly up to about 100 T.The experimental verification of these predictions,which are of crucial importance for the validity of the theory,has not been attempted as yet,although for the longitudinal MR the required field strengths for the saturation to be observable are well within the reach of the (Nijmegen (193)) experimental facilities.

From the non-intrinsic explanations the inclusion models of Sampsell and Garland (149),Stroud and Pan (150) and Van Gelder (151) remain the most promising.But as yet no systematic experimental study of the effects of inclusions or voids on the magnetoresistance has been reported, although we know of experiments where these aspects are currently being investigated (165,166).

As in a high purity sample at cryogenic temperatures the mean free path is of the order of 0.1 mm and as the theory requires the volume inclusions to be larger than the mean free path,the inclusions would be of the order of 0.1 $\sim$ 1 mm.It remains doubtful if volume inclusions that large are always present in a natural way in even the most pure and well prepared single crystals.In this respect,the Van Gelder theory is more attractive in that it considers sheetlike defects,which are physically more easily visualised as edge or screw dislocations,crystallite or grain boundaries,etc.

B) The validity of the theories of the linear MR are mostly gauged by comparing their predictions with experimental results obtained for Potassium.This is due to the fact that its Fermi surface is almost completely spherical and of all metals,Potassium approximates the free electron metal to the highest possible degree.One hoped, that an explanation of the observed facts could also be constructed within the framework of the free electron theory.

However,until now,this hope has been proved unfounded. The close correspondence to the free electron model has in no way facilitated theoretical interpretation of the linear MR,while from an experimental point of view,all the salient experimental features as they appear for Potassium,both of the electrical as well as of the thermal MR,have also and equally well been observed in the slightly more complicated metals Aluminium and Indium.

Furthermore,the experimental difficulties one encounters in the case of Potassium are many and considerable (163).

Because of its highly reactive and corrosive nature,Potassium samples can only be prepared in an environment of dehydrated inert gases or in well-dried paraffin oil. Homogeneous polycrystalline samples or single crystals of well-defined form are difficult to prepare and the construction of small,well-determined probe contacts poses a great challenge.Annealing for long periods,even in a dehydrated and deoxygenized environment,more often than

not result in chemical contamination and a decreased residual ratio resistance (RRR),oxydation of the probe contacts or loss of electrical continuity.X-ray analysis of single crystal samples are well-nigh impossible.Even if one has overcome these difficulties by dint of ingenuity,perseverance and plain hard work,the results are unpredictable and strongly dependent on sample preparation,annealing and induced strain during preparation and cooling to helium temperatures.
In Na,these difficulties are further enhanced by a martensic transformation at low temperatures (198).

In contrast to this,the experimental handling and sample preparation of Al and In poses no problem.Moreover, several well-developed metallurgical techniques exist to obtain information on their dislocation densities,grain boundaries and other lattice defects.
In view of these facts,a strong case should be made for Aluminium and Indium as the prime metals where the linear magnetoresistance should be investigated,especially where non-intrinsic properties are being studied.

4.2.9 The Corbino Effect

In a theoretical study of the Hall effect,Boltzmann (171) pointed out that in a circular metal disk with one electrode attached to the center and the second electrode to the outer edge of the disk,the radial flow lines obtain a circular component and reach the peripherical edge in logarithmic spirals when a magnetic field is applied normal to the disk.The deviation of the radial flow at each point of the disk occurs at a constant angle whose tangent depends upon the strength of the field and the material of the disk.The circular currents are due to the short-circuiting of the circumferential Hall field,induced in the disk by the orthogonal electric and magnetic field vectors.

It was Corbino (172),however,who first demonstrated experimentally the following related galvanomagnetic effects in circular metallic disks where the current enters in the center :

i) If a steady current and a steady magnetic field normal to the disk is applied,the radial current acquires a circular component.
If the disk hangs suspended,a torque can be measured due to the production of the circular current.

ii) If an alternating current and a steady magnetic field is applied,the inductive effect of the changing circular current can be revealed by means of a galvanometer connected to a coil,surrounding the disk.

iii) If no current and an alternating magnetic field is applied while the center and edge of the disk are connected to a galvanometer,a potential is measured. As Corbino pointed out,this effect may be regarded as a Hall effect on the induced circular currents.

(The fourth variant,where both an alternating current and an alternating field are applied,was not considered by Corbino,but have been discussed in refs.(173-175).) Since then,several articles on the Corbino effect have appeared (176-192),all connected with electrical phenomena,e.g. electrical magnetoresistance and Hall effect phenomena in semiconductors (180,181,183,185,189,190),liquid metals (191,192),semimetals (177,178,179) and normal metals (182,188),but none of them concerned with thermal effects

It was Gorter and Miedema (159,194) who were the first to realize that the enhanced magnetoresistance of the Corbino geometry can be used effectively for the separation of the electronic and the lattice conductivity of metals.

To obtain the relevant expressions for the thermal MR it is convenient to consider the electrical MR first. The situation in the Corbino geometry can be analysed by means of the Hall-Ohm equation

$$E = \rho J - R_H (J \times H) \qquad (4.40)$$

where E is the electric field vector,J is the current density vector,H the magnetic field vector,ρ the scalar

resistivity and R_H the Hall coefficient.(For a more elaborate analysis,see refs.(184,187,188))

In cylindrical coordinates

$$E_r = \rho J_r - R_H J_\phi H \qquad (4.40a)$$

$$E_\phi = \rho J_\phi - R_H J_r H \qquad (4.40b)$$

where the subfixes r and ϕ indicate the radial and angular components,respectively.

In the steady state we have

$$\nabla \times E = -\frac{\partial H}{\partial t} = 0 \qquad (4.41)$$

yielding $E_\phi = 0$

or $E_\phi \sim \frac{1}{r}$

as solutions for the angular component of the electric field vector.The line integral of the circumferential field is zero,however,i.e.

$$\int_0^{2\pi} E_\phi r d\phi = 0$$

leaving $E_\phi = 0$ as the only solution.

Defining the field dependent resistivity as

$$\rho(H) = E_r / J_r$$

one obtains from Eq.(4.40a)

$$\rho(H) = \rho\left(1 + \left(\frac{R_H H}{\rho}\right)^2\right) \qquad (4.43)$$

In terms of the resistivity tensor (Eq.(4.36b)),this is equivalent to

$$\rho(H)= \rho_{xx}\left(1 + \left(\frac{\rho_{xy}}{\rho_{xx}} \right)^2 \right) \qquad (4.44)$$

where ρ_{xx} is the resistivity in a transverse magnetic field and $\rho_{xy} = R_H H$ is the (isothermal) Hall resistivity.
For very high fields,where ρ_{xx} is assumed to saturate for closed orbit,uncompensated metals,one finds for the field dependent conductivity $\sigma(H)$

$$\sigma(H)= \frac{1}{\rho(H)} = \frac{\rho_{xx}}{\rho_{xx}^2 + \rho_{xy}^2} \underset{(H \to \infty)}{\to} \frac{\rho_{xx}}{(R_H H)^2} \qquad (4.45)$$

In the high field limit,Eq.(4.45) can be transformed to the thermal case by means of the WF-law and Eq.(4.38),and one obtains for the field dependent electronic thermal conductivity in the Corbino geometry

$$\lambda_e(H) \underset{(H \to \infty)}{\to} \frac{W_{xx}}{(A_{RL} H)^2} \qquad (4.46)$$

where W_{xx} is the thermal resistivity in a transverse magnetic field and A_{RL} is the Righi-Leduc coefficient.
Here,$A_{RL}T$ is taken to be constant,i.e. independent of field and temperature,in confirmation with the LAK-theory.
Hence,A_{RL} has a T^{-1}-dependence.
If one takes the observed non-saturating linear thermal MR into consideration,the transverse thermal resistivity component W_{xx} cannot be taken as constant as in Eq.(4.36a).

For W_{xx} we define ad hoc

$$W_{xx} = W_o(1 + bH) \tag{4.47}$$

Here,b is an adjustable parameter and the slope

$$s = W_o b$$

may be dependent upon temperature.
It should be pointed out that W_o is not the actual zero-field value of the electronic thermal resistivity,but the value of W_{xx} extrapolated to H= 0. In general

$$W_o = W(0,T) + a(T) \tag{4.48}$$

where W(0,T) is the measured zero-field value of the thermal resistivity and a(T) is a constant which again may be temperature dependent.

The total thermal conductivity as a function of field can now be expressed as

$$\lambda(H) = \lambda_g + \frac{s}{A_{RL}^2} H^{-1} + \frac{W_o}{A_{RL}^2} H^{-2} \tag{4.49}$$

We have used Eq.(4.49) to analyse the results of our thermal conductivity measurements of Al and In in the Corbino geometry.This shall be discussed in the next section.

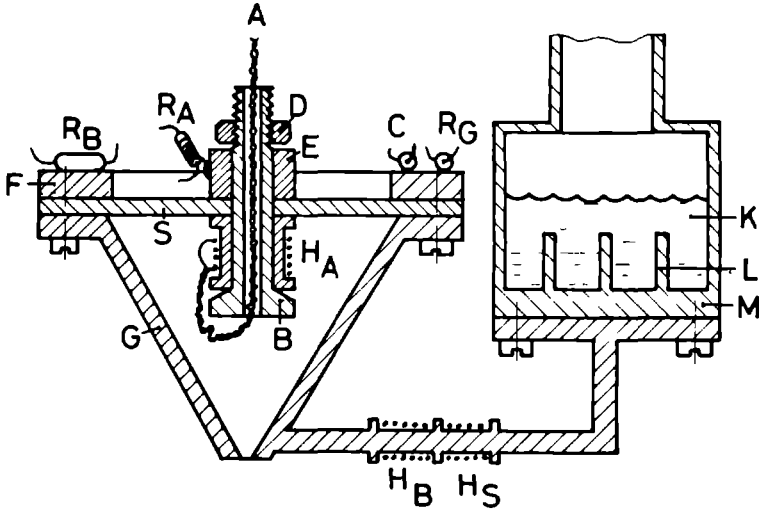

Fig.4.7 : Sample holder for the Corbino measurements.
(See text for the interpretation of the symbols)

4.3 Experimental Details and Results.

4.3.1 Experimental Arrangement.

The thermal conductivity measurements have been made in the Blue Monster (Chapter 2),in fields up to 6.5 T and temperatures down to 0.3 K for In and 1.5 K for Al.

The sample holder (Fig.4.7) consists of a hollow gold-plated copper cone (G),attached to the base of the ^{3}He-chamber (M) with copper screws.The cold end heaters(H_B and H_S) are used to stabilize the temperature.The hot end heater (H_A) consists of a manganine wire,wound a-round a copper,gold plated spool and is clamped to the inner edge of the Corbino sample (S) by means of a gold-plated copper washer (E) and a hollow PTFE screw (B), through which the leads (A) of the heater (H_A) are guided out.The gold plated inner (E) and outer (F) copper rings act as isothermal surfaces.No anisotropic temperature distribution could be detected in the outer ring (F) or in the cone (G),within accuracy of measurement.To avoid pressure differences between the inside and the outside of the sample holder,a hole is drilled in the top of the cone.The thermometers R_A and R_B consist of 10 Ω 1/10 W Allen-Bradley resistors for the In-measurements and 220 Ω 1/10 W resistors for the Al-experiment.To attach R_A,a copper wire is soldered at one end to E,while the

other end is wrapped tightly around the resistor,then greased with Apiezon-N vacuum grease to enhance thermal contact.R_B is glued to the ring F with GE-varnish. The resistors R_A and R_B are calibrated against a Germanium resistor R_G in zero field.In the presence of a field the temperature is kept constant by means of a glass capacitance thermometer,which remains unaffected by a magnetic field.All resistors are measured with ac-resistance bridges.The accuracy of the measured thermal conductivities is estimated to be 4 %.

4.3.2 Samples.

The Corbino samples consist of thin,cylindrical polycrystalline disks of Al and In,with a concentric cylindrical hole .The current flows between the inner and the outer perimeter,both of which are equipotential (or rather isothermal) surfaces in the case of isotropic metals.Due to the circular symmetry,the electrical field or temperature gradient must be radial.The geometrical factor

$$g = \text{area/length}$$

can be calculated in the following way.
Be d: the thickness of the sample,r_o:the outer radius and r_i: the inner radius (i.e. the radius of the central hole)
From the radial current

$$I_r = d\ 2\pi r\ J_r = d\ 2\pi r\ \sigma E_r$$

the voltage difference V between the inner and the outer edge can be obtained, i.e.

$$V = \int_{r_i}^{r_o} E_r dr = \frac{I_r}{d2\pi\sigma} \int_{r_i}^{r_o} \frac{dr}{r} = \frac{I_r}{d2\pi r} \ln(r_o/r_i)$$

This yields for the conductance $S = g\sigma$

$$S = \frac{I_r}{V} = \frac{2\pi d}{\ln(r_o/r_i)} \sigma$$

and therefore one obtains for the geometrical factor g

$$g = \frac{2\pi d}{\ln(r_o/r_i)} \qquad (4.50)$$

The Indium sample was kindly provided by Dr.W.F.Druyvesteyn (Philips Physical Laboratory, Eindhoven), the Aluminium was obtained from theVereinigte Aluminium-Werke AG, Bonn, W-Germany. Both samples are polycrystalline and the relevant parameters are summarized in Table 4.8.

Table 4.8. Corbino samples : Al and In

	Al	In
purity	6N5	6N
RRR	40 000	10 000
d (mm)	1.0	0.5
r_o (mm)	8.5	8.5
r_i (mm)	2.0	2.0

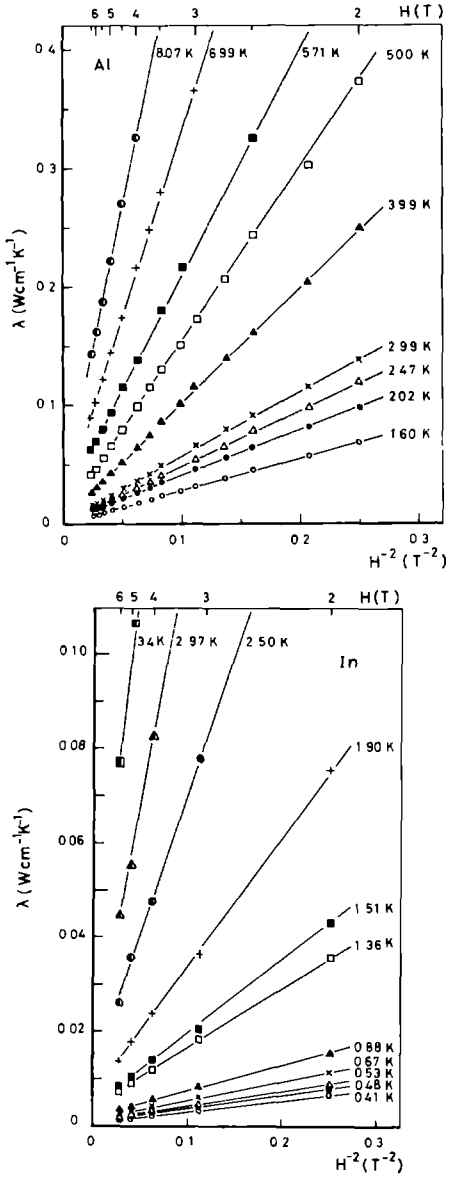

Fig.4.8 and 4.9 : The measured lattice conductivity as a function of H^{-2} for Al and In.

4.3.3 The Lattice Conductivity.

Fig.4.8 and Fig.4.9 plot the measured thermal conductivity of Al and In,respectively, as a function of H^{-2} at several constant temperatures.The resulting graphs are curved,rather than forming straight lines,as can be seen from Fig.4.10,where the vertical scale has been exploded.

The curves exhibit a downward bend at high fields and this effect is the more marked the lower the temperature.Assuming this deviation from the straight line behaviour to be a manifestation of the thermal linear MR,we have fitted our data to an expression of the form

$$\lambda(H)= a_o+ a_1H^{-1}+ a_2H^{-2} \qquad (4.51)$$

which is equivalent to Eq.(4.49).

The resulting coefficients a_o,a_1,a_2 of the computer-fits for Al and In are reproduced in Table 4.9 and Table 4.10,respectively.The values of a_o,which can be identified with the lattice thermal conductivity λ_g,are plotted as a function of temperature in Fig.4.11 and Fig.4.12. Both lie close to a line representing a T^2-behaviour.

For the lattice conductivity of Al we find from these results

$$\text{Al} : \quad \lambda_g = 1.0 \times 10^{-4}\, T^2 \quad Wcm^{-1}K^{-1} \qquad (4.52)$$

in close agreement with the values found by using the alloying method,e.g.

$\lambda_g = (0.9\text{-}2.5)\times10^{-4}T^2$ $Wcm^{-1}K^{-1}$ (Powell et al.(35))

$\lambda_g = \quad 0.8 \quad \times10^{-4}T^2$ $Wcm^{-1}K^{-1}$ (Klaffky et al.(32))

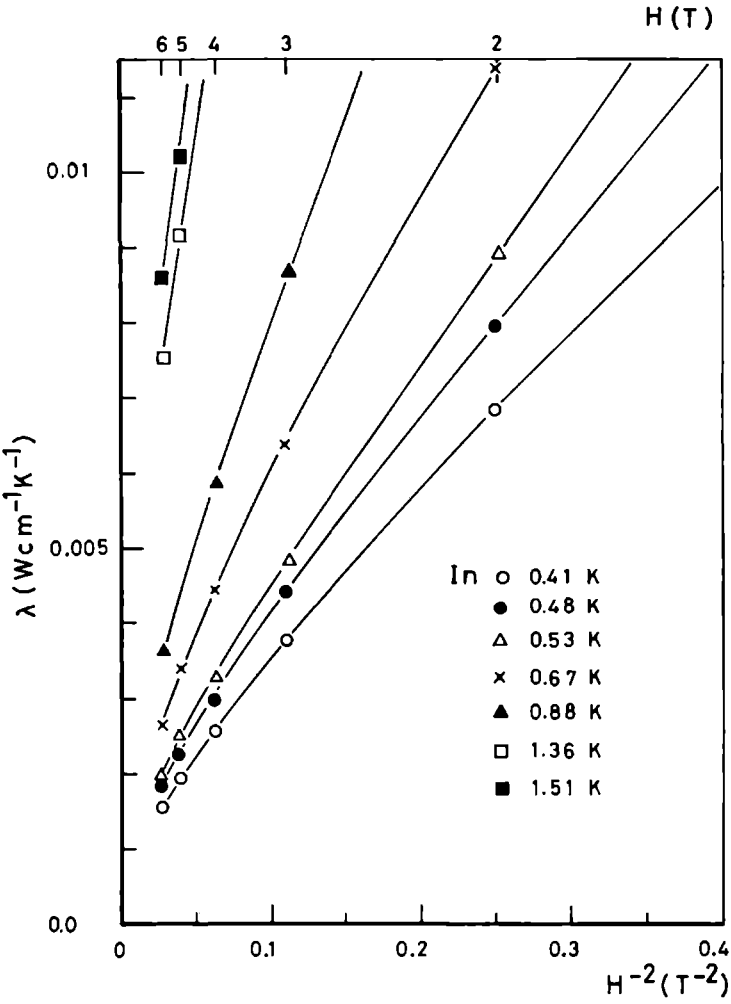

Fig.4.10 : Exploded view of the lattice conductivity as a function of H^{-2} for In.

$$\lambda_g = 1.0\times10^{-4}T^2 \ \text{Wcm}^{-1}\text{K}^{-1} \quad \text{(Amundsen et al.(33))}$$

For the lattice conductivity of In we find

$$\text{In}: \quad \lambda_g = 9 \times 10^{-4} T^2 \ \text{Wcm}^{-1}\text{K}^{-1} \qquad (4.53)$$

which is a factor 1.5 higher than the result from alloys i.e.

$$\lambda_g = 6 \times 10^{-4}T^2 \ \text{Wcm}^{-1}\text{K}^{-1} \quad \text{(Sladek (31))}$$

Including the effect of the linear MR in our extrapolation procedure thus proved successful in taking account of the downward bend of the experimental curves and provided us with values for the lattice conductivity of Al and In,which are in good agreement with those obtained from the alloying method.

If the linear MR would have been neglected,a computerfit to the expression

$$\lambda(H) = a_o + a_2 H^{-2} \qquad (4.54)$$

which is equivalent to Eq.(4.27),would give values for λ_g which are about a factor 3 and more higher than the corresponding results from the alloying technique,i.e.

$$\text{Al}: \ \lambda_g = 3 \times 10^{-4}T^2 \ \text{Wcm}^{-1}\text{K}^{-1}$$
$$\text{In}: \ \lambda_g = 2 \times 10^{-3}T^2 \ \text{Wcm}^{-1}\text{K}^{-1}$$

We would like to conclude this subsection with the following observations:

A) The results described in this section provide the first alternative and independent measurements,i.e. acquired by a method other than the alloying technique,of

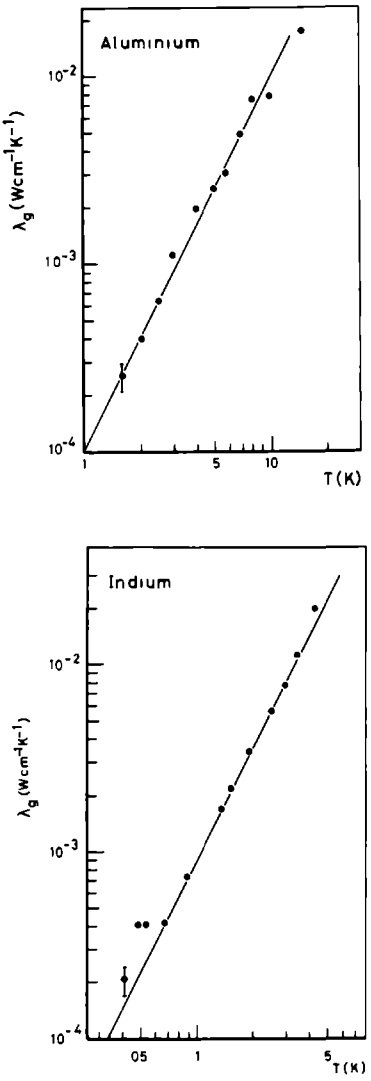

Fig.4.11 and 4.12 : The lattice conductivity as a function of temperature for Al and In. The solid line represents a T^2-dependence.

the thermal lattice conductivity of Aluminium and Indium. The difficulties inherent to the alloying and the magnetic field methods are described in subsections 4.2.5 and 4.2.6 respectively,but despite these difficulties one may conclude that the lattice conductivity of Al and In,determined by two independent methods,are in good agreement and do not disagree with the expected T^2-dependence.

B) The Corbino method is the most effective method to reduce the electronic thermal conductivity by means of an external magnetic field.The reason for its effectiveness lies in the fact that in the Corbino geometry the magnetoresistance acquire its maximum value,due to the absence of the Hall field.In contrast to this,the magnetoresistance in the conventional arrangement,whereby an electrical or thermal current is flown in a long thin wire perpendicular to the direction of a magnetic field,is minimal. In fact,because of the Hall effect,the simple free electron theory predicts a zero magnetoresistance for a measurement in the standard configuration.

A further advantage of the Corbino method is that it leads to measurements of conductivity rather than resistivity and therefore can be more directly compared with most transport theories.

C) In the case of the lattice conductivity of Potassium the Corbino method acquires an added importance.As yet,the lattice conductivity of K has not been properly measured. Ekin (207),using a realistic phonon spectrum and a number of different pseudopotentials,has calculated the lattice

Table 4.9 : Experimental Coefficients of Aluminium determined from computeral fitting

T K	a_o $10^{-3}Wcm^{-1}K^{-1}$	a_1 $10^{-3}WTcm^{-1}K^{-1}$	a_2 $10^{-3}WT^2cm^{-1}K^{-1}$
1.60	0.253	6.157	262
2.02	0.396	12.64	380
2.47	0.638	10.88	464
2.99	1.101	22.55	517
3.99	1.94	21.57	917
5.00	2.50	35.08	1452
5.71	3.02	53.76	1669
6.94	4.96	77.04	3068
8.07	7.50	138.3	4604
10.0	7.68	357.8	10234
14.9	17.12	3210.	27517

contribution to the thermal conductivity of Potassium, and found in the low temperature limit a value of about

$$K : \lambda_g = 2.5 \times 10^{-3} T^2 \ Wcm^{-1}K^{-1}$$

The available experimental data,however,are rather contradictory.As K is not a superconductor,the superconducting method to obtain λ_g cannot be employed.Archibald,Dunick and Jericho (41) have measured λ_g by using the alloying method with Cesium as the alloying metal.Their results do not show a T^2-dependence and are smaller in magnitude than the theoretical value.Apparently,not only does the alloying influence the electronic thermal conductivity, but the lattice thermal conductivity as well.This leaves the magnetic field method as the only means to measure the lattice conductivity of Potassium.

Fletcher (154) and Newrock and Maxfield (153,161,164) have measured λ_g ,by using the magnetic field method in the standard configuration.Both found an anomalous behaviour of λ_g,consisting in a maximum in the λ_g-values at about 3 K,of a magnitude ,5 to 8 times the theoretical value.Earlier,Stauder and Mielczarek (208) had also found a maximum,but in the total thermal conductivity of K and between 5 K and 6 K.However,careful measurements of Newrock and Maxfield (201) ruled out such anomalous behaviour of λ_{total}.

We believe that the anomalous behaviour in the lattice conductivity,as observed by Fletcher (154) and Newrock and Maxfield (161) are not real as well and can be ex-

Table 4.10 : Experimental Coefficients of Indium determined by computeral fitting

T K	a_o 10^{-3} Wcm^{-1}K^{-1}	a_1 10^{-3} WTcm^{-1}K^{-1}	a_2 10^{-3} WT^{2}cm^{-1}K^{-1}
0.41	0.211	5.47	15.5
0.48	0.408	4.89	20.4
0.53	0.409	5.81	22.7
0.67	0.413	10.0	24.0
0.88	0.744	10.8	39.7
1.36	1.69	18.3	98.8
1.51	2.19	15.4	138.6
1.90	3.44	22.2	244.3
2.50	5.64	58.9	437.6
2.97	7.83	82.2	819.3
3.45	11.4	172.9	1483.5
4.17	20.3	280.2	3072.

plained as due to a misinterpretation of a partial Corbino effect.This shall be expounded in section 4.3.5.

In view of the fact that all attempts to measure λ_g of Potassium have produced anomalous results which deviates considerably from the theoretical predictions but are most probably due to non-intrinsic effects,a careful, unambiguous measurement of the lattice thermal conductivity of K should have a high level of priority.We believe that the Corbino method forms a most suitable approach to such a study.

4.3.4 Thermal Linear Magnetoresistance.

In equating Eq.(4.49) to Eq.(4.51),i.e.

$$\lambda(H) = \lambda_g + \frac{s}{A_{RL}^2} H^{-1} + \frac{W_o}{A_{RL}^2} H^{-2} \qquad (4.49)$$

$$= a_o + a_1 H^{-1} + a_2 H^{-2} \qquad (4.51)$$

the Righi-Leduc value $A_{RL}T$ was assumed to be constant. As predicted theoretically (85) and measured experimentally both for Al (195,196) and In (157,158,196),this is indeed the case for sufficiently high fields and low temperatures.In the high field,low temperature limit $A_{RL}T$ is constant and equal to the free electron value R_H/L_o (Eq.(4.38)) within about 5 %.Hence for

$$\begin{aligned} &\text{Al} : A_{RL}T = 0.418 \ \text{cmK}^2\text{W}^{-1}\text{T}^{-1} \\ &\text{In} : A_{RL}T = 0.653 \ \text{cmK}^2\text{W}^{-1}\text{T}^{-1} \end{aligned} \qquad (4.55)$$

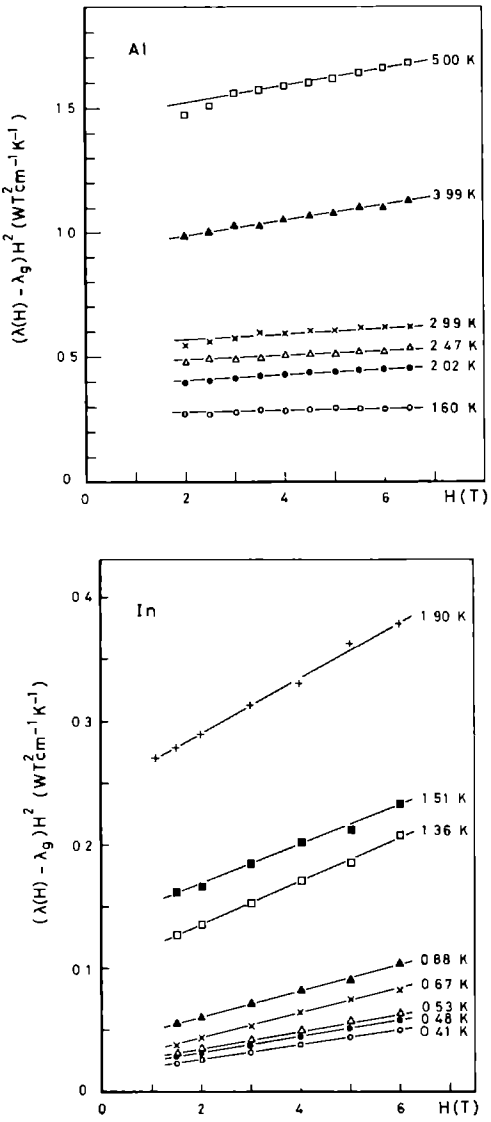

Fig.4.13 and 4.14 : $(\lambda(H) - \lambda_g)H^2$ plotted as a function of field to exhibit the linear magnetoresistance for Al and In.

Rewriting Eq.(4.49) yields back the thermal resistivity, divided by the square of the Righi-Leduc coefficient A_{RL}, which is constant at constant temperatures,i.e.

$$\frac{W_{xx}}{A_{RL}^2} = (\lambda(H) - \lambda_g)H^2 = a_2 + a_1 H \qquad (4.56)$$

The thermal linear MR can be made apparent by plotting $(\lambda(H) - \lambda_g)H^2$ against H,as in Fig.4.13 and Fig.4.14,and the resulting curves are indeed straight lines with slopes a_1,crossing the vertical axis at values a_2.

When dealing with the electrical linear MR,it is customary to characterize it by a Kohler slope defined by Eq.(4.39).Analogous to the electrical case,a dimensionless Kohler slope S_{th} can be defined by

$$S_{th} = \frac{W(H,T) - W(0,T)}{W(0,T)\omega_c\tau} = \frac{\Delta W/W}{\omega_c\tau} \qquad (4.57)$$

However,one has to be careful in the interpretation of the relaxation time τ for the thermal transport processes. Although it is reasonable to assume that the electrical relaxation time τ_{el} is equal to the thermal relaxation time τ_{th},since both relaxation processes involve the same conduction electrons,a single relaxation time can be defined only when the scattering is elastic,i.e.when the initial and final states have the same energy values. This occurs in the limit of rather high ($T > \theta$) and rather low ($T \approx 0$,for very pure metals) temperatures.It is only at these limiting temperatures that the WF-law is strictly valid,independent of the detailed nature of the

bandstructure,the Fermi surface,etc. i.e.

$$\frac{\rho}{WT} = \frac{\pi^2}{3}(k_B/e)^2 = L_o = 2.443\times10^{-8}\ W\Omega K^{-2} \quad (4.58)$$

At intermediate temperatures inelastic scattering , involving change in the energy of the electrons at collision,becomes important and which is more effective at restricting the thermal rather than the electrical conductivity,hence $\tau_{el} > \tau_{th}$ and

$$\frac{\rho}{WT} = L(T) = L_o \frac{\tau_{th}}{\tau_{el}} \quad (4.59)$$

This should be visualized,not as a difference of the rate at which the electrons experience collisions in the electrical and in the thermal case,but rather as a difference in the effectiveness of each single collision in degrading the electrical and thermal currents.

Obviously,the difference in relaxation times bears an influence on the high field condition

$$\omega_c\tau \gg 1 \quad (4.60)$$

To investigate this point we shall first rewrite Eq.(4.60) in terms of the applied field.Realizing that $\tau=l_e/v_F$, and $\omega_c = v_F/R_c$,where l_e is the electron mean free path,v_F is the Fermi velocity and R_c is the cyclotron radius,one arrives at the equivalent condition

$$\omega_c\tau = l_e/R_c \gg 1$$

which expresses the fact that in high fields the electrons will undergo many complete circulations before being

scattered. The cyclotron radius for a free electron is

$$R_c = \hbar k_F / eH$$

The electron mean free path l_e can be expressed as a function of the residual resistance ratio RRR= $\rho(295\ K)/\rho(0\ K)$,

$$l_e = \frac{\rho_o l_e}{\rho(295\ K)}\ (RRR) \qquad (4.61)$$

where for metals $(\rho_o l_e)$ has a constant value and ρ_o constitutes the residual resistivity for T= 0 K.
Hence, in the electrical case we obtain for the high field condition

$$\omega_c \tau_{el} = \frac{eH}{\hbar k_F} \left(\frac{\rho_o l_e}{\rho(295\ K)}\right)(RRR) \gg 1 \qquad (4.62)$$

Table 4.11. Estimate of high field condition $\omega_c \tau \gg 1$

	Al	In	Ref.
$\rho_o l_e$ (Ωcm^2)	$7. \times 10^{-12}$	5.8×10^{-12}	(203)
$\rho(295\ K)$ (Ωcm)	2.74×10^{-6}	8.75×10^{-6}	(204)
k_F (cm^{-1})	1.78×10^{8}	1.5×10^{8}	(47)
v_F (cms^{-1})	2.02×10^{8}	1.74×10^{8}	(47)
RRR	40 000	10 000	exp.
$R_c H$ (cmT)	11.5×10^{-4}	9.9×10^{-4}	calc.
l_e (cm)	$9. \times 10^{-2}$	$7. \times 10^{-3}$	calc.
H_o (T)	0.023	0.141	calc.

Table 4.12 : Calculated parameters of Aluminium.

T	A_{RL}	$S_{th} = a_1 A_{RL}$	$s = a_1 A_{RL}^2$	$b = a_1/a_2$	$W_o = a_2 A_{RL}^2$	τ
K	$cmKW^{-1}T^{-1}$	10^{-3}	$10^{-4} cmKW^{-1}T^{-1}$	$10^{-2}T^{-1}$	$10^{-2} cmKW^{-1}$	10^{-11} sec
1.60	0.261	1.607	4.194	2.350	1.785	8.33
2.02	0.207	2.617	5.417	3.324	1.630	7.25
2.47	0.169	1.838	3.107	2.345	1.325	7.25
2.99	0.140	3.157	4.420	4.365	1.012	7.87
3.99	0.105	2.265	2.378	2.352	1.011	5.92
5.00	0.0836	2.932	2.452	2.416	1.015	4.67
5.71	0.0732	3.935	2.881	3.22	0.894	4.65
6.94	0.0602	4.638	2.792	2.51	1.112	3.08
8.07	0.0518	7.166	3.712	3.005	1.235	2.39
10.0	0.0418	14.96	6.251	3.496	1.788	1.33
14.9	0.0281	90.22	25.35	11.667	2.173	0.74

Rewritten in explicit terms of the applied field, this yields

$$H \gg H_o = \left(\frac{\hbar}{e}\right)\frac{k_F \rho(295\ K)}{(\rho_o l_e)(RRR)} \qquad (4.62a)$$

The relevant values for Al and In are summarized in Table 4.11.

For the thermal case one obtains in view of Eq.(4.59)

$$\omega_c \tau_{th} = \omega_c \tau_{el} \frac{L(T)}{L_o} = \frac{H}{H_o}\frac{L(T)}{L_o} \qquad (4.63)$$

L(T) is critically dependent on sample purity and sample treatment, and cannot be derived generally. However, White (202) has analysed the L(T) behaviour of several metals, i.e. Al, Cu, Fe, Pb, Pt, W at elevated temperatures. Plotting L(T) as a function of the reduced temperature T/θ, he found that the $L(T/\theta)$-values of the different metals coincide, going through a deep minimum of about 0.34 L_o at 0.1 T/θ and reaching the L_o-value again at about 2 T/θ. Estimating from these results the high field condition in the thermal case, i.e.

$$\omega_c \tau_{th} \gg 1 \qquad (4.64)$$

we find from Eq.(4.63) that Eq.(4.64) transform into

$$H \gg 3\ H_o \qquad (4.65)$$

It can be seen from Table 4.11 that for Al and In, H_o lies between 0.02 T and 0.20 T. Therefore, above 1 T one is in the high field region for the thermal case as well.

Table 4.13 : Calculated parameters of Indium.

T	A_{RL}	$S_{th} = a_1 A_{RL}$	$s = a_1 A_{RL}^2$	$b = a_1/a_2$	$W_o = a_2 A_{RL}^2$	τ
K	$cmKW^{-1}T^{-1}$	10^{-3}	$10^{-4} cmKW^{-1}T^{-1}$	$10^{-2}T^{-1}$	$10^{-2} cmKW^{-1}$	10^{-11} sec
0.41	1.593	8.71	13.87	0.353	3.93	2.30
0.48	1.360	6.65	9.05	0.239	3.78	2.05
0.53	1.232	7.16	8.82	0.256	3.45	2.03
0.67	0.975	9.77	9.55	0.418	2.28	2.43
0.88	0.742	7.99	5.93	0.271	2.19	1.93
1.36	0.480	8.79	4.22	0.185	2.28	1.20
1.51	0.432	6.67	1.16	0.111	2.79	0.95
1.90	0.344	7.64	2.63	0.091	2.89	0.68
2.50	0.261	15.37	4.01	0.135	2.98	0.50
2.97	0.220	18.08	3.98	0.100	3.97	0.32
3.45	0.189	32.67	6.17	0.117	5.30	0.20
4.17	0.157	44.0	6.91	0.912	7.57	0.12

However, besides the temperature dependence of the Lorenz number L(T) an extra difficulty arises from its field dependence L(H).
For Al, Amundsen and Olsen (205) have measured the field dependence of the Lorenz constant L(H) in Al films of thickness d= 0.07 ∿ 0.2 mm, at a constant temperature (4.2 K) and in fields up to 1.3 T. They found that after an initial maximum $L(H)/L_o$ decreases to a value of about 85 %.
For In, the temperature and field dependence of L were measured by Wyder (2) and De la Cruz et al. (13) in polycrystalline samples and by Challis et al. (53) in a single crystal, in the temperature region between 1.5 K and 4 K and in fields up to 1 T. The results show a decrease of $L(T)/L_o$ with increasing temperature to about 50 % at 4 K. As for the field dependence, $L(H)/L_o$ appears to increase slightly with increasing field up to about 120 % at 0.05 T, after which it decreases again to about 70 % at 1 T, for all temperatures between 1.5 K and 4 K.
No good theory exists as yet to explain the field dependence of the Lorenz number.

Returning to Eq. (4.57), we shall explicitly define the thermal Kohler slope S_{th} by

$$S_{th} = \frac{\Delta W/W_o}{\omega_c \tau_{th}} \qquad (4.66)$$

where we have identified W= W(0,T) (Eq. (4.57)) with W_o (Eq. (4.48)). From Eqs. (4.47), (4.49) and (4.51) it follows

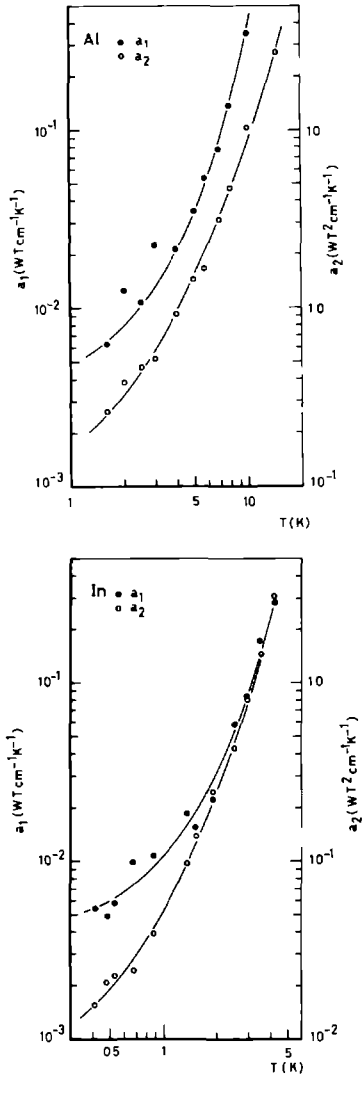

Fig.4.15 and 4.16 : a_1 and a_2 as a function of T for Al and In.

that

$$\Delta W/W_o = bH = \frac{a_1 A_{RL}^2 H}{W_o} \tag{4.67}$$

In the free electron model

$$\omega_c \tau_{th} = \frac{A_{RL} H}{W_o} \tag{4.68}$$

Hence, using Eqs.(4.67) and (4.68), we arrive at

$$S_{th} = \frac{\Delta W/W_o}{\omega_c \tau_{th}} = a_1 A_{RL} \tag{4.69}$$

However, comparison of the slopes with data found by other investigators have often been complicated by the use of different definitions of slopes to describe the linear MR. For that reason, besides the thermal Kohler slope S_{th}, we shall also define the slope s of the linear portion of the thermal resistivity $W_{xx}(H)$, which from Eqs.(4.47) and (4.67) can be expressed as

$$s = \frac{\Delta W}{H} = a_1 A_{RL}^2 \tag{4.70}$$

as well as the slope b of the thermal MR (Eq.(4.67))

$$b = \frac{\Delta W/W_o}{H} = a_1/a_2 \tag{4.71}$$

Here, W_o has been taken as

$$W_o = a_2 A_{RL}^2 \tag{4.72}$$

which follows from Eqs.(4.49) and (4.51).

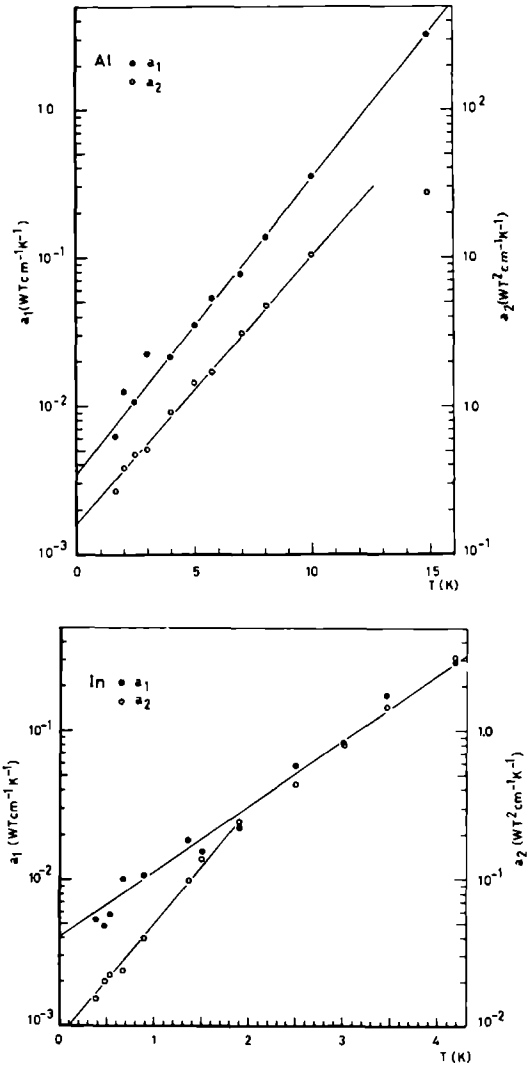

Fig.4.17 and 4.18 : a_1 and a_2 as a function of T for Al and In, plotted on a half-log. scale to show the exponential temperature dependence.

The values for S_{th},s,b, and W_o have been collected in Table 4.12 and Table 4.13 for Al and In,respectively.

We shall first concern ourselves with the results of S_{th} as a function of temperature.To arrive at the temperature dependence of S_{th},we have plotted a_1 and a_2 as a function of T in Fig.4.15 and Fig.4.16.It follows from those figures that $a_1$and a_2 of both Al and In do not follow a simple power law of the form

$$a_i \sim T^{x_i} \quad (i=1,2;\ x= \text{real number}) \qquad (4.73)$$

over the temperature range investigated.However,a_1 and a_2 can be fairly well represented over the temperature region under consideration by an exponentional function of T (Fig.4.17 and Fig.4.18),i.e.

$$a_i \sim \exp(y_i T) \quad (i=1,2;\ y= \text{real number}) \qquad (4.74)$$

As $A_{RL}T$ is constant in the high field,low temperature limit,A_{RL} can be taken to have a T^{-1} dependence. Combining these results we have plotted S_{th} as a function of T in Fig.4.19 and Fig.4.20.For reasons of comparison, s and b have also been plotted.Several conclusions can be drawn from these results:

i) Both for Al and In the Kohler slope S_{th} does not remain constant but increases with increasing temperature. This suggests that Kohler's rule is <u>not</u> obeyed and progressively less so the higher the temperature.

ii) S_{th} spans the range between 10^{-3} and 10^{-1} which,compared to $S_{el}=10^{-4} \sim 10^{-2}$,is generally an order of magnitude higher.

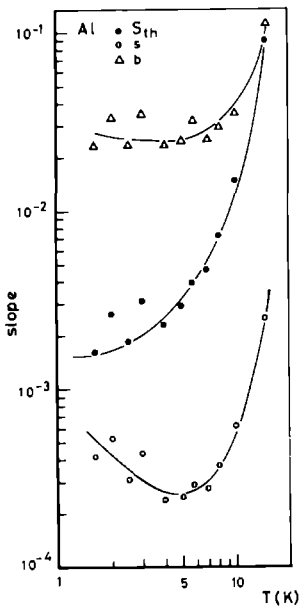

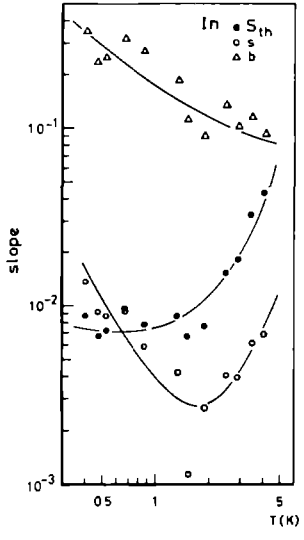

Fig.4.19 and 4.20 : The different slopes for Al and In.

iii) In most experimental investigations of the linear MR, the changes of S_{el} and S_{th} were attributed to differences in sample preparation, impurity content, strain, etc. and the Kohler slope was correlated to the RRR only. In our case and in contrast to former studies, the change in S_{th} is due solely to its temperature dependence. Although at low temperatures the increase of S_{th} with T is relatively small, at higher temperatures the increase of S_{th} with T is considerable and far steeper than the increase due to impurity enhancement. It follows from our results that the temperature is a highly significant parameter in determining the slope of the linear MR. Theoretical models attempting to explain the linear MR should take the pronounced temperature dependence of the Kohler slope into account. As yet, this has been done by none of the currently available theories. In view of these arguments it appears rather interesting to investigate the temperature dependence of S_{el} and S_{th} over an extended range of temperatures for samples of different purity.

iv) It follows from Eqs.(4.69), (4.70) and (4.71) that the differently defined slopes S_{th}, s and b are characterized by different temperature dependences. To illustrate this point we have also plotted s and b in Figs.4.19 and 4.20. When comparing data one should always be careful to establish if the same definitions of the different slopes is being used. The ambiguity in the definition of the slopes and the subsequent difference in their temperature behaviour are the main reasons that one often encounters

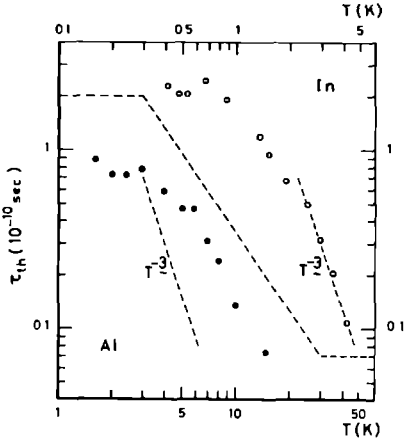

Fig.4.21 : The thermal relaxation time as a function of temperature for Al and In.

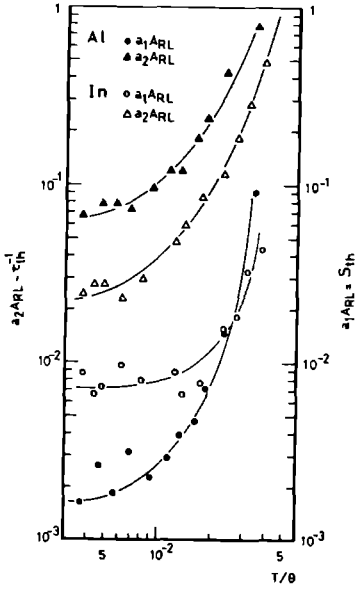

Fig.4.22 : Thermal Kohler slope and thermal relaxation time as a function of the reduced temperature.

conflicting reports in the literature.The situation is further compounded by the fact that in most cases the slopes are measured in a small temperature range in the helium region only.As our measurements have shown,conclusions valid for a small,low temperature range cannot in general be straightforwardly extended to a higher temperature region.

v) Using Eqs.(4.69) and (4.71), the thermal relaxation time τ_{th} can be written as

$$\tau_{th} = \frac{bH}{S_{th}\omega_c} = (a_2 A_{RL}(\frac{e}{m}))^{-1} \text{ sec} \qquad (4.75)$$

where for free electrons the charge-mass ratio is constant,

$$(e/m) = 1.7588 \times 10^{11} \text{ Ckg}^{-1} \qquad (4.76)$$

As can be seen from Fig.4.21,after an initial constant value of

$$\text{Al} : \tau_{th} = 8 \times 10^{-11} \text{ sec}$$
$$\text{In} : \tau_{th} = 2 \times 10^{-10} \text{ sec}$$

τ_{th} reduces sharply with an order of magnitude when the temperature is increased.Assuming

$$A_{RL} \sim T^{-1}$$
$$W \sim \beta T^{-1} + \alpha T^2$$

and using Eq.(4.68),the temperature dependence of τ_{th} can be estimated,i.e.

$$\tau_{th} \sim \frac{A_{RL}}{W} \sim T^{-3} \qquad (4.77)$$

It follows from Fig.4.21 that with increasing temperature τ_{th} drops less steeply than a T^{-3}-dependence; a T^{-3}-behaviour is only followed by In at the highest measured temperature.

From

$$l_{th} = v_F \tau_{th} \tag{4.78}$$

the thermal electron mean free path l_{th} can also be estimated, using the v_F-values of Table 4.11, i.e.

$$\begin{aligned} \text{Al: } l_{th} &= 1.6 \times 10^{-2} \text{ cm } (T < 3 \text{ K}) \\ &= 1.5 \times 10^{-3} \text{ cm } (T \approx 15 \text{ K}) \\ \text{In: } l_{th} &= 3.8 \times 10^{-2} \text{ cm } (T < 1 \text{ K}) \\ &= 2. \times 10^{-3} \text{ cm } (T \approx 4 \text{ K}) \end{aligned} \tag{4.79}$$

which is of about the same order of magnitude as those obtained for the electrical electron mean free path l_e by means of Eq.(4.61) (Table 4.11).

vi) When one plots the several parameters as a function of the reduced temperature T/θ, where θ is the Debye temperature (Table 4.3) a striking similarity between the results obtained for Al and In appears. This is demonstrated in Fig.4.22 where we have plotted $a_1 A_{RL} = S_{th}$ and $a_2 A_{RL} \sim \tau_{th}^{-1}$ as a function of T/θ. The similarity is also present in the curves of s, b, W_o as functions of T/θ.

vii) Still another difficulty is manifested by the temperature and field dependence of the Righi-Leduc value $A_{RL}T$. Theory (85) predicts it to be constant in the high field limit and equal to the free electron value

$$A_{RL}T = R_H/L_o \tag{4.38}$$

The experimental results for Al (195,196) and In (157,158, 196) agree with this prediction only in the low temperature,high magnetic field limit.With increasing field,the free electron value of $A_{RL}T$ is reached the sooner the lower the temperature,but for higher temperatures the available fields were not of sufficient strength to show a saturation of $A_{RL}T$ at the free electron value R_H/L_o (158).

Measurements on the alkali metals Na,K,Li,and Rb (134,197) at temperatures ranging from 2 K to 120 K and in fields up to 1 T also show the low temperature high field limiting value of A_{RL} and R_H to be as expected from Eq.(4.38).The temperature dependence of $A_{RL}T$,however, shows a pronounced peak at temperatures between 10 K and 40 K (134,197) although R_H varies only weakly with temperature (199).At higher temperatures $A_{RL}T$ drops below the free electron value R_H/L_o.

When plotted against the reduced temperature T/θ,the $A_{RL}T$ versus T/θ-curves of Na,K and Rb show a similar behaviour with their peaks at the same T/θ-value (197).The reason for this anomalous behaviour of $A_{RL}T$ is not clear.

An increase of $A_{RL}T$ may be provided by anisotropic relaxation time (134,210) but the observed enhancement of $A_{RL}T$ is far too high to be completely accounted for by the proposed mechanism.

Another possible explanation could be the influence of inelastic scattering.As at intermediate temperatures and at zero field this mechanism is working with different effectiveness on the electrical and thermal currents, thereby reducing the Lorenz number L(T),it could equally

well have the same effect in the intermediate temperature high field limit,both on $\rho(H,T)$ and $W(H,T)$,as well as on $R_H(H,T)$ and $A_{RL}(H,T)$,i.e.

$$\frac{\rho(H,T)}{W(H,T)T} = \frac{R_H(H,T)}{A_{RL}(H,T)T} = L(H,T) \qquad (4.80)$$

Fletcher (134,197) rejected this explanation with the following argumentation:
When on a heat current U_x a magnetic field H in the z-direction is applied,a transverse heat current

$$U_y = \omega_c \tau_{th} U_x \qquad (\omega_c \tau_{th} \gg 1)$$

is established.Experimentally,the condition $U_y = 0$ is maintained,so that a transverse temperature gradient is created of

$$(\partial T/\partial y) = - U_y/\lambda$$

Hence,one finds for the Righi-Leduc coefficient (Eq.(4.36))

$$A_{RL} = \frac{-(\partial T/\partial y)}{H U_x} = \frac{\omega_c \tau_{th}}{H\lambda} = \frac{R_H}{L_o T}$$

using $\lambda = \pi^2 k_B^2 n T \tau_{th}/3m$,appropriate for the free electron model and neglecting λ_g.
A similar argument holds in the case of an electric current and for the resulting Hall coefficient R_H.

These arguments,however,are based on the free electron model,which is well known to be deficient in explaining magnetic field effects on transport theory,as is

illustrated by its prediction of a zero magnetoresistance. Assuming the effects of inelastic scattering to be visible in the Righi-Leduc and Hall coefficients also, we can generalize the LAK-result of Eq.(4.38) into

$$\frac{R_H}{A_{RL}T} = L(H,T) \qquad (4.81)$$

If one neglects the field dependence of L for the moment, L(H,T) is equivalent to Eq.(4.59), i.e.

$$L(H,T) \approx L(T) = L_o \frac{\tau_{th}}{\tau_{el}} \qquad (4.82)$$

The observed peak in A_{RL} can now be interpreted as follows:

To compare the measured values of A_{RL} and R_H on an equal footing, Fletcher has plotted $A^m_{RL}L_oT$ and R^m_H versus T (m indicates the measured values), and found e.g. for Na, the peak value of $A^m_{RL}L_oT$ about 21 % higher than the equivalent value of R^m_H, at a peak temperature of 23 K. Compared with the values in the low temperature limit, where $A^m_{RL}L_oT$ and R^m_H are indeed equal, the peak value of $A^m_{RL}L_oT$ is about 32 % higher.

In our opinion, to arrive at equivalent values of R^m_H, one should plot according to Eq.(4.81) and (4.82), i.e.

$$\begin{aligned} A^m_{RL}L(T)T &= A^m_{RL}L_oT(L(T)/L_o) \\ &= A^m_{RL}L_oT(\tau_{th}/\tau_{el}) \end{aligned} \qquad (4.83)$$

Hence, the plotted values of $A^m_{RL} L_o T$ are a factor $L_o/L(T)$ higher than the equivalent values $A^m_{RL} L(T) T$ of R^m_H.
If our assumptions are correct, the peak of $A^m_{RL} L_o T$ should correspond to the peak in $L_o/L(T)$, both with regard to its magnitude as with regard to its peak temperature.
Of the alkali metals under consideration only of Na could we find references (215,216), which provide measurements of $L_o/L(T)$, with a peak 70 $\sim$ 80 % higher than the zero field value, at peak temperatures between 12 and 16 K.
This is in reasonable agreement with Fletcher's Na-results for $A^m_{RL} L_o T$, when one takes into account that the field dependence of L(H,T) is completely neglected and that both the magnitude of the peak and the temperature at which it occurs in $L_o/L(T)$ is highly dependent on the handling and the purity of the samples.
viii) In the interpretation of our data of Al and In, we have consistently taken $A_{RL} T$ to be constant, in accordance with the LAK-theory. This entails a T^{-1}-dependence of A_{RL} for the whole temperature range.
In view of the results obtained by Fletcher for the alkali metals and if our assumptions that the LAK-prediction, expressed by Eq.(4.38) should be generalized to Eq.(4.81) at intermediate temperatures prove to be true, the employed temperature dependence of A_{RL} is not correct and our results should be analysed more carefully. Due to a complete lack of the necessary data, this proved to be impossible.
We should like therefore to conclude this subsection with the following observations:

A) For most metals the field dependence of the different transport properties have been well investigated in the region of low temperatures.A paucity of information concerning the field behaviour of the different transport parameters exist,however,in the intermediate and high temperature ranges.This information cannot be obtained by a simple extrapolation from the low temperature limit. The cited results of Fletcher for the alkali metals and the magnetoresistance measurements of Al for temperatures up to 32 K of Krevet and Schauer (209) show that interesting results are to be expected in these temperature ranges.

In view of these considerations it would be desirable if the measurement of transport properties in high fields and in temperatures,say,between 5 K and 50 K or higher, gains more emphasis in the near future.

B) In particular,it would be highly interesting to measure the field dependence of the Lorenz number L via the electrical resistivity ρ and the thermal resistivity W,i.e.

$$\rho(H,T)/W(H,T)T = L(H,T)$$

and via the Hall coefficient R_H and the Righi-Leduc coefficient A_{RL},i.e.

$$R_H(H,T)/A_{RL}(H,T)T = L(H,T)$$

in one and the same sample for an extended range of temperatures.The results would provide a check on the LAK-prediction Eq.(4.38) or its generalization Eq.(4.81).

4.3.5 The (so-called) Quadratic Magnetoresistance.

In several recent articles on measurements of the thermal MR of Potassium,Newrock and Maxfield (NM)(153,161, 164) and Fletcher (F)(154) have reported a gradual transformation from a linear to a quadratic field dependenc of W(H,T)T as the temperature is lowered.The electrical MR of some of their samples has also been measured using helicon techniques and found to be linear over the field range in question.Former electrical measurements by Taub et al.(124) on long wires also displayed a linear MR only. Consequently,since W(H,T)T is quadratic and $\rho(H,T)$ linear in H,the prediction of the LAK-theory(85) that the high field Lorenz ratio should be constant,i.e. independent of field,appears to be violated,and the departure from L_o increases as the temperature decreases.
According to NM,the quadratic field dependence of WT is a new aspect of the thermal MR behaviour (of Potassium) which has no analogue in the electrical MR.No theory exists,however,to explain this effect and NM suggested that a possible origin may lie in inelastic scattering processes or a field dependence of some parameters in the Boltzmann equation.

We shall demonstrate here,that a far more plausible explanation can be found by taking into account the influence of the sample geometry on the MR and that the observed anomalous behaviour can consistently be explained as the result of a partial Corbino effect.

As evidenced by Figs.4.23 and 4.24,the thermal resistivity of both Al and In also show the phenomenon of a quadratic field dependence.But here,as explained in section 4.2.9,the quadratic field dependence has a natural geometrical cause and finds its origin in the utilized Corbino configuration.When one takes the Corbino effect and the lattice conductivity into account (Eq.(4.55)), the quadratic field dependence disappears and the thermal MR reduces to a linear field behaviour (Fig.4.13 and Fig.4.14),in complete agreement with the electrical results.
An explanation for the close parallel between the F and NM-results which were obtained without using the Corbino geometry,and our measurements on Al and In,which were acquired with full use of the Corbino effect,can be found in the theoretical papers of Lippmann and Kuhrt (70).

For a rectangularly shaped plate the MR and the Hall effect deviates strongly from the bulk behaviour when the length and width of the samples become comparable.This deviation is usually small for the Hall effect and can be neglected when the length of the specimen is about four times longer than its width.But the magnetoresistance may be strongly modified,even for samples with a much smaller width to length ratio.
This effect occurs because the Hall field is reduced at the ends of a specimen,allowing the Lorentz force to remain partly uncompensated.What one obtains is a partial Corbino effect.

Lippmann and Kuhrt (70) have analysed this effect in detail and have obtained approximate formulas for the electrical resistivity.Transforming their results to the thermal case one finds for the thermal resistivity in the different limiting cases

$$\frac{W(H,b/a)}{W(0,b/a)} = \frac{W(H,0)}{W(0,0)} \times \begin{cases} (1+tg^2\theta_{RL}) & ;\frac{b}{a} \to \infty \\ (1+tg^2\theta_{RL})^{1/2} & ;\frac{b}{a} = 1 \\ (1+\frac{b}{a}(tg\theta_{RL} - \frac{4\ln 2}{\pi}) & ;\frac{b}{a} \to 0 \end{cases} \tag{4.84}$$

Here,W(H,b/a) is the thermal resistivity of a plate with length a and width b in a field H perpendicular to the plate,$\theta_{RL}$is the Righi-Leduc angle and

$$tg\ \theta_{RL} = A_{RL}H/W \tag{4.85}$$

The configuration where $b/a \to \infty$,corresponds to the complete Corbino geometry;the other limit of Eq.(4.84),i.e. $b/a = 0$,corresponds to the geometry of an infintely long wire.In this case the geometry effect is absent and one re-obtains the geometry of the standard configuration of most MR measurements.

The thermal MR measurements of Newrock and Maxfield (161),however,were done on plate like specimen of rectangular shape (201),i.e. conform to the configuration $1 < b/a < 0$.

It follows from Eq.(4.84) and Eq,(4.85),that if W(H,0) shows a linear field dependence,W(H,b/a) would display a quadratic field behaviour.
The electrical MR measurements performed by helicon techniques woul obviously not show this particular geometry effect,nor would electrical MR measurements on long thin wires.It is to be expected,however,that electrical MR measurements with the same geometrical configuration would show the same quadratic field dependence.

Hence,the quadratic field dependence is not an intrinsic phenomenon but an effect due to the specific geometry of the specimen and the experimental arrangement.

Consequently,the conclusion drawn by NM,that,since W(H,T)T shows a quadratic and $\rho(H,T)$ a linear field behaviour,the Lorenz ratio

$$L(H,T)= \rho(H,T)/W(H,T)T$$

would always display a field dependence - in contrast to the LAK-theory which predicts it to be constant in the high field limit - is rather premature.
At high fields,<u>both</u> the electrical and the thermal MR show a linear field dependence,and a <u>linear</u> field dependence only,and this would not affect the Lorenz ratio.
Experiment,where the electrical and thermal MR are measured at the same rectangular sample in the same configuration are needed to investigate these problems in a clear-cut way.

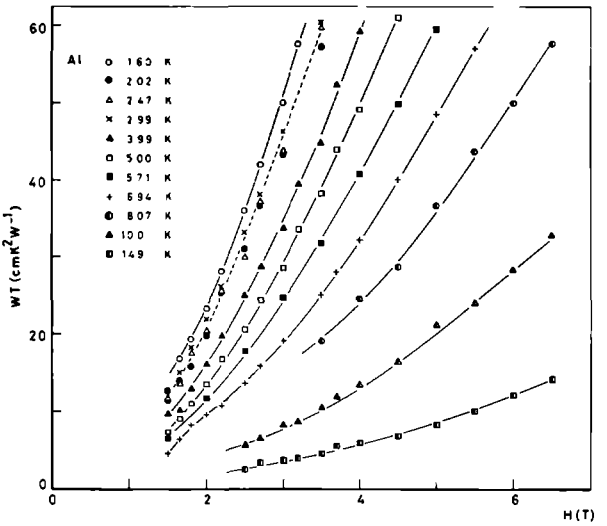

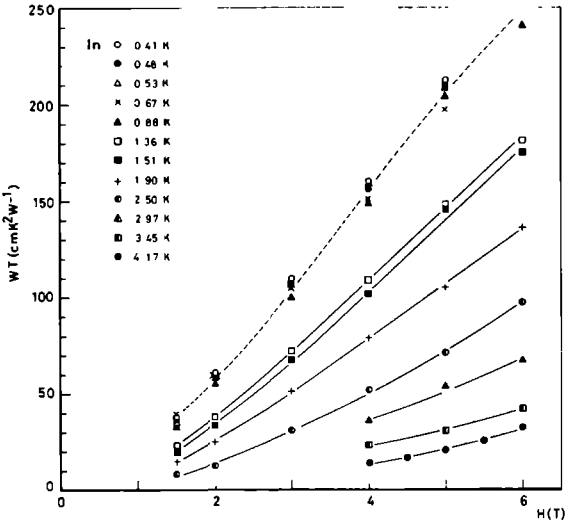

Fig.4.23 and 4.24 : Field dependence of WT for Al and In, at different constant temperatures.The temperature region where the curve-crossing occurs have been indicated by a broken line.

4.3.6 Curve-Crossing : the Kagan Effect.

Another effect ,observed by F (154) and NM (153, 161,164),involves the crossing of the curves at the lowest temperatures in plots of W(H,T)T versus H.They noted that with decreasing temperatures the field behaviour of W(H,T)T increases from a nearly linear to a nearly quadratic dependence.Hence,a curve of low temperature will eventually cross one of higher temperatures.

Although obviously all W(H,T)T vs.H curves obtained in the Corbino configuration show a quadratic field dependence,without the occurrence of linear curves,the curve crossing is also displayed in our results of Al (Fig.4.23) and,less pronounced,of In (Fig.4.24).
The crossing of the curves disappears however, if W(H,T) rather than W(H,T)T is plotted against H (Figs.4.25 and 4.26).Moreover,decreasing the temperature appears not to be a sufficient or even necessary condition to observe curve crossing.The curves seem to cross in a certain small temperature region only,i.e. between 2 K and 3 K for Al and in a small interval around 0.5 K for In.
As can be seen from Figs 4.27 and 4.28 where W(H,T)T is plotted against T for Al and In,respectively,the curve crossing is due to the appearance of a local maximum and minimum,which become more pronounced at higher fields.For K,these local extremes occur in an interval around 3 K,as can be surmised from the results of NM (e.g.ref.(161) Fig.2) and F(ref (154) Fig.1 and 3)

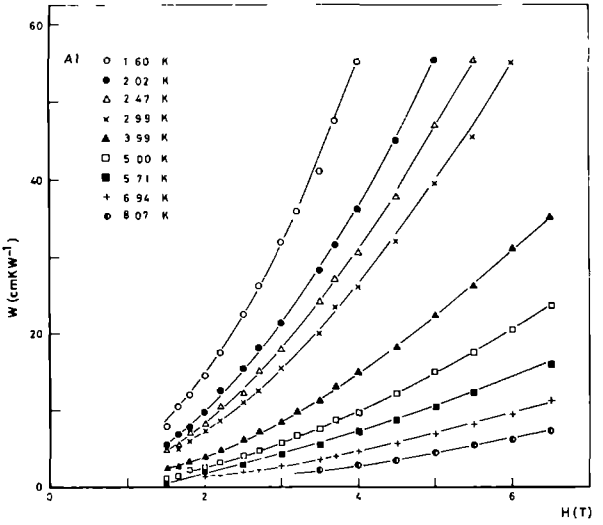

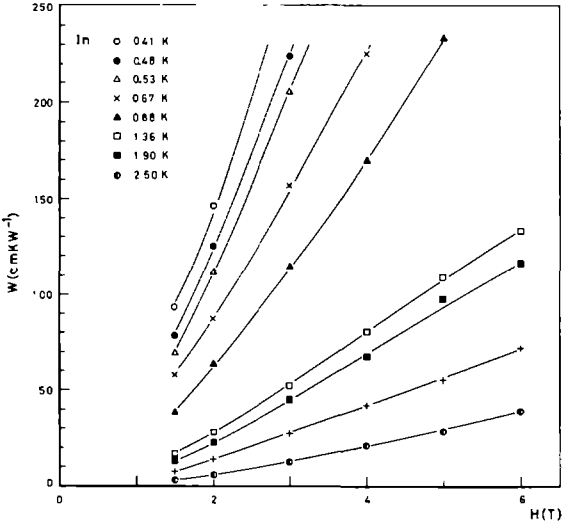

Fig.4.25 and 4.26 : Field dependence of W for Al and In.

When W(H,T)T is plotted against the reduced temperature T/θ,the temperature regions where the curve crossing occur,i.e. where the maxima appear,seem to coincide for Al and In (Fig.4.29).As to what causes the appearance of these localized extremes,when a magnetic field is applied,remains still to be investigated.

A possible interpretation may be found in the recent theoretical studies of Kagan and collaborators (213, 214),which have provided new insight and understanding of the unusual temperature behaviour of the electrical MR at intermediate temperatures.

It was found earlier by several workers(99,101,209) that with increasing temperatures in high fields the electrical MR of Al exhibited a maximum,the magnitude of which depended on the impurity concentration.According to Kagan, the explanation of this effect stems from the fact that in the limit of zero impurity the electron distribution function in metals is highly anisotropic,causing a considerable reduction of the electrical resistivity.The appearance of this anisotropy is due mainly to umklapp processes in the electron-phonon interaction,but is also caused by the anisotropy of the phonon spectrum and the Fermi surface.Even in the case of a nearly spherical Fermi surface,the scale of the anisotropy of the electron distribution in polyvalent metals is so great that taking it into account can change the resistivity of an ideal metal in a given temperature range by an order of magnitude.Any scattering or other mechanism which decreases

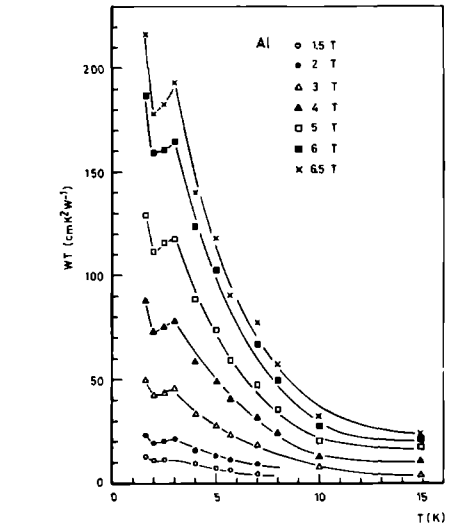

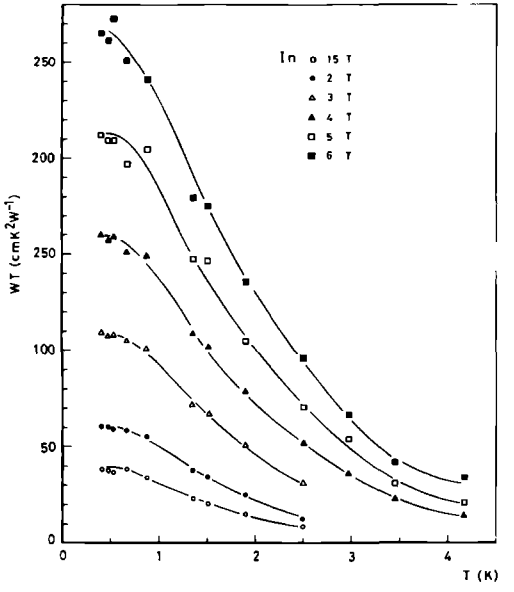

Fig.4.27 and 4.28 : Temperature dependence of WT for Al and In at different constant fields.

the anisotropy will thus considerably influence the magnitude of the resistivity.Hence,by applying a magnetic field or introducing impurities,isotropy may be restored more and more leading to an increase of the resistivity.

A finite MR exists only to the extent that the electron distribution function possesses anisotropy depending on the crystal structure.Therefore,for a closed orbit,uncompensated metal of very high purity,one expects to find in the high field limit where saturation occurs, that the temperature dependence of the MR should reflect the temperature dependence of the anisotropy of the distribution function of the conduction electrons. According to Kagan,this anisotropy function increases with temperature,passes through a maximum,then decreases to zero as T is enhanced still further.

To put this qualitative description of the Kagan theory on a more quantitative footing,we shall follow the treatment of Krevet and Schauer (209)

Consider the resistivity $\rho(H,T,r)$ at a given magnetic field H,a temperature T and of purity r,i.e.

$$\rho(H,T,r) = \rho_{res}(H,r) + \rho_{temp}(H,T,r) \qquad (4.86)$$
$$= \rho_{res}(H,r) + \rho_{ph}(T) + \Delta(H,T,r)$$

ρ_{res} is temperature independent and is due to electron-impurity scattering

ρ_{temp} is the temperature dependent part and consists of

ρ_{ph} ,which is the pure phonon contribution

Δ ,which represents the coupling between ρ_{ph} and ρ_{res}

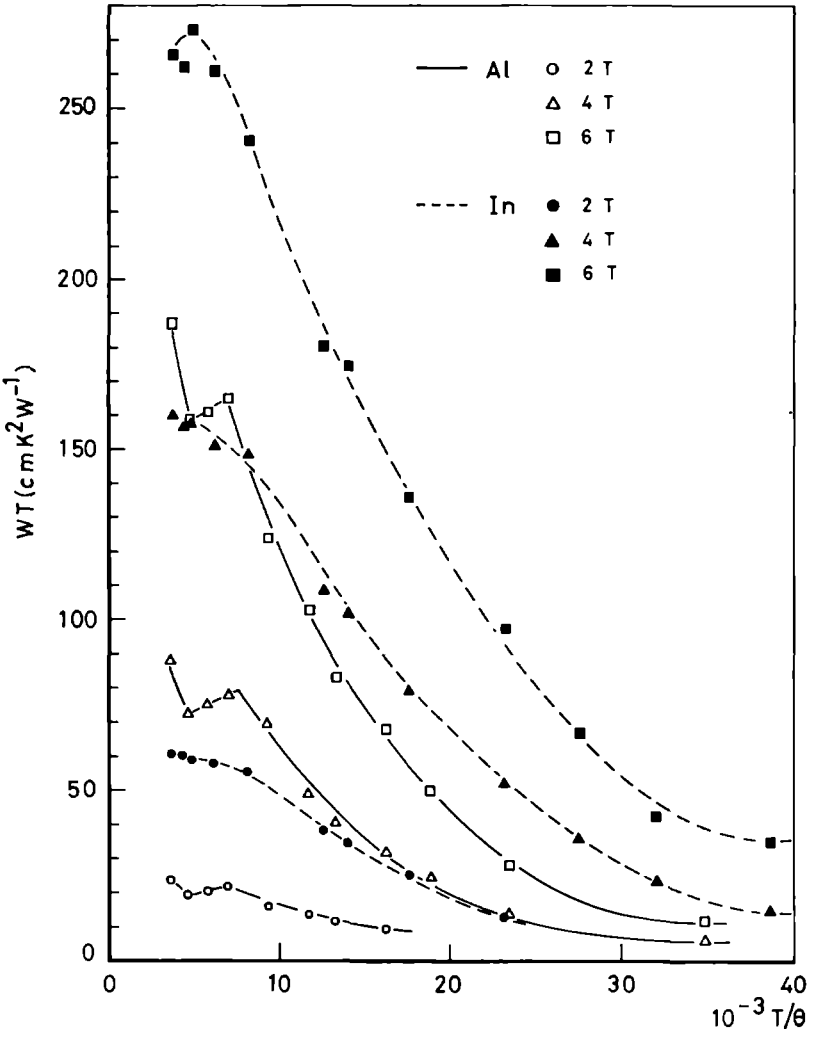

Fig.4.29 : WT as a function of the reduced temperature for Al and In.

and describes the deviation from Matthiessen's rule.

In the clean limit (infinite purity) and zero field, i.e.

$$H = 0, r \to \infty, \rho_{res} = \Delta = 0$$

where the anisotropy in the electron distribution is most effective, Kagan introduces the theoretical conception

$$\rho(0,T,r \to \infty) = \rho_{ph}(T) = \rho^{o}_{ph}(T)(1-\eta(T)) \quad (4.87)$$

Here, $\rho^{o}_{ph}(T)$ represents the phonon contribution corresponding to an isotropic electronic distribution function while $\eta(T)$ is a measure of the anisotropy of the electronic distribution function over the Fermi surface and which for Aluminium exhibits a maximum at $T_m \approx 5$ K (209, 214).

Isotropization of the electron distribution function occurs when purity is decreased or the magnetic field is increased. Both for the dirty limit $\rho_{res} \gg \rho_{temp}$ as well as for the high field limit $\omega_c \tau \gg 1$, the coupling term Δ is given by

$$\Delta(0,T,r)\Big|_{\rho_{res} \gg \rho_{temp}} = \Delta(H,T,r)\Big|_{\omega_c \tau \gg 1} = \rho^{o}_{ph}(T)\eta(T) \quad (4.88)$$

Combining Eqs. (4.86), (4.87) and (4.88) leads us to the important result of Kagan, that for both limits

$$\rho(0,T,r)\Big|_{\rho_{res} \gg \rho_{temp}} = \rho_{res}(0,r) + \rho^{o}_{ph}(T) \quad (4.89)$$

$$\rho(H,T,r)\Big|_{\omega_c \tau \gg 1} = \rho_{res}(H,r) + \rho^{o}_{ph}(T) \quad (4.90)$$

i.e. the resistivity in the high field limit exhibits the same temperature dependence as the resistivity in the dirty limit at zero field.

For a sample of very high purity (clean limit): $\rho_{res} = 0$. Hence, the magnetoresistance of a very pure sample in the high field limit (Eq. (4.90)) should be equal to the " phonon magnetoresistance"

$$\underset{\substack{r \to \infty \\ \omega_c\tau \gg 1}}{(\Delta\rho/\rho)} = \underset{\omega_c\tau \gg 1}{(\Delta\rho/\rho)_{ph}} = \eta(T)/(1-\eta(T)) \qquad (4.91)$$

Eq. (4.91) has a maximum at the same temperature T_m as the anisotropy function $\eta(T)$ itself. However, as purity decreases, this maximum shifts to higher temperatures and increases in magnitude.

For Al, the peak temperature T_m is about 5 K (209,214). The experimental results of electrical MR measurements on Al on the other hand display a maximum at about 17 K (99,209) for samples with an RRR between 20 000 and 30 000; for samples with a lower RRR the peak occurs at even higher temperatures. This may be due to the simplifying assumptions in the theory (spherical Fermi surface, Debye phonon spectrum) and the finite impurity content of the samples.

No theoretical extension of the Kagan theory to the thermal MR exists as yet, but this same mechanism, as discovered by Kagan and based on the anisotropy of

the electron distribution function,should be equally effective,mutatis mutandis,in influencing the thermal magnetoresistivity.Presumably,the maxima as displayed in the thermal MR curves of Al (Fig.4.27) and In (Fig.4.28) are but a manifestation of the Kagan mechanism.
The theory of Kagan is couched in general terms and not aimed at a specific metal,i.e. the results can be expressed as functions of the reduced temperature T/θ.
For different metals of the same impurity concentration, the difference in T_m,i.e. the temperature at which the maximum occurs,is determined only by the different values of the Debye temperature θ.In view of this argument,it is significant that,when plotted as a function of T/θ, the maxima in the WT-curves of Al and In seem to occur at about the same reduced temperature (Fig.4.29).
We know of no other references where the thermal MR of Al and In are displayed as a function of temperature and which would allow more unambiguous pronouncements.

4.3.7 The Thermal Lattice Conductivity of Potassium.

Recently,Fletcher (206) has developed a method to obtain the thermal lattice conductivity of pure uncompensated metals from thermal magnetoresistivity measurements at rather low fields.As shown by Fletcher (206),for uncompensated metals in not too high fields the measured thermal resistivity W_{xx}^{m} can be approximated by

$$W^m_{xx} \approx W^e_{xx} + (W^e_{xy})^2 \lambda_g \qquad (4.92)$$

Here, W^e_{xx} and W^e_{xy} are the electronic transverse and Righi-Leduc thermal resistivities, respectively. As

$$W^e_{xy} = A_{RL} H \qquad (4.93)$$

Eq.(4.92) can be transformed into

$$W^m_{xx} = W^e_{xx} + \lambda_g A^2_{RL} H^2 \qquad (4.94)$$
$$= c_o + c_2 H^2$$

Hence, Eq.(4.94) provides a convenient method to measure λ_g, especially in the case of Potassium which has a large W_{xy} (134) and a small W_{xx} for samples of sufficient purity. However, by measuring the thermal resistivity of K as a function of field up to 1 T in the temperature region between 1.5 K and 4.5 K and in samples, typically 50x4x1 mm^3 in size, Fletcher found that his results fitted far better an equation of the form

$$W^m_{xx} = c_o + c_1 H + c_2 H^2 \qquad (4.95)$$

rather than Eq.(4.94).

The interpretation by Fletcher (F) (154) and Newrock and Maxfield (NM) (161) of the coefficients c_o, c_1, c_2, connected with Eq.(4.95) invites some comments.

i) F and NM identified c_o with W(0,T), the thermal resistivity at zero field. However, as explained earlier (Eq.(4.48)), c_o is equal to W_o, which is the linear extrapolation of W(H,T) to H= 0, and which is not identical to

the actually measured zero field value of the thermal resistivity W(0,T),i.e.

$$W_o = a(T) + W(0,T) \qquad (4.48)$$

where a(T) is a constant.

This is supported by the fact that the zero field values of W^m_{xx} are the only points which did not lie on the curves,represented by Eq.(4.95) but invariably lower,as noted by both F and NM.

ii) F(154) indicated that the origin of c_1 is not understood,as indeed a linear term in H does not appear in the approximation of W^m_{xx} as expressed by Eq.(4.94).

For closed orbit,uncompensated metals however,W^e_{xx} does not saturate but acquires a linear field term at sufficiently high fields,i.e.

$$W^e_{xx} = c_o + c_1 H \qquad (4.96)$$

which explains the origin of c_1.

NM have also used this interpretation of c_1 (161) and have connected it to the thermal Kohler slope S_{th},i.e.

$$S_{th} = \frac{c_1}{A_{RL} T} \qquad (4.97)$$

However,care should be taken when comparing their results with those presented in this thesis,as in the pure Corbino geometry one would have obtained (Eqs(4.56),(4,69))

$$S_{th} = c_1 A_{RL} \qquad (4.97a)$$

The difference between Eq.(4.97) and Eq.(4.97a) stems from the fact that NM have used

$$W^{e}_{xx}T = W(H,T)T\Big|_{lin} = c_o + c_1 H \tag{4.98}$$

and have defined S_{th} as

$$S_{th} = \frac{\Delta W(H,T)T}{W(H,T)T}\Big|_{lin} / \omega_c \tau_{th} \tag{4.99}$$

where

$$\frac{\Delta W(H,T)T}{W(H,T)T}\Big|_{lin} = \frac{W(H,T)T - W(0,T)T}{W(H,T)T} = \frac{c_1}{W(H,T)T} \tag{4,100}$$

while in the pure Corbino geometry one would have used (compare with Eq.(4.56) where $a_1 = c_1$ and $a_2 = c_o$)

$$\frac{W^{e}_{xx}}{A^{2}_{RL}} = c_o + c_1 H \tag{4.100a}$$

and S_{th} is defined as

$$S_{th} = \frac{\Delta W/W_o}{\omega_c \tau_{th}} \tag{4.69}$$

where

$$\frac{\Delta W}{W} = \frac{W(H,T) - W_o}{W_o} \tag{4.57}$$

iii) F (154) has equated c_2 to the coefficient of the quadratic field term according to Eq.(4.94), i.e.

$$c_2 = \lambda_g A_{RL}^2 \qquad (4.101)$$

This interpretation was also followed by NM (161). Hence, using Eq.(4.101), λ_g can be evaluated as

$$\lambda_g = \frac{c_2}{A_{RL}^2} = c_2 (neL_o T)^2 \qquad (4.102)$$

However, when using the measured data to get c_2-values, the resulting λ_g-values evaluated according to Eq.(4.102), show a highly unexpected and unusual behaviour.

Ekin (207) has calculated the lattice thermal conductivity of K, employing variational methods and using realistic pseudopotentials and phonon spectra, and found λ_g to be a smooth, monotonically increasing function of T. The results of F (154) and NM (161) however, showed $\lambda_g(T)$ to possess a maximum at about 3 K and to have a magnitude which for different temperatures is about a factor 5 to 8 times the values calculated by Ekin.
This means that the values of c_2, as extracted from the experimental data according to Eqs.(4.101) and (4.102) are much too high.
F (154) suggested that, apart from the influence of λ_g, no other mechanism could be found in the literature capable of providing a quadratic field dependence of W_{xx}^m for uncompensated metals. To explain the enhanced value of λ_g, speculations were advanced about possible contributions to the heat current by uncharged excitations like spin-

and charge -density waves (154).

However,as can be seen from Eq.(4.84),the Lippmann-Kuhrt theory (70) does produce a purely geometrical H^2-contribution to W^m_{xx} if one takes the linear field dependence of W^e_{xx} into account.In view of the close similarity between the W^m_{xx}-results obtained by F and NM for rectangularly sized samples of K and those obtained by us,using the Corbino configuration,of Al and In,the explanation of the seemingly anomalous behaviour of λ_g in K is simple. The quadratic field term,apart from a small contribution due to λ_g,is largely due to a partial Corbino effect,i.e.

$$c_2 = c_g + c_{Cor} \qquad (4.103)$$

where c_{Cor} is the Corbino contribution
$c_g = \lambda_g A^2_{RL}$ and
$c_g \ll c_{Cor}$
The occurrence of a maximum in the temperature region around 3 K,where the curve crossings occur,also points in that direction as a similar behaviour is observed in our Al and In measurements performed in the Corbino geometry.Due to the misinterpretation,this maximum appears for K in the $\lambda_g(T)$-values instead of in the W^m_{xx} versus T curves,similar to the results for Al and In. This means,however,that in K,even for a b/a-ratio of 0.08 (154) the partial Corbino effect is still clearly measurable,although for other metals (e.g. Al as checked by Fletcher (154)),in samples of the same b/a-value the partial Corbino effect may already be too small to be experimentally noticeable.

This may be due to the fact that the Righi-Leduc coefficient A_{RL} is much larger for K than for Al and In,i.e. using Eq.(4.38) we find

$$\begin{aligned} K &: A_{RL}T = 1.821 \quad cmK^2W^{-1}T^{-1} \\ Al &: A_{RL}T = 0.418 \quad cmK^2W^{-1}T^{-1} \\ In &: A_{RL}T = 0.653 \quad cmK^2W^{-1}T^{-1} \end{aligned}$$

so that for K,A_{RL} appears about 3 to 5 times larger than for Al or In.

In summary,one can conclude that due to the presence of a partial Corbino effect,the thermal lattice conductivity of K cannot be obtained using the low field method,as developed by Fletcher (206).To avoid this partial Corbino effect,the thermal magnetoresistivity of K should be measured on very long wires,to obtain a very low b/a-ratio

Of course,an alternative high field method to extract the lattice conductivity of K,consists of measuring the thermal magnetoresistivity in the pure Corbino geometry.This will presently be done in our laboratory.

References.

1) S G Lipson,Proc.Roy.Soc.(London) 293 A(1966)275

2) P Wyder,Phys.Kondens.Mater. 3(1965)263

3) P G Klemens in "Handbuch der Physik" (ed.S Flügge, Springer,Berlin,1956),vol.14,p.198

4) P G Klemens,Solid State Physics,7(1958)1

5) P G Klemens in "Thermal Conductivity" (ed.R P Tye, Academic Press,New York,1969),vol.1,p.2

6) K Mendelssohn and H M Rosenberg,Solid State Physics, 12(1961)223

7) J E Parrot and A D Stuckes,"Thermal Conductivity of Solids"(Academic Press,New York,1975)

8) F J Blatt,"Physics of Electronic Conduction in Solids"(McGraw-Hill,New York,1968)

9) J M Ziman,"Electrons and Phonons"(Clarendon Press, Oxford,1960)

10) A H Wilson,"The Theory of Metals",2nd ed.(Cambridge University Press,London,1953)

11) A M Guénault,Proc.Roy.Soc.(London),A 262(1961)420

12) R E Jones and A M Toxen,Phys.Rev. 120(1960)1167

13) M E De la Cruz,F De la Cruz,J M Cotignola,O J Bressan,and C A Luengo,Phys.Rev.176(1968)871

14) O J Bressan,A E Ridner and F De la Cruz,J.Phys.F. 5(1975)1902

15) M W Ackerman,Phys.Rev.B 5(1972)2751

16) J K Hulm,Proc.Roy.Soc.(London),A 204(1950)98

17) J Bardeen,L N Cooper and J R Schrieffer,Phys.Rev. 108(1957)1175

18) J Bardeen,G Rickayzen and L Tewordt,Phys.Rev.113 (1959)982

19) L P Kadanoff and P C Martin,Phys.Rev.124(1961)670

20) C B Satterwaite,Phys.Rev.125(1962)873

21) M H Jericho,Phil.Trans.Roy.Soc.(London),A 257 (1965)385

22) S G O'Hara and A C Anderson,Phys.Rev.B 9(1974)3730

23) A M Toxen,G K Chang and R E Jones,Phys.Rev.126 (1962)919

24) P Lindenfeld and H Rohrer,Phys.Rev.139(1965)A 206

25) G M Graham,Proc.Roy.Soc.(London),A 248(1958)522

26) N E Philips,Phys.Rev.100(1955)1719

27) T Amundsen and B Verbeek,Physica 81 B(1976)319

28) E W Fenton,J S Rogers and S B Woods,Canad.J.Phys. 41(1963)2026

29) P Seeberg and T Olsen,Physica Norvegica 2(1967)197

30) P Kessener,Chem.Phys.Letters 31(1975)212

31) R J Sladek,Phys.Rev. 97(1955)902

32) R W Klaffky,N S Mohan and D H Damon,Phys.Rev.B 11 (1975)1297

33) T Amundsen,D Furuseth and R P Søvik,J.Phys.F. 7(1977)L159

34) P Tâubert,F Thom and U Gammert,Cryogenics 13 (1973)149

35) R Powell,W Hall and H Roder,J.Appl.Phys.31(1960) 496

36) J B Sousa,Phys.Letters 26A(1968)607

37) W R G Kemp,P G Klemens,A K Sreedhar and G K White, Proc.Roy.Soc.(London),A 233(1956)480

38) A B Pippard,Phil.Mag. 46(1955)1104;Proc.Roy.Soc. (London) A 257(1960)165;"Dynamics of Conduction Electrons" in "Low Temperature Physics,Les Houches 1961 Summerschool Lectures"(ed.C.De Witt,Gordon and Breach,New York,1962)

39) J E Zimmerman,J.Phys.Chem.Solids 11(1959)299

40) P Lindefeld and W B Pennebaker,Phys.Rev.127(1962) 1881

41) M Archibald,J Dunick and M H Jericho,Phys.Rev. 153(1967)787

42) A C Anderson and S G O'Hara,J.Low Temp.Phys.15 (1973)323

43) P Lindenfeld,E A Lynton,D S McLachlan and R Souler Phys.Rev.143(1966)434

44) B Mühlschlegel,Z.Physik 155(1959)313

45) P Rhodes,Proc.Roy.Soc.(London),A 204(1950)396

46) E D Ramos and D H Sanchez,Cryogenics 14(1974)341

47) C Kittel,"Introduction to Solid State Physics", 5th ed.(John Wiley,New York,1976)

48) J M Ziman,"Principles of the Theory of Solids", 2nd ed.(Cambridge University Press,London,1972)

49) C Kittel,"Quantum Theory of Solids",(John Wiley, New York,1963)

50) M P Sharma and G H Wannier,Phys.Letters 41A(1972) 377

51) G H Wannier,Phys.Rev. B 5(1972)3836

52) E H Sondheimer and A H Wilson,Proc.Roy.Soc.(London),A 190(1947)435

53) L J Challis,J D N Cheeke and P Wyder in"Proc.9th Int.Conf.on Low Temp.Phys."(Plenum Press,London, 1965),part B,p.839

54) E H Sondheimer in "Progress in Low Temp.Physics" (ed.C J Gorter,North Holland,Amsterdam,1957),vol.2 p.151

55) J Bardeen,Phys.Rev. 52(1937)688

56) R E B Makinson,Proc.Camb.Phil.Soc. 34(1938)474

57) P Cotti,Helv.Phys.Acta 34(1961)777

58) P Cotti,Phys.Kondens.Mater. 3(1964)40

59) J Thorn and P Wyder,Phys.Letters 13(1964)11

60) E H Sondheimer,Proc.Roy.Soc.(London),A 203(1950)75

61) I A Campbell,Solid State Commun. 9(1971)1513

62) F A Andrews,R T Webber and D A Spohr,Phys.Rev. 84(1951)994

63) H M Rosenberg,Phil.Trans.Roy.Soc. A 247(1955)441

64) K Mendelssohn and H M Rosenberg,Proc.Phys.Soc. A 65(1952)385

65) K Mendelssohn and C A Renton,Proc.Roy.Soc.(London) A 230(1955)157

66) P G Klemens and L Tewordt,Rev.Mod.Phys.36(1964)118

67) Th zur Nieden,Ph.D.-thesis Univ.of Heidelberg,1973

68) A R de Vroomen,"Transport door Electronen en Fononen in Metalen",Ph.D-thesis Univ.of Leiden,(Excelsior,The Hague,1959)

69) J P Jan,Solid State Physics,5(1957)1

70) H J Lippmann and F Kuhrt,Z.Naturforsch.13a(1958) 462,474

71) N N Sirota,V I Gostishchev and A A Drozd,Sov. Phys.JETP Letters,16(1972)170

72) W B Willott,Phil.Mag.16(1967)691

73) I I Hanna and E H Sondheimer,Proc.Roy.Soc.(London) A 239(1957)247

74) M Bailyn,Phys.Rev. 112(1958)1587

75) M Tsuji,J.Phys.Soc.Japan 14(1959)618

76) V N Flerov,Sov.Phys.Solid State 16(1974)33

77) D I Paul,Phys.Rev. 111(1958)1086

78) E H Sondheimer,Proc.Roy.Soc.(London),A 193(1948) 484

79) N W Ashcroft,Phil.Mag.8(1963)2055

80) N W Ashcroft and W E Lawrence,Phys.Rev.175(1968) 938

81) M Kohler,Naturwissenschaften 36(1949)186;Ann.Phys. (Leipzig),6(1949)18

82) R G Chambers,Proc.Roy.Soc.(London),A 238(1956)344

83) M C Steel and J Babiskin,Phys.Rev. 98(1955)359

84) I M Lifshitz,M Y Azbel and M I Kaganov,Sov.Phys. JETP,4(1957)41

85) M Y Azbel,M I Kaganov and I M Lifshitz,Sov.Phys. JETP,5(1957)967

86) I M Lifshitz and M I Kaganov,SOV.Phys.Uspekhi, 2(1960)831;5(1963)878;8(1966)805

87) E Fawcett,Adv.Phys. 13(1964)139

88) I M Lifshitz,M Y Azbel and M I Kaganov,"Electron Theory of Metals"(Consultants Bureau,New York,1973)

89) A A Abrikosov,"The Theory of Normal Metals"(Hindustan Publishing Corporation,Delhi,1968) and "Introduction to the theory of Normal Metals",Solid State Physics,Suppl.12,1972

90) P Kapitza,Proc.Roy.Soc.(London),A 123(1929)292

91) J S Lass,private communication

92) J R Purcell and R B Jacobs,Cryogenics 1(1961)109

93) R J Balcombe,Proc.Roy.Soc.(London),A 275(1963)113

94) V G Volotskaya,Sov.Phys.JETP 17(1963)56

95) E S Borovik and V G Volotskaya,Sov.Phys.JETP 21 (1965)1041

96) R Stevenson,Canad.J.Phys.45(1967)4115

97) T Alstadheim and R Risnes,Phil.Mag. 18(1968)885

98) T Amundsen and P Seeberg,J.Phys.C.2(1969)694

99) Yu N Chiang,V V Eremenko and O G Shevchenko,Sov. Phys.JETP 30(1970)1040

100) R J Balcombe and R A Parker,Phil.Mag.171(1970)533

101) F R Fickett,Phys.Rev. B 3(1971)1941;Cryogenics 11(1971)349

102) W Kesternich and H Ullmaier,Phys.Letters 36A(1971) 411

103) Yu N Chiang and O G Shevchenko,Phys.Stat.Sol. 54(1972)K47

104) T Amundsen and P Jerstad,J.Phys.F.2(1972)657

105) T Amundsen and P Jerstad,J.Low Temp.Phys.15 (1974)459

106) J A Delaney,J.Phys.F.4(1974)247

107) R J Douglas and W R Datars,Solid State Commun. 14(1974)461

108) P Janssen and J Witters,J.Phys.Chem.Solids 36 (1975)1261

109) W Kesternich,H Ullmaier and W Schilling,Phil.Mag. 31(1975)471

110) W Kesternich,H Ullmaier and W Schilling,J.Phys.F. 6(1976)1867

111) J L Olsen,Helv.Phys.Acta 31(1958)713

112) E S Borovik and V G Volotskaya,Sov.Phys.JETP 11 (1960)189

113) V G Volotskaya,Sov.Phys.JETP 18(1964)36

114) Yu P Gaidukov,Sov.Phys.JETP 22(1966)730

115) F De la Cruz,M E De la Cruz and J M Cotignola Phys.Rev. 163(1967)575

116) F J Blatt,A Burmester and B LaRoy,Phys.Rev. 155 (1967)611

117) J C Garland and R Bowers,Phys.Rev. 188(1969)1121

118) J Babiskin and P G Siebenmann,Phys.Kondens.Mater. 9(1969)113

119) P A Penz and R Bowers,Solid State Commun.5(1967) 341

120) P A Penz and R Bowers,Phys.Rev.172(1968)991

121) J S Lass,J.Phys.C. 3(1970)1926

122) J Babiskin and P G Siebenmann,Phys.Rev.Letters 27(1971)935

123) S A Schaefer and J A Marcus,Phys.Rev.Letters 27 (1971)935

124) H Taub,R L Smidt,B W Maxfield and R Bowers,Phys. Rev. B 4(1971)1134

125) A M Simpson,J.Phys.F.3(1973)1471

126) P G Siebenmann and J Babiskin,Phys.Rev.Letters 30(1973)380

127) S A Werner,T K Hunt and G W Ford,Solid State Commun.14(1974)1217

128) F W Holroyd and W R Datars,Can.J.Phys.53(1975)2517

129) B K Jones,Phys.Rev.179(1969)637

130) D E Chimenti and B W Maxfield,Phys.Rev. B 7(1973) 3501

131) D Shoenberg and P J Stiles,Proc.Roy.Soc.(London) A 281(1964)62

132) M J G Lee and L M Falicov,Proc.Roy.Soc.(London) A 304(1968)319

133) L M Falicov and H Smith,Phys.Rev.Letters 29(1972) 124

134) R Fletcher and A J Friedman,Phys.Rev.B 8(1973)5381

135) J M Ziman,Phil.Mag.3(1958)1117

136) Yu P Gaidukov,Sov.Phys.JETP 10(1960)913

137) J R Reitz and A W Overhauser,Phys.Rev.171(1968)749

138) A W Overhauser,Phys.Rev.Letters 27(1971)938;Phys. Rev. B 3(1971)3173;Phys.Rev. B 9(1974)2441

139) P M O'Keefe and W A Goddard,Phys.Rev.Letters 23 (1969)300

140) J S Lass,Phys.Letters A39(1972)343

141) J S Lass,Phys.Rev. B 13(1976)2247

142) R A Young,Phys.Rev.175(1968)813

143) W Y Hsu and L M Falicov,Phys.Stat.Sol.B 66(1974) 639;B 67(1975)325

144) P M Cardon de Lichtbuer,Solid State Commun.19(1976) 127

145) H Höjgaard Jensen and H Smith,J.Phys.C.5(1972)2867

146) C Herring,J.Appl.Phys.31(1960)1939

147) J C Garland,B W Maxfield,P A Penz,H Taub and D K Wagner,Phys.Rev.B 9(1974)1987

148) K D Schotte and D Jacob,Phys.Stat.Sol.A 34(1976) 593

149) J B Sampsell and J C Garland,Phys.Rev.B 13(1976) 583

150) D Strout and F P Pan,Phys.Rev.B 13(1976)1434

151) A P van Gelder,to be published

152) J C van Dongen,"Transversale Magnetoweerstand van Metalen",doctoraal-thesis,Cath.Univ.Nijmegen,1977, unpublished.

153) R S Newrock and B W Maxfield,Solid State Commun. 13(1973)927

154) R Fletcher,Phys.Rev.Letters 32(1974)930

155) T Amundsen and O Kverndalen,Phys.Letters 43A(1973)9

156) T Amundsen and R P Søvik,J.Low Temp.Phys.2(1970)121

157) C H Stephan and B W Maxfield,Solid State Commun. 7(1969)1039

158) C H Stephan and B W Maxfield,Phys.Rev.B 6(1972)2893

159) M Hubers,J F M Klein,H van Kempen,H N de Lang,J S Lass,A R Miedema and P Wyder in "Proc.Int.Conf.on Phonon Scattering in Solids"(ed.H L Albany,Service de Documentation du CEN,Saclay,1972),p.169

160) H van Kempen,H N de Lang,J S Lass and P Wyder, Phys.Letters 42A(1972)277

161) R S Newrock and B W Maxfield,J.Low Temp.Phys.23 (1976)119

162) A B Pippard,Proc.Roy.Soc.(London),A 282(1964)464

163) J H H M Ribot,private communication

164) R S Newrock and B W Maxfield in "Proc.13th Int. Conf.on Low Temp.Phys."(eds. K D Timmerhaus,W J O'Sullivan and E F Hammel,Plenum Press,New York, 1974),vol.4,p.343

165) C J Beers,H van Kempen and P Wyder,to be published

166) G Bruls,H van Kempen and P Wyder,to be published

167) B Lüthi,Helv.Phys.Acta 33(1960)2

168) A B Pippard,Proc.Roy.Soc.(London),A 305(1968)291

169) J C Milliken and R C Young,Phys.Rev.148(1966)558

170) R C Young,Phys.Rev.163(1967)676

171) L Boltzmann,Phil.Mag.22(1886)226

172) O M Corbino,Phys.Zeit.12(1911)561,842

173) B R Russell and C Wahlig,Rev.Sci.Instr.21(1951)513

174) G Busch and Y Tiecke,Phys.Kondens.Mater.1(1963)78

175) J C Perron, Rev.Phys.Appl.5(1970)611

176) L L Campbell,"Galvanomagnetic and Thermomagnetic Effects"(Longmans,New York,1923);contains a comprehensive bibliography of the older measurements.

177) C A Beck,Phys.Rev. 40(1932)607

178) A L Perrier,Helv.Phys.Acta 24(1951)637;25(1952)469

179) G Busch,R Jaggi and P Braunschweig,Helv.Phys.Acta, 26(1953)392

180) H Weiss and H Welker,Z.Phys. 138(1954)322

181) A C Beer,Phys.Rev. 107(1957)1506;J.Appl.Phys.32 (1961)2107

182) G Lautz and G Tittes,Z.Naturforsch.13a(1958)866

183) T C Harman,Phys.Rev.118(1960)1541

184) D A Kleinman and A L Schawlov,J.Appl.Phys.31(1960) 2176

185) M Green,J.Appl.Phys.32(1961)1286,2047

186) T C Harman and J M Honig,J.Appl.Phys.33(1962)3178, 3188

187) T C Harman and J M Honig,"Thermoelectric and Thermomagnetic Effects and Applications"(McGraw Hill, New York,1967)

188) A Fortini and A Le Bourgeois,J.Phys.Radium(appl) 23(1962)163A;J.Phys.25(1964)175A

189) C B Burckhardt,M J O Strutt and F K von Willisen, Sol.State Electr.7(1964)343

190) H H Wieder,J.Appl.Phys.40(1969)3320

191) P W Shackle,Phil.Mag.21(1970)987

192) J P Velly,A M Martin and E J Picard,Phys.Kondens. Mater.15(1972)36

193) H N de Lang and P Wyder,Ned.Tijdschr.v.Natuurk. 43(1977)95

194) F W Gorter,"Some Physics behind Heat Switches" Ph.D-thesis,Univ.of Amsterdam,1969

195) T Amundsen,Phil.Mag.17(1968)1303

196) T Amundsen,Phil.Mag.20(1969)687

197) R Fletcher,Phys.Rev.B 15(1977)3602

198) J S Dugdale and D Gugan,Proc.Roy.Soc.(London) A 254(1960)184

199) B Hayman and J P Carbotte,Phys.Rev.B 6(1972)1154

200) R Berman,"Thermal Conduction in Solids"(Oxford University Press,London,1977)

201) R Newrock and B W Maxfield,Phys.Rev.B 7(1973)1283

202) G K White in "Proc.8th Conf.on Thermal Conductivity" (eds.C Y Ho and R E Taylor,Plenum Press,New York, 1969)

203) D C Larson,Phys.of Thin Films,6(1971)81

204) G T Meaden,"Electrical Resistance of Metals"(Heywood,London,1966)

205) T Amundsen and T Olsen,Phil.Mag.11(1965)561

206) R Fletcher,J.Phys.F.4(1974)1155

207) J W Ekin,Phys.Rev.B 6(1972)371

208) R F Stauder and E V Mielczarek,Phys.Rev.158(1967) 630

209) B Krevet and W Schauer,J.Appl.Phys.47(1976)3656

210) J E A Alderson and T Farrell,Phys.Rev.185(1969)876

211) K Böning,H J Fenzl,E Olympios,J M Welter and H Wenzl,Phys.Stat.Sol.34(1969)365

212) K Böning,H J Fenzl,J M Welter and H Wenzl,Phys.Stat. Sol.40(1970)609

213) Yu Kagan and A P Zhernov,Sov.Phys.JETP 33(1971)990

214) Yu Kagan and V N Flerov,Sov.Phys.JETP 39(1974)673

215) R Berman and D K C MacDonald,Proc.Roy.Soc.(London) A 209(1951)368

216) J G Cook,M P van der Meer and M J Laubitz,Can.J. Phys.50(1972)1386

217) M L Snodgrass,F J Blatt,J L Opsal and C K Chiang, Phys.Rev.B 13(1976)574

218) J Bass,Adv.Phys.21(1972)431

219) M R Cimberle,G Bobel and C Rizzuto,Adv.Phys.23(1974) 639

220) C Kittel,Solid State Physics,22(1968)1

221) J Kondo,Solid State Physics,23(1969)184

222) Yu Kagan and A P Zhernov,Sov.Phys.JETP 23(1966)737

223) L Landau and I Pomerantchuk,Phys.Z.Sov.10(1936)649 (English transl.in:"Collected Papers of L.D.Landau" ed.D.ter Haar,Pergamon,London,1965)

224) W E Lawrence and J W Wilkins,Phys.Rev.B 7(1973)2317

225) H van Kempen,J S Lass,J H J M Ribot and P Wyder, Phys.Rev.Letters 37(1976)1574

226) H van Kempen in "Proc.EPS Conf. on Transport Properties of Normal Metals",Cavtat,1977 (invited paper)(Sveučilišna Naklada Liber,Zagreb,1977).

227) H van Kempen,J H J M Ribot and P Wyder,Phys.Rev. to be published.

5. METASTABLE STATES IN SUPERCONDUCTORS : SUPERCOOLING AND SUPERHEATING

5.1 Introduction.

Kamerlingh Onnes (1) discovered superconductivity in 1911 at Leiden University. It derives its name from the fact that below a certain critical temperature T_c, the electrical resistance of certain metals abruptly disappears. Its other basic property, the magnetic flux expulsion or Meissner effect, was discovered by Meissner and Ochsenfeld in 1933 (2). They found that even at $T < T_c$ the superconductor (SC) behaves as a normal metal if magnetic fields above a critical value H_c were present, but when the magnetic field is lowered beneath H_c, the SC becomes superconducting again while at the same time the induction B inside the SC vanishes to zero, i.e. the SC behaves like a perfect diamagnet (the Meissner state). These striking electromagnetic properties are manifestations of a thermodynamic phase transition, which consists of an ordening of the motion of the conduction electrons.

A superconductor is classified as Type I if this phase transition is of first order, involving an abrupt change between normal magnetic permeability and complete diamagnetism at the thermodynamic critical field H_c and for suitable sample geometry, and as

Type II if the phase transition is of second order, with a gradual change in permeability for all sample geometries.

However, it was soon found experimentally, that metastable states (magnetic supercooling and superheating) do also exist in superconductors with first order phase transitions. Supercooling was first discovered by De Haas en Voogd (3) in 1928, superheating by Garfunkel and Serin (4) in 1952, but it was not until 1958 that a first quantitative theoretical explanation by Ginzburg (5) appeared, based on the Ginzburg-Landau (GL) equations (6). These are non-linear second order differential equations which describe the behaviour of a superconductor in terms of a spatial variable order parameter. With these equations transitions between the normal and the superconducting state in a variable magnetic field can be investigated. Where formerly was found that these transitions took place at the thermodynamical critical field H_c, on the base of the GL-equations Ginzburg (5) could show that in a decreasing magnetic field the transition from the normal (N) to the superconducting (S) state occurs at the field

$$H_{sc} = H_{c2} = \kappa\sqrt{2}\, H_c = 1.414\, \kappa H_c \qquad (5.1)$$

while in an increasing magnetic field the SN-transition can be estimated to occur at (5,11)

$$H_{sh} = H_c/(\kappa\sqrt{2})^{\frac{1}{2}} = 0.841\ \kappa^{-\frac{1}{2}} H_c \qquad \kappa \ll 1 \qquad (5.2)$$

$$H_{sh} \to H_c \qquad \kappa \to \infty$$

Here $\kappa = \lambda(T)/\xi(T)$ is the famous dimensionless Ginzburg-Landau parameter, $\lambda(T)$ is the penetration depth of the magnetic field and $\xi(T)$ the GL-coherence length (7,10). The GL-theory also provides for a clear-out distinction between Type I and Type II superconductors, i.e.

$$\text{Type I} \quad \text{if} \quad \kappa < 1/\sqrt{2} \qquad (5.3)$$

$$\text{Type II} \quad \text{if} \quad \kappa > 1/\sqrt{2}$$

Thus a Type I superconductor ($H_{c2} < H_c$) in a decreasing magnetic field can persist in a (metastable) normal state in fields lower than H_c : supercooling. (In contrast, a Type II superconductor ($H_{c2} > H_c$) gradually becomes superconducting at fields higher than H_c.)

Similarly, for a Type I superconductor in an increasing magnetic field, the superconducting state can exist metastably in fields higher than H_c : superheating.

Hence it follows that supercooling and superheating is the more pronounced the lower the κ-value.

A simple physical criterion for supercooling and superheating to occur is that the surface energy $(H_c^2/8\pi)\delta$ be positive. Here δ is a parameter with the dimensions of length, i.e. $\delta \sim (\xi - \lambda)$ (7-10). Type I superconductors always have positive surface energies

and the crossover from positive to negative surface energies occurs for $\kappa = 1/\sqrt{2} = 0.7071$. The expression for the supercooling field H_{sc} (Eq. (5.1)), as derived by Ginzburg applied to a bulk SC. By considering the influence of the boundaries on the order parameter in the GL-theory, Saint-James and De Gennes (7,12) could show that in a decreasing field superconductivity usually first nucleates at the surface, inducing a superconducting surface sheath supposed on a normal interior. They predicted for the surface nucleation field a value

$$H_{sc} = H_{c3} = 1.695\ H_{c2} = 2.39\ \kappa\ H_c \qquad (5.4)$$

and the existence of the sheath and the magnitude of H_{c3} was first verified by Bon Mardion et al. (18), Joseph and Tomasch (19) and subsequently by a host of other experimenters.

If one boundary leads to an increase of the supercooling field, it seems obvious to suspect that two intersecting boundaries might lead to an even greater enhancement of the nucleation field of the superconducting phase. This idea was worked out quantitatively by Van Gelder (13), who considered a SC of a wedge-like shape and found that superconductivity nucleates along the wedge in a region with a thickness of order ξ at a nucleation field

$$H_{c4} \geq (\tfrac{1}{2}\sqrt{3}\ \alpha)H_{c2} \qquad (5.5)$$

Here ξ is the coherence length and 2α the angle between the intersecting boundaries forming the wedge. An experimental verification of these theoretical results were subsequently provided by Van Gelder, Hendriks and Wyder (14,15,16).

The next and - so it seems - last step would be to consider configurations where three or more boundaries converge into a point. Experimentally, such a system might be represented by a thin whisker (17) or a small particle (63).

The theoretical predictions of the supercooling (Eqs. (5.1), (5.4)) and superheating (Eq. (5.2)) fields were obtained, by reducing the GL-equations into a one-dimensional form. This could be achieved by a judicious choice of the geometry involved, i.e. a semi-infinite halfspace ($x \geqslant 0$, $-\infty < y,z < +\infty$) with the magnetic field in the z-direction parallel to the boundary. Ginzburg (5) showed that the Meissner state of a SC could only exist as solutions of these one-dimensional GL-equations, if the applied field was smaller than a certain maximum field H_{sh}, and he interpreted this maximum field as the superheating field. In the limit of $\kappa \to 0$, H_{sh} tends to infinity and for $\kappa \to \infty$, $H_{sh} = H_c$.

The superheating field could not be obtained as an analytical expression for the whole κ-range, however, but had to be tabulated numerically.

De Gennes and his Orsay group (11), and independently Bean and Livingston (20), introduced the theoretical concept of an electrodynamic surface barrier which opposes the entry of vortices and which is induced by the surface supercurrents. In this conception, the superheating field is equated to the field at which the surface barrier is overcome. Taking the influence of the boundary into account, Matricon and Saint-James (22,23) arrived at slightly higher values for H_{sh}, however, than were formerly obtained (5,11), but their results could only be expressed numerically.

Recently, Parr (24) has derived an analytical expression for H_{sh}, correct to second order in κ, which agrees well with the sc numerical results in the limit of low κ, i.e.

$$H_{sh} = (1 + \frac{15}{32}\sqrt{2}\kappa)H_c/(\kappa\sqrt{2})^{\frac{1}{2}} \qquad (5.6)$$
$$= (0.841\ \kappa^{-\frac{1}{2}} + 0.558\ \kappa^{\frac{1}{2}})H_c$$

for $\kappa << 1$.

The influence of the boundary on H_{sc} and H_{sh} can be modified by covering the SC with a normal metal. This changes the boundary conditions, leading to a depression of the superconducting order parameter at the surface (proximity effect) (7,48). Surface superconductivity is suppressed by normal metal coating (33,34,35) and the supercooling field H_{sc} tends towards the bulk value H_{c2}, below H_{c3}, hence leading to a 'greater' supercooling effect. For the same reason the

superheating field H_{sh} is also suppressed and the normal state induced at smaller fields, especially for temperatures near T_c (11), hence leading to a 'smaller' syperheating effect. In BCS-terms : a Cooper pair formed in the boundary region, tends to diffuse into the normal metal where it is destroyed, i.e. the proximity effect serves as a pair-breaking mechanism.

The interest in metastable states of superconductors continues up to the present time (25-32), mainly because it constitutes one of the few available methods to determine the very important Ginzburg-Landau parameter κ in Type I superconductors. Measurements of H_{sc} and H_{sh} can be done, using resistive transitions (36,37), magnetization (37,47), susceptibility (25-31) or tunneling (15,32) techniques. Due to the presence of flaws in the surface (38). It appears well-nigh impossible to observe ideal supercooling and superheating in macroscopically large samples. These flaws can act as nucleation centers for superconductive regions, thereby destroying the supercooling state, or can induce large demagnetization factors locally, detrimental to the superheating state. Once the transition to a normal or a superconducting state has started at such a flaw, the new phase propagates over the entire sample and what one observes is only the transition, typical for the defect. This can be avoided with powders where a phase, nucleated in one particle, will not propagate to other particles, so that in each

particle a nucleation process is necessary. Furthermore, the chance of having a flaw which can act as a nucleation center decreases with size. Indeed, almost ideal supercooling and superheating were first observed by Feder et al. (39) in Indium powder samples.

The powder technique, however, entails several encumbrances. Due to size, shape and quality of the powder particles as well as clustering and other effects that can distort the magnetic field seen by the particles, the transition is smeared out, making the final interpretation of the supercooling and superheating fields rather arbitrary. Therefore, a sophisticated technique consists of measuring the metastable state of small, perfect, single speres, typically $10 \sim 100$ μm in diameter (25,28-31).

A variant of the powder method was developed by Pellan et al. (41) : by means of a photomask small squares of metal films, of dimensions 20×20 μm^2 were evaporated on a glass substrate. In this way the form of the squares is rather well controlled, with less chance of smear-out effects. Furthermore the sample can be arbitrarily oriented against the magnetic field and also the thickness of the film can be varied. This allows the measurement of the supercooling and superheating fields of thin films and their thickness dependence. Another aspect which may be studied by this method is the systematic discrepancy which exist between the κ-values obtained from the metastable

transitions in thin films and those obtained from measurements on bulk samples (42).

On powders, both magnetization and susceptibility measurements can be performed, but for single spheres only the susceptibility technique (40) can be used. A drawback of this method however, lies in the fact that in the presence of a supercooling-superheating hysteresis, the critical field H_c cannot be measured on the same sample directly and has to be culled from other sources.

For films, the tunneling technique is also useful to measure magnetic transitions, since it probes the bulk of the film and is relatively insensitive to contributions from the edges.

Besides these rather sophisticated techniques, it is also possible to measure the metastable transitions by a simple dc-resistive method on comparatively large cylindrical wires (36).

We have performed such measurements on thin, cylindrical unplated and goldplated Indium wires, using a configuration originally devised by Wyder and Deltour (43), whereby the magnetic field is taken perpendicular to the wire. Due to the geometry of the arrangement an intermediate state is established between the normal and the superconducting state and the transition between the two states is gradual. The advantage of this geometry is, that in principle the critical thermodynamic field H_c can be extrapolated

from the intermediate state. In addition, by employing the quench effect (38,44) we were able to directly measure H_c, which is usually not possible by the other techniques.

In almost all theoretical treatments, the influence of sample-shape is taken into account by phenomenologically introducing an appropriate demagnetization factor into the solutions for the superheating field of the one-dimensional GL-equations, e.g. (7,11,25,26,28-31). (As for supercooling in a decreasing field, the demagnetization factor leaves the nucleation of normal state unaffected.)

The question remains, however, if this simple approach is justified. The maximum local magnetic field which corresponds to superheating is in general dependent on the shape of the superconductor. The demagnetization factor takes account of this shape dependence, but any local variation of the penetration depth is completely neglected. However, by using a multipole expansion, we could extend the one-dimensional calculations of the semi-infinite halfspace (11) to the case of a cylinder in a perpendicular magnetic field. This indeed, leads to the appropriate demagnetization factor enhanced by a negligibly small correction factor. Fink and Presson (45) and Doll and Graf (49) have calculated the superheating field for a cylinder in a field parallel to its axis (zero demagnetization factor) which for large cylinder radius turned out to be indeed equivalent to

the result obtained for a semi-infinite halfspace. Voetmann Christiansen and Smith (50) have computed numerical solutions of the GL-equations for a cylinder with its axis perpendicular to the field. In this chapter we shall develop analytical solutions of the GL-equations for the configuration of a cylinder in a perpendicular magnetic field, exact to first order in $f_o r$ (f_o = orderparameter in zero magnetic field, r = radius of the cylinder).

This chapter is organised as follows:
In section 5.2 a quantitative description of the supercooling and superheating effects is given, based on the Ginzburg-Landau theory, as well as of the influence of the boundary conditions. In section 5.3 we have theoretically explored the influence of the penetration depth on the demagnetization factor, while in the last section 5.4 we shall report and discuss the results of our measurements.

5.2 The Metastable States.

5.2.1 The Ginzburg-Landau Equations.

According to a phenomenological theory published in 1950 by Ginzburg and Landau (6), the difference in free energy between the superconducting and the normal state can be described by $\Delta G = \int d^3r\ F(r)$, where $F(r)$

is defined by

$$F(r) = -|f|^2 + \tfrac{1}{2}|f|^4 + \left|\left(-\frac{i}{\kappa}\nabla f - Af\right)\right|^2 + (\nabla \times A - H)^2 \qquad (5.7)$$

Here, $f(r)$ is the order parameter, $A(r)$ the vector potential, H the external magnetic field and $\kappa = 1/\xi(T)$ the GL parameter. $\xi(T)$ is the temperature dependent coherence length: All entities are written in reduced units, where the length is measured in units λ, the magnetic field in units $\sqrt{2}\ H_c$, and the energy in units $H_c^2/8\pi$.

The GL equations follow from Eq. (5.7), by minimizing ΔG with respect to f^* and A, i.e.

$$\delta(\Delta G)_{f^*} = 0 : \left(\frac{i}{\kappa}\nabla + A\right)^2 f - f + f|f|^2 = 0 \qquad (5.8)$$

$$\delta(\Delta G)_A = 0 : \frac{i}{2\kappa}(f^*\nabla f - f\nabla f^*) + |f|^2 A = -\ \mathrm{rot\ rot}\ A \qquad (5.9)$$

$$\hat{n} \cdot \left(\frac{i}{\kappa}\nabla + A\right) f = 0 \qquad (5.10)$$

Eq. (5.10) is the boundary condition if the superconductor is bounded by an insulator, and $\hat{n}$ is a unit vector normal to the surface. Physically, Eq. (5.10) means that no current will flow through the boundary. Furthermore it is to be noted, that always a gauge can be found, where f is real.

Supercooling and superheating in superconductors were for the first time discussed in terms of the GL-theory by Ginzburg[5]. In the next sections, however, we shall

mainly follow the expositions of De Gennes[7] and his Orsay-group (71,23).

5.2.2 Supercooling.

Consider a SC in a decreasing magnetic field H with a temperature $T < T_c$. The SC is contained in the semi-infinite halfspace $x > 0$, while for $x < 0$, the space is filled by an insulator or a vacuum. The magnetic field $H = (0,0,H)$ is parallel at the surface, while $A = (0,Hx,0)$ is choosen as the gauge.

In those regions where the superconducting phase starts to nucleate, $|f|$ is very small, so Eq. (5.8) can be linearized, i.e.

$$(\frac{i}{\kappa} \nabla + A)^2 f = f \tag{5.11}$$

This eigenvalue equation can, in analogy to the familiar Schrödinger equation, be solved by variational methods. We use as trial function

$$f(x,y,z) = f(x)\, e^{i(k_y y + k_z z)} \tag{5.12}$$

This leads to an equation of the same form as the Schrödinger equation for a harmonic oscillator.

$$\begin{aligned} &- \frac{d^2 f}{dx^2} + (\kappa H)^2 (x-x_o)^2 f = (\kappa^2 - k_z^2) \ ; \\ &x_o = \frac{k_y}{H\kappa} \end{aligned} \tag{5.13}$$

with eigenvalues

$$\varepsilon = (\kappa^2 - k_z^2) = (n + \tfrac{1}{2})\, 2\kappa H \tag{5.14}$$

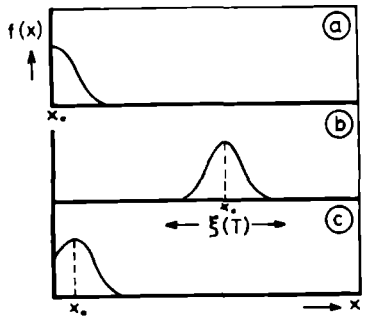

Fig.5.1: GL-solutions for
a) $x_o = 0$
b) $x_o^o \gg \xi(T)$
c) $0^o < x_o < \xi(T)$

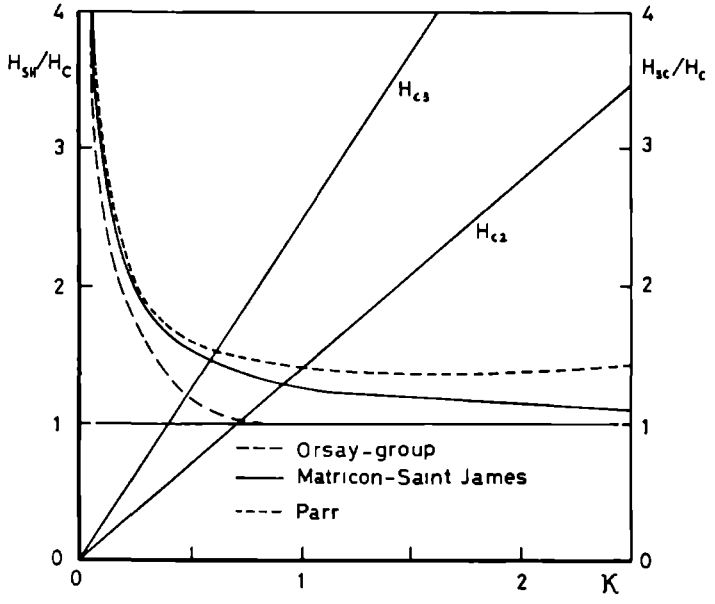

Fig.5.2: Reduced values of the superheating and supercooling fields as a function of κ.
Superheating: Matricon/ aint ames:Eq.(5.40)
: Orsay-group:Eq.(5.39)
: Parr:Eq.(5.6)
Supercooling: H_{c2}-Ginzburg Landau: Eq.(5.16)
H_{c3}-Saint James/de Gennes:Eq.(5.23)

The state of lowest energy is obtained for n = 0, $k_z = 0$, i.e.

$$H_{c2} = \kappa \tag{5.15}$$

In conventional units:

$$H_{c_2} = \sqrt{2}\,\kappa H_c \tag{5.16}$$

For Type I SC ($\kappa < 1/\sqrt{2}$), Eq. (5.16) defines the minimal supercooling field, i.e. H_{c_2} is the lowest possible field in which a superconductor can remain in a normal state.

For the solutions of Eq. (5.13) we find

$$f(x) = \exp\{-\tfrac{1}{2}\kappa^2(x-x_o)^2\} \text{ (GL solution)} \tag{5.17}$$

These have the form of a Gaussian curve, centered around x_o and decreasing exponentially to zero over a distance $1/\kappa = \xi(T)$, the coherence length. Thus x_o can be interpreted as the nucleation center of the superconducting regions. The solutions (Eq. (5.17)) has still to be submitted to the boundary condition (10), i.e.

$$\frac{df}{dx} = 0 \quad \text{for} \quad x = 0 \tag{5.18}$$

As one can readily verify, f(x) cannot satisfy the boundary condition (Eq. (5.18)) for all possible values of x_o; this can only be done for $x_o = 0$ (nucleation on the surface) or for $x_o \gg 1/\kappa$ (nucleation in the bulk) (Fig. 5.1)

Saint-James and De Gennes (12) showed, that for $0 < x_o < 1/\kappa$ a solution f of Fq. (5.17) exists, which satisfies the boundary condition (Eq. (5.18)) and which has lower energy eigenvalues than $\varepsilon = \kappa^2$.
To prove this, they remarked, that Eq. (5.13), with potential $V(\text{harm}) = (\kappa H)^2(x-x_o)^2$ and valid in the region $x > 0$, may be replaced by the equivalent equation

$$-\frac{d^2f}{dx^2} + V(x)\, f = \kappa^2\, f \qquad (5.19)$$

valid for $-\infty < x < +\infty$ and with the symmetrized potential

$$V(x) = \begin{cases} (\kappa H)^2(x-x_o)^2 & x > 0 \\ V(-x) & x < 0 \end{cases} \qquad (5.20)$$

For the minimum energy eigenvalue they found

$$\varepsilon = \kappa^2 = \mu^2\, \kappa\, H \qquad (5.21)$$

where $\mu^2 = 0.59010$. For a Type I SC this yields a minimal supercooling field

$$H_{c_3} = \frac{\kappa}{\mu^2} = 1.695\, \kappa \qquad (5.22)$$

In conventional units

$$H_{c_3} = 1.695\ \ H_{c_2} = 2.397\, \kappa\, H_c \qquad (5.23)$$

The corresponding solution of Eq. (5.19), which satisfies the boundary condition (Fq. (5.18)), is

$$f(x) = \alpha\, U(a,\xi) \qquad (5.24)$$

where $U(a,\xi)$ is a Weber function (46) (parabolic cylindrical function), α an arbitrary constant,

$a = -\kappa/2H$ a normalisation constant and $\xi = (2\kappa H)^{\frac{1}{2}}(x-x_o)$ with

$$x_o = \frac{\mu^2}{\kappa} = 0.59\ \xi(T) \qquad (5.25)$$

The presence of a surface boundary thus leads to a nucleation field $H_{c_3} > H_{c_2}$, while the nucleation will take place in a surface layer of thickness smaller than $\xi(T)$: surface nucleation.

The above calculation is only applicable when H is parallel to the surface. If H is perpendicular to the surface, the boundary condition is automatically satisfied and the original GL result valid. However, there always exist a boundary parallel to the applied field H, so that the minimal supercooling field has always to be identified with H_{c_3}.

5.2.3 Superheating

When the magnetic field of a superconductor is increased, a metastable situation can exist, in which the flux cannot penetrate, although H is above the thermodynamical critical value. According to the Orsay group (11), this is due to a surface barrier opposing the macroscopic penetration of flux.
For a Type I SC this corresponds to a situation $H > H_c$: superheating.
The Orsay group identified the maximal barrier field with the superheating field i.e. the maximal field in

which a SC can persist in a complete Meissner state.

To calculate this maximal field we consider again a semi-infinite Type I SC ($\kappa << 1$) with the applied field H parallel to the surface. This geometry yields one-dimensional GL-equations

$$\frac{1}{\kappa^2}\frac{d^2f}{dx^2} - A^2 f + f - f^3 = 0 \qquad (5.26)$$

$$\frac{d^2A}{dx^2} = f^2 A. \qquad (5.27)$$

We assume that the field penetrates only in a region of thickness $\delta << \xi(T)$ (complete Meissner state). In this region, f is nearly constant, i.e. $f = f(o) \neq 0$. Then Eq. (5.27) yields

$$A(x) = A(o)\, e^{-x\, f\,(o)} \qquad (5.28)$$

The field at the surface is

$$H = \frac{dA}{dx}\Big|_{x=o} = A(o)\, f(o) \qquad (5.29)$$

and the boundary condition now becomes

$$\begin{aligned} h = H = A(o)\ f(o) \quad & f = f(o) \quad \text{for } x = 0 \\ h = A = 0 \quad & f = 1 \quad \text{for } x > \delta \end{aligned} \qquad (5.30)$$

where h(x) is the local field.

The GL-equations (5.26) and (5.27) are equivalent with the conduction that ΔG, the free energy difference between the superconducting and the normal state (per cm^2 of the surface), is minimized with regard to f

and A, where

$$\Delta G = \int_0^\infty dx\, F(x) =$$

$$= \int_0^\infty dx \{-f^2+\tfrac{1}{2}f^4 - \frac{1}{\kappa^2}(\frac{df}{dx})^2 + \qquad (5.31)$$

$$+ A^2f^2 - (\frac{dA}{dx})^2 + \tfrac{1}{2}\}$$

The $+\frac{1}{2}$-term is added to fulfill the boundary condition for $x > \delta$. Because in equilibrium $\delta G = 0$, F is an arbitrary constant. Assume $A = 0$ and consider

$$F(x) = -\frac{1}{\kappa^2}(\frac{df}{dx})^2 + f^2(-1+\tfrac{1}{2}f^2) = \text{constant}$$

As $f = 1$ for $x > \delta$, this yields $F(x) = -\frac{1}{2}$. Thus

$$-\frac{1}{\kappa^2}(\frac{df}{dx})^2 + f^2(-1+\tfrac{1}{2}f^2) + \tfrac{1}{2} = 0 \qquad (5.32)$$

$$\frac{1}{\kappa^2}(\frac{df}{dx})^2 = \tfrac{1}{2}(1-f^2)^2 \qquad (5.33)$$

$$\frac{df}{dx} = \frac{\kappa}{\sqrt{2}}(1-f^2) \qquad (5.34)$$

The integral (Eq. (5.31)) can now be evaluated. The contributions of the A-terms yield

$$G_1 = \int_0^\infty dx \{A^2f^2 - (\frac{dA}{dx})^2\}$$

$$= -\int_0^\infty (\frac{dA}{dx})\, dA$$

$$= -A \frac{dA}{dx} \Big|_0^\infty$$

$$= A^2(o)\, f(o) \qquad (5.35)$$

The contributions of the f-terms give

$$G_2 = \int_o^\infty dx \{\tfrac{1}{2}+f^2(-1+\tfrac{1}{2}f^2) - \frac{1}{\kappa^2}(\frac{df}{dx})^2\}$$

$$= \int_o^\infty dx \{-\frac{2}{\kappa^2}(\frac{df}{dx})^2\}$$

$$= \int_o^\infty dx \{-\frac{2}{\kappa^2}(\frac{df}{dx})\frac{\kappa}{\sqrt{2}}(1-f^2)\}$$

$$= \frac{\sqrt{2}}{\kappa} \int_{f(o)}^1 (1-f^2)\, df$$

$$= \frac{\sqrt{2}}{\kappa}\{\frac{2}{3} - f(o) + \frac{1}{3} f^3(o)\} \qquad (5.36)$$

so

$$\Delta G = G_1 + G_2 = A^2(o)\, f(o) +$$

$$+ \frac{\sqrt{2}}{\kappa}\{\frac{2}{3} - f(o) + \frac{1}{3} f^3(o)\} \qquad (5.37)$$

Minimizing with regard to f(o), while keeping A(o) constant, we obtain

$$A^2(o) = \frac{\sqrt{2}}{\kappa}\{1-f^2(o)\}$$

or

$$H^2 = A^2(o)f^2(o) = \frac{\sqrt{2}}{\kappa} f^2(o)\{1-f^2(o)\} \qquad (5.38)$$

For f = 1, H has a minimum H = 0.

For $f = 1/\sqrt{2}$, H has a maximum $H_{sH} = \kappa^{-\frac{1}{2}}\, 2^{-3/4}$.
In conventional units

$$H_{SH} = \kappa^{-\frac{1}{2}}\, 2^{-\frac{1}{4}}\, H_c \qquad (5.39)$$

Eq. (5.39) for the superheating field is only valid in the clean limit $\kappa << 1$. For arbitrary values of κ, Matricon and Saint-James (22,23) have solved the one-dimensional GL-equations (5.26), (5.27) with the boundary condition

$$\begin{aligned} h &= H \qquad \frac{df}{dx} = 0 \quad \text{for } x = 0 \\ h &= A = 0 \quad f = 1 \quad \text{for } x \to \infty \end{aligned} \qquad (5.40)$$

numerically.
Their result, as well as that from the Orsay group is shown in Fig. 5.2. As expected, agreement is obtained for low κ values. In deriving Eq. (5.39) the Orsay group has assumed rather boldly that all instabilities of interest will be displayed by the one-dimensional GL equations. To prove the validity of that assumption, one has to show that the obtained solution is locally stable for variations of the order parameter in the y- and z-directions. This has been verified theoretically by Kramer (51) and Voetman Christiansen and Smith (50). Kramer has examined the second variation $\delta^2(\Delta G)$ of the GL free energy and found it positive definite, exactly up to H_{sh} (Eq. (5.39)), for arbitrary but one-dimensional perturbations. The same result was obtained for two-dimensional perturbations in the limit of

small κ. For large κ (> 0.5) a periodic modulation in the y-direction could induce instabilities in the Meissner state, at fields slightly lower than H_{sh}, as first predicted by Galaiko (52). The difference may not be experimentally detectable, however. Furthermore, the GL-theory is essentially a local theory, and strictly valid only under the condition $\lambda >> \xi$. For a Type I SC this condition is but satisfied in a small temperature range near T_c i.e. $(1-t) < \kappa^2$. By using generalized GL-equations, in which the non-local electrodynamic effects are taken into account (53), Smith et al. (26) have extended the Orsay approach to cover the whole temperature range. For pure, low κ superconductors they found

$$H_{sh} = C\ \kappa_o^{-1/3}\ (1-t)^{-1/12}\ H_c \qquad (5.41)$$

where κ_o is the κ-value at T_c, $t = T/T_c$ is the reduced temperature, and $C = 0.8$-0.9 is a constant.

5.2.4 Influence of the Boundary Condition.

The equations (5.23) and (5.39) are obtained with the boundary condition (Eq. (5.10)), i.e. where the SC is surrounded by an insulator. The supercooling and the superheating fields are highly dependent on the boundary condition.

Indeed, H_{c_3} is directly connected with Eq. (5.10). If the surface is coated with a normal metal, the boundary

condition to be imposed on the order-parameter will change and H_{SC} and H_{SH} are modified.

To obtain the most general boundary condition, we require the current across the boundary to vanish, i.e.

$$-\frac{4\pi}{c}\, j\cdot\hat{n} = \frac{i}{2\kappa}\,(f^{*}\hat{n}\cdot\nabla f - f\hat{n}\cdot\nabla f^{*}) + f^{*}f\;\hat{n}\cdot A = 0$$

$$\hat{n}\cdot\left(\frac{i}{\kappa}\nabla + A\right) f = i\,\gamma\, f$$

In conventional units (7,11,48)

$$\hat{n}\cdot\left(\nabla - i\,\frac{2e}{c}\,A\right)\Psi = \frac{1}{b}\,\Psi \qquad (5.42)$$

γ and b are arbitrary real constants.
If the SC is bounded by an insulator, b is infinite, giving back Eq. (5.10); if it is bounded by a normal metal, b is finite. The effect of the normal layer can thus be described by a single parameter, the extrapolation length b.

A similar boundary condition was found by Zaitzev (35)

$$\hat{n}\cdot\left(\nabla - i\,\frac{2e}{c}\,A\right)\Psi = -\frac{1}{\tilde{\gamma}_{\beta}}\,\frac{\kappa}{\lambda(T)}\,(1-t)^{-\frac{1}{2}} \qquad (5.43)$$

$\tilde{\gamma}_{\beta} = C_1\,\beta$ with

$$C_1 = \begin{cases} (12/7\zeta\,(3))^{\frac{1}{2}} & \text{for } l \to \infty \\ 2/\pi & \text{for } l \ll \xi_o \end{cases}$$

Here l is the mean free path of the electron in the SC and $\zeta(x)$ the Riemann zeta function. β is a parameter which goes to infinity if the transmission coefficient

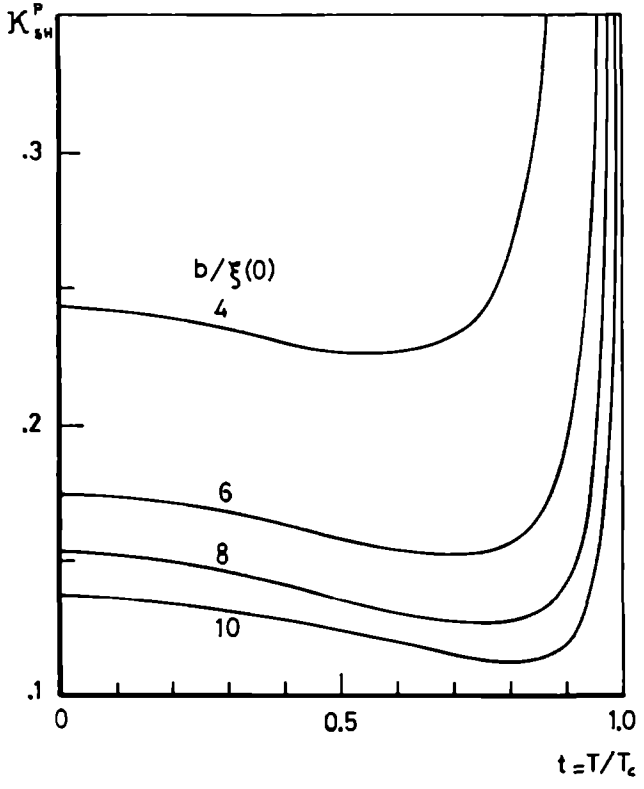

Fig.5.3: κ^p_{SH} as a function of the reduced temperature and $b/\xi(0)$ (After ref.(25))

for the electrons at the surface becomes zero, giving back Eq. (5.10).

For the effect of the normal metal on the supercooling field, Zaitsev finds in the clean limit ($\kappa << 1$)

$$H_{c_3} = H_{c_2} \{1 + \frac{(1-t)^{\frac{1}{2}}}{2\sqrt{\pi}} \gamma\beta \exp\left(\frac{1}{\gamma^2\beta^2(1-t)}\right)\} \tag{5.44}$$

provided the contact between the normal and the superconducting metal is good. According to Eq. (5.44) surface superconductivity is completely suppressed near T_c, so that the supercooling field becomes

$$H_{SC} = H_{c_2} \tag{5.45}$$

In the dirty limit ($\kappa >> 1$) Hurault (34) found a similar result, again provided there was good electrical contact between the normal and the superconducting metal.

The influence of the normal coating on the superheating effect has, in the clean limit $\kappa << 1$, been discussed by the Orsay group[11], using the boundary condition (42) and the assumption that b is independent of the temperature and the magnetic field. Indeed, from Eq. (5.43) we find b to be temperature independent near T_c, because $\lambda(T)$ diverges as $(1-t)^{\frac{1}{2}}$. The Orsay group found H_{SH} to be strongly dependent on $b/\xi(T)$, where $\xi(T)$ is the coherence length. In the range $\kappa\,\xi^2(T) < b^2 < \xi^2(T)$, H_{SH} is significantly reduced and can be approximated by

$$H_{SH} = \frac{2\sqrt{2}}{9} \frac{b}{\xi(T)} \kappa^{-\frac{1}{2}} 2^{-\frac{1}{4}} H_c \qquad (5.46)$$

$$= \frac{0.26}{\sqrt{\kappa}} \frac{b}{\xi(T)} H_c$$

For $b > \xi(T)$, H_{SH} tends towards H_c.

Using these results of the Orsay group, Feder and McLachlan (25) have plotted the temperature dependence of κ_{SH} for different values of b/ξ_o where $\xi(T) = \xi_o/(1-t^4)^{\frac{1}{2}}$ and ξ_o is the Pippard coherence length. Their results are pictured in Fig. 5.3. The curves show the effect of the normal coating to be strongly dependent on temperature and b/ξ_o. The increase of κ_{SH} near T_c they interpreted as proximity and size effects. Size effects will occur when $\xi(T)$ becomes comparable to the dimensions of the sample.

5.2.5 Flaws as Nucleation Centers.

Nucleation of the superconducting phase has been assumed by Faber and Pippard[38] to originate at local flaws, i.e. irregularities of the crystalstructure caused by strain, dislocations and impurities. These imperfections reduce the mean free path l of the electrons, and as $\xi^{-1} = (\xi_o^{-1} + l^{-1})$, this lowers the value of ξ. This in turn reduces the surface energy $(\xi-\lambda)H_c^2/8\pi$, which may even become negative, and

nucleation can occur with greater ease than elsewhere. When the most stable phase nucleates locally, it propagates quickly over the whole sample. Thus the values of H_{SC} and H_{SH} measured may not be really characteristic of the pure sample, but may be determined by a local inhomogeneity, giving too high values for H_{SC} or too low values for H_{SH}. Many flaws are extremely stable, so that their supercooling or superheating behaviour remains remarkably reproducible. The observed supercooling and superheating, however, do not seem to be caused by one and the same flaw.
Superheating is more difficult to observe than supercooling. For bulk samples this is attributed to end effects, where the magnetic field is most distorted. The largest supercooling and superheating effects, i.e. the lowest κ values are found in the close vicinity of T_c. This is due to the fact, that $\xi(T)$ presumably grows larger than the size of the defect, which then becomes uneffective as a nucleation-center.

5.2.6 The Quench Effect.

The degree of the attainable supercooling is affected by the strength of the maximum field to which the specimen has previously been subjected. This effect is called the quench-effect (55). Suppose the sample to be in a very high field, which is then decreased steadily. It supercools in the usual way at a field H_{S1}.

If the field is now increased to a value above H_c but not above the quenching field H_q, and then decreased again, the sample will supercool at a field $H_{S2} > H_{S1}$, thus showing a 'smaller' supercooling effect. To restore the supercooling to its original value H_{S1}, it is necessary to exeed H_q. It seems that a trace of the superconducting phase persist above the critical field H_c, probably in the neightbourhood of some flaw. This serves, below H_c, as a center of nucleation, but once the quenching field is reached, this trace is irreversibly destroyed.

We have employed the quench effect to determine the critical field H_c directly in our measurements. By using the same method the bulk critical field H_c could also be measured directly in susceptibility measurements, as was first demonstrated by F. Meier (62). This was hitherto thought to be not possible.

5.3 Influence of the Geometry.

The above results were calculated for a semi-infinite halfspace with the external field parallel to the surface. For a sample of arbitrary form and in an arbitrary position with respect to the field, a correction factor has to be applied.

Consider for instance a cylindrical SC in a transverse magnetic field. For the supercooling field

H_{SC}, no correction-factor needs to be used. The only effect of the geometry is the establishment of an intermediate state, i.e. a thermodynamically stable state in which superconducting regions can exist alongside normal ones.

As for the superheating field H_{SH}, the usual procedure is, to take the same Eq. (5.39), derived for the semi-infinite case, but now corrected with an appropriate demagnetisation factor. In the case of the cylinder this is $\frac{1}{2}$, hence

$$H_{SH} = \tfrac{1}{2}\,\kappa^{-\frac{1}{2}} 2^{-\frac{1}{4}} H_c \qquad (5.47)$$

This is by no means an obvious procedure (54). The demagnetisation factor gives only a correction for the shape of the sample. But because the magnetic field penetrates the superconductor, its value at the surface is not only determined by the shape but is also dependent on the penetration depth. However, this turns out to be a begligible effect. To prove this, we have used the three-dimensional expressions of the linearized GL-equations, i.e.

$$\nabla^2 f = \kappa^2 \{f^3 - f + A^2 f\} \qquad (5.48)$$

$$\text{rot rot } A + f^2 A = 0 \qquad (5.49)$$

These equations are equivalent to the condition that the functional $\Delta G = \int d^3r\, F(r)$ is minimized with respect to the order parameter $f(r)$ and the vector potential $A(r)$, if $F(r)$ is defined as

$$F(r) = \tfrac{1}{2}f^4 - f^2 + \frac{1}{\kappa^2}(\nabla f)^2 + A^2 f^2 + \tag{5.50}$$

$$+(\nabla \times A - H)^2 + \tfrac{1}{2}$$

The integration extends over both the SC and the surrounding vacuum. $h(r) = \text{rot } A(r)$ is the local field and $H = \text{rot } A_o$ the uniform external field. Away from the SC, $h(r)$ approaches asymtotically to H.

In order to minimize ΔG, we consider an infinite set of trial functions, which we simply denote with the same symbols f and A. These functions must be twice differentiable except at the vacuum interface, where the normal components of A and ∇f are required to vanish. Finally both A and rot A should be continuous across the surface. For the vacuum we have $f = o$ without loss of generality we may restrict the choice of trial-functions by letting A be determined by Eq. (5.49). This means that we only have to vary $f(r)$. These considerations outlines the framework for our approach. In the following we shall attempt to rewrite ΔG in terms of f only, taking the appropriate boundary conditions into account. Minimizing with respect to f will then lead to the desired results.

To calculate the contributions of the A-terms, we use the general result that, as $h \to H$ for $r \to \infty$:

$$\int d^2r(A-A_o) \times (h-H_o) = 0 \tag{5.51}$$

if the surface of integration is far removed from the SC. Hence

$$0 = \int d^2r(A-A_o) \times (h-H_o) =$$

$$\int d^3r \; \mathrm{div}\,\{(A-A_o) \times (h-H_o)\}$$

$$= \int d^3r \,\{(A-A_o)\,\mathrm{rot}\,(h-H) - (h-H)\,\mathrm{rot}\,(A-A_o)\}$$

$$= \int d^3r \,\{(A-A_o)(-f^2A) - (h-H)^2\} \qquad (5.52)$$

$$= \int d^3r \; f^2 A \, A_o - \int d^3r \,\{f^2A^2 - (h-H)^2\}$$

Using the fact that Eq. (5.49) rot h = rot rot A = $-f^2$A and rot H = 0, because H is kept fixed. Thus we find

$$G_1 = \int d^3r \,\{(\mathrm{rot}\,A-H)^2 + f^2A^2\} = \int d^3r \; f^2 A \, A_o \qquad (5.53)$$

To calculate the contribution of the f-terms, we use Eqs. (5.33) and (5.34), i.e.

$$G_2 = \int d^3r \,\{\tfrac{1}{2} - f^2 + \tfrac{1}{2}f^4 + \frac{1}{\kappa^2}(\nabla f)^2\} =$$

$$\int d^3r \,\{\frac{2}{\kappa^2}(\nabla f)^2\} \qquad (5.54)$$

$$= \int d^3r \,\{\frac{\sqrt{2}}{\kappa}\,(1-f^2)\nabla f\} =$$

$$\frac{\sqrt{2}}{\kappa} \int d^2r \int_{f_o(r)}^{1} df(1-f^2)$$

Here, $f_o(r)$ is the value of f(r) at the surface. Hence

$$\Delta G = \frac{\sqrt{2}}{\kappa} \int d^2r \int_{f_o(r)}^{1} (1-f^2)\, df + \qquad (5.55)$$

$$+ \int d^3r \; f^2 \, A \, A_o$$

The first integral must be performed over the surface of the SC, the second one over its volume.

Consider now the superconductive cylinder (with radius r_o and lateral axis in the z-direction) in a uniform magnetic field $H = \text{rot } A_o$ in the xy-plane.

We choose the gauge

$$A = (0,0,A_z)(r,\varphi)) \tag{5.56}$$

In cylindrical coordinates (r,φ,z):

$$h_r = \frac{1}{r}\frac{dA_z}{d\varphi} \quad h_\varphi = -\frac{dA_z}{dr} \quad h_z = 0 \tag{5.57}$$

Using the multipole expansion we find for the field outside and at the surface of the SC.

$$A_z = H\, r \sin\varphi + \sum_{n=1} \frac{a_n}{r^n} \sin n\varphi \tag{5.58}$$

For large r:

$$A_z = A_o = H\, r \sin\varphi \tag{5.59}$$

Furthermore, Eq. (5.57) yields

$$rh_\varphi = -r\frac{dA_z}{dr} =$$

$$= -H\, r \sin\varphi + \sum_{n=1} n \frac{a_n}{r^n} \sin n\varphi \tag{5.60}$$

and again from Fq. (5.57) follows

$$\frac{a_n}{r^n} = \frac{1}{\pi}\int d\varphi \sin n\varphi$$

$$\{A_z(\varphi) + H\, r \sin\varphi\}$$

$$= \frac{1}{\pi} \int d\varphi \sin n\varphi \, A_z(\varphi) -$$

$$- \frac{Hr}{\pi} \int d\varphi \sin n\varphi \sin\varphi$$

$$= \frac{1}{\pi} \int d\varphi \sin n\varphi \, A_z(\varphi) + \tag{5.61}$$

$$\begin{cases} -\frac{Hr}{\pi} \int \sin^2\varphi = -Hr & \text{if } n = 1 \\ 0 & \text{if } n \neq 1 \end{cases}$$

hence:

$$h_\varphi = -2H \sin\varphi + \sum_{n=1} n \sin n\varphi \, \frac{1}{\pi} \int d\varphi' \sin n\varphi' \left\{\frac{A_z(\varphi')}{r}\right\} \tag{5.62}$$

Eq. (5.62) constitutes a general result, i.e. valid for general $A_z(\varphi)$ (Eq. (5.58)).

However, we consider only A's, which satisfy Eq. (5.49):

$$\text{rot rot } A + f^2 A = 0$$

With the gauge (Eq. (5.56)) this becomes:

$$-\nabla^2 A_z + f^2 A_z = 0 \tag{5.63}$$

or in cylindrical coordinates ($d^2A_z/dz^2 = 0$, because A_z is independent of z)

$$\frac{d^2A_z}{dr^2} + \frac{1}{r}\frac{dA_z}{dr} + \frac{1}{r^2}\frac{d^2A_z}{d\varphi^2} - f^2 A_z = 0 \tag{5.64}$$

Using the approximation $f(r) = f_o$ and neglecting all

terms of order $(f_o r)^{-2}$ and lower, we finally arrive at

$$\frac{d^2 A_z}{d(f_o r)^2} + \frac{1}{f_o r}\frac{dA_z}{d(f_o r)} - A_z = 0 \qquad (5.65)$$

For the solution we use the trial function

$$A_z = C(f_o r)^{-\frac{1}{2}} e^{f_o(r-r_o)} \qquad (5.66)$$

C is a constant to be determined by considering

$$\begin{aligned} h_\varphi \Big|_{r=r_o} &= -f_o \frac{dA_z}{d(f_o r)} \Big|_{r=r_o} \\ &= f_o C(f_o r)^{\frac{1}{2}} e^{f_o(r-r_o)} \{\frac{1}{2f_o r} - 1\} \Big|_{r=r_o} \\ &= C(\frac{f_o}{r_o})^{\frac{1}{2}} \{\frac{1}{2f_o r_o} - 1\} \\ C &= h_\varphi \Big|_{r=r_o} (\frac{r_o}{f_o})^{\frac{1}{2}} \{\frac{1}{2f_o r_o} - 1\}^{-1} \end{aligned} \qquad (5.67)$$

Hence

$$A_z = \frac{h_\varphi}{f_o}(\frac{r_o}{r})^{\frac{1}{2}} e^{f_o(r-r_o)} \{\frac{1}{2f_o r_o} - 1\}^{-1} \qquad (5.68)$$

Eq. (5.68) is not an exact solution of Eq. (5.65). Substituting Eq. (5.68) into Eq. (5.65) however, gives a term of order $(f_o r_o)^{-2}$ at the surface, which can be neglected.

With Eq. (5.67) we can approximate Eq. (5.66) by

$$A_z = -\frac{h_\varphi}{f_o}\{1 - \frac{1}{2f_o r_o}\}^{-1}$$
$$= -\frac{h_\varphi}{f_o}\{1 + \frac{1}{2f_o r_o}\} \qquad (5.69)$$

Substituting Eq. (5.69) into Eq. (5.62) we obtain

$$h_\varphi = -2H \sin\varphi - \frac{1}{\pi}\sum_{n=1} n \sin n\varphi$$
$$\int d\varphi' \sin n\varphi' \frac{h_{\varphi'}}{f_o r} \qquad (5.70)$$

in which again terms of order $(f_o r)^{-2}$ has been neglected. Substituting Eqs. (5.59) and (5.68) into Eq. (5.53) and taking $f(r) = f_o(r)$ gives

$$G_1 = \int d^3r\, f^2\, A\, A_o$$
$$= -\int d(f_o r)\, d\varphi\, dz\, r_o^2 (\frac{r}{r_o})^{3/2}$$
$$(1 + \frac{1}{2f_o r_o})\, e^{f_o(r-r_o)}\, h_\varphi\, H \sin\varphi \qquad (5.71)$$

Using the approximation

$$(\frac{r}{r_o})^{3/2} = (\frac{r-r_o+r_o}{r_o})^{3/2} =$$
$$(1 + \frac{f_o(r-r_o)}{f_o r_o})^{3/2} =$$
$$1 + \frac{3}{2}\frac{f_o(r-r_o)}{f_o r_o} \qquad (5.72)$$

yields

$$G_1 = - r_o^2 \int d\varphi \; d \; z \; h_\varphi \; H \sin \varphi$$
$$\{1 + \frac{1}{2 f_o r_o} + \frac{3}{2} \frac{f_o (r - r_o)}{f_o r_o}\}$$
$$e^{f_o (r - r_o)} \, d(f_o r)$$
$$= - (1 - \frac{1}{f_o r_o}) \; r_o^2 \int d\varphi d \; z \; h_\varphi \; H \sin \varphi \qquad (5.73)$$

Substituting Eq. (5.70), and neglecting $(f_o r_o)^{-2}$-terms we obtain

$$G_1 = - (1 - \frac{1}{f_o r_o}) r_o^2 \int dz d\varphi \; H \sin \varphi$$
$$\{-2 \; H \sin \varphi - \frac{1}{\pi} \sin \varphi \int d\varphi' \sin \varphi' \frac{h_{\varphi'}}{f_o r}\}$$
$$= (1 - \frac{1}{f_o r_o}) \{ \int d^3 r \; 2 \; H^2 +$$
$$r_o^2 H \int dz d\varphi' \sin\varphi' \{\frac{-2H \sin\varphi'}{f_o r}\}\}$$
$$= (1 - \frac{1}{f_o r_o}) \{ \int d^3 r \; 2 \; H - \int d^3 r \; \frac{2H^2}{f_o r}\}$$
$$= 2 \int d^3 r \; H^2 - 4 \int d^2 r \; \frac{H^2}{f_o} \qquad (5.74)$$

Out of Eq. (5.54) we find

$$G_2 = \int d^2 r \; \frac{\sqrt{2}}{\kappa} \{ \frac{2}{3} - f_o + \frac{1}{3} f_o^3 \} \qquad (5.75)$$

and finally

$$\Delta G = 2 \int d^3r\, H^2 - \int d^2r \{\frac{4H^2}{f_o} - \frac{\sqrt{2}}{\kappa} (\frac{2}{3} - f_o + \frac{1}{3} f_o^3)\} \quad (5.76)$$

Minimizing with respect to f_o gives

$$4H^2 = \frac{\sqrt{2}}{\kappa} f_o^2 (1-f_o^2) \quad (5.77)$$

and this leads to a maximum field for $f_o = 1/\sqrt{2}$ i.e.

$$H_{SH} = \tfrac{1}{2} \kappa^{-\frac{1}{2}} 2^{-\frac{3}{4}} \quad (5.78)$$

In conventional units

$$H_{SH} = \tfrac{1}{2} \kappa^{-\frac{1}{2}} 2^{-\frac{1}{4}} H_c \quad (5.79)$$

Hence the demagnetisation factor $\frac{1}{2}$ emerges in a most natural way into the equation of the superheating field and the effect of the field penetration is shown to be of negligible consequence.

5.4 Experimental Results.

5.4.1 Sample Preparation.

Small chips were cut from an indiumbar (99.9999% pure from the Hollandse Metallurgische Industrie Biliton Ltd.) which were gathered in a holder. In the perspex bottom of the holder a small hole was drilled, with the diameter, required for the wire. We used diameters of 0.5 mm, 0.3 mm, 0.2 mm and 0.12 mm. Using

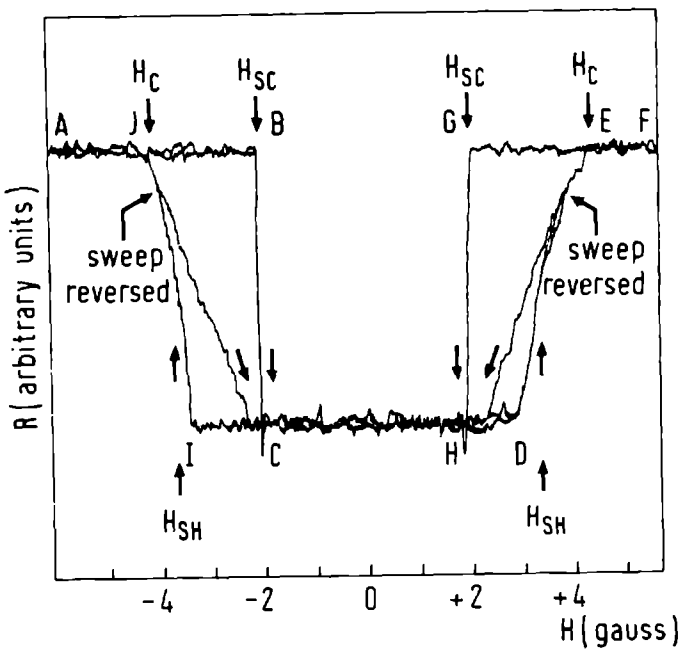

Fig.5.4: Typical curve representing the resistance transitions as a function of the applied magnetic field for unplated wires.

a press, the indium was slowly pressed out of the holder, yielding a wire of about 80 cm length. Examined under a 30x microscope, the surface of the wires showed regular shallow lateral scratches over their whole length, presumably because the hole through which the indium was pressed, did not have a clean-cut edge. Those parts of the wires, which showed other irregularities than the shallow scratches, were not used for measurements. To remove strains and dislocations (flaws) the wires were annealed for about one or two weeks.
Clean pieces of the wires, with a length of about 28 mm, were used as samples. Their residual resistance ratio ($RRR = \rho_{295K}/\rho_{4.2K}$) are shown in Table 1.

Table 1 : RRR of the Indium samples.

ϕ in mm	RRR
0.5	5000
0.3	4500
0.2	3700
0.12	3300

The coating of the samples was accomplished by vacuum evaporation of gold. As good contact between the normal and superconducting metal was compulsory, the oxide layer on the sample was removed before evaporation by dipping the wire in a concentrated solution of HNO_3 until the metallic glint returned.

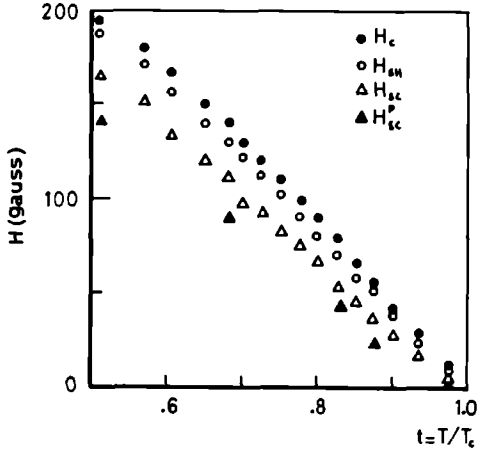

Fig.5.5: The critical fields as a function of the reduced temperature.

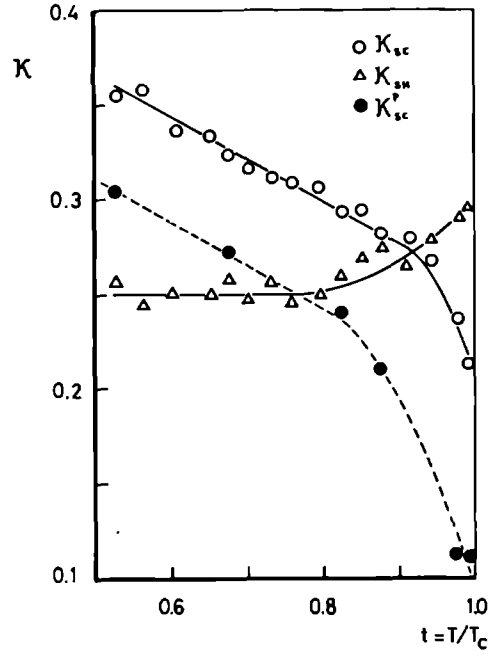

Fig.5.6: Temperature dependence of κ_{SC}, κ_{SH} and κ^{p}_{SC}

We have not attempted to measure the thickness of the evaporated gold film.

The resistivity of the samples was measured by the conventional four-probe method in a temperature range between 2 and 4.2 K. The magnetic field was applied perpendicular to the direction of the current through the wires and was generated by a Varian V-3950 electromagnet, with a sweep of excellent linearity. The voltage across the wires, as measured by a Keithley Nanovolt meter, was recorded on a Hewlett-Packard XY-recorder, against the sweep of the magnetic field.

5.4.2 Unplated Wires.

A typical example of the curves measured, is shown in Fig. 5.4. As the magnetic field sweeps back and forth, only the curve ABCDEFGHIJ is traced. To produce the intermediate state curves EH and JC, we have made use of the quench effect, by reversing the sweep just before the horizontal upper curve was reached.
The zero-point H = 0 was determined from the symmetry properties of the curve.
Some samples display a slight asymmetry in their curves, i.e. the supercooling or superheating fields at the left side may be slightly smaller or bigger than at the right side. Presumable this is due to the fact, that the Indium wires bend slightly under the pressure of the clamps of the sample holder. To side-step eventual

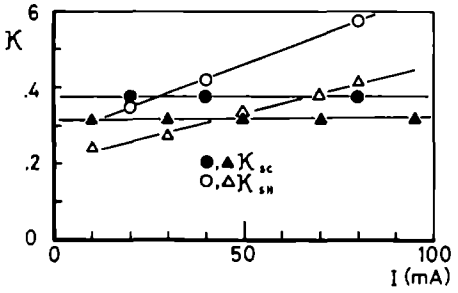

Fig.5.7: Dependence of κ_{SC} and κ_{SH} on the measuring current for wires of diameter ϕ= 0.2 mm (circles) and ϕ= 0.3 mm (triangles)

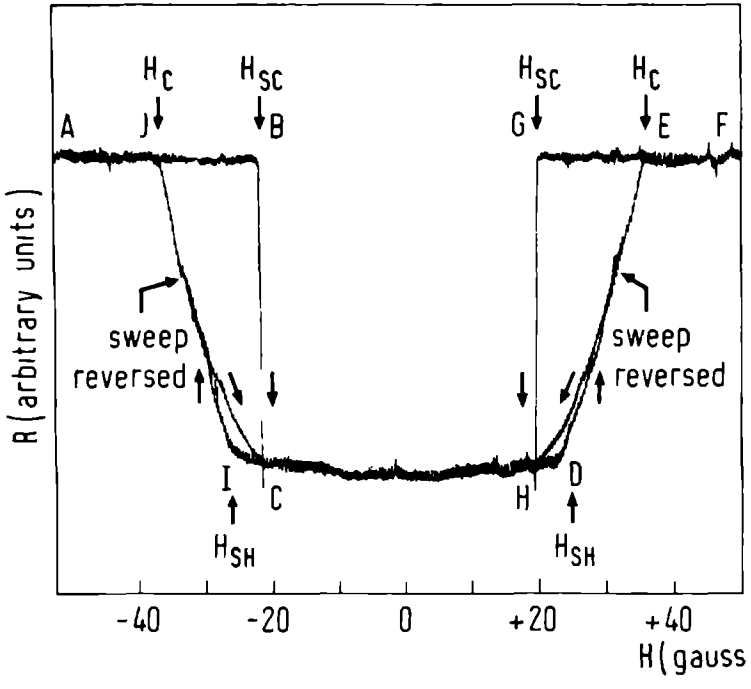

Fig.5.8: Typical curve, representing the resistance transitions as a function of the applied magnetic field for goldplated wires.

asymmetry effects, we define H = 0 as the middle of the distance between H_c and H_c'. At the supercooling field the curve displays a reproducible jump and H_{SC} can thus be determined accurately.

Fig. 5.5 shows the fields, as well as the supercooling field for the case of the goldplated wire, as they change with temperature.

For low values of T, these measured $H_c(T)$-values are about 4% less than the ones, determined by Finnemore and Mapother (55). Presumably this is due to the current in the wire. The current appears to have no effect on the κ_{SC}-values, but a considerable influence on κ_{sh} as is shown by Fig. 5.6. For relatively large current values, the superheating effect disappears.

$\kappa_{SC}(t)$ is calculated from Eq. (5.23), i.e.

$$\kappa_{SC}(t) = \frac{1}{2.397} \frac{H_{sc}(t)}{H_c(t)} = 0.4172 \frac{H_{sc}(t)}{H_c(t)} \qquad (5.80)$$

As for the superheating values $\kappa_{sh}(t)$, those are found by calculating $2H_{sh}(t)/H_c(t)$ and determining the corresponding κ_{sh}-value by means of the Orsay-curve, represented in Fig. 5.2. The results show no influence of size-effects and we believe all our samples to be bulk superconductors. A typical example of the obtained values is shown in Fig. 5.7.

The steep slope of the κ_{SC}-curve makes it dubious, if not impossible to determine $\kappa_{SC}(T_c)$ by extrapolation. The lowest κ_{SC}-value we have actutally <u>measured</u> at

$T \approx T_o$ is $\kappa_{SC} = 0.194$. As the GL-theory is strictly valid for $T = T_c$, the κ_{SC}- and κ_{SH}-values should converge for $t = 1$. This is not seen to happen. Indeed, for $t \to 1$, κ_{SH} increases steeply and the superheating effect is diminished. We believe this is due to end-of-fects, rather than to size-effects.
Furthermore, as is shown by Fig. 5.2, for $2H_{SH}/H_c \approx 1$, small changes in H_{SH} give rise to a tremendous increase of κ_{SH}.

5.4.3 Gold-plates Wires.

In Fig. 5.7 we have also drawn the κ^P_{SC}-curve for the gold-plated wire, where $\kappa^P_{SC}(t)$ is defined by again Eq. (5.80) as for the unplated case. However, when plated with a normal metal, the supercooling field becomes (Eq. (5.23)):

$$H_{SC} = H_{c_2} = 0.59\ H_{c_{3_P}} \tag{5.81}$$

Correspondingly, κ_{SC} should be lower than κ_{SC} by a factor 0.59. We found at $T \approx T_c$ for the 0.3 mm wire :

$$\frac{\kappa^P_{SC}}{\kappa_{SC}} = 0.66 \tag{5.82}$$

and for the 0.2 mm wire:

$$\frac{\kappa^P_{SC}}{\kappa_{SC}} = 0.52 \tag{5.83}$$

$\kappa^P_{SC}/\kappa_{SC}$ increases with decreasing temperature.
No gold was evaporated on the 0.12 mm wire, as it turned out to be too tender for manipulation.
As is explained in section 5.2.4 and borne out by our experiments, H^P_{SH} is greatly reduced for $T \approx T_c$ and completely destroyed for lower T-values. That in the latter case, one has $H_{SH} = H_c$, can be demonstrated experimentally by the quenching-method (see Fig. 5.8): the "superheating curve" HDE closely follows the "intermediate state curve" EH. For $T \approx T_c$ we do however find a small superheating effect.

5.4.3 Discussion.

It has been known from the work of Faber (56) that Indium exhibits considerable supercooling. At T_c both κ_{sc} and κ_{sh} should equal the GL-parameter κ and from the supercooling data of Faber, De Gennes (7) extrapolated $\kappa(T_c)$ of Indium to be

$$\kappa(T_c) = 0.066 \qquad (5.84)$$

The very sophisticated measurements of Feder and McLachlan (25), who were the first to measure on small single Indium spheres, yielded

$$\kappa(T_c) = 0.062 \pm 0.001 \qquad (5.85)$$

Equally measuring on single spheres as well, Parr (31) found

$$\kappa(T_c) = 0.061 \pm 0.001 \qquad (5.86)$$

while, using the powder technique, Smith et al. (26) obtained

$$\kappa(T_c) = 0.060 \pm 0.002 \tag{5.87}$$

which values agree quite well with the Feder-McLachlan result. All these authors also found $\kappa_{sc}(T)$ and $\kappa_{sh}(T)$ to converge indeed to a common value κ for $T = T_c$, and no discrepancy thus exist between the κ-value as derived from supercooling or superheating data. $\kappa_{sc}(T)$ and $\kappa_{sh}(T)$ differ only in their temperature dependence. Microscopic theory (7-10) gives

$$\kappa = 0.96\ \lambda_L/\xi_o \tag{5.88}$$

where, in the free electron model,

$$\lambda_L = (mc^2/4\pi n_s e^2)^{\frac{1}{2}} \tag{5.89}$$

is the London penetration depth and n_s the density of superconducting electrons in the two-fluid model, while

$$\xi_o = 0.18\ \hbar V_F/\kappa_B T_c \tag{5.90}$$

is the coherence length.
For Indium, this leads to $\lambda_L = 155$ Å and $\xi_o = 7070$ Å. Using these values one gets

$$\kappa = 0.021 \tag{5.91}$$

However, using the experimental values, i.e. $\lambda_L(\text{exp}) = 250$ Å (57) and $\xi_o(\text{exp}) = 2000$ Å (58) one obtains

$$\kappa = 0.120 \tag{5.92}$$

The discrepancy between these last two κ-values and the experimentally observed values of Eqs. (5.85), (5.86), (5.87) cannot be attributed to the presence of flaws in the samples, in view of the fact that flaws become ineffective as T nears T_c, and that κ_{sc} and κ_{sh} both converge to the same value at T_c. Instead, we believe them to be the result mainly of the non-local electrodynamics, inherent to low κ, superconductors. Well before the microscopic non-local BCS-theory, Pippard (59) introduced a non-local reformulation of the local London electrodynamics, which satisfactorily explained the large observed penetration depths as compared to λ_L. The Pippard result involves a complicated integral, and only in the limits $\lambda >> \xi$ (local London limit) and $\lambda << \xi$ (non-local Pippard limit) could an explicit relation be formulated. For Type I superconductors, $\lambda << \xi$ and the non-local limit has to be used, i.e. (8-10)

$$\lambda(o) = (\sqrt{3}/2\pi)\xi_o\lambda_L^2)^{1/3} \qquad (5.93)$$

which for Indium leads to a value (0)-360 A. Hence (Eq. (5.88))

$$\kappa = 0.049 \qquad (5.94)$$

Although agreeing far better than Fq. (5.91) with the bulk κ-values of Eqs. (5.85), (5.86), (5.87), a discrepancy still exists. This might be due to the fact that not the complete Pippard integral has been used to describe $\lambda(o)$, but the limiting approximation of Eq. (5.93).

As for the difference between Eq. (5.92) and the bulk experimental values, this is also most probably caused by non-local effects. The experimental values constituting Eq. (5.92) are usually derived from experiments on thin films. As noted by Cody (42) and others, κ-values obtained from thin film transition data are systematically higher than κ-values obtained from supercooling experiments. Tinkham (60) has shown, that thin films are essentially Type II superconductors, even if their κ-values are smaller than $1/\sqrt{2}$. Because of this, Gray (32) has questioned the validity of comparing supercooling data of κ with those obtained from thin film transitions, as they involve superconductors of different type. A clearcut answer to these questions remains to be given as yet.

Our measured values of $\kappa(T_c)$ are about three times higher than those of Eqs. (5.85), (5.86), (5.87). These results were not unexpected. The resistive method we have used, unavoidably induces flaws and local strain, e.g. there where the contacts for the current and voltage measurements touch the sample. Furthermore, by pressing the Indium through a small hole, a wire with a completely smooth surface can never be ontained. And as the propagation effect of the nucleating phases is the main drawback, these induced nucleation centers will highly hinder the observation of ideal supercooling and superheating states.

Yet, despite these impediments, it is surprising, how well qualitatively the theoretically predicted behaviour of the metastable states, as verified for instance by highly accurate susceptibility measurements (25-31), are also borne out by our simple experiments of dc-transport.

Besides these investigations, the following experiments were also attempted :

i) We have tried to stimulate a transition between the metastable and the stable states by neutron irradiation. The sample was kept, by means of a constant applied field, in a metastable state close to H_{sc} or H_{sh} and then bombarded with neutrons, emanating from a radioactive source. As is well known the neutrons have no charge, they will deeply penetrate the sample. We hoped that, while traversing the sample, their magnetic spin moment will sufficiently enhance or diminish the applied magnetic field locally, so that the sample would be pushed out of its metastable state and superconducting or normal nucleation centers would be formed. Due to the weakness of the neutron source, however, no definite results could be obtained. A similar experiment with β-rays has been performed by Bernas et al. (61) with no clear results.

ii) We have also tried to measure the Van Gelder effect or the ridge-nucleation field H_{c4} (13-16) on a Type I superconductor, again with no definite results. The main difficulty hereby arrises from the

fact, that beneath a certain critical thickness the Type I superconductor behaves as one of Type II.

References

1) H Kamerlingh Onnes,Leiden Comm.122b(1911)147

2) W Meissner and R Ochsenfeld,Naturwiss.21(1933)787

3) W J de Haas and J Voogd,Leiden Comm.191d(1928)37

4) M P Garfunkel and J Serin,Phys.Rev.85(1952)834

5) V L Ginzburg,Sov.Phys.JETP 7(1958)78

6) V L Ginzburg and L D Landau,Zh.Eksperim.i Teor.Fiz. 20(1950)1064 (English transl. in:"Collected Papers of L.D.Landau",ed.D.ter Haar,Pergamon,London,1965)

7) P G de Gennes,"Superconductivity in Metals and Alloys",(Benjamin,New York,1966)

8) E A Lynton,"Supraleitung"(Bibliograph.Inst.,Mannheim,1966)

9) G Rickayzen,"Theory of Superconductivity"(John Wiley,New York,1964)

10) M Tinkham,"Introduction to Superconductivity"(Mc Graw Hill,New York,1975)

11) The Orsay group in"Quantum Fluids"(ed.D.F.Brewer, North Holland,Amsterdam,1966),p.26

12) D Saint James and P G de Gennes,Phys.Letters 7(1963)306

13) A P van Gelder,Phys.Rev.Letters 20(1968)1435

14) A P van Gelder,J W Hendriks and P Wyder in "Proc. 11th Int.Conf. on Low Temp.Phys."(eds.J F Allen, D M Finlayson and D M McCall,St.Andrews,1968), vol.2,p.956

15) A P van Gelder,J W Hendriks and P Wyder,Phys.Rev. B 4(1971)2950

16) J W Hendriks,"Measurements on Superconducting Films" Ph.D-thesis Cath.Univ.Nijmegen (Krips Repro,Meppel, 1976)

17) D S McLachlan,J.Low Temp.Phys.6(1972)385

18) G Bon Mardion,B B Goodman and A Lacaze,Phys.Letters 8(1964)15

19) W J Tomasch and A S Joseph,Phys.Rev.Letters 12(1964) 148

20) P G de Gennes,Solid State Commun.3(1965)127

21) C P Bean and J D Livingston,Phys.Rev.Letters 12 (1964)14

22) J Matricon and D Saint James,Phys.Letters 24A(1967) 241

23) J P Burger and D Saint James in "Superconductivity" (ed.R D Parks,Marcel Dekker,New York,1969)

24) H Parr,Z.Physik,B 25(1976)359

25) J Feder and D S McLachlan,Phys.Rev.177(1969)763

26) F W Smith,A Baratoff and M Cardona,Phys.Kondens. Mater.12(1970)145

27) F de la Cruz,M D Maloney and M Cardona,Physica 55(1971)749

28) H Parr and J Feder,Phys.Rev.B 7(1973)166

29) H Parr,Phys.Rev.B 10(1974)4572

30) H Parr,Phys.Rev.B 12(1975)4886

31) H Parr,Phys.Rev.B 14(1976)2842,2849

32) K E Gray,Phys.Rev.B 13(1976)3774

33) P G de Gennes,Rev.Mod.Phys.36(1964)225

34) J P Hurault,Phys.Letters 20(1966)587

35) R O Zaitsev,Sov.Phys.JETP 23(1966)702

36) R Deltour,H N de Lang and P wyder,Phys.Letters 31A(1970)515

37) S Gygax,Phys.Kondens.Mater.4(1965)207

38) T E Faber and A B Pippard in "Progress in Low Temperature Physics"(ed.C J Gorter,North Holland, 1964),vol.1,p.127

39) J Feder,S R Kiser and F Rothwarf,Phys.Rev.Letters 17(1966)87

40) D S McLachlan and J Feder,Rev.Sci.Instr.39(1968)1340

41) Y Pellan,J Blot,J C Pineau and J Rosenblatt,Phys. Letters,44A(1973)415

42) G D Cody,Phys.Letters 37A(1971)295

43) P Wyder and R Deltour,1966 (unpublished)

44) J F Cochran,D E Mapother and R E Mauld,Phys.Rev. 103(1956)1657

45) H J Fink and A G Presson,Phys.Rev.168(1968)399

46) "Handbook of Mathematical Functions"(eds.M Abramowitz and I A Stegun,NBS,Washington,1964)

47) R Doll and P Graf,Phys.Rev.Letters 19(1967)897

48) G Deutscher and P G de Gennes in "Superconductivity"(ed.R D Parks,Marcel Dekker,New York,1969) vol.2,ch.17

49) R Doll and P Graf,Z.Physik,197(1966)172;204(1967) 205

50) P Voetmann Christiansen and H Smith,Phys.Rev.171 (1968)445

51) L Kramer,Phys.Rev.170(1968)475

52) V Galaiko,Sov.Phys.JETP 23(1966)475

53) R S Thompson and A Baratoff,Phys.Rev.167(1968)361

54) A P van Gelder,private communication

55) D K Finnemore and D E Mapother,Phys.Rev.140(1965) A507

56) T E Faber,Proc.Roy.Soc.(London),A 241(1957)531

57) K Fossheim,Phys.Rev.Letters 19(1967)81

58) E Guyon,F Meunier and E S Thompson,Phys.Rev.156 (1967)452

59) A B Pippard,Proc.Roy.Soc.(London),A 216(1953)547

60) M Tinkham,Phys.Rev.129(1963)2413

61) H Bernas,J P Burger,G Deutscher,C Valette and S J Williamson,Phys.Letters 24A(1967)721

6. SUMMARY

Electrical and thermal conductivity measurements are the main techniques by which we have investigated the transport properties in solids. The conductivity experiments were performed in the temperature range between 0.3 K and 25 K and in magnetic fields up to 6.5 tesla.

Ch.1 provides a general introduction to these measurements and the concepts of transport theory,while Ch.2 describes the measuring apparatus and techniques. In Ch.3 we report on the thermal conductivity measurements of two-dimensional magnetic systems.Not only does the thermal transport in these systems occur by phonons, but by magnons as well and we have measured a thermal magnon conductivity comprising between 70 % and 90 % of the total heat transport,the largest fractional magnon contribution observed as yet.

Besides magnon conductivity we have also observed thermal conductivity by paramagnons for temperatures above T_c.This is the first time that paramagnon conductivity has been observed but a comparison with theory has been compounded by a lack of the latter.

Apart from a discussion of these experimental results we have examined theoretically the magnon conduction in two-dimensional systems and the criteria for its appearance.

In Ch.4 the main aim has been to determine the lattice conductivity of Aluminium and Indium by reducing the electronic thermal conductivity by means of a magnetic field.This was done using the Corbino configuration, which prevents the thermal Hall field from forming,hence produces the largest magnetoresistance for a given field strength.In this way we were able for the first time to measure the lattice conductivity of Al and In by the magnetic field method.Apart from a discussion of these results we have comprehensively and critically examined the different methods to determine the lattice conductivity of metals,the phenomenon of the linear magnetoresistance, the quadratic field dependence of the MR and the anomalous lattice conductivity of Potassium and the phenomenon of curve crossing.
The appearance of a maximum at high fields in the thermal MR as a function of temperature could be interpreted as the Kagan effect.This is the first experimental verification of the Kagan effect in the thermal MR.

In Ch.5 we have investigated the metastable states of superconductors by resistive dc-measurements.We have also developed analytical solutions of the 3-dimensional Ginzburg-Landau equations for the configuration of a cylinder in a perpendicular magnetic field.

SAMENVATTING

De transport eigenschappen van vaste stoffen werden onderzocht m.b.v. electrische en warmtegeleiding in het temperatuurgebied tussen 0.3 en 25 K en in magnetische velden tot aan 6.5 tesla.

Hoofdstuk 1 geeft een algemene inleiding op de metingen en op de concepten die bij de transport theorie een rol spelen.

Hoofdstuk 2 beschrijft de meettechniek en het meet-instrumentarium.

Hoofdstuk 3 beschrijft de metingen van de warmtegeleiding in 2-dimensionale magnetische systemen.Het warmte transport daarbij gebeurt niet alleen via fononen, doch ook via magnonen en de door ons gemeten magnongeleiding bedroeg 70 tot 90 % van de totale warmtegeleiding.Dit is de grootste fractionele magnon bijdrage tot het warmte transport dat tot nog toe ooit is gemeten.

Naast magnongeleiding hebben we ook warmtegeleiding via paramagnonen waargenomen.Dit is voor het eerst dat paramagnon warmtegeleiding kon worden gemeten.Een vergelijking met de theorie was niet mogelijk door het ontbreken van de laatste.

Hoofdstuk 4 had als hoofddoel de bepaling van de roostergeleiding van Aluminium en Indium,door het reduceren van de electron warmtegeleiding m.b.v. een magnetisch veld.De Corbino configuratie,die daartoe werd

benut,heeft het voordeel dat daarbij het thermische Hall-veld zich niet kan opbouwen,waardoor voor een bepaalde veldsterkte de grootst mogelijke magnetoweerstand kan worden verkregen.Op deze wijze waren wij in staat om voor het eerst m.b.v. een magnetische methode de roostergeleiding van Al en In te bepalen.
Naast een bespreking van onze experimentele resultaten hebben we in hoofdstuk 4 ook een uitgebreid en critisch overzicht gegeven van de verschillende methoden om de roostergeleiding in metalen te meten,het verschijnsel van de lineaire magnetoweerstand,de anomale roostergeleiding en de kwadratische veld-afhankelijkheid van de magnetoweerstand van Kalium alsmede van het verschijnsel van de curve doorkruising.
Het in hoge velden ontstaan van een maximum in de magnetoweerstand als een functie van de temperatuur,kon worden verklaard m.b.v. het Kagan-effect.Dit is de eerste experimentele verificatie van het voorkomen van het Kagan-effect in de thermische magnetoweerstand.

Hoofdstuk 5 beschrijft metingen aan metastabiele toestanden in supergeleiders.We hebben daarbij een analytische oplossing ontwikkeld van de 3-dimensionale Ginzburg-Landau vergelijkingen voor het probleem van een cylinder in een magnetisch veld,loodrecht op de as van de cylinder.

Job 42:3

Curriculum Vitae:

Na mijn eindexamen HBS-B in 1955,liet ik mij datzelfde jaar inschrijven aan de Universiteit van Amsterdam, alwaar ik de eer en het zeer grote genoegen had lid te zijn van het Vrij Disputgezelschap "Honestas et Rata Amicitia". Na mijn militaire dienstplicht vervuld te hebben,begon ik in 1963 de wis- en natuurkunde studie aan de Katholieke Universiteit te Nijmegen,waar ik in 1967 het candidaatsexamen (natuur- en wis- met scheikunde) aflegde, en het doctoraalexamen in 1969.Het promotie-onderzoek werd sinds 1971 in FOM-verband verricht op de afdeling Vaste Stof Fysica II,Experimentele Natuurkunde IV,onder leiding van Prof.P. Wyder en Dr.H. van Kempen.

November 1977 H.N. de Lang

Transport Properties of Solids at Low Temperatures in High Magnetic Fields

STELLINGEN

23 november 1977

H. N. de Lang

I

Het meten van de warmtegeleiding van metalen bij lage temperaturen en hoge magneetvelden heeft naast grote wetenschappelijke, ook grote karaktervormende waarde. In het bijzonder kweekt het aan zachtmoedigheid, geduld en doorzettingsvermogen, en maakt zodoende de beoefenaar ervan tot een beter mens.

II

Met behulp van de warmtepulsmethode zou de voortplantingssnelheid van het energietransport zowel in het fonon- alsook in het magnonsysteem kunnen worden bepaald. In het bijzonder zou via de warmtepulsmethode „second sound" in het magnonsysteem kunnen worden gemeten.

III

Roosterdefecten kunnen de magnon-fonon koppeling vergroten. Bij lagerdimensionale magnetische systemen kan dit leiden tot energietransport via magnon-achtige excitaties boven T_c. Het is van belang dit aspect systematisch te onderzoeken.

Dit proefschrift.

IV

Het is van belang een theorie te ontwerpen voor het energietransport door langlevende spinfluctuaties boven T_c (paramagnonen).

Dit proefschrift.

V

De z.g. supergeleidende methode, d.i. de methode om de elektron warmtegeleiding te reduceren door het metaal in de supergeleidende toestand te brengen, is niet geschikt voor het meten van de roostergeleiding in metalen.

Dit proefschrift.

VI

De theorie van Pippard over de ultrasone afzwakking (ultrasonic attenuation) in metalen kan niet worden gebruikt om de roostergeleiding in zuivere metalen af te schatten.

Dit proefschrift.

VII

Voor een non-intrinsieke verklaring van de lineaire magnetoweerstand in ongecompenseerde metalen met een gesloten Fermi-oppervlak verdienen twee-dimensionale kristaldefecten de voorkeur boven driedimensionale inclusies.

Dit proefschrift.

VIII

De o.a. door Newrock en Maxfield gemeten anomale kwadratische veldafhankelijkheid van de thermische magnetoweerstand kan eenvoudig worden verklaard.

R. S. Newrock and B. W. Maxfield,
J. Low Temp. Phys. 23(1976)119
Dit proefschrift.

IX

Het verdient aanbeveling het Lorenz getal L van metalen, aan een en hetzelfde sample als functie van de temperatuur T en het magnetisch veld H op twee verschillende manieren te meten, n.l

i) als evenredig aan het quotient van de elektrische en thermische weerstand

$$L(H, T) = \frac{\rho(H, T)}{W(H, T)\,T}$$

ii) als evenredig aan het quotient van de elektrische en thermische Hall constante

$$L(H, T) = \frac{R_H(H, T)}{A_{RL}(H, T)\,T}$$

en de resultaten onderling te vergelijken.

Dit proefschrift.

X

Van vele metalen en legeringen zijn de transporteigenschappen boven 10 K onbekend. Het is een vermetele werkwijze de transporteigenschappen bij die hogere temperaturen te extrapoleren vanuit metingen bij lagere (< 4.2 K) temperaturen m.b.v. de geldende theorieen. Daarom verdient het experimenteel onderzoek van de transporteigenschappen van metalen bij temperaturen tussen 5 en 100 K meer nadruk en aandacht te krijgen.

Dit proefschrift.

XI

Bij de onderlinge vergelijking van de elektrische en thermische Kohler hellingen S_{el} en S_{th} van diverse magnetoweerstandsmetingen aan dezelfde of verschillende metalen, dient gelet te worden op het temperatuurgebied waarin de metingen zijn verricht.

Dit proefschrift.

XII

De door Fletcher gevonden anomale bult in de temperatuurafhankelijkheid van de roostergeleiding van Kalium, kan eenvoudig worden verklaard.

R. Fletcher, Phys. Rev. Letters, 32(1974)930

Dit proefschrift.

XIII

De roostergeleiding van Kalium kan het best met de magnetische methode gemeten worden. Van de beschikbare magnetische methoden is de Corbino-methode daartoe het meest geschikt

Dit proefschrift.

XIV

De bepaling van het z.g. „superheating field" H_{SH} van bol- en cylindervormige supergeleiders door het superheating field van een supergeleidende, oneindige halfruimte te vermenigvuldigen met een geeigende demagnetisatie-factor geschiedt ongemotiveerd. Analytisch en exact kan worden aangetoond dat de bij deze werkwijze optredende correctietermen verwaarloosbaar klein zijn.

Dit proefschrift.

XV

In navolging van het Amerikaanse OTA (Office of Technology Assessment) dient zo spoedig mogelijk een EOTA (European Office of Technology Assessment) te worden opgericht.

H. N. de Lang, "Technology Assessment"
Technische Winkler Prins, Elsevier, Amsterdam.

XVI

Toekomstverkenningen hebben mede tot doel de eigen prognoses niet uit te laten komen. Daarom dienen ze tijdig te worden verricht.

XVII

De huidige wetenschapsjournalistiek en wetenschapsvoorlichting in de media concentreren zich (te) vaak op slechts de succesvolle en spectaculaire resultaten en geven aldus een eenzijdig en gefalsificeerd beeld van de wetenschap, dat mythevorming in de hand kan werken.

XVIII

De sinds 1931 voor het classificeren van aardbevingen gebezigde, doch sinds 1954 door de schaal van Richter vervangen, gemodificeerde schaal van Mercalli kan nog zeer wel worden gebruikt om de verwoestende kracht van peuters en kleuters aan te geven.

XIX

Moederliefde verlaagt de entropie.

XX

Of het leven waard is geleefd te worden is mede afhankelijk van de lever.